

PORTOFOLIULUCRĂRI RELEVANTE - dr Horia Ștefănescu

in extenso

1. **Articolul 1**, cu titlul "*Liver Stiffness Assessed by Ultrasound Shear Wave Elastography from General Electric Accurately Predicts Clinically Significant Portal Hypertension in Patients with Advanced Chronic Liver Disease*" - **pagina 2**
2. **Articolul 2**, cu titlul "*A novel spleen-dedicated stiffness measurement by FibroScan® improves the screening of high-risk esophageal varices.*" - **pagina 10**
3. **Articolul 3**, cu titlul "*What's in Metabolomics for Alcoholic Liver Disease?*" - **pagina 41**
4. **Articolul 4**, cu titlul "*Non-invasive menage a trois for the prediction of high-risk varices: stepwise algorithm using Lok score, liver and spleen stiffness.*" - **pagina 49**
5. **Articolul 5**, cu titlul "*Spleen stiffness measurement using fibroscan for the noninvasive assessment of esophageal varices in liver cirrhosis patients.*" - **pagina 58**
6. **Articolul 6**, cu titlul "*Bidimensional shear wave ultrasound elastography with supersonic imaging to predict presence of oesophageal varices in cirrhosis.*" - **pagina 65**
7. **Articolul 7**, cu titlul "*Development and prognostic relevance of a histologic grading and staging system for alcohol-related liver disease.*" - **pagina 66**
8. **Articolul 8**, cu titlul "*Identification of optimal therapeutic window for steroid use in severe alcohol-associated hepatitis: A worldwide study.*" - **pagina 75**
9. **Articolul 9**, cu titlul "*The EFSUMB Guidelines and Recommendations for the Clinical Practice of Elastography in Non-Hepatic Applications: Update 2018.*" - **pagina 84**
10. **Articolul 10**, cu titlul "*Noninvasive Tools and Risk of Clinically Significant Portal Hypertension and Varices in Compensated Cirrhosis: The "Anticipate" Study*" - **pagina 113**

Liver Stiffness Assessed by Ultrasound Shear Wave Elastography from General Electric Accurately Predicts Clinically Significant Portal Hypertension in Patients with Advanced Chronic Liver Disease

Lebersteifigkeit mittels Ultraschall-Scherwellenelastografie von General Electric zur treffsicheren Vorhersage einer klinisch signifikanten portalen Hypertonie bei Patienten mit fortgeschrittener chronischer Lebererkrankung

Authors

Horia Stefanescu^{1, 5}, Corina Rusu^{2, 5}, Monica Lupsor-Platon³, Oana Nicoara Farcau^{2, 5}, Petra Fischer^{2, 5}, Crina Grigoras^{1, 5}, Adelina Horhat^{1, 5}, Oana Stancu^{4, 5}, Andreea Ardelean^{1, 5}, Marcel Tantau², Radu Badea³, Bogdan Procopet^{1, 2, 5}

Affiliations

- 1 Hepatology Department, Regional Institute of Gastroenterology and Hepatology, Cluj Napoca, Romania
- 2 3rd Medical Clinic, Iuliu Hatieganu University of Medicine and Pharmacy, Cluj-Napoca, Romania
- 3 Medical Imaging Department, Iuliu Hatieganu University of Medicine and Pharmacy, Cluj-Napoca, Romania
- 4 Central Military Hospital, Carol Davila University of Medicine and Pharmacy, Bucharest, Romania
- 5 Liver Research Club, Cluj-Napoca, Romania

Key words

liver stiffness, ultrasound elastography, portal hypertension, noninvasive

received 26.09.2018

accepted 12.06.2019

Bibliography

DOI <https://doi.org/10.1055/a-0965-0745>

Published online: September 2, 2019

Ultraschall in Med

© Georg Thieme Verlag KG, Stuttgart · New York

ISSN 0172-4614

Correspondence

Dr. Horia Stefanescu

Hepatology Department, Regional Institute of Gastroenterology and Hepatology, 19–21 Croitorilor str, 400162 Cluj-Napoca, Romania
Tel.: ++40/7 66/31 82 83
horia.stefanescu@irgh.ro

ABSTRACT

Purpose Clinically significant portal hypertension (CSPH) is responsible for most of the complications in patients with cirrhosis. Liver stiffness (LS) measurement by vibration-controlled transient elastography (VCTE) is currently used to evaluate CSPH. Bi-dimensional shear wave elastography from

General Electric (2D-SWE.GE) has not yet been validated for the diagnosis of PHT. Our aims were to test whether 2D-SWE.GE-LS is able to evaluate CSPH, to determine the reliability criteria of the method and to compare its accuracy with that of VCTE-LS in this clinical setting.

Materials and Methods Patients with chronic liver disease referred to hepatic catheterization (HVPG) were consecutively enrolled. HVPG and LS by both VCTE and 2D-SWE.GE were performed on the same day. The diagnostic performance of each LS method was compared against HVPG and between each other.

Results 2D-SWE.GE-LS was possible in 123/127 (96.90 %) patients. The ability to record at least 5 LS measurements by 2D-SWE.GE and IQR < 30 % were the only features associated with reliable results. 2D-SWE.GE-LS was highly correlated with HVPG ($r = 0.704$; $p < 0.0001$), especially if HVPG < 10 mmHg and was significantly higher in patients with CSPH (15.52 vs. 8.14 kPa; $p < 0.0001$). For a cut-off value of 11.3 kPa, the AUROC of 2D-SWE.GE-LS to detect CSPH was 0.91, which was not inferior to VCTE-LS (0.92; $p = 0.79$). The diagnostic accuracy of LS by 2D-SWE.GE-LS to detect CSPH was similar with the one of VCTE-LS (83.74 % vs. 85.37 %; $p = 0.238$). The diagnostic accuracy was not enhanced by using different cut-off values which enhanced the sensitivity or the specificity. However, in the subgroup of compensated patients with alcoholic liver disease, 2D-SWE.GE-LS classified CSPH better than VCTE-LS (93.33 % vs. 85.71 %, $p = 0.039$).

Conclusion 2D-SWE.GE-LS has good accuracy, not inferior to VCTE-LS, for the diagnosis of CSPH.

ZUSAMMENFASSUNG

Ziel Klinisch signifikante portale Hypertonie (CSPH) ist für die meisten Komplikationen bei Patienten mit Zirrhose verantwortlich. Die Messung der Lebersteifigkeit (LS) mittels vibrationsgesteuerter transienter Elastografie (VCTE) wird derzeit zur Abschätzung einer CSPH verwendet. Die 2-dimensionale Scherwellenelastografie von General Electric (2D-SWE.GE)

wurde für die Diagnose der PHT noch nicht validiert. Unser Ziel war es zu untersuchen, ob die LS mittels 2D-SWE.GE in der Lage ist, eine CSPH abzuschätzen, die Zuverlässigkeitskriterien der Methode zu bestimmen und ihre Treffsicherheit in diesem klinischen Anwendungsbereich mit der VCTE-LS zu vergleichen.

Material und Methoden Patienten mit chronischer Lebererkrankung, die für einen Lebervenenendruckgradienten (HVPG) mittels Lebervenenkatheter vorgesehen wurden, wurden nacheinander eingeschlossen. HVPG und LS wurden sowohl mittels VCTE als auch 2D-SWE.GE am selben Tag durchgeführt. Die diagnostische Leistung jeder LS-Methode wurde mit dem HVPG sowie untereinander verglichen.

Ergebnisse 2D-SWE.GE-LS war bei 123/127 (96,90 %) Patienten durchführbar. Die Fähigkeit, mindestens 5 LS-Messungen mit 2D-SWE.GE und einer IQR < 30 % aufzuzeichnen, waren die einzigen Parameter, die zu zuverlässigen Ergebnissen führten. Die 2D-SWE.GE-LS korrelierte stark mit dem HVPG ($r = 0,704$;

$p < 0,0001$), insbesondere bei HVPG < 1 mmHg, und war bei Patienten mit CSPH signifikant höher (15,52 vs. 8,14 kPa; $p < 0,0001$). Bei einem Cut-off von 11,3 kPa betrug die AUROC der 2D-SWE.GE-LS zum Nachweis einer CSPH 0,91, was der VCTE-LS nicht unterlegen war (0,92; $p = 0,79$). Die diagnostische Genauigkeit der LS mittels 2D-SWE.GE-LS zur Erkennung von einer CSPH war ähnlich wie bei VCTE-LS (83,74 % gegenüber 85,37 %; $p = 0,238$). Die diagnostische Genauigkeit wurde durch den Einsatz unterschiedlicher Cut-offs, die die Sensitivität oder Spezifität erhöhten, nicht verbessert. In der Untergruppe der kompensierten Patienten mit alkoholbedingter Lebererkrankung klassifizierte die 2D-SWE.GE-LS eine CSPH jedoch besser als die VCTE-LS (93,33 % gegenüber 85,71 %, $p = 0,039$).

Schlussfolgerung Für die Diagnose der CSPH zeigt die 2D-SWE.GE-LS eine gute Treffsicherheit – diese ist nicht schlechter als die der VCTE-LS.

Introduction

In compensated advanced chronic liver disease (cACLD), the occurrence of portal hypertension (PHT) is responsible for most of the complications [1]. The standard method for the assessment of PHT is hepatic venous pressure gradient (HVPG) measurement that is not widely available and is invasive and costly [2]. HVPG ≥ 10 mmHg represents the threshold for clinically significant PHT (CSPH), from where PHT-related complications may occur [3].

Liver stiffness (LS) measurement by vibration-controlled transient elastography (VCTE) was validated as an accurate surrogate for CSPH and it is currently recommended as a noninvasive tool for its diagnosis [4, 5]. Values ≥ 21.1 kPa have very good diagnostic and prognostic accuracy, not inferior to HVPG [6–8]. However, it is not technical feasible in a significant number of patients [9].

Lately, point and bi-dimensional shear wave elastographic (2D-SWE) methods were developed to assess liver fibrosis. They have the advantage of visual control over VCTE, being implemented on ultrasound machines, but still need validation for PHT diagnosis. 2D-SWE from General Electric (2D-SWE.GE) is one of the newest methods developed for fibrosis staging [10], but has not yet been validated for the assessment of CSPH.

The aims of the study were (1) to test whether 2D-SWE.GE is able to estimate CSPH assessed by HVPG, (2) to determine its reliability criteria in this scenario and (3) to compare the method's accuracy with that of VCTE in this clinical setting.

Methods

The study protocol was approved by the local ethics committee and was designed in accordance with the 2000 review of the Human Rights Declaration and following the liver-FibroSTARD checklist [11] – see Appendix for details. All participants gave their informed consent.

Patients and study protocol

All patients with chronic liver disease of various etiologies, referred for HVPG measurement or transjugular liver biopsy for the management of their disease were enrolled consecutively.

Exclusion criteria were: pacemaker or heart defibrillator; pregnancy; liver transplantation; unresectable hepatocellular carcinoma (HCC); patients unable or unwilling to sign the consent.

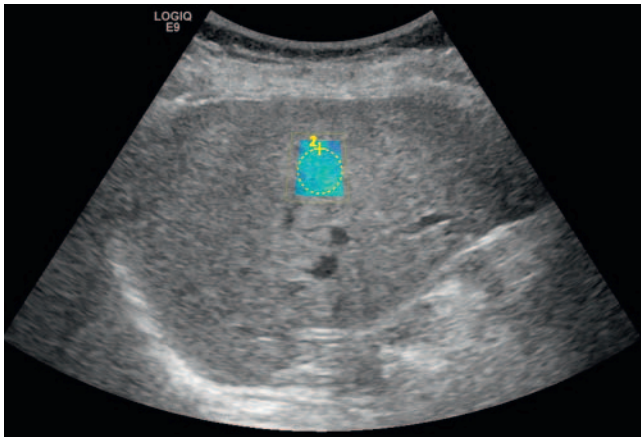
HVPG and liver stiffness measurement with both VCTE and 2D-SWE.GE were performed on the same day after at least 6 hours (overnight) fasting [12–14].

Liver stiffness measurements

Liver stiffness was measured by different experienced operators (more than 500 examinations for VCTE and certified ultrasound examiner) for each technique, blinded to one another and also blinded to the clinical, biological and hemodynamic data.

LS by VCTE was assessed using the FibroScan[®] device equipped with the M-probe (Echosens, Paris, France), as previously reported [15]. For each patient, LS values were considered reliable if at least 10 valid measurements were obtained with an inter-quartile range (IQR) < 30 % of the median value if LS > 7.1 kPa [16].

LS by 2D-SWE (► **Fig. 1**) was performed using a LOGIQ E9 system equipped with the C1-6-D convex probe (GE Healthcare, Chalfont St Giles, United Kingdom). The patient was placed in a supine position with the right arm in maximum abduction. The probe was located in the right intercostal spaces in order to obtain the best possible acoustic window for liver assessment. The SWE region of interest (ROI) was placed at least 2 cm below the liver capsule, in a region free of large vessels. On a suitable section, with the patient in exhaling apnea, 2–3 colored SWE image frames were recorded for 5 seconds. A total of 10 SWE frames were eventually acquired. A circular (1 cm wide) ROI was placed within each SWE frame and the stiffness inside the ROI was calculated. Each stiffness measurement represents the average of Young Modulus values of every point inside the circular ROI and



► **Fig. 1** Estimation of 2D-SWE.GE-LS: An elasticity map is obtained inside the trapezoidal ROI and the stiffness is calculated inside the circular ROI with a diameter of 1 cm.

is expressed in kilopascals. Eventually, the median and IQR values of 10 SWE measurements are automatically calculated. The 2D-SWE.GE operator was experienced in ultrasound elastography and blinded to other patient data.

HVPG measurement

Under ultrasonographic guidance and after local anesthesia, a 9F venous catheter introducer (St. Jude Medical, Minnesota, USA) was placed using the Seldinger technique in the right internal jugular vein. Thereafter, under fluoroscopic guidance a 7F balloon-tipped catheter (Edwards Lifesciences, Irvine, CA, USA) was advanced into the hepatic vein. Wedged and free hepatic venous pressures were measured in triplicate. HVPG was calculated as the difference between wedged and free hepatic venous pressures. Clinically significant portal hypertension was defined as HVPG \geq 10 mmHg [3]. The operator was blinded to elastography measurement results.

Statistical analysis

The statistical analysis was performed using the SPSS software version 20.0 (SPSS Inc. Chicago, IL, USA). Quantitative data is reported as median and range, while qualitative data is reported as percentage (%). Shapiro-Wilk test was used to evaluate the normal distribution of data. Spearman's test was used for correlations among continuous variables. Medians were compared using the Mann-Whitney test.

The concordance between LS by 2D-SWE.GE calculated as a median of 3, 5 or 10 distinct measurements was tested using absolute interclass correlation agreement (ICC).

The diagnostic performance of each elastographic technique was assessed by receiver operating characteristic (ROC) curves analysis. Optimal cut-off values were calculated using a common optimization step that maximized the Youden index [17]. For comparison of the ROC curves, the DeLong test was used, via an online tool available at http://vassarstats.net/roc_comp.html.

The performance of tested noninvasive methods to predict CSPH was estimated by calculating the proportion of correctly

classified patients – diagnostic accuracy (DA), together with the sensitivity (Se), specificity (Sp), positive predictive value (PPV), negative predictive value (NPV), and likelihood ratios (LR). The Fischer exact test and McNemar test were used in the 2×2 contingency table for assessing differences in the proportion of misclassified patients with dichotomous cut-offs, as well as for comparing categorical variables.

For all calculations, a p-value < 0.05 was considered to indicate statistical significance.

Results

Baseline characteristics of patients

A comprehensive overview of our cohort is detailed in ► **Table 1**. Briefly, 127 consecutive patients admitted for HVPG measurement with or without concomitant transjugular liver biopsy were prospectively included. The indication for HVPG measurement was: cirrhosis of viral cause prior to antiviral therapy (n = 24), suspicion of severe alcoholic hepatitis (n = 46) or for diagnosis and severity assessment in patients with suspected advanced liver disease (n = 57). 70 % (n = 89) had CSPH and 35.5 % (n = 45) were decompensated at the moment of inclusion due to severe alcoholic hepatitis (n = 30) or sepsis (n = 15).

Applicability and feasibility of LS by 2D-SWE.GE

LS by 2D-SWE.GE was possible in 123/127 patients (96.9%). In most of the patients (103/127, 81.1 %), 10 distinct measurements were recorded, while less than 5 measurements could be obtained in 11 patients (8.6%). Overall, at least 5 separate measurements were obtained in 112 (88.2 %) patients, and at least 3 measurements in 118 (92.91 %).

In the 103 patients with 10 measurements, no differences were observed in the median LS values if they were calculated using 3, 5 or 10 measurements: 13.87 (95%CI: 9.34–17.17) kPa vs. 13.96 (9.00–17.64) kPa vs. 13.93 (9.34–17.54) kPa, respectively (p = 0.82). The concordance between the three values is almost perfect: ICC = 0.989; p < 0.0001 .

IQR/median < 0.3 could be used as reliability criteria for 2D-SWE.GE-LS, similarly with VCTE. This criteria is met in 71/118 (60.16 %) patients with at least 3 measurements, in 108/112 (96.42 %) patients with ≥ 5 measurements and in 100/103 (97.08 %) patients with 10 measurements.

LS by 2D-SWE.GE, irrespective of the number of measurements performed, is very well correlated with HVPG, when assessed in the entire cohort or only in patients with reliable results (► **Table 2**).

Based on these results, LS by 2D-SWE.GE was calculated as the median of 5 distinct measurements for further analysis.

Ascites, the depth where the LS was measured, the skin-liver distance, and BMI were not associated with failure to measure the LS by 2D-SWE.GE. However, failure to record at least 5 measurements was associated with a higher IQR, suggesting less reliable results.

The correlation between 2D-SWE.GE-LS and HVPG is much better in patients without CSPH (HVPG < 10 mmHg) compared with those with more advanced disease (► **Fig. 2**).

► **Table 1** Baseline characteristics of patients.

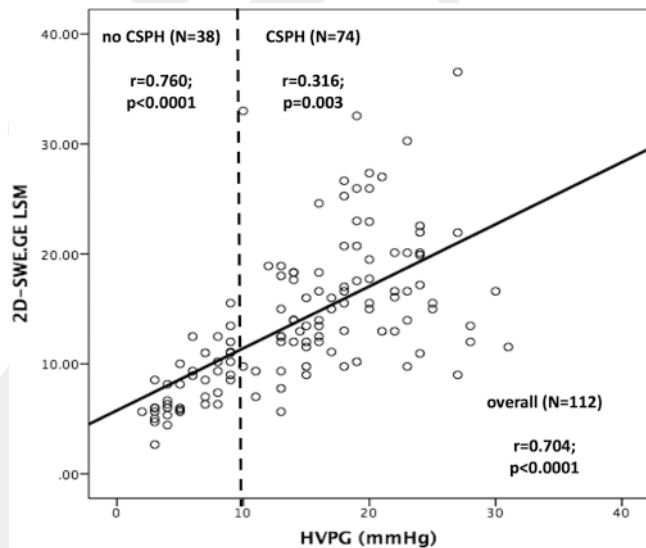
variable	n (%) or median (range)
age (years)	57 (20–78)
gender (male)	79 (62.20%)
BMI (kg/m ²)	26.97 (20.45–37.32)
etiology of liver disease	
▪ viral	46 (36.22%)
▪ alcohol	52 (40.94%)
▪ viral + alcohol	3 (2.36%)
▪ other	26 (20.47%)
lab values	
▪ AST (UI/ml)	83.43 (69.98–96.87)
▪ ALT (UI/ml)	49.72 (41.37–58.07)
▪ Bil T (mg/dl)	1.80 (0.23–42.00)
▪ Alb (g/dl)	3.56 (3.41–3.71)
▪ INR	1.56 (1.46–1.66)
▪ platelet count (x10 ³ /ml)	131 (15–441)
▪ creatinine (mg/dl)	0.72 (0.29–5.51)
cirrhosis	102 (80.31%)
▪ CPT class (A/B/C)	53 (51.96%)/24 (23.52%)/25 (24.50%)
▪ CPT score	6 (5–13)
▪ MELD	11.02 (9.56–12.47)
▪ ascites [mild-moderate/severe]	43 (33.85%) [34(79.06%)/9(20.94%)]
endoscopy	
▪ esophageal varices/HREV	62 (48.81%)/42 (32.28%)
HVPG (mmHg)	15 (2–31)
CSPH	89 (70.10%)
elastography (LS)	
▪ VCTE	n = 115
– median (kPa)	39.26 (34.24–44.28)
– IQR (kPa)	9.68 (4.74–16.23)
– IQR/M	0.21 (0.16–0.28)
▪ 2D-SWE.GE	n = 123
– median (kPa)	13.96 (12.77–15.15)
– IQR (kPa)	1.06 (0.00–6.64)
– IQR/M	0.09 (0.00–0.37)

ALT – alanine amino transferase; AST – aspartate amino transferase; Alb – albumin; Bil T – total bilirubin; BMI – body mass index; CPT – Child-Pugh-Turcotte; CSPH – clinically significant portal hypertension; HREV – high-risk esophageal varices; INR – international normalized ratio; IQR – interquartile range; MELD – model for end-stage liver disease; LS – liver stiffness measurement; kPa – kilopascals; VCTE – vibration-controlled transient elastography; 2D-SWE.GE – real-time shear wave elastography.

► **Table 2** Correlation between LS by 2D-SWE.GE and HVPG measurement according to the number of LS recordings.

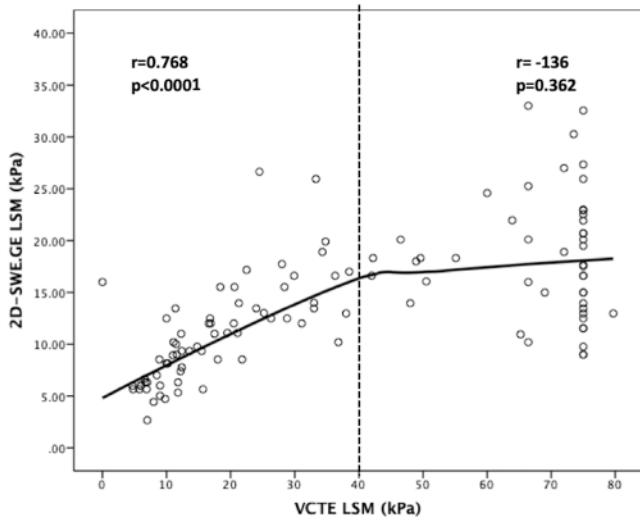
	3 measurements	5 measurements	10 measurements
entire population			
N	118	112	103
r ¹	0.694	0.704	0.704
P	<0.0001	<0.0001	<0.0001
patients with reliable results			
N	71	108	100
r ¹	0.787	0.802	0.801
p	<0.0001	<0.0001	<0.0001

¹ Spearman correlation test.

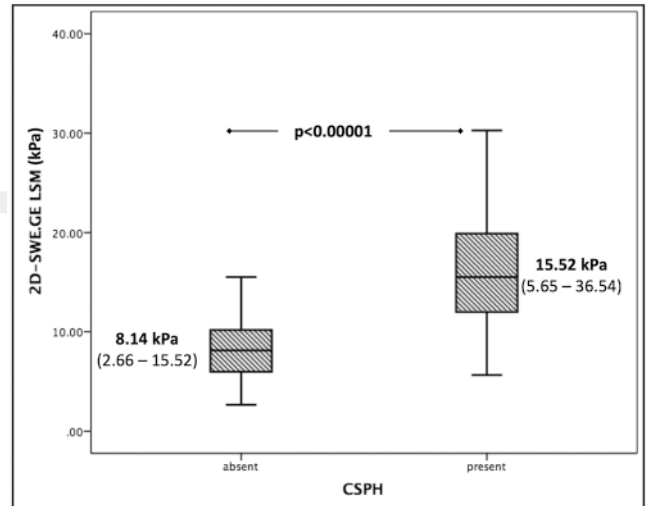
► **Fig. 2** Scatter-dot plot demonstrating the correlation between 2D-SWE.GE-LS and HVPG values. The correlation is better in patients without CSPH (HVPG < 10 mmHg).

In contrast, LS by VCTE was possible in only 115/127 (90.6%), which is not significantly different from LS by 2D-SWE.GE ($p = 0.331$). BMI ($p = 0.132$), ascites ($p = 0.096$) and other clinical parameters were not significantly associated with failure to perform VCTE-LS, although a tendency could be observed for the former. The correlation between LS by VCTE and HVPG was also high for the entire population ($r = 0.700$; $p < 0.0001$), especially for patients without CSPH ($r = 0.774$; $p < 0.0001$), while it was weaker for patients with HVPG ≥ 10 mmHg ($r = 0.489$; $p < 0.0001$).

LS values obtained by either technique were well correlated as well ($r = 0.704$; $p < 0.0001$), but the correlation disappeared for VCTE-LS values higher than 40 kPa (► **Fig. 3**).



► **Fig. 3** Scatter-dot plot demonstrating the correlation between 2D-SWE.GE-LS and VCTE-LS. The correlation is lost for high (>40 kPa) VCTE-LS values.



► **Fig. 4** Box plots showing the significant difference between median values of 2D-SWE.GE-LS in patients with/without CSPH.

Performance for diagnosing CSPH in the entire population

LS by 2D-SWE.GE was significantly higher in patients with CSPH as compared with those without, as shown in ► **Fig. 4**. The same trend is observed for LS by VCTE (11.10 vs. 60.00 kPa, $p < 0.0001$).

Using the Youden index, the best cut-off value for LS by 2D-SWE.GE to predict CSPH was 11.3 kPa. LS by 2D-SWE.GE and VCTE had a similar AUROC for the prediction of CSPH (► **Table 3**), showing the non-inferiority of 2D-SWE.GE compared to VCTE.

The cut-off value for LS by 2D-SWE.GE is 9 kPa for a sensitivity of 0.95, while the cut-off for better specificity (0.95) is 13 kPa. The cut-off that favors sensitivity (9 kPa) does not have significantly better accuracy in comparison with the cut-off of 11.3 kPa (84.5% vs. 83.7%, McNemar-test $p = 0.243$). In contrast, when using the cut-off value that favors specificity, the diagnostic accuracy significantly decreased from 83.74% to 75% (McNemar-test $p < 0.001$). Therefore, for further comparison with VCTE-LS, we used the cut-off of 11.3 kPa.

The generally accepted cut-off values for VCTE-LS to predict CSPH are 13.6 kPa (favoring Se)[18] and 21.1 kPa (favoring Sp)[6]. In our cohort, the accuracy of CSPH diagnosis with a threshold of 13.6 kPa for VCTE-LS is significantly lower (McNemar-test $p < 0.001$) than 21.1 kPa.

For CSPH prediction, the diagnostic accuracy of 11.3 kPa (2D-SWE.GE-LS) is significantly better than 13.6 kPa (VCTE-LS) and similar with 21.1 kPa (VCTE-LS), McNemar-test $p < 0.001$ and $p = 0.238$, respectively.

In our cohort with a high pretest probability of CSPH (0.70), using the thresholds of 21.1 kPa (LS by VCTE) or 11.3 kPa (LS by 2D-SWE.GE) results in an increase in the posttest probability of more than 20% (0.94 for VCTE and 0.93 for 2D-SWE.GE).

Diagnostic performance in compensated patients

82 (65.5%) patients were compensated at the moment of inclusion. In this subgroup, LS by 2D-SWE.GE was reliably obtained in 79 (96%) patients, while LS by VCTE could only be obtained in 74 (90%) ($p = 0.268$).

The AUROCs of LS by 2D-SWE.GE and VCTE were almost identical. The best cut-off value for 2D-SWE.GE-LS to predict CSPH was also 11.3 kPa (► **Table 4**). For this value, 65/79 (82.27%) patients were correctly classified as having or not having CSPH. The diagnostic accuracy of 2D-SWE.GE-LS was not different from that of VCTE-LS using the cut-off of 21.1 kPa (McNemar-test $p = 0.338$), but significantly better than the cut-off of 13.6 kPa (McNemar-test $p < 0.001$).

The post-test probability to detect CSPH is 87% (2D-SWE.GE-LS) and 70% (VCTE-LS). Considering the prevalence of 55%, the probability gain is significantly higher for 2D-SWE.GE-LS (32% vs. 15%, respectively; $p < 0.001$).

Influence of etiology

In the subgroup of compensated patients, 16 (19.51%) had alcoholic liver disease. LS by 2D-SWE.GE was significantly higher in the case of an alcoholic etiology as compared with other etiologies (18.10 vs. 10.70 kPa; $p = 0.002$). The AUROC value of 2D-SWE.GE-LS for predicting CSPH was higher in alcoholic patients (1.00, 95% CI: 1.00–1.00) than in non-alcoholic ones (0.846, 95% CI: 0.744–0.948) but was not significantly different from VCTE-LS in either situation (DeLong test, $p = 0.85$ and 0.88, respectively).

The proportion of patients correctly classified as having CSPH based on LS, assessed by both techniques, was also higher in patients with alcohol-related liver disease compared with those without (► **Table 5**). In alcoholic patients, the diagnostic accuracy of 2D-SWE.GE-LS is significantly better than VCTE-LS ($p = 0.039$).

► **Table 3** Prediction of CSPH by LS, assessed either by 2D-SWE.GE or by VCTE in the entire population (N = 127). Pre-test probability (prevalence of CSPH) is 70.1 %.

	2D-SWE.GE			VCTE		
AUROC¹	0.91 (0.86–0.96)			0.92 (0.87–0.97)		
cut-off (kPa)	11.3 ²	9	13	24.25 ²	13.6 ³	21.1 ⁴
Se	0.82	0.95	0.66	0.81	0.94	0.84
Sp	0.87	0.71	0.95	0.97	0.54	0.88
PPV	93.33 %	87.50 %	96.50 %	98.50 %	82.60 %	94.40 %
NPV	68.75 %	77.10 %	55.40 %	69.38 %	79.16 %	70.50 %
+LR	6.25	3.12	12.51	28.51	2.05	7.34
–LR	0.20	0.13	0.36	0.19	0.11	0.18
accuracy	83.74 % (103/123)	84.50 % (104/123)	75.00 % (92/123)	86.20 % (100/116)	82 % (95/116)	85.34 % (99/116)

¹ p (de Long test) = 0.79; difference = 0.01 [$\Delta = -0.26$ (for non-inferiority)].

² calculated according to Youden Index.

³ generally accepted cut-off value for VCTE-LS with 90 % sensitivity.

⁴ generally accepted cut-off value for VCTE-LS with 90 % specificity.

► **Table 4** Prediction of CSPH by LS, assessed either by 2D-SWE.GE or by VCTE, in the subgroup of compensated patients (N = 82). Pre-test probability (prevalence of CSPH) is 55 %.

	2D-SWE.GE	VCTE	
AUROC¹	0.882 (0.808–0.957)	0.886 (0.808–0.964)	
cut-off (kPa)	11.3 ²	11.6 ³	21.1 ⁴
Se	0.79	0.92	0.73
Sp	0.85	0.51	0.90
PPV	87.50 %	70.37 %	90.10 %
NPV	76.92 %	85.00 %	73.17 %
+LR	5.56	1.91	8.04
–LR	0.23	0.14	0.29
accuracy	82.27 % (65/79)	74.32 % (55/74)	81.08 % (60/74)

¹ p (de Long test) = 0.94; difference = 0.004 [$\Delta = -0.07$ (for non-inferiority)].

² calculated according to Youden Index.

³ generally accepted cut-off value for VCTE-LS with 90 % sensitivity.

⁴ generally accepted cut-off value for VCTE-LS with 90 % specificity.

► **Table 5** Comparisons of correctly classified patients (diagnostic accuracies) of LS by 2D-SWE.GE (11.3 kPa) and VCTE (21.1 kPa) for diagnosing CSPH in compensated patients with/without alcohol-related liver disease (n = 82).

	2D-SWE.GE-LS	VCTE-LS	p (McNemar test)
entire population (n = 82)	65/79 (82.27 %)	60/74 (81.08 %)	0.338
alcohol-related (n = 16)	14/15 (93.33 %)	12/14 (85.71 %)	0.039
not alcohol-related (n = 66)	51/64 (79.68 %)	47/60 (78.33 %)	0.413

LS in advanced liver disease was found to be a good noninvasive surrogate marker for CSPH [6, 18] and may assess patients at risk of having esophageal varices that need treatment [19].

LS by VCTE is the most validated method but its feasibility is limited in up to 55 % of cases [20] mainly due to ascites, high BMI and narrow intercostal spaces. In our cohort, the failure rate of VCTE-LS was only 10 %, but the proportion of patients with massive ascites and high BMI was low. As previously reported [20, 21], the feasibility of real-time SWE techniques is very high. In our cohort, 2D-SWE.GE-LS was feasible in a similar proportion. Although not statistically significant, the feasibility of 2D-SWE.GE-LS in cirrhotic patients tends to be higher than that of VCTE-LS, while the situation appears to be the other way around in healthy subjects [22].

As previously shown for another 2D-SWE technique [23], we demonstrated that 5 distinct measurements are enough for reliable and accurate results. No clinical factor was associated with

Discussion

This study is the first to demonstrate the usefulness of LS by 2D-SWE available on the GE Logiq E9 ultrasound machine for the diagnosis of CSPH in patients with advanced liver diseases. In this cohort we found better feasibility of the method compared with LS by VCTE and very good diagnostic accuracy for CSPH that is not inferior to VCTE.

failure to obtain elastograms in advanced CLD patients. However, in difficult patients obtaining 5 distinct elastograms is reliable enough to estimate liver stiffness by 2D-SWE.GE.

In cirrhosis, LS evaluated by 2D-SWE.GE shows a very good correlation with HVPG measurement, especially if < 10 mmHg, while in patients with CSPH, the correlation is weaker, confirming that LS, irrespective of which technique is used to assess it [18, 24, 25], does not entirely reflect the hemodynamic changes that occur at high portal pressure. However, the accuracy of 2D-SWE.GE-LS for predicting the risk of variceal bleeding or the response to beta-blockers has not yet been investigated, but considering this behavior it can be speculated that it would not differ from LS by VCTE [26].

The diagnostic performance of 2D-SWE.GE-LS for CSPH is good both in the entire population and in the subgroup of compensated patients, and it is not inferior to VCTE-LS. The performance is in line with 2D-SWE.SSI [21, 25], thus confirming the role of LS for CSPH prediction, irrespective of the method used.

The best cut-off value for predicting CSPH is 11.3 kPa with a diagnostic accuracy of almost 84%. Contrary to previous studies that used different cut-off values for LS to rule-in or rule-out CSPH [6, 21, 25], using this approach did not increase the diagnostic accuracy in our population. It is difficult to say whether this is an intrinsic characteristic of the specific algorithm that calculates LS since the values are very close (9 kPa for 95% sensitivity and 13 kPa for 95% specificity), or whether it is a consequence of the high prevalence of CSPH in our population (70%). However, in the compensated subgroup the post-test probability of diagnosing CSPH was 17% higher using 2D-SWE.GE than VCTE. While the post-test probability for VCTE (70%) is in line with the data from the Anticipate study [27], the higher value obtained for 2D-SWE.GE (87%) suggests its better feasibility.

Although the issue of an exact cut-off value is not important per se, the co-existence of different devices on the market that use various methods to generate the shear wave and to transform the estimated velocity into kilopascals [28] is confusing. For healthy subjects or patients with mild/moderate disease, the concordance between elastographic techniques appears to be higher [29]. A much detailed comparison of seven different elastographic techniques with VCTE as a reference [30], revealed that 2D-SWE from GE and from SSI differ from one another and from VCTE. In our study, the correlation between techniques is better than previously observed, but only for VCTE-LS values \leq 40 kPa (► Fig. 3). This finding could be explained on one hand by the ceiling effect of the FibroScan (20 patients had the maximum possible value – 75 kPa – measured by the machine), and on the other hand by the method-specific algorithm used to estimate LS (the biggest LS value on 2D-SWE.GE was not higher than 35 kPa). It could be speculated that the actual shear wave velocities would have been better correlated than their corresponding LS estimates. This issue was not assessed in this study, but it has been previously demonstrated that shear wave velocity values by GE are best correlated with the values measured on Siemens S3000 [31], and not with the FibroScan.

Many studies that validated LS were performed in highly selected populations, mainly with HCV-related disease. As our study group was a heterogeneous one, an ancillary finding of this analysis

was that the diagnostic accuracy for CSPH provided by 2D-SWE.GE is significantly higher ($p = 0.039$) in compensated alcoholic patients as compared with VCTE. This suggests that 2D-SWE.GE-LS might be the elastographic method of choice in this subset of patients. This finding, however, needs to be further validated due to the small number of patients in this subgroup ($n = 16$).

This is the first study validating LS by 2D-SWE.GE for the diagnosis of CSPH using HVPG as a reference and demonstrates the non-inferiority compared to VCTE. However, this study has some limitations. The first is the heterogeneity of the population and the high prevalence of CSPH patients. The subgroup analysis performed in fully compensated patients ($n = 82$) overcame this limitation. Secondly, the cross-sectional design of the study doesn't allow prognosis assessment.

In conclusion, 2D-SWE.GE-LS is a good noninvasive method for predicting CSPH in patients with advanced liver diseases and is not inferior to VCTE-LS. It appears to be easier to perform (obtaining 5 measurements is enough for an accurate estimation of LS) and tends to have better feasibility, especially in compensated patients with alcoholic liver disease.

Conflict of Interest

The authors declare that they have no conflict of interest.

References

- [1] Bosch J, Berzigotti A, Garcia-Pagan JC et al. The management of portal hypertension: Rational basis, available treatments and future options. *J Hepatol* 2008; 48: 68–92
- [2] Targownik LE, Spiegel BMR, Dulai GS et al. The Cost-Effectiveness of Hepatic Venous Pressure Gradient Monitoring in the Prevention of Recurrent Variceal Hemorrhage. *Am J Gastroenterol* 2004; 99: 1306–1315
- [3] Bosch J, Abraldes JG, Berzigotti A et al. The clinical use of HVPG measurements in chronic liver disease. *Nat Rev Gastroenterol Hepatol Nature Publishing Group* 2009; 6: 573–582
- [4] Castera L, Yuen Chan HL, Arrese M et al. EASL-ALEH Clinical Practice Guidelines: Non-invasive tests for evaluation of liver disease severity and prognosis. *J Hepatol* 2015; 63: 237–264
- [5] Franchis RD, Abraldes JG, Bajaj J et al. Expanding consensus in portal hypertension Report of the Baveno VI Consensus Workshop: Stratifying risk and individualizing care for portal hypertension. *J Hepatol European Association for the Study of the Liver* 2015; 63: 743–752
- [6] Bureau C, Metivier S, Peron JM et al. Transient elastography accurately predicts presence of significant portal hypertension in patients with chronic liver disease. *Aliment Pharmacol Ther* 2008; 27: 1261–1268
- [7] Robic MA, Procopet B, Métivier S et al. Liver stiffness accurately predicts portal hypertension related complications in patients with chronic liver disease: a prospective study. *J Hepatol* 2011; 55: 1017–1024
- [8] Singh S, Fujii LL, Murad MH et al. Liver stiffness is associated with risk of decompensation, liver cancer, and death in patients with chronic liver diseases: A systematic review and meta-analysis. *Clin Gastroenterol Hepatol Elsevier, Inc* 2013; 11: 1573–1584
- [9] Castéra L, Foucher J, Bernard P-H et al. Pitfalls of liver stiffness measurement: a 5-year prospective study of 13369 examinations. *Hepatology* 2010; 51: 828–835
- [10] Bende F, Sporea I, Sirli R et al. Performance of 2D-SWE.GE for predicting different stages of liver fibrosis, using Transient Elastography as the reference method. *Med Ultrason* 2017; 19: 143

- [11] Boursier J, de Ledinghen V, Poynard T et al. An extension of STARD statements for reporting diagnostic accuracy studies on liver fibrosis tests: The Liver-FibroSTARD standards. *J Hepatol European Association for the Study of the Liver* 2015; 62: 807–815
- [12] Arena U, Lupsor Platon M, Stasi C et al. Liver stiffness is influenced by a standardized meal in patients with chronic hepatitis C virus at different stages of fibrotic evolution. *Hepatology* 2013; 58: 65–72
- [13] Berzigotti A, de Gottardi A, Vukotic R et al. Effect of meal ingestion on liver stiffness in patients with cirrhosis and portal hypertension. *PLoS One* 2013; 8: e58742
- [14] Simkin P, Rattansingh A, Liu K et al. Reproducibility of 2 Liver 2-Dimensional Shear Wave Elastographic Techniques in the Fasting and Postprandial States. *J Ultrasound Med* 2018; 38: 1739–1745
- [15] Ziol M, Handra-Luca A, Kettaneh A et al. Noninvasive assessment of liver fibrosis by measurement of stiffness in patients with chronic hepatitis C. *Hepatology* 2005; 41: 48–54
- [16] Boursier J, Zarski JP, de Ledinghen V et al. Determination of reliability criteria for liver stiffness evaluation by transient elastography. *Hepatology* 2013; 57: 1182–1191
- [17] Fluss R, Faraggi D, Reiser B. Estimation of the Youden Index and its Associated Cutoff Point. *Biometrical J* 2005; 47: 458–472
- [18] Vizzutti F, Arena U, Romanelli RG et al. Liver stiffness measurement predicts severe portal hypertension in patients with HCV-related cirrhosis. *Hepatology* 2007; 45: 1290–1297
- [19] Augustin S, Pons M, Maurice JB et al. Expanding the Baveno VI criteria for the screening of varices in patients with compensated advanced chronic liver disease. *Hepatology* 2017; 66: 1980–1988
- [20] Elkrief L, Rautou PE, Ronot M et al. Prospective Comparison of Spleen and Liver Stiffness by Using Shear-Wave and Transient Elastography for Detection of Portal Hypertension in Cirrhosis. *Radiology* 2015; 275: 589–598
- [21] Procopet B, Berzigotti A, Abraldes JG et al. Real-time shear-wave elastography: Applicability, reliability and accuracy for clinically significant portal hypertension. *J Hepatol* 2015; 62: 1068–1075
- [22] Bende F, Mulabecirovic A, Sporea I et al. Assessing Liver Stiffness by 2-D Shear Wave Elastography in a Healthy Cohort. *Ultrasound Med Biol* 2018; 44: 332–341
- [23] Schellhaas B, Strobel D, Wildner D et al. Two-dimensional shear-wave elastography. *Eur J Gastroenterol Hepatol* 2017; 29: 723–729
- [24] Attia D, Schoenemeier B, Rodt T et al. Evaluation of liver and spleen stiffness with acoustic radiation force impulse quantification elastography for diagnosing clinically significant portal hypertension. *Ultraschall der Medizin* 2015; 36: 603–610
- [25] Jansen C, Bogs C, Verlinden W et al. Shear-wave elastography of the liver and spleen identifies clinically significant portal hypertension: A prospective multicentre study. *Liver Int* 2017; 37: 396–405
- [26] Berzigotti A. Non-invasive evaluation of portal hypertension using ultrasound elastography. In: *Journal of Hepatology* 2017; 67: 399–411
- [27] Abraldes JG, Bureau C, Stefanescu H et al. Noninvasive tools and risk of clinically significant portal hypertension and varices in compensated cirrhosis: The “Anticipate” study. *Hepatology* 2016; 64: 2173–2184
- [28] Christoph Dietrich AF, Bamber J, Berzigotti A et al. EFSUMB Guidelines and Recommendations on the Clinical Use of Liver Ultrasound Elastography, Update 2017 (Long Version) EFSUMB-Leitlinien und Empfehlungen zur klinischen Anwendung der Leberelastographie, Update 2017 (Langversion). *EFSUMB Guidel and ... Ultraschall in Med* 2017; 38: 16–47
- [29] Mulazzani L, Salvatore V, Ravaoli F et al. Point shear wave ultrasound elastography with Esaote compared to real-time 2D shear wave elastography with supersonic imagine for the quantification of liver stiffness. *J Ultrasound* 2017; 20: 213–225
- [30] Piscaglia F, Salvatore V, Mulazzani L et al. Differences in liver stiffness values obtained with new ultrasound elastography machines and Fibroscan: A comparative study. *Dig Liver Dis* 2017; 49: 802–808
- [31] Gress V, Glawion E, Schmidberger J et al. Comparison of Liver Shear Wave Elastography Measurements using Siemens Acuson S3000, GE LOGIQ E9, Philips EPIQ7 and Toshiba Aplio 500 (Software Versions 5.0 and 6.0) in Healthy Volunteers. *Ultraschall der Medizin – Eur J Ultrasound* 2018. doi:10.1055/a-0651-0542

DR. HORIA STEFANESCU (Orcid ID : 0000-0002-4034-5471)
DR. GIOVANNI MARASCO (Orcid ID : 0000-0001-7167-8773)
DR. PAUL CALES (Orcid ID : 0000-0003-4866-5274)
DR. VICTOR DE LEDINGHEN (Orcid ID : 0000-0001-6414-1951)
DR. FEDERICO RAVAIOLI (Orcid ID : 0000-0002-1142-8585)
PROF. PIETRO ANDREONE (Orcid ID : 0000-0002-4794-9809)

Article type : Original Articles
Editor : Christophe Bureau

A novel spleen-dedicated stiffness measurement by FibroScan® improves the screening of high-risk esophageal varices.

Horia Stefanescu¹, Giovanni Marasco², Paul Calès³, Mirella Fraquelli⁴, Matteo Rosselli⁵,
Nathalie Ganne-Carriè⁶, Victor de Ledinghen⁷, Federico Ravaioli², Antonio Colecchia²⁻⁸,
Corina Rusu¹, Pietro Andreone², Giuseppe Mazzella², Davide Festi².

Authors' institutions:

¹Liver Unit, Regional Institute of Gastroenterology and Hepatology, Cluj-Napoca, Romania;

²Department of Medical and Surgical Sciences, University of Bologna, Bologna, Italy;

³Hepato-Gastroenterology Department, University hospital, Angers, France;

⁴Gastroenterology and Endoscopy Unit, Fondazione IRCCS Ca' Granda Ospedale Maggiore Policlinico, Milan, Italy;

⁵University College of London, Institute for Liver and Digestive Health, Royal Free Hospital, London, UK;

⁶Hepato-Gastroenterology Department, APHP Jean Verdier Hospital, University Paris 13, INSERM UMR 1162, France;

This article has been accepted for publication and undergone full peer review but has not been through the copyediting, typesetting, pagination and proofreading process, which may lead to differences between this version and the Version of Record. Please cite this article as doi: 10.1111/liv.14228

This article is protected by copyright. All rights reserved.

⁷Haut-Lévêque Hospital, Hepatology Department, Bordeaux, France;

⁸Gastroenterology Unit, University Hospital Borgo Trento, Verona, Italy.

Corresponding author:

Davide Festi, Department of Medical and Surgical Sciences, University of Bologna, Italy

Phone: +39 0512144123, fax. +39 0512144123 e-mail: davide.festi@unibo.it,

List of abbreviations: PH, portal hypertension; CLD, chronic liver disease; EV, esophageal varices; EGD, esophagogastroduodenoscopy; HRV, high-bleeding risk varices; CSPH, clinically significant portal hypertension; LSM, liver stiffness measurement; VCTE, vibration controlled transient elastography; HVPG, hepatic venous gradient pressure; SSM, spleen stiffness measurement; SSM@50Hz: SSM with the standard liver dedicated VCTE examination; SSM@100Hz: SSM with the novel spleen-dedicated VCTE examination; HCV, hepatitis C virus; HBV, hepatitis B virus; BMI, body mass index; NSBB, non-selective beta-blockers; HCC, hepatocellular carcinoma; INR, international normalized ratio; ALT, alanine amino-transferase; AST, aspartate amino-transferase; GGT, gamma glutamyl-transferase; MELD, model for End-Stage Liver Disease; LSPS, LSM-spleen diameter to platelet ratio score; Fib-4, Fibrosis-4 score; APRI, AST to platelets ratio index PSR, platelet count/spleen ratio; kPa, kiloPascals; IQR, inter quartile range; OR, odds ratio; CI, confidence interval at 95%; AUC, area under receiving operator characteristics curve.

Conflict of interest statement: Paul Calès was consultant for Echosens until January 2019.

Financial Support: The study has been sponsored by Echosens.

Clinical Trial number: NCT02180113

Acknowledgments:

Co-investigators: Alina Habic, Radu Badea, Jean-Baptiste Hiriart, Juliette Foucher, Sarah Shili, Sara Massironi, Etienne Pateu, Frédéric Oberti, Elton Dajti.

Echosens sponsor: Khalide Seddik, Hecham Azrak, Cécile Bastard, Aymeric Labourdette, Anne Llorca, Véronique Miette, Céline Fournier

Abstract

Background and Aims

Several non-invasive tests (NITs) have been developed to diagnose esophageal varices (EV), including the recent Baveno VI criteria to rule out high-risk varices (HRV). Spleen stiffness measurement (SSM) with the standard FibroScan® (SSM@50Hz) has been evaluated. However, the EV grading could be underestimated due to a ceiling threshold (75 kPa) of the SSM@50Hz. The aims were to evaluate SSM by a novel spleen-dedicated FibroScan® (SSM@100Hz) for EV diagnosis compared with SSM@50Hz, other validated NITs and Baveno VI criteria.

Methods

This prospective multicenter study consecutively enrolled patients with chronic liver disease; blood data, endoscopy, liver stiffness measurement (LSM), SSM@50Hz and SSM@100Hz were collected.

Results

Two-hundred and sixty patients met inclusion criteria. SSM@100Hz success rate was significantly higher than that of SSM@50Hz (92.5% vs 76.0%, $p < 0.001$). SSM@100Hz accuracy for the presence of EV (AUC=0.728) and HRV (AUC=0.756) was higher than in other NITs. SSM@100Hz AUC for large EV (0.782) was higher than SSM@50Hz (0.720, $p = 0.027$). AUC for HRV with SSM@100Hz (0.780) was higher than with LSM (0.615,

p<0.001). The spared endoscopy rate of Baveno VI criteria (8.1%) was significantly increased by the combination to SSM@50Hz (26.5%) or SSM@100Hz (38.9%, p<0.001 vs others). The missed HRV rate was, respectively, 0% and 4.7% for combinations.

Conclusions

SSM@100Hz is a new performant non-invasive marker for EV and HRV providing a higher accuracy than SSM@50Hz and other NITs. The combination of Baveno VI criteria and SSM@100Hz significantly increased the spared endoscopy rate compared to Baveno VI criteria alone or combined with SSM@50Hz.

Keywords: Liver stiffness measurement, Spleen stiffness measurement, Portal hypertension, Baveno VI criteria.

LAY SUMMARY

- A novel spleen-dedicated examination (SSM@100Hz) has recently been developed and found to have a better accuracy in detecting EV and large EV.
- A sequential algorithm to rule out HRV, starting with Baveno VI criteria and followed optionally by SSM@100Hz, allowed to spare more EGD compared to Baveno VI criteria alone or combined with standard SSM@50Hz.

INTRODUCTION

Variceal bleeding represents one of the most severe and life-threatening complications in chronic liver disease (CLD) ¹. The prevalence of esophageal varices (EV) among cirrhotic patients is about 50-60% ¹. The incidence of variceal bleeding is approximately 5% to 15% yearly, and variceal re-bleeding rate is 30% to 40% within the first 6 weeks ¹. Despite the clinical progress, the 6-week mortality associated with variceal bleeding is still in the order of

10 to 20%¹. Esophagogastroduodenoscopy (EGD) is the reference diagnostic tool for detecting and grading EV and for the recognition of indicators of at high-bleeding risk EV (HRV)². However, EGD is an invasive method with constraints and may lead to complications³. In addition, it is an expensive method and its use is limited to specialized clinical setting.

In the last decade, several authors tried to assess the presence and severity of portal hypertension (PH) by using non-invasive methods, among which liver stiffness measurement (LSM) proved to have a primary role^{4,5}. Along these lines, the recent 2015 Baveno VI consensus workshop⁶ highlighted the diagnostic accuracy of LSM in defining the presence of clinically significant PH (CSPH), EV and HRV. In particular, patients with LSM <20 kPa (assessed by vibration controlled transient elastography, VCTE) and a platelet count >150 G/l were considered very unlikely to have HRV (<5%), and EGD could be safely avoided.

Nevertheless, LSM have a poor correlation with portal pressure and its complications when hepatic venous pressure gradient (HVPG) is >10 mmHg⁷. Once this critical threshold is reached, portal-systemic collaterals develop and extra-hepatic factors contribute to increase HVPG⁸. Hence, at this stage, LSM might underestimate the PH severity and the risk of variceal bleeding.

Recently, spleen stiffness measurement (SSM)⁹⁻¹² has also been proposed as a non-invasive marker for the prediction of CSPH and EV. It has been postulated that SSM could overcome some of the limitations of LSM^{9,12}. Several authors found a good correlation between SSM by standard VCTE (SSM@50Hz) and PH degree, EV and the natural history of cirrhotic patients^{9,10,12}.

However, the spleen is stiffer than the liver and the use of the current VCTE examination dedicated to the liver on the spleen leads to overestimation of the SSM¹³. To overcome those limitations, a novel spleen-dedicated examination (SSM@100Hz) based on VCTE has recently been developed¹³ and found to have a better accuracy in detecting EV and large EV. The aim of the present study was to evaluate new SSM@100Hz as a surrogate non-invasive marker for the presence of EV, large EV and HRV in patients with CLD. Secondary objectives were (i) to compare the EV prediction by this new SSM@100Hz with the SSM@50Hz and other non-invasive tests (NITs), (ii) to evaluate the correlation between SSMs and HVPG, and (iii) to test whether SSM@100Hz might improve the Baveno VI criteria to better select patients for HRV screening by EGD.

PATIENTS AND METHODS

Study population

This is a multicenter European prospective study conducted in Bologna and Milan (Italy), Cluj (Romania), Angers, Bordeaux and Bondy (France) and London (United Kingdom); patients with CLD undergoing a VCTE examination and scheduled for EGD were prospectively and consecutively enrolled, according to the following criteria: Inclusion criteria were: CLD due to hepatitis virus C (HCV), hepatitis virus B (HBV) or alcoholic liver disease; 18-79 years old; health insurance; ultrasound (US) examination, blood examination, and EGD performed within 6 months of VCTE examination. Exclusion criteria were: consuming illness (HIV infection, malignancy); pacemaker or heart defibrillator; pregnancy; obese patients (body mass index (BMI) ≥ 35 kg/m²); ascites; previous endoscopic treatment of EV; serum aminotransferases ≥ 250 IU/l; ongoing non-selective β -blockers (NSBB) treatment at the time of the study; HCV or HBV treatment ongoing or ended within 2 months from inclusion, liver transplantation, acute alcoholic hepatitis, jaundice (defined by total

serum bilirubin ≥ 50 $\mu\text{mol/l}$) and hepatocellular carcinoma. This study was conducted in compliance with the Declaration of Helsinki and approved by the local Ethical Committee of each center and other national Competent Authority if required. The study was initially approved by the Ethics Committee of S.Orsola-Malpighi Hospital in Bologna (Italy, coordinating center). This study was also registered on ClinicalTrials.gov (NCT 02180113) in 2014. In 2015 the design of the study was modified before knowing the statistical results to account for the new definitions for compensated advanced CLD (cACLD) (defined as $\text{LSM} \geq 10$ kPa) and HRV provided by the Baveno VI Consensus Conference ⁶. All patients provided written informed consent before any inclusion procedure. A sub-group of 193 patients was previously reported for the development of the acquisition algorithm for SSM@100Hz¹³. This study follows the liver-FibroSTARD statements ¹⁴.

Study assessment

For each patient the following demographic and clinical characteristics were recorded: age, gender, body weight, height and BMI. Blood variables (platelet count, INR, AST, ALT, total bilirubin, creatinine) were obtained from each local laboratory. A standard ultrasound examination was performed by an experienced sonographer blinded to the other exams to measure the longitudinal spleen length and the mean portal vein velocity. According to published formula, LSM-longitudinal spleen diameter to platelet ratio score (LSPS) ¹⁵, platelet count/longitudinal spleen diameter ratio (PSR) ¹⁶, Lok-index ¹⁷, Fib-4 ¹⁸ and APRI ¹⁹ were calculated. In a single center (Bologna), HVPG was also measured ²⁰ and collected within 6 months from SSM and LSM. A standard EGD was performed by a senior or experienced operator blinded to the other exams. The endoscopic findings for EV were recorded as follows: grade of EV and presence of red signs. Patients were also categorized

according to the Baveno VI criteria²¹ and the recently published expanded Baveno VI criteria

22

Definitions

Outcomes - The main outcomes were: EV, large EV and HRV. The HRV were defined as large EV (grade 2 or 3 EV i.e. diameter $\geq 5\text{mm}$ ²³) or grade 1 EV with red signs according to Baveno VI consensus⁶.

The outcome measures were AUC for outcome diagnosis by NITs and HVPG, and two clinical descriptors for outcome diagnosis by algorithms as follows.

The spared EGD rate was calculated as the ratio between the number of patients with EGD that could be avoided, due to a low HRV risk according to the diagnostic test or algorithm, and the total number of patients.

The missed HRV rate was measured as the rate of patients with missed HRV either among the patients with HRV (privileged definition) or patients with spared EGD or all patients²⁴.

Diagnostic tests - Success rate: a successful LSM or SSM was defined by at least 10 or 8¹³, respectively, single valid measures obtained in a patient. The success rate refers to the rate of patients with successful LSM in the whole population. The lack of success was called failure.

Reliability is defined as diagnostic test measures having better accuracy according to precise patient characteristics. Thus, reliable LSM (for successful LSM only) was defined as LSM < 7 kPa or LSM > 7.1 kPa with inter-quartile range (IQR) < 30%²⁵. As reliability criteria are not yet defined for SSM, the largest subgroup comprised patients with successful SSM and reliable LSM.

Sub-populations - Four sub-populations were used according to the maximum of suitable stiffness results available in patients with available EGD: sub-population A with successful SSM@100Hz, used for SSM@100Hz evaluation, from which two sub-populations were

extracted; sub-population B with successful SSM@50Hz used for comparison of SSM@100Hz with SSM@50Hz, and sub-population C with successful and reliable LSM, used for comparison of SSM@100Hz and LSM. Finally, sub-population D included patients with successful and reliable LSM, successful SSM@50 and available platelets, used for Baveno VI criteria evaluation.

Liver and spleen stiffness measurement

LSM and SSM@50Hz procedure was performed as previously reported²⁶. The technical characteristics of the SSM@100Hz examination are detailed elsewhere¹³.

Statistical analysis

Continuous variables were reported as median [Q1-Q3] and categorical variables were reported as proportion (percentage). For group comparisons of categorical and continuous variables, Kruskal Wallis test and Wilcoxon's test were used, as appropriate. To compare categorical variables, Chi square test (unpaired samples) and McNemar's test (paired samples) were used as appropriate. Spearman's rank test was used for correlations among continuous variables. To evaluate the variables associated with the failure of SSM@100Hz and SSM@50Hz, a multivariate logistic regression was used: p values and odds ratio (OR) were reported. In order to measure the accuracy of the different NITs for EV, large EV or HRV presence, area under the receiver operator characteristic curve (AUC) was assessed. Paired Delong's test was used for the AUC comparison. In algorithm construction, a combined model was constructed for ruling-out HRV using first Baveno VI criteria and, consecutively, SSM using a cut-off for ruling-out HRV calculated with sensitivity at 95% in remaining patients, i.e. at high risk for HRV according to Baveno VI criteria. As various methods are currently used in the literature to calculate the rate of patients with HRV left

without EGD (missed HRV), we calculated this rate with all the three following calculations: the numerator is always the number of missed HRV and the denominator can be the total number of HRV ²⁷, or the number of spared endoscopy ²⁸ or the total number of patients ²⁸. According to a recent study, we privilege the first calculation. We selected for our study patients with a large spectrum of liver disease severity; therefore, in order to evaluate the impact of liver disease severity on test performance, we also applied the sequential model Baveno VI criteria and SSM@100Hz in two sub-groups of sub-population D defined by median MELD score. All statistical analyses were performed using Microsoft R Open 3.4.2, for Windows.

RESULTS

Patient characteristics

During the study period from September 2011 to January 2017, 403 patients with CLD were enrolled; 28 were excluded for protocol deviation. Among the remaining 375 enrolled patients, 91 (24.3%) patients did not undergo EGD within 6 months of SSM; among the remaining 284 patients, SSM@100Hz fully failed (no valid measurement) in 11 patients (2.9%) and did not reach the success criterion in further 13 patients (3.5%). A total of 260 patients were thus included in the core sub-population A (Figure 1). The bio-clinical characteristics of these 260 patients are presented in Table 1.

SSM descriptors

SSM@100Hz - Successful SSM@100Hz was obtained in 347 patients out of 375 (92.5%). A

multivariate logistic regression found the following independent predictors of SSM@100Hz failure:

longitudinal spleen diameter ($p=0.016$, OR: 0.733 [0.569-0.944]) and a higher BMI ($p=0.050$, OR: 1.136 [1.000-1.290]). Among the 260 patients with EGD within 6 months of successful SSM@100Hz (sub-population A), patients with EV had a median SSM@100Hz of 55.2 kPa [40.9-72.3] which was significantly higher ($p<0.001$) than that of patients without EV (39.7 kPa [27.6-49.6]). Among patients with EV, SSM@100Hz values of grade 2 EV (61.4 kPa [49.2-78.5]) were significantly higher ($p<0.001$) than in grade 1 (48.5 kPa [38.3-65.7]) but not significantly different ($p=0.328$) from grade 3 (78.3 kPa [68.2-88.0]) as shown in Figure 2A. The AUC of SSM@100Hz for EV presence was 0.728 (95% CI: 0.665-0.791) and for large EV (grade ≥ 2): 0.767 (0.700-0.834). SSM@100Hz in the 69 patients with HRV (65.0 kPa [51.6-80.1]) was significantly higher than in those without HRV (43.0 kPa [33.9-57.9], $p<0.001$). The AUC of SSM@100Hz for HRV presence was 0.756 (0.691-0.821).

SSM@50Hz - SSM@50Hz was successful in 285 out of 375 patients (76.0%) which was significantly lower than the success rate of SSM@100Hz (92.5%, $p<0.001$). A multivariate logistic regression found the following independent predictors of SSM@50Hz failure: a smaller longitudinal spleen diameter ($p<0.001$, OR: 0.764) and a smaller mean portal vein velocity ($p=0.010$, OR: 0.946). Out of the 260 patients with EGD within 6 months of successful SSM@100Hz (sub-population A), 222 patients also had a successful SSM@50Hz. In this sub-population B, SSM@50Hz was significantly higher ($p<0.001$) in patients with EV (65.9 kPa [48.0-75.0]) than in patients without EV (50.0 kPa [32.4-67.5]). In patients with EV, SSM@50Hz values were not significantly different between adjacent EV grades (Figure

2B). The AUC of SSM@50Hz was 0.672 (0.598-0.746) for EV presence, 0.720 (0.639-0.802) for large EV (grade ≥ 2) and 0.737 (0.665-0.809) for HRV presence.

SSM comparison - SSM@50Hz and SSM@100Hz were highly correlated (Spearman's $r=0.820$, $p<0.001$). AUC of SSM@100Hz and SSM@50Hz were not significantly different for EV presence ($p=0.113$), and HRV presence ($p=0.105$) as shown in Table 2. However, for the presence of large EV (grade ≥ 2), the AUC of SSM@100Hz (0.782 [0.709-0.855]) was significantly higher ($p=0.027$) than the AUC of SSM@50Hz (0.720 [0.639-0.802]).

SSM comparison with LSM and other NITs.

Out of the 260 cases with EGD within 6 months of successful SSM@100Hz (sub-population A), 225 patients had also a reliable LSM. Among patients with EV, LSM was not significantly different between adjacent EV grades (Figure 2C). The AUCs for the presence of EV and HRV were compared between SSM@100Hz, LSM and other NITs in Table 2 and detailed in Supplemental materials 1.

Combination with Baveno VI criteria

The comparison of the performances of the different methods to identify patients for whom EGD can be safely avoided (low risk for HRV) was conducted on the 185 patients with EGD within 6 months of successful SSM@100Hz or SSM@50Hz and reliable LSM and of platelet count. In this sub-population D, applying Baveno VI criteria, 15 out of 185 patients (8.1%) were classified at low risk for HRV (Table 3). Among them, none had HRV so that the missed HRV rate was 0% (regardless of the way to calculate it). In the remaining 170 patients identified as at high risk for HRV (using the Baveno VI criteria alone), we investigated if the consecutive use of SSM would help to safely spare more EGD. Indeed, SSM@100Hz and SSM@50Hz when tested alone with a cut-off for the detection of 95% of HRV, allowed to

spare more EGD when compared to Baveno VI criteria alone ($p < 0.001$). To do so, we identified, in this high HRV risk group, the cut-off for the detection of 95% of HRV (i.e. 95% sensitivity) at 40.1 kPa for SSM@50Hz and 41.3 kPa for SSM@100Hz. Table 3 compares the rate of spared EGD and of missed HRV. The sequential combination of SSM@100Hz to Baveno VI criteria spared further 30.8% of unneeded EGDs; thus, the total spared EGD rate was 38.9%. The missed HRV rate was 4.7% (using the total number of HRV as the denominator, i.e. the calculation based on sensitivity). No difference in spared EGD was found comparing SSM@100Hz alone with the combination Baveno VI criteria+SSM@100Hz (37.8% Vs 38.9%, $p = 0.480$). When the combination of Baveno VI criteria and SSM@50Hz was considered, a greater number of EGD were spared than with Baveno VI alone (26.5% vs 8.1%, $p < 0.001$) but it was significantly lower than with the combination of Baveno VI criteria and SSM@100Hz (26.5% vs 38.9%, $p < 0.001$). Figure 3 therefore proposes a new sequential diagnostic algorithm for the detection of patients at high risk of HRV. The superiority of the combined model Baveno VI+SSM@100Hz was highlighted also when dichotomizing the sub-population D for the severity of liver disease according to the median MELD score (Supplemental material 2). Additionally, we applied expanded Baveno VI criteria for trying to spare more EGD (Supplemental material 3), but the missed HRV rate of those criteria alone was too high (12.6%) precluding to determine a useful combination to SSM@100Hz.

SSM comparison with HVPG.

HVPG (available in 102 patients), which was significantly higher in patients with EV than in those without EV and different among EV grades ($p < 0.001$), was better correlated with SSM@100Hz values (Spearman's $r = 0.532$, $p < 0.001$) than SSM@50Hz (Figure 4). Additionally, we evaluated the accuracy of SSM@100Hz in detecting patients with CSPH

(78 out of 102, 76,5%) finding a best cut-off of 34.15 kPa with an AUC of 0.811 (95% CI: 0.672; 0.950); furthermore, for detecting patients with HVPG \geq 12mmHg the best cut-off was 44.95 kPa with an AUC of 0.782 (95%CI: 0.677; 0.887). The results of these comparisons are detailed in Supplemental material 4.

DISCUSSION

In the last decade, LSM and SSM by the standard VCTE liver dedicated examination (SSM@50Hz) were proposed as accurate diagnostic tools for EV diagnosis^{9,11,12}. The aims of the present study were the evaluation of a new spleen dedicated VCTE examination (SSM@100Hz) as surrogate non-invasive marker for the presence of HRV in patients with CLD and its comparison with other NITs to select patients for endoscopic screening of HRV.

In addition, we compared the new SSM@100Hz with standard SSM@50Hz.

First, SSM@100Hz showed a higher success rate than SSM@50Hz. Second, diagnostic accuracy of SSM@100Hz for EV, large EV and HRV presence was significantly higher than with most other NITs. Moreover, SSM@100Hz accuracy was significantly higher than SSM@50Hz for large EV (grade \geq 2). Then, the combination of Baveno VI criteria and SSM@100Hz for the diagnosis of HRV allowed to almost triple the spared EGD rate, without missing more than 5% of HRV, compared to Baveno VI criteria alone. Finally, cSSM@100Hz was more closely correlated to HVPG than SSM@50Hz.

Several studies identified SSM@50Hz as a good surrogate marker of PH^{9,10} and a good non-invasive test for EV presence and grading^{9,29,30}. In addition, for the evaluation of PH and EV grading, a better diagnostic accuracy for SSM compared to LSM has been demonstrated. This was attributed to the inability of LSM in evaluating the extra-hepatic component of PH that is present for high degree of PH (HVPG $>$ 10 mmHg)⁷.

In almost all the available studies done so far, SSM was performed with the same device used for LSM²⁹. As the spleen is significantly stiffer than the liver, the use of the standard VCTE liver dedicated device (SSM@50Hz) leads to SSM overestimation¹³. Moreover, most patients with severe PH reached upper detection limit for tissue stiffness of VCTE by FibroScan®, which is set at 75 kPa, thus potentially limiting its accuracy^{5,9,13}. To overcome this limitation, one monocentric study³¹ of patients with HCV related liver disease, using VCTE with an algorithm for SSM, was performed by simply expanding the range of stiffness values up to 150 kPa and reported a good accuracy for large EV. Recently, a spleen adapted version of VCTE (SSM@100Hz) was developed and subsequently tested in a pivotal study¹³, finding a greater accuracy for EV presence than SSM@50Hz. Indeed, in addition to the wider range stiffness values (from 5 to 100 kPa), the use of a higher shear wave frequency (100 Hz) and adapted measurement depths (25 to 55 mm) reduced the sources of overestimation by SSM@50Hz¹³.

In the present multicentric European study using the SSM@100Hz, the good diagnostic accuracy for EV presence was confirmed. Furthermore, regarding EV grading, we found SSM@50Hz values in agreement with those previously reported^{11,32} but without significant differences between EV grades. SSM@100Hz showed a greater accuracy for EV grading than SSM@50Hz and thus, it had a significant higher diagnostic accuracy for large EV presence (grade ≥ 2) than SSM@50Hz. Moreover, our results confirm previous studies^{9,31,33} that highlighted the greater diagnostic accuracy of SSM when compared to LSM, PSR, APRI test and LSPS, especially for large EV or HRV presence.

In the past, several authors tried to assess the performance of NITs for HRV with good results^{30,34,35}, in particular a recent meta-analysis stated the superiority of SSM@50Hz compared to LSM for HRV presence¹¹. Our findings are in contrast with a previous report³⁶ which found

a greater diagnostic accuracy of LSPS than SSM@50Hz for HRV presence. The difference with the present study could be explained by the use of SSM@100Hz¹³.

The Baveno VI consensus conference⁶ proposed new criteria for ruling-out the presence of HRV by the combination of LSM by VCTE and platelet count and, since then, several papers^{27,35,37-42} provided validation of those Baveno VI criteria. The limitation of the Baveno VI criteria⁶ is the low rate of spared EGDs (15-25%)^{37,38}. To date, one recent meta-analysis⁴³, merging 15 studies, documented that Baveno VI criteria for ruling out HRV were satisfied in 10-40% of patients and the rate of missed HRV among HRV varied from 0% to 9% with a pooled estimate rate at 4.0%. Another review, merging 13 studies, reported 9.6% of HRV prevalence, 2.1% of missed HRV rate (recalculated in²⁴) and 20.6% of spared EGD⁴⁴. Different calculations were used for missed HRV rate in the different studies. In our opinion, the missed HRV rate should be obtained using the number of patients with HRV as denominator because it corresponds to the test sensitivity which is the standard in test construction⁴⁵. In the present study, the spared EGD rate by the Baveno VI criteria (8.1%) were into the range of reported studies^{43,44} with a 0% missed HRV rate. The low rate of spared EGD in our population may be due to more severe CLD which resulted in a higher prevalence of large EV (20.8%) and HRV (26.5%). In our study CLD, instead of cACLD as recommended by Baveno VI⁶, was an inclusion criterion since the study protocol was finalized in 2011 (before 2015 Baveno VI workshop). However, cACLD (defined by LSM ≥ 10 kPa) was observed in 92.4% of our patients. This is also the reason why large EV, instead of HRV, was initially an outcome in the study protocol.

Moreover, since SSM@100Hz was the most accurate NIT for HRV presence, we tried to combine it with the Baveno VI criteria, in order to spare more unneeded EGDs. Using SSM@100Hz, with a cut-off ≤ 41.3 kPa, in addition to Baveno VI criteria, the spared EGD rate was significantly increased to 38.9%, while the missed HRV rate was $< 5\%$ in accordance

with the Baveno VI recommendation. A similar rate of spared EGD was reached using SSM@100Hz alone in all patients, thus the use of the sequential algorithm Baveno VI+SSM@100Hz proposed (Figure 3) could be debated; however, we support the sequential algorithm since clinically simpler. Thus, SSM@100Hz use is restricted to patients at high-risk according to Baveno VI criteria.

A possible explanation for SSM@100Hz greater performance in ruling out HRV when compared to Baveno VI criteria alone, which includes LSM, could be due to the fact that LSM is known to have a lower correlation with high degree of PH, if compared to SSM^{7,9}. Indeed, the correlation between LSM and PH is lost when HVPG >10 mmHg⁷. On the other hand, the HVPG correlation was good with SSM@50Hz, as previously demonstrated⁹, and significantly higher with SSM@100Hz in the present study. Thus, SSM, especially SSM@100Hz, can better reflect PH severity or its complications than LSM⁹ and, consequently, than Baveno VI criteria. In addition, according to our results, we confirmed the high accuracy of SSM@100Hz for detecting CSPH. Furthermore, SSM@100Hz overcomes the potential technical limitations of SSM@50Hz. In addition, the failure rate of SSM@100Hz (7.5%) was lower than the rates of SSM@50Hz (24.0%) and literature^{1,5}. Thus, the higher success rate of SSM@100Hz improve its spared EGD rate compared to SSM@50Hz also when we performed an intention to diagnose analysis ($p < 0.05$), as reported in Supplemental material 5. This good success rate could be attributable to the new dedicated VCTE examination for the spleen; indeed, the use of a 100Hz frequency appeared to be a good compromise between a sufficiently low shear wave length and a good tissue penetration tissue¹³. The only factors associated with SSM@100Hz failure were a smaller spleen longitudinal diameter and an higher BMI, the same as those reported^{9,12} for SSM@50Hz.

The main limitation of the present exploratory study is the lack of a validation population. However, prospective studies in the field of non-invasive diagnosis of HRV are

very rare; this characteristic, as well as the limitations due to the innovation of this device, precluded other methodological aspects such as validation population. Another limitation is the high rate of missing EGD (24.3%) data. Patients were enrolled at VCTE examination and scheduled for an EGD in the next 6 months; however, several patients did not show-up or refused to undergo the EGD after the enrollment, especially when they already had done one in the past 6-12 months. Furthermore, HCV infection was prevalent in our population since the study protocol was designed in a pre-DAA era and HCV was the most prevalent cause of CLD in Italy and Romania ⁴⁶. Moreover, we excluded NAFLD and obese patients since we aimed to perform this pivotal study in best standardized conditions. Indeed, a validation in population with NASH will need a separate study given the specific cut-offs of elastography in NAFLD. Furthermore, a high failure rate of LSM was expected with M probe in these patients and XL probe wasn't considered in this study.

On the other hand, this study has several strengths. First, to our knowledge, this is the first fully prospective study devoted on Baveno VI criteria since previous studies had retrospective recruitment and/or design. Second, this was a multicenter study of tertiary centers including a large number of patients. Third, one can argue that patients were not selected as cACLD but as CLD. This difference provided the advantage of a prevalence of HRV sufficiently high (26.5%). Indeed, 8 out 13 previous studies had a HRV prevalence <10% and the mean HRV prevalence was 9.6% ⁴⁴. This precluded to evaluate performance of Baveno VI criteria in adequate methodological conditions. Therefore, the HRV prevalence should be >10% ²⁴. Moreover, as patient selection according to severity of the underlying liver disease is concerned, we applied our Baveno VI and SSM@100Hz model considering two groups defined by the median MELD score in the sub-population D (Supplemental material 1); accordingly, we found in both groups that the combination with SSM@100Hz significantly improved the rate of EGD spared compared to Baveno VI criteria (p<0.001).

Additionally, when we considered expanded Baveno VI criteria to spare more EGD, we observed a too high rate of missed HRV (12.6%). This precluded a combination to SSM@100Hz.

In conclusion, the new SSM@100Hz has a greater accuracy for the HRV presence than other NITs. A sequential algorithm to rule out HRV, starting with Baveno VI criteria and followed optionally by SSM@100Hz, allowed to spare more EGD compared to Baveno VI criteria alone or combined with standard SSM@50Hz, while keeping missed HRV rate <5%.

REFERENCES

1. Garcia-Tsao G, Abraldes JG, Berzigotti A, Bosch J. Portal hypertensive bleeding in cirrhosis: Risk stratification, diagnosis, and management: 2016 practice guidance by the American Association for the study of liver diseases. *Hepatology*. 2017;65:310–335.
2. Garcia-Tsao G, Sanyal AJ, Grace ND, Carey WD, Practice Guidelines Committee of American Association for Study of Liver Diseases, Practice Parameters Committee of American College of Gastroenterology. Prevention and management of gastroesophageal varices and variceal hemorrhage in cirrhosis. *Am J Gastroenterol*. 2007;102:2086–102.
3. Eisen GM, Baron TH, Dominitz JA, et al. Complications of upper GI endoscopy. *Gastrointest Endosc*. 2002;55:784–793.
4. Clinical Practice Guidelines EASL-ALEH Clinical Practice Guidelines : Non-invasive tests for evaluation of liver disease severity and prognosis European Association for the Study of the Liver , Clinical Practice Guidelines. 2015;63:237–264.
5. Berzigotti A. Non invasive evaluation of portal hypertension using ultrasound elastography. *J Hepatol*. 2017; 67:399-411.
6. de Franchis R, Baveno VI Faculty. Expanding consensus in portal hypertension: Report of the Baveno VI Consensus Workshop: Stratifying risk and individualizing care for portal

hypertension. *J Hepatol.* 2015;63:743–52.

7. Vizzutti F, Arena U, Romanelli RG, et al. Liver stiffness measurement predicts severe portal hypertension in patients with HCV-related cirrhosis. *Hepatology.* 2007;45:1290–7.

8. Bosch J, Navasa M, Garcia-Pagán JC, DeLacy AM, Rodés J. Portal hypertension. *Med Clin North Am.* 1989;73:931–53.

9. Colecchia A, Montrone L, Scaiola E, et al. Measurement of spleen stiffness to evaluate portal hypertension and the presence of esophageal varices in patients with HCV-related cirrhosis. *Gastroenterology.* 2012;143:646–54.

10. Colecchia A, Colli A, Casazza G, et al. Spleen stiffness measurement can predict clinical complications in compensated HCV-related cirrhosis: A prospective study. *J Hepatol.* 2014;60:1158–1164.

11. Ma X, Wang L, Wu H, et al. Spleen Stiffness Is Superior to Liver Stiffness for Predicting Esophageal Varices in Chronic Liver Disease: A Meta-Analysis. *PLoS One.* 2016;11:e0165786.

12. Stefanescu H, Grigorescu M, Lupsor M, et al. Spleen stiffness measurement using Fibroscan for the noninvasive assessment of esophageal varices in liver cirrhosis patients. *J Gastroenterol Hepatol.* 2011;26:164–70.

13. Bastard C, Miette V, Calès P, Stefanescu H, Festi D, Sandrin L. A Novel FibroScan Examination Dedicated to Spleen Stiffness Measurement. *Ultrasound Med Biol.* 2018;44:1616–1626.

14. Boursier J, de Ledingham V, Poynard T, et al. An extension of STARD statements for reporting diagnostic accuracy studies on liver fibrosis tests: The Liver-FibroSTARD standards. *J Hepatol.* 2015;62:807–815.

15. Kim BK, Han K-H, Park JY, et al. A liver stiffness measurement-based, noninvasive prediction model for high-risk esophageal varices in B-viral liver cirrhosis. *Am J*

Gastroenterol. 2010;105:1382–90.

16. Giannini E, Botta F, Borro P, et al. Platelet count/spleen diameter ratio: proposal and validation of a non-invasive parameter to predict the presence of oesophageal varices in patients with liver cirrhosis. *Gut.* 2003;52:1200–5.

17. Lok ASF, Ghany MG, Goodman ZD, et al. Predicting cirrhosis in patients with hepatitis C based on standard laboratory tests: results of the HALT-C cohort. *Hepatology.* 2005;42:282–92.

18. Sterling RK, Lissen E, Clumeck N, et al. Development of a simple noninvasive index to predict significant fibrosis in patients with HIV/HCV coinfection. *Hepatology.* 2006;43:1317–25.

19. Lebensztejn DM, Skiba E, Sobaniec-Lotowska M, Kaczmarski M. A simple noninvasive index (APRI) predicts advanced liver fibrosis in children with chronic hepatitis B. *Hepatology.* 2005;41:1434–5.

20. Bosch J, Abraldes JG, Berzigotti A, García-Pagan JC. The clinical use of HVPG measurements in chronic liver disease. *Nat Rev Gastroenterol Hepatol.* 2009;6:573–582.

21. de Franchis R, Baveno VI Faculty. Expanding consensus in portal hypertension. *J Hepatol.* 2015;63:743–752.

22. Augustin S, Pons M, Maurice JB, et al. Expanding the Baveno VI criteria for the screening of varices in patients with compensated advanced chronic liver disease. *Hepatology.* 2017;00:1–9.

23. Calès P, Oberti F, Bernard-Chabert B, Payen J-L. Evaluation of Baveno recommendations for grading esophageal varices. *J Hepatol.* 2003;39:657–9.

24. Calès P, Buisson F, Ravaioli F, et al. How to clarify the Baveno VI criteria for ruling out varices needing treatment by noninvasive tests. *Liver Int.* 2018; 39:49-53.

25. Boursier J, Zarski J-P, de Ledinghen V, et al. Determination of reliability criteria for liver

stiffness evaluation by transient elastography. *Hepatology*. 2013;57:1182–91.

26. Sandrin L, Fourquet B, Hasquenoph J-M, et al. Transient elastography: a new noninvasive method for assessment of hepatic fibrosis. *Ultrasound Med Biol*. 2003;29:1705–13.

27. Calès P, Sacher-Huvelin S, Valla D, et al. Large oesophageal varice screening by a sequential algorithm using a cirrhosis blood test and optionally capsule endoscopy. *Liver Int*. 2018;38:84–93.

28. Augustin S, Pons M, Maurice JB, et al. Expanding the Baveno VI criteria for the screening of varices in patients with compensated advanced chronic liver disease. *Hepatology*. 2017;66:1980–1988.

29. Colecchia A, Marasco G, Taddia M, et al. Liver and spleen stiffness and other noninvasive methods to assess portal hypertension in cirrhotic patients: a review of the literature. *Eur J Gastroenterol Hepatol*. 2015;27:992–1001.

30. Colecchia A, Ravaoli F, Marasco G, et al. A combined model based on spleen stiffness measurement and Baveno VI criteria to rule out high-risk varices in advanced chronic liver disease. *J Hepatol*. 2018;69:308-317

31. Calvaruso V, Bronte F, Conte E, Simone F, Craxi A, Di Marco V. Modified spleen stiffness measurement by transient elastography is associated with presence of large oesophageal varices in patients with compensated hepatitis C virus cirrhosis. *J Viral Hepat*. 2013;20:867–874.

32. Singh S, Eaton JE, Murad MH, Tanaka H, Iijima H, Talwalkar JA. Accuracy of spleen stiffness measurement in detection of esophageal varices in patients with chronic liver disease: systematic review and meta-analysis. *Clin Gastroenterol Hepatol*. 2014;12:935–45.e4.

33. Sharma P, Kirnake V, Tyagi P, et al. Spleen stiffness in patients with cirrhosis in

predicting esophageal varices. *Am J Gastroenterol*. 2013;108:1101–1107.

34. Kim HY, Jin EH, Kim W, et al. The Role of Spleen Stiffness in Determining the Severity and Bleeding Risk of Esophageal Varices in Cirrhotic Patients. *Medicine (Baltimore)*.

2015;94:e1031.

35. Abraldes JG, Bureau C, Stefanescu H, et al. Noninvasive tools and risk of clinically significant portal hypertension and varices in compensated cirrhosis: The “Anticipate” study.

Hepatology. 2016;64:2173–2184.

36. Stefanescu H, Radu C, Procopet B, et al. Non-invasive menage a trois for the prediction of high-risk varices: stepwise algorithm using lok score, liver and spleen stiffness. *Liver Int*.

2015;35:317–325.

37. Maurice JB, Brodtkin E, Arnold F, et al. Validation of the Baveno VI criteria to identify low risk cirrhotic patients not requiring endoscopic surveillance for varices. *J Hepatol*.

2016;65:899–905.

38. Jangouk P, Turco L, De Oliveira A, Schepis F, Villa E, Garcia-Tsao G. Validating, deconstructing and refining Baveno criteria for ruling out high-risk varices in patients with compensated cirrhosis. *Liver Int*. 2017; 37:1177-1183.

39. Llop E, Lopez M, de la Revilla J, et al. Validation of non invasive methods to predict the presence of gastroesophageal varices in a cohort of patients with compensated advanced chronic liver disease. *J Gastroenterol Hepatol*. 2017; 32:1867-1872.

40. Silva MJ, Duarte P, Mendes M, et al. Baveno VI Recommendation on Avoidance of Screening Endoscopy in Cirrhotic Patients based on Liver Elastography and Platelet Count –

Are We There Yet? *J Hepatol*. 2016;64:S731.

41. Sousa M, Fernandes S, Proença L, et al. The Baveno VI criteria for predicting esophageal varices: validation in real life practice. *Rev Española Enfermedades Dig*. 2017;109.

42. Bae J, Sinn DH, Kang W, et al. Validation of the Baveno VI and the expanded Baveno VI

criteria to identify patients who could avoid screening endoscopy. *Liver Int.* 2018; 38:1442-1448.

43. Marot A, Trépo E, Doerig C, Schoepfer A, Moreno C, Deltenre P. Liver stiffness and platelet count for identifying patients with compensated liver disease at low risk of variceal bleeding. *Liver Int.* 2017;37:707–716.

44. Roccarina D, Rosselli M, Genesca J, Tsochatzis EA. Elastography methods for the non-invasive assessment of portal hypertension. *Expert Rev Gastroenterol Hepatol.* 2018;12:155–164.

45. Cassinotto C, Charrie A, Mouries A, et al. Liver and spleen elastography using supersonic shear imaging for the non-invasive diagnosis of cirrhosis severity and oesophageal varices. *Dig Liver Dis.* 2015;47:695–701.

46. Deuffic-Burban S, Deltenre P, Buti M, et al. Predicted effects of treatment for HCV infection vary among European countries. *Gastroenterology.* 2012;143:974–85.e14.

Figure legend

Figure 1. Study flow chart. Abbreviations: EGD: esophagogastroduodenoscopy, SSM@100Hz: new spleen stiffness measurement with transient elastography, LSM: liver stiffness measurement, SSM@50Hz: standard spleen stiffness measurement with transient elastography.

Figure 2. Box plots of (A) SSM@100Hz (n=260); (B) SSM@50Hz (n=222) and (C) LSM (n=225) versus esophageal varices grade assessed by EGD. Abbreviations: EGD: esophagogastroduodenoscopy, SSM@100Hz: new spleen stiffness measurement with transient elastography, LSM: liver stiffness measurement, SSM@50Hz: standard spleen stiffness measurement with transient elastography.

Figure 3. New algorithm combining Baveno VI and SSM@100Hz for ruling-out patients at risk of HRV (* by VCTE). Abbreviations: CLD: chronic liver disease, HRV: high-bleeding risk esophageal varices, EGD: esophagogastroduodenoscopy, SSM@100Hz: new spleen stiffness measurement with transient elastography, LSM: liver stiffness measurement, PLT: platelet count.

Figure 4. Correlation between HVPG and SSM@100Hz (r_s : 0.532) or SSM@50Hz (r_s : 0.363, $p=0.008$). Abbreviations: SSM@100Hz: new spleen stiffness measurement with transient elastography; SSM@50Hz: standard spleen stiffness measurement with transient elastography; HVPG: hepatic venous pressure gradient.

Table 1. Demographics and clinical data of patients enrolled (sub-population A).

Characteristics	N	Median [Q1-Q3] or n (%)
Male	260	169 (65)
Female	260	91 (35)
Age (years)	260	59 [51-68]
BMI (kg/m ²)	260	26.0 [23.7-28.6]
ALT (IU/L)	251	51 [29-88]
AST (IU/L)	242	56 [36-93]
Platelets (G/l)	254	101 [77-142]
Grade of EV	260	
• G0		95 (36.5)
• G1		111 (42.7)
• G2		42 (16.2)
• G3		12 (4.6)
Cherry spots	260	29 (11.2)
Red wale marks	260	42 (16.2)
Presence of HRV	260	69 (26.5)
Spleen longitudinal length (cm)	260	13.6 [11.9-15.5]
Aetiology	260	
• HCV		155 (59.6)
• HBV		19 (7.3)
• Alcohol		79 (30.4)
• Others		7 (2.7)
MELD score	204	9.2 [7.9-11.7]
LSM (kPa) §	225	23.4 [15.4-35.3]
SSM@100Hz (kPa) *	260	48.0 [36.6-66.1]
SSM@50Hz (kPa) *	222	60.0 [41.3-74.6]
HVPG (mmHg)	102	13 [11-15]

Abbreviations: IQR, inter quartile range; BMI, body mass index; ALT, alanine amino-transferase; AST, aspartate amino-transferase; EV: esophageal varices, HRV: high-bleeding risk esophageal varices; HCV, hepatitis C virus; HBV, hepatitis B virus; HVPG, hepatic venous pressure gradient; LSM: liver stiffness measurement; SSM spleen stiffness measurement; MELD, model for end-stage liver disease; kPa, kilopascal.

§ in patients with reliable LSM

* in patients with successful SSM

Table 2. AUC (CI 95%) of SSM@100Hz for EV presence, large EV and HRV presence compared to SSM@50Hz, LSM, HVPG, and other non-invasive tests (sub-population A).

Comparator ^N	EV		Large EV		HRV		p [§]	p [§]		
	Comparator [¶]	SSM@100Hz	Comparator [¶]	SSM@100Hz	Comparator [¶]	SSM@100Hz				
SSM@50Hz	222	0.672 (0.598 - 0.746)	0.709 (0.639 - 0.779)	0.113	0.720 (0.639 - 0.802)	0.782 (0.709 - 0.855)	0.027	0.737 (0.665 - 0.809)	0.778 (0.709 - 0.846)	0.105
LSM	225	0.712 (0.642 - 0.782)	0.742 (0.676 - 0.808)	0.424	0.618 (0.527 - 0.709)	0.811 (0.749 - 0.872)	<0.001	0.615 (0.532 - 0.697)	0.780 (0.714 - 0.846)	<0.001
LSPS	191	0.718 (0.640 - 0.795)	0.749 (0.678 - 0.821)	0.435	0.654 (0.562 - 0.746)	0.784 (0.714 - 0.854)	0.010	0.637 (0.549 - 0.724)	0.760 (0.685 - 0.834)	0.007
Lok-index	198	0.687 (0.606 - 0.769)	0.736 (0.663 - 0.810)	0.273	0.723 (0.648 - 0.799)	0.743 (0.667 - 0.819)	0.686	0.704 (0.625 - 0.784)	0.721 (0.644 - 0.799)	0.732
PSR	219	0.299 (0.223 - 0.375)	0.731 (0.661 - 0.800)	<0.001	0.285 (0.210 - 0.361)	0.755 (0.684 - 0.825)	<0.001	0.323 (0.245 - 0.401)	0.737 (0.666 - 0.808)	<0.001
Fib-4	236	0.598 (0.516 - 0.679)	0.713 (0.645 - 0.782)	0.009	0.623 (0.547 - 0.700)	0.764 (0.694 - 0.833)	0.005	0.609 (0.534 - 0.684)	0.743 (0.673 - 0.813)	0.005
APRI	235	0.549 (0.465 - 0.632)	0.712 (0.643 - 0.780)	<0.001	0.588 (0.507 - 0.669)	0.767 (0.697 - 0.836)	<0.001	0.555 (0.476 - 0.633)	0.746 (0.676 - 0.816)	<0.001
HVPG	102	0.760 (0.663 - 0.857)	0.761 (0.667 - 0.855)	0.979	0.764 (0.652 - 0.877)	0.822 (0.740 - 0.905)	0.343	0.749 (0.643 - 0.854)	0.835 (0.757 - 0.913)	0.109

Abbreviations: AUC: area under receiving operator characteristics curve; CI: confidence interval; N: number; EV: esophageal varices; HRV: high-bleeding risk esophageal varices; IQR, inter quartile range; LSPS: LSM-spleen diameter to platelet ratio score; PSR: platelet count/spleen ratio; Fib-4: Fibrosis-4 score; APRI: AST to platelets ratio index; HVPG: hepatic venous pressure gradient; LSM: liver stiffness measurement; SSM@100Hz: SSM with the novel spleen-dedicated VCTE examination; SSM@50Hz: SSM with the standard liver dedicated VCTE examination.

[¶] The result is variable since corresponding to the maximum size of the group with comparator available

[§] Delong's test

Table 3. Comparison of diagnostic performance of Baveno VI, SSM@100Hz, SSM@50Hz, Baveno VI + SSM@100Hz and Baveno VI + SSM@50Hz for ruling-out HRV. Sub-population D including 185 patients.

	Baveno VI	SSM@100Hz	<i>p</i> [¶]	SSM@50Hz	<i>p</i> [¶]	<i>p</i> [°]	Baveno VI + SSM@100Hz*	<i>p</i> [¶]	<i>p</i> [°]	Baveno VI + SSM@50Hz§	<i>p</i> [¶]	<i>p</i> [°]
Spared endoscopy	15 / 185 8.1 % (4.6%-13.0%)	70 / 185 37.8 % (30.8%-45.2%)	<0.001	44 / 185 23.8 % (17.8%-30.6%)	<0.001	<0.001	72 / 185 38.9 % (31.9%-46.3%)	<0.001	0.480	49 / 185 26.5 % (0.3%-33.5%)	<0.001	<0.001
Missed HRV / number of HRV	0 / 43 0 % (0%-6.7%)	2 / 43 4.7 % (0.6%-15.8%)	0.480	2 / 43 4.7 % (0.6%-15.8%)	0.480	1.000	2 / 43 4.7 % (0.6%-15.8%)	0.480	1.000	2 / 43 4.7 % (0.6%-15.8%)	1.000	1.000
Missed HRV / number of spared endoscopy	0 / 15 0 % (0%-18.1%)	2 / 70 2.9 % (0.3%-9.9%)	1.000	2 / 44 4.5 % (0.6%-15.5%)	0.989	1.000	2 / 72 2.8 % (0.3%-9.8%)	1.000	1.000	2 / 49 4.1 % (0.5%-14.0%)	1.000	1.000
Missed HRV / all patients	0 / 185 0 % (0%-1.6%)	2 / 185 1.1 % (0.1%-3.9%)	0.480	2 / 185 1.1 % (0.1%-3.9%)	0.480	1.000	2 / 185 1.1 % (0.1%-3.9%)	0.480	1.000	2 / 185 1.1 % (0.1%-3.9%)	1.000	1.000

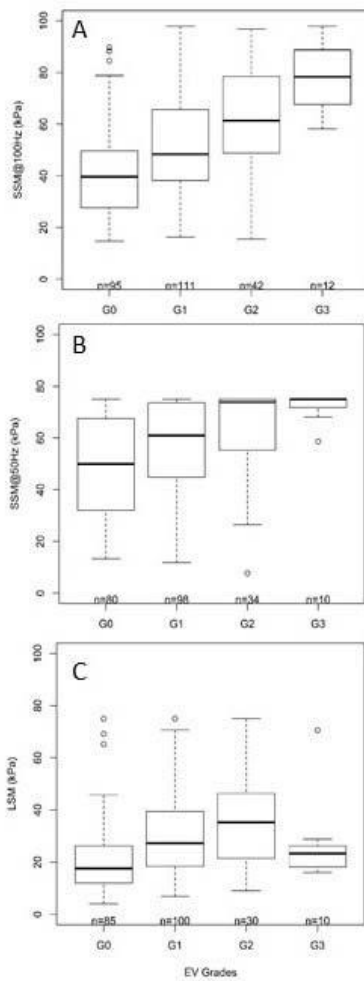
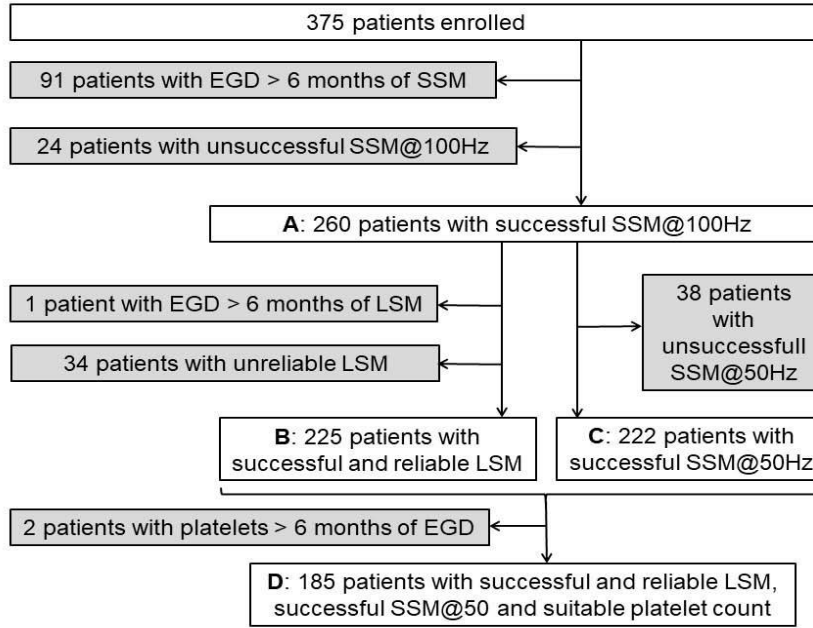
[¶] *p*-value of the proportion comparison with Baveno VI alone by McNemar test (except for missed HRV among spared endoscopy: Chi² test)

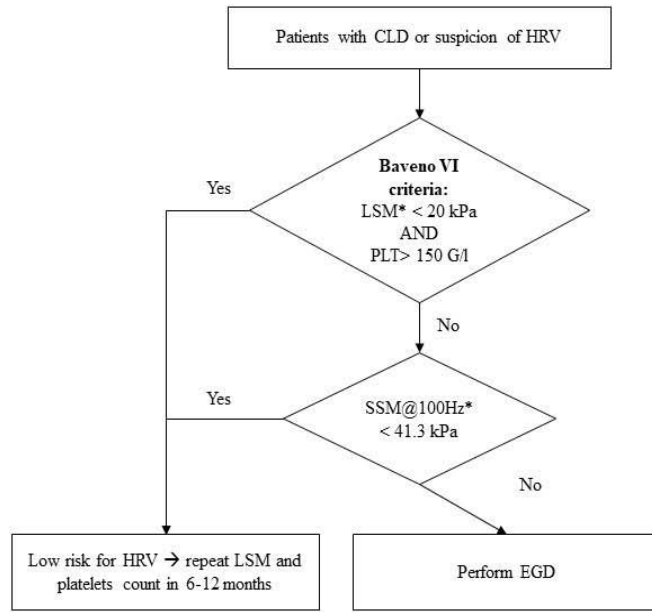
[°] *p*-value of the proportion comparison with SSM@100Hz by McNemar test (except for missed HRV among spared endoscopy: Chi² test)

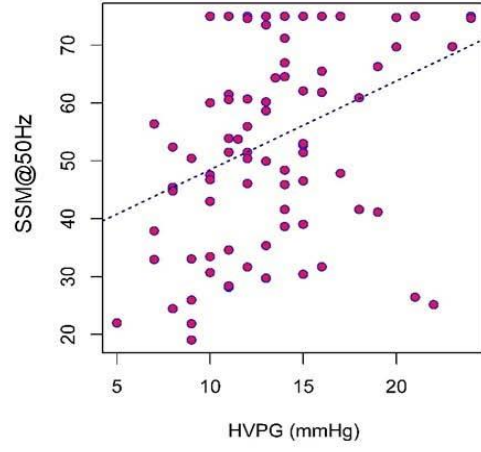
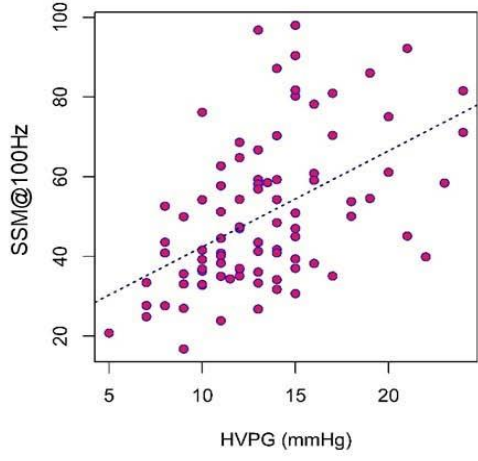
[¶] *p*-value of the proportion comparison with Baveno VI+SSM@100Hz by McNemar test (except for missed HRV among spared endoscopy: Chi² test)

* The cut-off of 41.3 kPa was calculated on the sub-group of 170/185 patients with available SSM@100Hz and at high-risk for HRV according to Baveno VI by setting sensitivity of SSM@100Hz for HRV at 95 %.

§ The cut-off of 40.1 kPa was calculated on the sub-group of 170/185 patients with available SSM@50Hz and at high-risk for HRV according to Baveno VI by setting sensitivity of SSM@50Hz for HRV at 95 %.







What's in Metabolomics for Alcoholic Liver Disease?

Alina M. Suciu^{1,2}, Dana A. Crisan³, Bogdan D. Procopet^{1,2}, Corina I. Radu^{1,2}, Carmen Socaciu⁴, Marcel V. Tantau^{1,2}, Horia O. Stefanescu², Mircea Grigorescu¹

1) 3rd Medical Clinic, Iuliu Hatieganu University of Medicine and Pharmacy;
2) Hepatology Unit, Regional Institute of Gastroenterology and Hepatology Cluj;
3) 5th Medical Clinic, Iuliu Hatieganu University of Medicine and Pharmacy;
4) RTD Center for Applied Biotechnology. BIODIATECH, SC Proplanta, Cluj-Napoca, Romania

Address for correspondence:

Horia O. Stefanescu
Regional Institute of Gastroenterology and Hepatology Cluj,
19-21 Croitorilor Street,
Cluj-Napoca, Romania
horia.stefanescu@irgh.ro

Received: 15.10.2017

Accepted: 14.12.2017

ABSTRACT

Background & Aims: Current management of alcoholic liver disease (ALD), especially for alcoholic hepatitis (AH) is still driven by liver biopsy. Therefore, the identification of novel and accurate noninvasive biomarkers for the diagnosis and assessment of severity is important. Metabolomics, because it unravels changes closest to the phenotype, may represent the key for novel biomarkers. The aim of this study was to identify and characterize potential metabolomic biomarkers for diagnosis, staging and severity assessment of ALD.

Methods: 30 consecutive ALD patients and 10 healthy controls were included in this proof-of-concept cross-sectional study. Baseline assessment consisted in evaluation of Maddrey's Discriminant Function, Model for End-Stage Liver Disease (MELD) and ABIC scores as well as ASH-Test (Fibromax) as a surrogate for the confirmatory diagnosis of AH in suggestive clinical and biologic settings. Additionally, SOP metabolomics and lipidomics were performed from serum samples by liquid chromatography mass-spectrometry analysis.

Results: From the 127 and 135 serum/urine candidate metabolites initially identified, only 11/5 metabolites were characteristic for ALD patients. None of them correlated with alcohol intake, and only 5/1 metabolites could differentiate cirrhotic from non-cirrhotic patients. Of those, N-Lauroglycine (NLG) was the best for identifying cirrhosis (100% sensitivity and 90% negative predictive value, NPV) and decatrienoic acid (DTEA) was the best for assessing disease severity (evaluated by ABIC score) with 100% sensitivity and 100% NPV.

Conclusion: Due to their high NPV, NLG and DTEA could be used in conjunction in ALD patients to exclude cirrhosis or a severe disease. If further validated, they could become biomarkers for better management and risk assessment in ALD.

Key words: metabolomics – lipidomics – alcoholic liver disease – noninvasive.

Abbreviations: ABIC: age-bilirubin-INR-cholesterol; ALD: alcoholic liver disease; AH: alcoholic hepatitis; AST/ALT: aspartate/alanine aminotransferase; DF: Maddrey's Discriminant Function; DTEA: decatrienoic acid; LC-MS: liquid chromatography–mass spectrometry; LRD: liver related clinical decompensation; MELD: Model for End-Stage Liver Disease; NLG: N-Lauroglycine; NPV: negative predictive value; PPV: positive predictive value; PT: prothrombin time; Se: sensibility; Sp: specificity.

INTRODUCTION

Alcoholic liver disease (ALD) represents a wide spectrum of liver pathology, beginning with fatty liver, present in almost all heavy alcohol drinkers and mostly asymptomatic, and continuing with progressive fibrosis that eventually leads to cirrhosis [1, 2]. In the Western world, alcohol is the leading cause of cirrhosis and its complications: portal hypertension, ascites,

spontaneous bacterial peritonitis, hepatic encephalopathy, variceal bleeding and hepato-renal syndrome [3]. However, ALD is marked by the spectrum of alcoholic hepatitis (AH), which may develop anytime during the natural history. Alcoholic hepatitis is a clinical syndrome characterized by rapid hepatic decompensation (jaundice, coagulation impairment and encephalopathy) that causes death in up to 50% of patients in the absence of treatment [4]. Since 20–40% of alcoholics develop fibrosis and 10–22% will eventually progress to cirrhosis, of whom 1.5–2% will develop hepatocellular carcinoma every year [5], it is very important to diagnose and treat early and accurately ALD and alcohol misuse. In none of the stages of ALD are clinical and biological changes characteristic, and the clinical scenario of AH is very similar to

the one of severe cirrhotic decompensation of another etiology. In this context, liver biopsy remains the gold standard for diagnosis, mainly for AH, despite its invasiveness and relatively high cost. Therefore, the identification of novel and accurate noninvasive biomarkers for the diagnosis and assessment of severity is of utmost importance.

The metabolome represents the endpoint of the omics cascade and it is also the closest point to the phenotype [7, 8]. Metabolomics is a rapidly evolving field, which identifies characteristic changes in the metabolome associated with any physiological perturbations. The use of metabolomics in ALD represents a powerful means not only to unravel the molecular mechanism of its pathogenesis, but also to identify the earliest biomarkers [9, 10]. The earliest change in ALD pathogenesis is the accumulation of free fatty acids in the liver. In this context, the majority of new studies are focused on the understanding of ALD pathogenesis by identifying the pathways involved in fatty acid metabolism.

The aim of this proof-of-concept study was to identify and further characterize the potential metabolomic biomarkers for the diagnosis, staging and severity assessment of ALD.

METHODS

The study was designed as a cross-sectional one, in full accordance with the 2000 review of Human Rights Declaration and was approved by the Ethical Committee of the Cluj-Napoca Regional Institute of Gastroenterology and Hepatology. All participants gave their informed consent prior to inclusion into the study.

Patients

Consecutive patients previously diagnosed with different stages of ALD, aged 18–80 years and with ongoing alcohol consumption (> 20 g/day for women and > 40 g/day for men) were included. Patients with cirrhosis have been also previously diagnosed based on unequivocal clinical, biological, imaging and endoscopic features.

Additionally, consecutive subjects without liver disease and without significant alcohol intake (<20 g/day for women and <40 g/day for men) were included and were considered as control group.

Baseline assessment

Fasting serum, plasma and urine samples were collected from all participants for metabolomic analysis (see below).

Patients with ALD underwent in the same day a full laboratory work-up assessing liver function tests, coagulation, platelets count, serum lipids and glucose. ASH-Test (BioPredictive, France) was performed in all patients in order to evaluate the level of necro-inflammation and was used as a surrogate for AH diagnosis in suggestive clinico-biologic settings. Demographic and anthropometric data were noted. Clinical examination, abdominal ultrasound and liver stiffness measurements were performed.

For the evaluation of the severity of ALD the following scores were calculated:

- Maddrey's Discriminant Function (DF), which depends on bilirubin levels and PT: a cut-off value ≥ 32 is correlated

with a more severe outcome, lack of response to corticotherapy and death in almost 50% of the patients [11];

- Model for End-Stage Liver Disease (MELD), which uses bilirubin, INR and creatinine to assess liver disease severity and predict mortality [12];

- ABIC score, which integrates age, bilirubin level, INR, creatinine, being able to predict 90 days mortality [14]. ABIC allows mortality risk stratification into low, moderate or high.

Standard Operation Procedure (SOP) Metabolomics

Blood sample preparation

The serum samples were diluted (1:5) with methanol, vortexed, ultrasonicated at 4°C for 5 minutes and centrifuged at 15 000g for 15 minutes to remove particulates and proteins by precipitation. The supernatant was collected, filtered through 0.2 μm filters and kept in the deep freezer until analysis.

Liquid chromatography mass spectrometry analysis

Aliquots of 5 μl of each sample were subjected to chromatography on a Bruker DaltonicsMaXis Impact device with a Thermo Scientific HPLC UltiMate 3000 system with a quaternary pump delivery system DionexUltiMate and MS detection, on C18 reverse-phase column [5 μm , 2.1 x 100 mm], (Acclaim, Dionex) maintained at 40°C.

Mobile phase: A - water containing 0.1% formic acid; B - acetonitrile containing 0.1% formic acid. Gradient: 95% A:5% B with linear gradient to 85% A: 15% B from 0 to 3 min, followed by linear gradient to 50% A: 50% B at 6 min, linear gradient to 5% A: 95% B at 9 min, isocratic on 5% A: 95% B for 6 min and then returned to the initial condition 95% A: 5% B at 15.1 min for 5 min. Flow rate, 0.500ml/min.

Mass spectrometry was performed on a Bruker Daltonics MaXis Impact Q-TOF operating in positive ion mode. The mass range was set between 50–1000 m/z. The nebulizing gas pressure was set at 2.8 bar, the drying gas flow at 12 L/min, the drying gas temperature at 300°C. Before each chromatographic run, a calibrant solution of sodium formate was injected.

The control of the instrument and data processing were done using TofControl 3.2 and Data Analysis 4.2 (Bruker Daltonics).

SOP lipidomics

Blood sample preparation (lipid extraction)

Lipids were extracted from 0.1 ml serum diluted with 0.2 ml methanol, then vortexed for 20 s, next 1.66 ml chloroform was added and vortexed for 20 s, and an additional of 0.1 ml water was added to induce phase separation. The samples obtained were vortexed for 20 s, then were subjected to centrifugation at 8000 rpm for 10 min, then the lipid phase was collected and evaporated. Samples were reconstituted in 500 μl of acetonitrile/isopropyl alcohol/water (65:30:5) volume.

Liquid chromatography mass spectrometry analysis

Aliquots of 5 μl of each sample were subjected to chromatography on a Bruker DaltonicsMaXis Impact device with a Thermo Scientific HPLC UltiMate 3000 system with a quaternary pump delivery system DionexUltiMate and MS detection, on C18 reverse-phase column [5 μm , 2.1 x 100 mm], (Acclaim, Dionex) maintained at 55°C.

Mobile phase: A - water: acetonitrile (60:40) containing 0.1% formic acid and 10 mM ammonium formate; B - isopropyl

alcohol: acetonitrile (90:10) containing 0.1% formic acid and 10 mM ammonium formate. Gradient: 75% A: 25% B followed by linear gradient to 50% A: 50% B at 4 min, linear gradient to 3% A: 97% B at 19 min, isocratic on 3% A: 97% B for 4 min and then returned to the initial condition 75% A: 25% B at 24 min for 4 min. Flow rate, 0.260ml/min.

Mass spectrometry was performed on a Bruker Daltonics MaXis Impact Q-TOF operating in positive ion mode. The mass range was set between 50-1000 m/z. The nebulizing gas pressure was set at 2.8bar, the drying gas flow at 12 L/min, the drying gas temperature at 300 °C. Before each chromatographic run, a calibrant solution of sodium formate was injected.

The control of the instrument and the data processing were completed using Tof Control 3.2 and Data Analysis 4.2 (Bruker Daltonics).

RESULTS

Baseline characteristics of the patients

Ten controls and 30 patients with ALD were enrolled. Of them, 17 were known to have cirrhosis and 7 had previous liver related clinical decompensation (LRD) events. Of the 30 ALD patients at inclusion, 16 patients (of which 12 were known cirrhotics) had an ASH-Test ≥ 0.18 , indicating at least minimal activity.

Baseline patient characteristics are shown in Table I.

Identification of the candidate metabolites

Using liquid chromatography–mass spectrometry (LC-MS) of both serum and urine samples of the entire cohort of patients with ALD and compared with those of healthy controls (Fig. 1) we identified 127 serum candidate metabolites for ALD

Table I. Baseline ALD patients' characteristics

Variables	Value
Age (years)	53.2 (27-74)
Male/Female	19/11
Height (cm)	164.249 \pm 6.0412
Weight (kg)	69.561 \pm 14.9096
ALT (IU/ml)	67.43 (17-260)
AST (IU/ml)	47.8 (7-169)
Bilirubin (mg/dl)	8.25 (0.3- 68.43)
Cholesterol (mg/dl)	191.03 (89-394)
Triglycerides (mg/dl)	115.96 (3-228)
GGT (IU/ml)	242.86 (25-2229)
Glucose (mg/dl)	130.89 (66-405)
Platelets	162,493 (27,000 - 367,000)
Alcohol consumption (g/day)	109.7 (31.8-320)
Cirrhosis n (%)	17 (56.66%)
With decompensation	7 (23.33%)
MELD score	13.46 (6-29)
Maddrey DF	28 (8-36)
ABIC score	26 (6-29)

patients and 150 for controls. From the urine we identified 135 candidate metabolites for the ALD cohort and 129 for controls.

By using the Scores system, 35 major metabolites could be further identified (Fig. 2).

Further more, using the Loading system, based on m/z analysis (Fig. 3), we identified 11 serum and 5 urine metabolites that were significantly different in patients with ALD compared with controls. The serum and urine metabolites in patients with

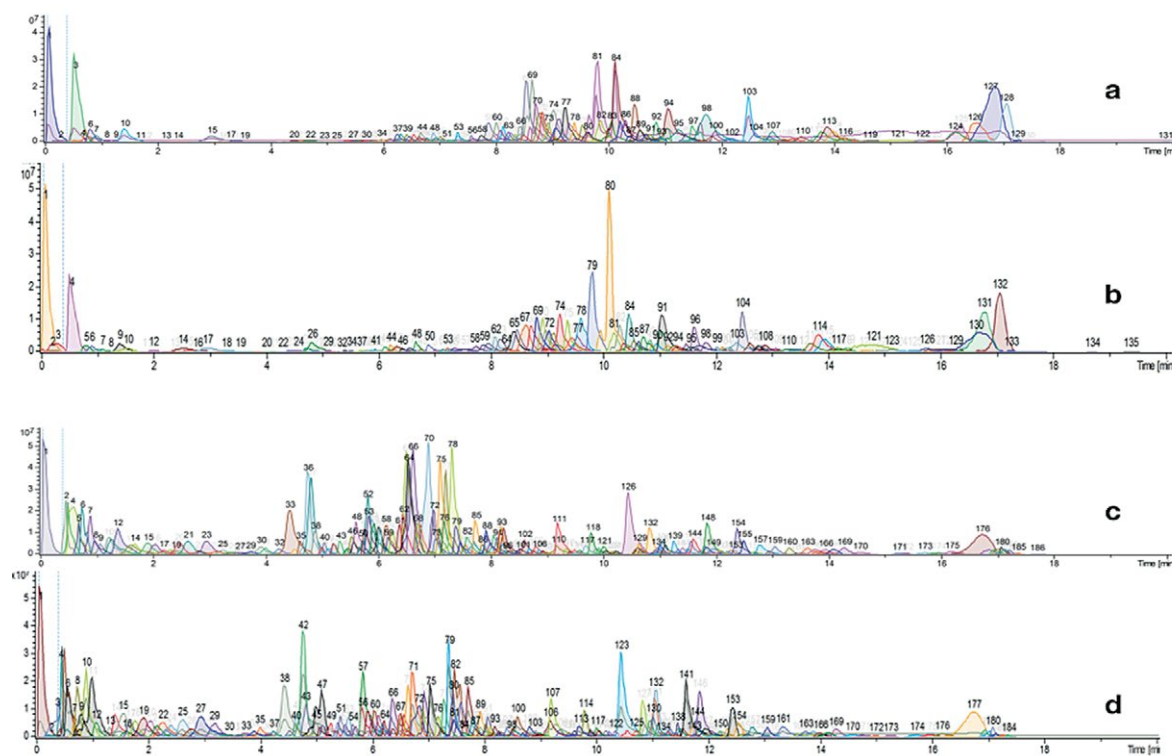


Fig. 1. Skyline graph demonstrating the metabolites identified in the serum of patients with ALD (a) and healthy controls (b) as well as in the urine of patients (c) and controls (d).

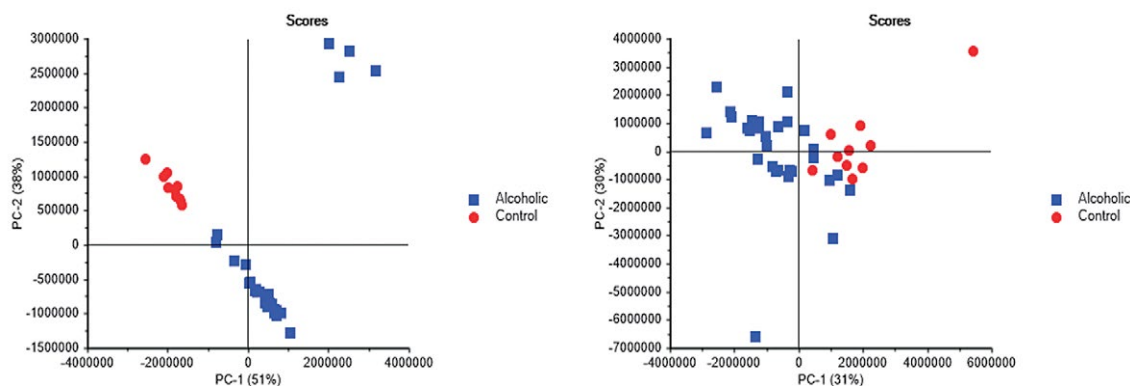


Fig. 2. Scores system-identification of 35 major metabolites from serum and urine in ALD patients vs controls

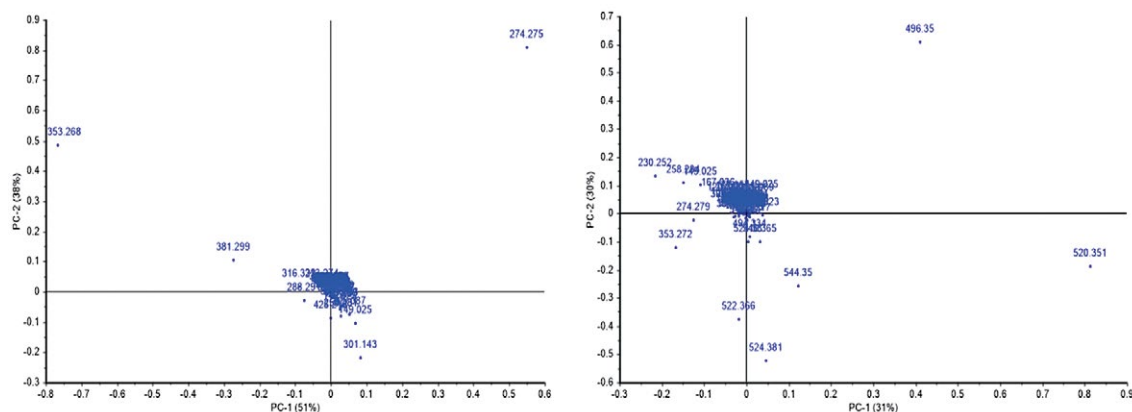


Fig. 3. Loadings system identifying the specific metabolites in serum and urine of ALD patients

ALD identified using sequential metabolomic techniques are shown in Table II.

Characterization of the selected metabolites

The signal areas of these 11 serum and 5 urine metabolites were further analyzed in patients with ALD. None of these

metabolites was correlated with the amount of alcohol consumption (units/day).

Only 5 serum (sM2, 3, 5, 10 and 11) and 1 urine (uM3) metabolites were able to further differentiate cirrhotic from non-cirrhotic patients with ALD. These 6 metabolites were chosen for further deeper analysis as represented in Fig. 4.

Table II. Serum and urine metabolites in patients with ALD identified using sequential metabolomic techniques

Serum Metabolites			Urine Metabolites		
Code	M/Z Value	Common Name	Code	M/Z Value	Common Name
sM1	149.022	2-Hydroxyglutarate	uM1	274.275	Glutaconylcarnitine
sM2	167.054	Decatrienoic acid	uM2	288.291	L-Octanoylcarnitine
sM3	177.0545	Ascorbic acid	uM3	301.142	2-Methoxyestrone
sM4	230.2486	Butenyl carnitine	uM4	353.266	MG(18:3/0/0/0) MG(0:0/18:3/0:0) Prostaglandin D2/E2
sM5	258.2797	N-Lauroylglycine	uM5	381.298	MG(20:3/0/0/0) MG(0:0/20:3/0:0)
sM6	353.272	Prostaglandin E2/D2/H2 MG (0:0/18:3/0:0)			
sM7	496.3407	PE(O-20:0/0:0) PS(16:1(9Z)/0:0)			
sM8	520.3407	LysoPC (18:2(9Z,12Z)/0:0)			
sM9	522.3569	LysoPC (18:1(9Z)/0:0)			
sM10	524.3721	Isom.LPC (16:0/2:0), LysoPC (0:0/18:0)			
sM11	544.341	LysoPC (20:4/0:0)			

Table III. Signal areas of 5 serum and 1 urine metabolites in cirrhotic vs. non-cirrhotic patients with ALD and their diagnostic performance for cirrhosis

	Signal areas			Ability to diagnose cirrhosis	
	Cirrhosis	Non-cirrhotic	p	AUROC	95% CI
sM2	684060.313 (±150311.430)	544880.286 (±165017.511)	0.022	0.763	0.574-0.898
sM3	902229.563 (±126759.965)	806594.357 (±109529.537)	0.037	0.759	0.569-0.895
sM5	2676623.06 (±320180.649)	2401624.71 (±253205.174)	0.015	0.835*	0.655-0.944
sM10	350893.875 (±133338.296)	545040.714 (±192818.251)	0.003	0.728	0.535-0.873
sM11	790748.438 (±493497.928)	1633634.14 (±755245.193)	0.001	0.728	0.535-0.873
uM3	288674.875 (±16968.302)	275233.214 (±24205.543)	0.08	0.656	0.456-0.858

* p (deLong test) = 0.05 (vs. sM2 and sM3) and 0.03 (vs. sM10 and sM11), respectively

Ability to diagnose cirrhosis

Analyzing only the ALD patients, all the selected serum metabolites had significantly different mean signal areas in patients with cirrhosis as compared with those without, while uM3 lost the significance. The diagnostic performance for cirrhosis was acceptable for all metabolites, but sM5 was significantly better than all the others (Table III).

Based on these data, sM5 (N-Lauroglycine, NLG) was chosen as the best metabolite for prediction of cirrhosis in patients with ALD. For a cut-off value of the signal area of 2478287, the sensitivity (Se) was 1 and specificity (Sp) 0.62, the positive predictive value (PPV) was 75% and negative predicted value (NPV) 90%, the positive and negative likelihood ratio (LR) were 2.62 and 0.09, respectively. Using this value to assess the diagnostic accuracy, 24/30 (80%) patients were correctly classified (chi-square=11.317, p=0.001).

Table IV. Correlation of serum metabolites with ALD severity indexes; the urine metabolite was not correlated with either of these scores.

		Maddrey score	ABIC
sM2	rho	0.529	0.679
	p	0.003	0.0001
sM3	rho	0.413	0.561
	p	0.01	0.001
sM5	rho	0.557	0.560
	p	0.001	0.001
sM10	rho	- 0.569	- 0.538
	p	0.001	0.002
sM11	rho	- 0.530	- 0.616
	p	0.003	0.0001

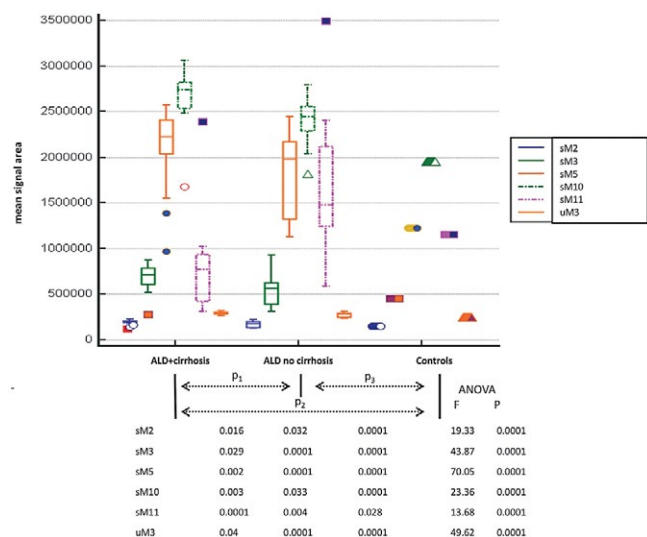


Fig. 4. Metabolites characterization. Boxplots representing signal areas for 5 serum and 1 urine metabolites in cirrhotic, non cirrhotic patients with ALD and healthy controls, as depicted by ANOVA test with Bonferroni post-hoc analysis. p₁, p₂ and p₃ represent the p values comparing mean signal areas between cirrhotic-non cirrhotic patients, cirrhotics-controls and non-cirrhotics-controls, respectively; P and F represent the values of overall ANOVA test for each metabolite).

Assessment of disease severity

All the five serum metabolites were well correlated with Maddrey and ABIC scores, as the most widely used in clinical practice to assess ALD severity and prognosis (Table IV).

Based on these data, sM2 and sM5 seem to be the best candidates to be further used to assess ALD severity. Both metabolites had similar AUROC to predict Maddrey score ≥ 32 (0.799 (95%CI: 0.613-0.922) vs. 0.837 (95%CI: 0.681-0.937); p (de Long test) = 0.12 and, respectively ABIC score ≥ 6.71 (0.844 (95%CI: 0.666-0.950) vs. 0.867 (95%CI:0.693-0.962); p (de Long test) = 0.73.

As for the ABIC score > 9 (associated with severe disease and bad prognosis), the AUROC for sM2 was significantly higher than the one for sM5: 0.946 (95%CI: 0.863-1.000) vs. 0.884 (95%CI: 0.714-0.971), p (de Long test)=0.05. Based on these findings, sM2 (decatrienoic acid, DTEA) was considered as being the best serum metabolite to assess the disease severity (Table V).

DISCUSSION

The purpose of this study was to identify and characterize new metabolomic biomarkers for the diagnosis, staging and severity assessment of ALD, as a noninvasive alternative to

Table V. Association between the decatrienoic acid (DTEA) area and prognostic scores.

	Maddrey >32	ABIC \geq 6.71	ABIC >9
Cut-off value	>624000	>624000	>819000
Sensitivity	0.86	0.79	1
Specificity	0.75	0.75	0.93
PPV	75.00%	80%	50
NPV	85.00%	78.60%	100
+LR	3.42	3.73	14
-LR	0.19	0.25	0
Diagnostic accuracy	80%	79.31%	93.33%
Correctly class pts	24/30	23/30	28/30

LR: likelihood ratio; NPV: negative predictive value; PPV: positive predictive value.

liver biopsy. Metabolomics is the last and rapidly expanding omic technique that explores the wide spectrum of metabolic pathways products. Theoretically, these products should be the first to change when a certain pathway is interfered by a specific condition, thus metabolomics appears to be the path to follow when trying to identify sensitive and specific biomarkers for early diagnosis. By using different methods to purify the metabolites' signature obtained from patients with ALD, we identified 5 serum and 1 urine metabolites, of which one (NLG) seemed accurate for identifying cirrhotic patients and another (DTEA) appeared to be more appropriate to select patients with severe disease.

Multiple studies have analyzed the metabolomics profile for other hepatic diseases such as nonalcoholic fatty liver disease (NAFLD), viral hepatitis and hepatocellular carcinoma [24-33], trying to identify possible biomarkers for disease progression. In NAFLD, elevated hepatic concentrations of various lysophosphatidylcholine (LPC), lysophosphatidylethanolamine (LPE) and phosphatidylcholine (PC) species have been reported for human steatotic vs. non-steatotic livers [24, 30]. Three studies reported elevated bile salts in the liver [24] that spilled over to elevated bile acids in serum and plasma [25, 26]. Regarding HCV infection, a metabolomic comparison of HCV-infected hepatocytes revealed small but significant increases in alanine, tyrosine and adenosine [27, 30, 32]. The metabolomic changes in hepatocellular carcinoma tend to point to increased fatty acid β -oxidation, with elevated acetate and 2-oxoglutarate (precursor of carnitine) and reduced free fatty acids, carnitine and carnitine esters [30, 31]. Further studies are required to validate these molecules as biomarkers for hepatocellular carcinoma.

Until now, only a few studies have focused on the metabolomic assessment of ALD [15-19]. The data available are heterogeneous, since the design of these studies differed substantially. Most of the studies identified protein metabolites associated with ALD in experimental [18] or clinical settings, either from serum [15] or urine [16] of drinking men. Overall, these studies found 19 metabolites associated with alcohol intake, most derived from the protein metabolism, and some of them, possible biomarker candidates of alcohol-induced liver injury.

Since the lipid metabolism appears to be the first dysregulated in the development of ALD, it seems rational to search for lipid metabolites as early biomarkers. In this respect, Li et al. [19] found in a murine model that metabolites of phosphatidyl choline, sphingomyelin as well as some aminoacids were associated with the development of hepatocellular carcinoma in ALD [19]. Our group previously identified an isoform of LPC to be a good predictor of liver related decompensation and death in patients with severe AH [33]. Similarly, all the relevant metabolites identified by this study using an untargeted approach are also related with the lipid pathway, demonstrating the importance of this pathway in the development and progression of ALD. There are multiple possible host or environmental factors that might interfere with the pathogenesis of ALD: drinking patterns, diet, microbiota composition. However, our study was not designed to evaluate neither of these factors, except the amount of alcohol intake and none of the identified metabolites were directly related with alcohol consumption.

The differential diagnosis between AH and cirrhotic decompensation is often difficult, because of similar clinical, biological and imaging aspects [20-22]. In this respect, the metabolite identified in our study (NLG), due to the high NPV, appears useful to select patients without cirrhosis. On the other hand, severity assessment in ALD and AH is extremely important and the performance of currently available systems (DE, MELD, ABIC) needs to be improved. In this respect, we identified DTEA as a possible biomarker to exclude severe AH.

The relevance of our data is hampered by the study limitations. There are some intrinsic limitations: the small number of patients, which is however acceptable for a proof-of-concept approach; the lack of biopsy-proven ALD and AH; the cross-sectional design and also the fact that the response to therapy was not assessed. Besides that, there are the limitations of the metabolomic approach, especially the untargeted one: lack of well established and standardized methods or procedures, metabolite identification difficult and time consuming, potentially thousands of compounds can match a given parent ion mass or a given atomic composition [34].

Despite these drawbacks, metabolomics seems to offer the premises of identifying an "ideal" biomarker for ALD: specific, easy to use, widely available and also with a low cost. Our study was not designed to prove any of these facts, but opened the gate of opportunity for a closer look into metabolomics' applications in ALD. Until now, we managed to identify two serum metabolites with a good diagnostic accuracy and high NPV that could be used in conjunction in patients with ALD for better stratification: NLG to exclude the presence of cirrhosis and DTEA to exclude a severe disease. Nevertheless, all these findings need to be further addressed in larger, prospective clinical trials, with relevant clinical and therapeutic end-points.

CONCLUSION

Based on this proof of concept study, metabolomics appears to offer both the opportunity and the means for better management and risk assessment of patients with ALD.

Conflicts of interest: No conflict to declare.

Authors' contribution: A.S. drafted the manuscript; H.S. critically revised and completed the manuscript; A.S., D.C., C.R., B.P. and H.S. evaluated the patients and revised the manuscript; CS performed metabolomic analysis; M.T. and M.G. approved and coordinated the study and revised the manuscript.

Acknowledgement: This study was financially supported by a grant from the Romanian Ministry of Education and Research (UEFISCDI): (PN-II-RU-TE-2014-4-0709 , PN-II-RU-TE-2014-4-0356).

REFERENCES

1. Miller AM, Horiguchi N, Jeong WI, Radaeva S, Gao B. Molecular mechanisms of alcoholic liver disease: innate immunity and cytokines. *Alcohol Clin Exp Res* 2011;35:787–793. doi:10.1111/j.1530-0277.2010.01399.x
2. Mandrekar P. Epigenetic regulation in alcoholic liver disease. *World J Gastroenterol* 2011;17:2456–2464. doi:10.3748/wjg.v17.i20.2456
3. Teli MR, Day CP, Burt AD, Bennett MK, James OF. Determinants of progression to cirrhosis or fibrosis in pure alcoholic fatty liver. *Lancet* 1995;346:987–990.
4. Poynard T, Mathurin P, Lai CL, et al. A comparison of fibrosis progression in chronic liver diseases. *J Hepatol* 2003;38:257–265. doi:10.1016/S0168-8278(02)00413-0
5. Peery AF, Dellon ES, Lund J, et al. Burden of gastrointestinal disease in the United States: 2012 update. *Gastroenterology* 2012;143:1179–1187. doi:10.1053/j.gastro.2012.08.002
6. Grant BF. Barriers to alcoholism treatment: Reasons for not seeking treatment in a general population sample. *J Stud Alcohol* 1997;58:365–371. doi:10.15288/jsa.1997.58.365
7. Nishiumi S, Suzuki M, Kobayashi T, Matsubara A, Azuma T, Yoshida M. Metabolomics for biomarker discovery in gastroenterological cancer. *Metabolites* 2014;4:547–571. doi:10.3390/metabo4030547
8. Rieder F, Kurada S, Grove D, et al. A Distinct Colon-Derived Breath Metabolome is Associated with Inflammatory Bowel Disease, but not its Complications. *Clin Transl Gastroenterol* 2016;7:e201. doi:10.1038/ctg.2016.57
9. Griffin JL, Nicholls AW. Metabolomics as a functional genomic tool for understanding lipid dysfunction in diabetes, obesity and related disorders. *Pharmacogenomics* 2006;7:1095–1107. doi:10.2217/14622416.7.7.1095
10. Lelliott CJ, Lopez M, Curtis RK, et al. Transcript and metabolite analysis of the effects of tamoxifen in rat liver reveals inhibition of fatty acid synthesis in the presence of hepatic steatosis. *Faseb J* 2005;19:1108–1119. doi:10.1096/fj.04-3196com
11. Maddrey WC, Boitnott JK, Bedine MS, Weber FL Jr, Mezey E, White RI Jr. Corticosteroid therapy of alcoholic hepatitis. *Gastroenterology* 1978;75:193–199.
12. Gholam PM. Prognosis and Prognostic Scoring Models for Alcoholic Liver Disease and Acute Alcoholic Hepatitis. *Clin Liver Dis* 2016;20:491–497. doi:10.1016/j.cld.2016.02.007
13. Dominguez M, Rincón D, Abrales JG, et al. A new scoring system for prognostic stratification of patients with alcoholic hepatitis. *Am J Gastroenterol* 2008;103:2747–2756. doi:10.1111/j.1572-0241.2008.02104.x
14. Yu M, Zhu Y, Cong Q, Wu C. Metabonomics Research Progress on Liver Diseases. *Can J Gastroenterol Hepatol* 2017;2017:8467192. doi:10.1155/2017/8467192
15. Harada S, Takebayashi T, Kurihara A, et al. Metabolomic profiling reveals novel biomarkers of alcohol intake and alcohol-induced liver injury in community-dwelling men. *Environ Health Prev Med* 2016;21:18–26. doi:10.1007/s12199-015-0494-y
16. Chang HS, Bai HC, Wang M. The urine metabolomics research of patients with alcoholic liver disease. *Heilongjiang Medicine and Pharmacy* 2013;5:44–45.
17. Nahon P, Amathieu R, Triba MN, et al. Identification of serum proton NMR metabolomic fingerprints associated with hepatocellular carcinoma in patients with alcoholic cirrhosis. *Clin Cancer Res* 2012;18:6714–6722. doi:10.1158/1078-0432.CCR-12-1099
18. Manna SK, Thompson MD, Gonzalez FJ. Application of mass spectrometry-based metabolomics in identification of early noninvasive biomarkers of alcohol-induced liver disease using mouse model. *Adv Exp Med Biol* 2015;815:217–238. doi:10.1007/978-3-319-09614-8_13
19. Li S, Liu H, Jin Y, Lin S, Cai Z, Jiang Y. Metabolomics study of alcohol-induced liver injury and hepatocellular carcinoma xenografts in mice. *J Chromatogr B Analyt Technol Biomed Life Sci* 2011;879:2369–2375. doi:10.1016/j.jchromb.2011.06.018
20. Dhanda AD, Collins PL, McCune CA. Is liver biopsy necessary in the management of alcoholic hepatitis? *World J Gastroenterol* 2013;19:7825–7829. doi:10.3748/wjg.v19.i44.7825
21. Stickel F, Datz C, Hampe J, Bataller R. Pathophysiology and Management of Alcoholic Liver Disease: Update 2016. *Gut Liver* 2017;11:173–188. doi:10.5009/gnl16477
22. Hernaez R, Solà E, Moreau R, Ginès P. Acute-on-chronic liver failure: an update. *Gut* 2017;66:541–553. doi:10.1136/gutjnl-2016-312670
23. Rachakonda V, Gabbert C, Raina A, et al. Serum metabolomic profiling in acute alcoholic hepatitis identifies multiple dysregulated pathways. *PLoS One* 2014;9:e113860. doi:10.1371/journal.pone.0113860
24. Garcia-Canaveras JC, Donato MT, Castell JV, Lahoz A. A comprehensive untargeted metabolomic analysis of human steatotic liver tissue by RP and HILIC chromatography coupled to mass spectrometry reveals important metabolic alterations. *J Proteome Res* 2011;10:4825–4834. doi:10.1021/pr200629p
25. Kalhan SC, Guo L, Edmison J, et al. Plasma metabolomic profile in nonalcoholic fatty liver disease. *Metabolism* 2011;60:404–413. doi:10.1016/j.metabol.2010.03.006
26. Barr J, Vazquez-Chantada M, Alonso C, et al. Liquid chromatography-mass spectrometry-based parallel metabolic profiling of human and mouse model serum reveals putative biomarkers associated with the progression of nonalcoholic fatty liver disease. *J Proteome Res* 2010;9:4501–4512. doi:10.1021/pr1002593
27. Roe B, Kensicki E, Mohney R, Hall WW. Metabolomic profile of hepatitis C virus-infected hepatocytes. *PLoS One* 2011;6:e23641. doi:10.1371/journal.pone.0023641
28. Di Poto C, Ferrarini A, Zhao Y, et al. Metabolomic Characterization of Hepatocellular Carcinoma in Patients with Liver Cirrhosis for Biomarker Discovery. *Cancer Epidemiol Biomarkers Prev* 2017;26:675–683. doi:10.1158/1055-9965.EPI-16-0366
29. Crisan D, Radu C, Suci A, et al. Metabolomics for genomics: the role of vitamin D in nonalcoholic fatty liver disease. *J Gastrointest Liver Dis* 2015;24:394–395.
30. Beyoğlu D, Idle JR. The metabolomic window into hepatobiliary disease. *J Hepatol* 2013;59:842–858. doi:10.1016/j.jhep.2013.05.030

31. Gao R, Cheng J, Fan C, et al. Serum Metabolomics to Identify the Liver Disease-Specific Biomarkers for the Progression of Hepatitis to Hepatocellular Carcinoma. *Sci Rep* 2015;5:18175. doi:[10.1038/srep18175](https://doi.org/10.1038/srep18175)
32. Sarfaraz MO, Myers RP, Coffin CS, et al. A quantitative metabolomics profiling approach for the noninvasive assessment of liver histology in patients with chronic hepatitis C. *Clin Transl Med* 2016;5:33. doi:[10.1186/s40169-016-0109-2](https://doi.org/10.1186/s40169-016-0109-2)
33. Stefanescu H, Suciu A, Romanciuc F, et al. Lyso-phosphatidylcholine: A potential metabolomic biomarker for alcoholic liver disease? *Hepatology* 2016;64:678-679. doi:[10.1002/hep.28630](https://doi.org/10.1002/hep.28630)
34. Scalbert A, Brennan L, Fiehn O, et al. Mass-spectrometry-based metabolomics: limitations and recommendations for future progress with particular focus on nutrition research. *Metabolomics* 2009;5:435-458. doi:[10.1007/s11306-009-0168-0](https://doi.org/10.1007/s11306-009-0168-0)

CIRRHOSIS AND LIVER FAILURE

Non-invasive *ménage à trois* for the prediction of high-risk varices: stepwise algorithm using lok score, liver and spleen stiffness

Horia Stefanescu^{1,*}, Corina Radu^{1,2,*}, Bogdan Procopet^{1,2}, Monica Lupsor-Platon³, Alina Habic², Marcel Tantau^{1,2} and Mircea Grigorescu^{1,2}

1 Hepatology Unit, Regional Institute of Gastroenterology and Hepatology, Cluj-Napoca, Romania

2 3rd Medical Clinic, Iuliu Hatieganu University of Medicine and Pharmacy, Cluj-Napoca, Romania

3 Medical Imaging Department, Iuliu Hatieganu University of Medicine and Pharmacy, Cluj-Napoca, Romania

Keywords

high-risk oesophageal varices – liver stiffness – prediction algorithm – spleen stiffness

Abbreviations

(AU)ROC, (area under) receiver operating curve; +/- LR, positive/negative likelihood ratio; ALT, alanine amino transferase; AST, aspartate amino transferase; CI, confidence interval; CSPH, clinically significant PH; DA, diagnostic accuracy; EV, oesophageal varices; EVRS, oesophageal varices risk score; HBV, hepatitis B virus; HCV, hepatitis C virus; HREV, high-risk EV; ICC, interclass correlation; INR, international normalized ratio; IQR, interquartile range; kPa, kilopascals; LS(M), liver stiffness (measurement); LSPS, LSM-spleen diameter to platelet ratio score; MRI, magnetic resonance imaging; NAFLD, non-alcoholic fatty liver disease; OR, odds ratio; P/N PV, positive/negative predictive value; PH, portal hypertension; PSR, platelets count/spleen diameter ratio; SD, standard deviation; Se, sensitivity; Sp, specificity; SS(M), spleen stiffness (measurement); VCTE, vibration controlled transient elastography.

Correspondence

Horia Stefanescu, MD, PhD
Hepatology Unit, Regional Institute of
Gastroenterology and Hepatology
19-21, Croitorilor str; 400162, Cluj-Napoca,
Romania
Tel: +40 766 318283
Fax: +40 378 102396
e-mail: horia.stefanescu@irgh.ro

Received 28 June 2014

Accepted 23 August 2014

DOI:10.1111/liv.12687

Liver Int. 2015; 35: 317–325

Abstract

Background & Aims: Liver stiffness (LS), spleen stiffness (SS) and serum markers have been proposed to non-invasively assess portal hypertension or oesophageal varices (EV) in cirrhotic patients. We aimed to evaluate the performance of a stepwise algorithm that combines Lok score with LS and SS for diagnosing high-risk EV (HREV) and to compare it with other already-validated non-invasive methods. **Methods:** We performed a cross-sectional study including 136 consecutive compensated cirrhotic patients with various aetiologies, divided into training (90) and validation (46) set. Endoscopy was performed within 6 months from inclusion for EV screening. Spleen diameter was assessed by ultrasonography. LS and SS were measured using Fibroscan. Lok score, platelet count/spleen diameter ratio, LSM-spleen diameter to platelet ratio score and oesophageal varices risk score (EVRS) were calculated and their diagnostic accuracy for HREV was assessed. The algorithm classified patients as having/not-having HREV. Its performance was tested and compared in both groups. **Results:** In the training set, all variables could select patients with HREV with moderate accuracy, the best being LSPS (AU-ROC = 0.818; 0.93 sensitivity; 0.63 specificity). EVRS, however, was the only independent predictor of HREV (OR = 1.521; $P = 0.032$). The algorithm correctly classified 69 (76.66%) patients in the training set ($P < 0.0001$) and 36 (78.26%) in the validation one. In the validation group, the algorithm performed slightly better than LSPS and EVRS, showing 100% sensitivity and negative predicted value. **Conclusion:** The stepwise algorithm combining Lok score, LS and SS could be used to select patients at low risk of having HREV and who may benefit from more distanced endoscopic evaluation.

*Equally contributed to the work.

Key Points

- Liver stiffness and serum biomarkers are associated with the presence of varices, but endoscopy cannot be yet replaced;
- Spleen stiffness was recently identified as a potential surrogate marker for varices and portal hypertension;
- The proposed algorithm is the first attempt to use a combination among serum biomarkers (Lok score), liver and spleen stiffness in a stepwise approach to predict high-risk varices;
- The algorithm is not inferior to liver stiffness \times spleen diameter/platelet count or oesophageal varices risk score, and seems to work better as a rule-out strategy as it has excellent negative predictive values in both training and validation groups.

Screening for oesophageal varices (EV) in cirrhotic patients is of major importance since they may occur in up to 90% of cases (1), with a rate depending on the severity of cirrhosis (2). Both American (3) and European (4) consensus on portal hypertension (PH) and variceal bleeding recommend endoscopic screening for EV at the time of diagnosis of cirrhosis and endoscopic surveillance according to variceal staging. It was demonstrated that EV incidence rate is only 7% per year (5), with a cumulative 5-year rate of 21% (6), so repetitive negative endoscopies would increase the costs of care of newly diagnosed cirrhotic patients. Hence, finding alternate non-invasive tools to estimate clinical outcomes such clinically significant portal hypertension (CSPH) and high-risk EV (HREV) became of growing importance and recognized as such by the Baveno V faculty (4).

Transient elastography is a very useful non-invasive physical method, especially for ruling out severe fibrosis or cirrhosis (7, 8) being also able to predict 5-year survival (9). In the settings of cirrhosis, vibration controlled transient elastography (VCTE) was used to estimate the presence (10) or to predict the development (11) of complications related to PH. Liver stiffness measurement (LSM) (12, 13) and serological scores (14, 15, 16) or combination of these ones (17, 18, 19) has been proved to correlate well with the presence of oesophageal varices (EV) in cirrhotic patients. Recently, spleen stiffness measurement (SSM) using VCTE was proposed as a surrogate method to estimate the presence of EV (20) and CSPH (21) but spleen elastography still has a limited accuracy (22).

Based on our previous experience in combining LSM, SSM and biochemical scores (20, 23) we aimed to develop, evaluate and validate a stepwise algorithm that combines Lok score with liver and spleen stiffness for predicting the presence of HREV in cirrhotic patients, in comparison with other already-validated integrative non-invasive methods.

Methods**Patients**

During a 24 months period (November 2011 – October 2013) 136 consecutive compensated cirrhotic patients from a tertiary referral hospital were enrolled for this cross-sectional study. All patients previously diagnosed with cirrhosis (either biopsy proven, or having unequivocal clinical, biological and imaging features) aged 18–80 years, and irrespective of aetiology were included. Patients with previous episodes of decompensation (history of variceal bleeding and currently on pharmacologic secondary prophylaxis, or ascites currently controlled by diuretic therapy) were still included, provided that at the time of evaluation they were in a compensated state. Presence of perihepatic and/or perisplenic ascites, portal vein thrombosis, non-reliable liver and/or spleen stiffness measurements, obstructive jaundice, advanced hepatocellular carcinoma (HCC) or tumours located in the right liver lobe, presence of a pacemaker or heart defibrillator, pregnancy or refusal to participate were the exclusion criteria.

The first two-thirds of the patients ($n = 90$) were considered as the training set, and their data were retrospectively analyzed. Only in this set were included patients with previous decompensation. The following 46 patients consisted the validation set and were prospectively included. All these patients were fully compensated. The diagnostic performance of non-invasive tests was evaluated in the training set and further validated in the second group.

All selected patients underwent VCTE for liver and spleen stiffness measurement and were evaluated by endoscopy for the assessment of EV. The main endpoint of the endoscopic evaluation was the detection of HREV. Spleen longitudinal diameter in mm was recorded by ultrasonography. Routine biological tests according to the follow-up protocol were obtained in the same day.

All patients were enrolled for this study after signing an informed consent that was previously revised and approved, together with the study protocol by the Ethical Committee of the Cluj-Napoca University of Medicine and Pharmacy in full accordance with the ethical guidelines issued by the 1975 Declaration of Helsinki and its further revisions.

Stiffness measurements

Both liver and spleen stiffness measurements were recorded by an experienced operator with more than 2000 examinations performed at the time of the study in patients with chronic liver diseases who was blinded regarding the endoscopic findings (the presence and grade of EV).

Liver stiffness measurement

Liver stiffness measurements were performed after overnight fasting (24, 25) in the right liver lobe using one-dimension transient (impulsional) elastography (FibroScan[®], Echosens, Paris, France) following the technical background and examination procedure as previously described (26). Liver stiffness measurement was performed only after ultrasound guidance, to avoid the presence of focal liver lesions into the acquisition window. The medium probe was used for all patients. The results were expressed in kilopascals (kPa). The median value of 10 successful measurements was kept as a representative of the liver stiffness, according to the manufacturer's recommendations and previous evidence (27). Only examinations with the interquartile range (IQR) lower than 30% of the median value were further analyzed (28). The success rate (calculated as the number of validated LS measurements divided by the number of total measurements) $\leq 60\%$ was not considered a failure, if 10 valid measurements were eventually acquired (29).

Spleen stiffness measurement

Spleen stiffness measurement was assessed in the same day as LSM using the standard Fibroscan machine by placing the transducer in the left intercostal spaces, usually on the posterior axillary line with the patient in supine position with his left arm in maximum abduction. Ultrasound was used to 'guide' stiffness measurements into the spleen parenchyma; 4 cm thickness at ultrasound was the minimum threshold for pursuing with stiffness measurements. The median of 10 valid measurements was recorded and the same quality standards as for LSM were used (IQR < 30%).

Calculation of non-invasive scores

The Lok Score, platelet count/spleen diameter ratio (PSR), LSM-spleen diameter to platelet ratio score (LSPS) and oesophageal varices risk score (EVRS) were calculated for all patients.

The Lok Score was calculated according to previously published formula: Lok Score: $\log \text{ odds} = -5.56 - 0.0089 \times \text{platelet count (103/mm}^3) + 1.26 \times (\text{AST/ALT}) + 5.27 \times \text{INR}$; Lok = $[\exp(\log \text{ odds})]/[1 + \exp(\log \text{ odds})]$ [15].

Platelet count/spleen diameter ratio was calculated as the ratio between platelets count and spleen longitudinal diameter, as previously described (30).

LSM-spleen diameter to platelet ratio score was also calculated as the product of liver stiffness and the ratio between spleen diameter and platelets count (LSPS = LSM \times spleen diameter/platelet count) (31).

Oesophageal varices risk score was also calculated as recently proposed using the following formula: $-4.364 - 0.538 \times \text{spleen diameter} - 0.049 \times \text{platelet count} - 0.044 \times \text{LS} + [0.001 \times \text{LS} \times \text{platelet count}]$ (32).

Construction of stepwise non-invasive algorithm

The algorithm (Fig. 1) proposes as a first step the use of LSM and calculation of Lok score. Based on previously published data [10, 12, 16, 23], we suggest that if LS is <19 kPa and Lok score <0.6, the risk of HREV is very low. Also, the concordance of LSM and Lok score over a certain cut-off value (to be calculated), may predict the presence of HREV. For the non-concordant cases, we suggest SSM as discriminant second step to rule in HREV.

Oesophageal varices evaluation

Esogastroduodenoscopy was performed using a flexible EVIS EXERA video gastroscope (Olympus Europe

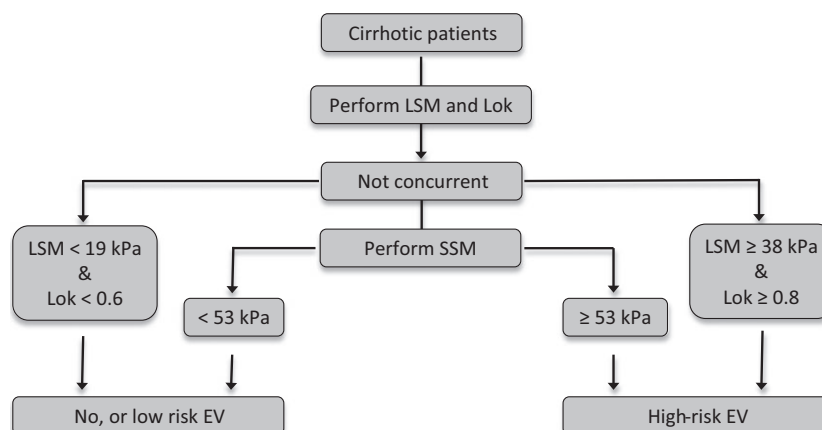


Fig. 1. Construction of the stepwise algorithm. First, liver stiffness is measured and Lok score is calculated. If the two are concurrent, large varices may be present or excluded. For the discordant cases, measurement of spleen stiffness as a second, discriminatory step is recommended.

Medical Systems, Hamburg, Germany). Oesophageal varices were graded according to their size as follows: (i) grade 1: small, straight EV; (ii) grade 2: enlarged, tortuous EV occupying less than one-third of the lumen; and (iii) grade 3: large, coil-shaped EV occupying more than one-third of the lumen. Grade 2 and 3 EVs were considered as large. Presence of red colour signs (red wale marking and cherry red spots) was also recorded. Grade 2 and 3 varices, together with grade 1 with red colour signs were considered high-risk varices. The endoscopic evaluation was not always synchronous with LSM and SSM, but did not exceed 6 months, and it was not always performed by the same examiner.

Statistical analysis

The statistical analysis was performed using the SPSS software version 20.0 (SPSS Inc. Chicago, IL, USA). Quantitative data in text and tables are reported as mean and standard deviation (SD) and confidence interval (95% CI) or as median and range and qualitative data as percentage (%). The relationships between different parameters were characterized using the non-parametric correlation coefficients. The data were compared using independent sample *t* test or Mann–Whitney, when appropriate. Multivariate logistic regression was used to determine the variables independently associated with an outcome. The diagnostic performance of LSM, SSM, PSR, LSPS and EVRS was assessed by receiver operating characteristic (ROC) curves analysis. Optimal cut-off values were calculated using a common optimization step that maximized the Youden index (33). For comparison of the ROC curves DeLong test was used, available through MedCalc v.9.2.1.0 software (MedCalc, Acaciaaam, Belgium). The sensitivity (Se), specificity (Sp), positive predictive value (PPV), negative predictive value (NPV), likelihood ratios (LR) and diagnostic accuracy (DA) were computed from the same data, without further adjustments. A *p* value of less than 0.05 was considered to indicate statistical significance.

The performance of tested non-invasive methods to predict HREV was estimated by calculating the proportion of correctly classified patients, together with Se, Sp, PPV, NPV, and LR. Chi-square and McNemar tests were used in the 2×2 contingency table for assessing differences in the proportion of misclassified patients with dichotomous cut-offs. They were also tested for absolute concordance against endoscopy findings using absolute interclass correlation agreement (ICC).

Results

Study population

In the training set ($n = 90$), 30 (33.33%) patients had HCV-related disease, while 12 (13.33%) HBV, 30 (33.33%) alcohol induced, 6 (6.67%) had mixed aetiology (viral + alcohol) and in 12 (13.33%) patients

cirrhosis was NAFLD related. In the validation group ($n = 46$), aetiology of cirrhosis was as follows: 16 (34.79%) – HCV; 8 (17.39%) – HBV; 11 (23.91%) – alcoholic; 4 (8.72%) – mixed; 7 (15.21%) – NAFLD. LSM and SSM were reliable in all patients, with good performances.

Biological, clinical, ultrasound and elastographic baseline characteristics of patients in both groups, according to the HREV status, are shown in Table 1. There are no relevant differences between patient groups as far the demographics or staging of the disease is concerned. There were no significant differences when comparing the same parameters in the training and validation set (Table S1).

Lok score, spleen size, platelets count, PSR, LSM, LSPS, EVRS and SSM were significantly higher in patients with HREV, in both training and validation set. In the training set, however, in multivariate analysis, only EVRS appeared to be independent predictor of HREV, with an OR of 1.521 ($P = 0.032$).

Performance of previously validated non-invasive scores in predicting LEV

In the training set, all tested scores (Lok, PSR, LSM, LSPS, EVRS and SSM) had a moderate performance for predicting HREV (Table 2). LSPS and EVRS appear to be the best, with an AUROC close to the 0.8 threshold, with a high statistical significance ($P < 0.0001$). However, as depicted by the DeLong test, there is no difference between AUROCs of all non-invasive tests.

As further showed in Table 2, for a certain cut-off value the diagnostic accuracy of the tested methods and composite scores varied from 65.55% (59 of 90 patients correctly classified) for LSM up to 80% (72/90) in the case of LSPS. Although in all cases the chi-square test was significant ($P < 0.003$ in all cases) and had moderate/high values (varying from 8.93 for LSM up to 34.30 for LSPS), the McNemar test was significant only for SSM ($P = 0.002$) and LSPS ($P = 0.008$).

Performance of the stepwise non-invasive algorithm

The cut-off values used in the algorithm (Fig. 1) to rule in HREV emerged from the training group (Table 2) and were as follows: ≥ 38 kPa for LSM, ≥ 0.8 for Lok and ≥ 53 kPa for SSM.

In the training set, the algorithm moderately correlated ($r = 0.558$; $P < 0.0001$) and was concurrent (ICC = 0.715; $P < 0.0001$) with endoscopy findings. The algorithm's diagnostic performance is shown also in Table 2 (right column). Post-test probability was 70.96%, while chi-square statistic was high (28.06; $P < 0.0001$) and McNemar test was significant ($P < 0.0001$).

Since our training group was heterogeneous, we tested the algorithms' diagnostic performance in some particular situations. As shown in Table S2, the algorithm appears to be more useful (diagnostic accuracy

Table 1. Baseline characteristics of patients in the training and validation groups, according to the presence/absence of high-risk oesophageal varices. When no otherwise specified, for each variable means (\pm standard deviation) or medians (range) are provided, based on the their normal/abnormal distribution as depicted by Shapiro–Wilk test

Variables*	Training Set			Validation set		
	no HREV (N = 43)	HREV (N = 47)	P	no HREV (N = 21)	HREV (N = 25)	P
EV status (N) (no/gr1/ gr2/gr3)	17/26/0/0	0/7/29/11		9/12/0/0	0/6/14/5	
gender (M/F)	26/24	24/16	NS	14/13	13/6	NS
Age (years)	56.47 (\pm 9.38)	54.98 (\pm 8.42)	NS	54.67 (\pm 9.13)	55.36 (\pm 9.13)	NS
BMI (kg/m ²)	26.35 (\pm 5.43)	27.07 (\pm 4.63)	NS	24.69 (\pm 2.33)	23.68 (\pm 0.98)	NS
AST (U/L)	87 (21–268)	78 (20–147)	NS	78 (26–278)	79 (21–278)	NS
ALT (U/L)	69 (14–256)	63 (14–159)	NS	64 (16–337)	62 (8–118)	NS
TBil (mg/dl)	1.25 (0.44–11.01)	1.58 (0.44–8.99)	NS	1.08 (0.55–1.55)	1.02 (0.70–1.34)	NS
AP (U/L)	276 (135–618)	302 (115–705)	NS	241 (151–262)	240 (163–258)	NS
GGT (U/L)	66.5 (13–824)	85.5 (24–672)	NS	60.5 (29–131)	128 (82–174)	NS
Platelets ($\times 10^9/L$)	111 (58.9–291)	77.5 (34.4–284)	0.005	109 (14–291)	79 (20–181)	NS
INR	1.44 (\pm 0.52)	1.41 (\pm 0.27)	NS	1.39 (\pm 0.36)	1.48 (\pm 0.39)	NS
Creatinine (mg/dl)	1.08 (\pm 0.32)	0.95 (\pm 0.30)	NS	0.90 (\pm 0.19)	1.52 (\pm 0.84)	NS
MELD	10 (2–17)	12 (4–23)	NS	8.55 (\pm 5.56) 10 (3–11)	11.68 (\pm 5.95) 12 (6–17)	NS
Child-Pugh Class (N: A/B/C)	29/12/2	27/20/0	NS	14/7/0	13/10/2	NS
Score	5 (5–10)	6 (5–9)		6 (5–9)	6 (5–10)	
Spl LD (mm)	133.31 (\pm 20.62)	153.54 (\pm 25.01)	<0.0001	147.99 (\pm 29.85)	163.60 (\pm 17.75)	0.032
PSR	840 (402–2487)	542 (155–1786)	<0.0001	730 (127–2279)	520 (112–1341)	0.027
Lok Score	0.73 (0.17–1.00)	0.94 (0.49–1.00)	<0.0001	0.8 (0.23–1)	0.94 (0.54–1)	0.022
LSM(kPa)	29.1 (14.3–75)	46.4 (16.8–75)	<0.0001	23.9 (11.6–63.9)	35.3 (16–75)	0.018
IQR/LSM	0.17 (0.07–0.30)	0.13 (0.09–0.30)	NS	0.14 (0.09–0.30)	0.11 (0.07–0.30)	NS
LSPS	3.12 (0.80–13.64)	8.39 (2.83–44.69)	<0.0001	3.02 (0.62–50.21)	6.35 (2.36–29.80)	0.006
SSM(kPa)	53.80 (\pm 17.08)	67.24 (\pm 11.11)	<0.0001	59.60 (\pm 18.46)	71.62 (\pm 9.18)	0.012
IQR/SSM	0.11 (0.08–0.30)	0.05 (0–0.20)	NS	0.09 (0.06–0.25)	0.03 (0–0.10)	NS
EVRS	−0.38 (\pm 2.40)	2.25 (\pm 2.08)	<0.0001	−0.60 (\pm 3.149)	2.03 (\pm 1.21)	0.001

Abbreviations: EV, oesophageal varices; BMI, body mass index; AST, aspartate amino transferase; ALT, alanine amino transferase; TBil, total bilirubin; AP, alkaline phosphatase; GGT, gamma glutamyltransferase; INR, international normalized ratio; MELD, model for end-stage liver disease; Spl LD, spleen longitudinal diameter; PSR, platelets count to spleen diameter ratio; LSM, liver stiffness measurement; LSPS, LSM-spleen diameter/platelets ratio; SSM, spleen stiffness measurement; IQR, interquartile range; SR, success ratio; EVRS, oesophageal varices risk score.

>80%) in patients with HCV aetiology than in alcoholic cirrhosis and in patients with previous decompensation.

Validation of the algorithm and comparison with other composite scores

In the validation set, the proposed algorithm performed better than composite scores (EVRS and LSPS) in identifying patients with HREV, reaching absolute sensitivity and negative predictive value (Table 3 and Fig. 2). Although the algorithm correctly classified the same number of patients as EVRS (36 out of 46; 78.26%), the level of significance was higher (McNemar test $P = 0.002$ vs. 0.1). The post-test probability was 71.42%.

Discussion

In this real-life scenario, we confirmed the value of several non-invasive methods in predicting the presence of

HREV, even if the diagnostic accuracy is not as good as those reported in carefully selected cohorts. We also developed and validated a new, stepwise algorithm that combines Lok score with liver and spleen stiffness, which proved to have a similar performance to predict HREV with other non-invasive composite methods (EVRS and LSPS).

Increased liver stiffness was associated with complications of cirrhosis [10] and its power to predict EVs was also studied, with conflicting results, varying from very good diagnostic accuracy (34) to no correlation at all (13). There is no consensus regarding the best cut-off value for predicting HREV, but it was proved to be influenced by the aetiology of the cirrhosis (35). Taking into account all these controversial data, together with the fact that the specificity and positive predictive values reported so far are too low and the results were not prospectively and independently validated, it was concluded that the ability of LS to predict EV is still a matter of

Table 2. Performance of Lok score (Lok), platelets count to spleen diameter ratio (PSR), liver stiffness measurement (LSM), liver stiffness – platelets to spleen ratio (LSPS), oesophageal varices risk score (EVRS) and spleen stiffness measurement (SSM) to detect high-risk varices (HREV) in the training group ($N = 90$; 52.2% having HREV)

	Lok	PSR	LSM	SSM	LSPS	EVRS	Algorithm
AUROC for HREV (95% CI)*	0.736 (0.628–0.844)	0.715 (0.590–0.812)	0.705 (0.596–0.813)	0.742 (0.637–0.848)	0.818 (0.727–0.908)	0.797 (0.703–0.891)	
Level of significance (P)	<0.0001	0.001	0.001	<0.0001	<0.0001	<0.0001	
Standard error	0.055	0.055	0.055	0.054	0.046	0.048	
Cut-off value	≥ 0.8	≤ 664	≥ 38	≥ 53	≥ 4.23	≥ 0.4	
Sensitivity	0.84	0.69	0.60	0.89	0.93	0.82	0.94
Specificity	0.61	0.66	0.71	0.54	0.63	0.63	0.58
PPV (%)	69.81	70.21	69.04	66.60	74.57	72.22	70.96
NPV (%)	75.75	60.44	62.5	81.48	90.32	77.72	89.28
+ LR	2.10	2.15	2.04	1.82	2.68	2.37	2.23
–LR	0.29	0.44	0.54	0.20	0.09	0.26	0.10
Diagnostic accuracy (correctly classified)	70% 63/90	68.88% (62/90)	65.55% (59/90)	71.11% (64/90)	80% (72/90)	74.44% (67/90)	76.66% (69/90)

*No significant differences between AUROC values (de Long test was not significant).

Table 3. Performance of the proposed non-invasive algorithm and other composite scores (LSPS and EVRS) to predict HREV in the validation set ($N = 46$; 54.34% having HREV)

	Algorithm	EVRS	LSPS
Sensitivity	1	0.92	0.80
Specificity	0.52	0.62	0.62
PPV (%)	71.42	74.19	71.42
NPV (%)	100	86.66	72.22
+LR	2.1	2.41	2.1
–LR	0.1	0.13	0.32
Post-test probability (%)	71.42	74.19	71.42
Diagnostic accuracy (correctly classified patients)	78.26 (36/46)	78.26 (36/46)	71.73 (33/46)
Chi-Square Test	17.21	15.09	8.41
P	<0.0001	<0.0001	0.04

P/N PV = positive/negative predictive value; +/- LR = positive/negative likelihood ratio.

debate, thus it cannot allow their use in current clinical practice (36). The median LSM value was significantly higher in patients with HREV as compared with ones without (46.4 vs. 29.1; $P < 0.0001$ in training set and 35.3 vs. 23.9; $P = 0.018$ in the validation set). What is intriguing from our data and can also be seen as a drawback of this study is the high mean values obtained for LSM, which may be the consequence of the relatively high proportion of alcoholic related cirrhosis (35, 37) in this study group. The best cut-off value for diagnosing HREV was 38 kPa, supporting the previously published data according to which in European population large EV are to be found most likely over 30 kPa (range 27.8–48) (38). However, at this cut-off and in our multietiological cohort LS showed a relatively modest performance to detect LEV (Se = 0.60; Sp = 0.70; AUROC = 0.705).

Spleen stiffness was only recently recognized to correlate with cirrhosis and PH. It was assessed by various techniques [MRI (39, 40) or shear wave ultrasound based elastography (41, 42)] with promising results in respect to EV and/or PH. SS measurement by VCTE was proposed as a surrogate marker for PH [21] and EV [20]. The cut-off value we found for SS to predict HREV (53 kPa) is concurrent with previously published data. Collechchia *et al.* found that SS ≥ 55 kPa rule in both CSPH and EV [21], with very good specificity values. We also found that the same SS value (42.7 kPa) is predictive for both CSPH and large EV, but the performance in a validation cohort was modest (AUROC = 0.633) (43). The study of Sharma *et al.* finds significant differences in SSM values in cirrhotic patients without EV (32 kPa), as compared with those with small EV (49 kPa), large EV (56 kPa) or those that bled (58 kPa)(44). Calvaruso *et al.*, for a SS value >54 kPa (using a modified calculation algorithm) obtained a 90% NPV for diagnosing large EV (45). All these findings lead to the conclusion that for a value of SSM >50 kPa the probability to find large or HREV at endoscopy is very high.

Platelets count to spleen longitudinal diameter ratio (PSR) was reported as a surrogate marker for detecting EV in cirrhotic patients (46) and was further validated that a value <909 is highly sensitive (91.5%) and has a good diagnostic accuracy (86%) in this respect [30]. In our cohort we found a lower cut-off value (664, which is expected, since our aim was to detect high-risk EV) with an acceptable sensitivity (0.69), but with a much lower accuracy (AUROC = 0.715). This tendency was previously observed by Calvaruso *et al.* that found a cut-off value <640 for detecting large EV in a cohort of HCV cirrhotics [45].

Both LSPS and EVRS were proposed in order to overcome the moderate performance of LSM alone to

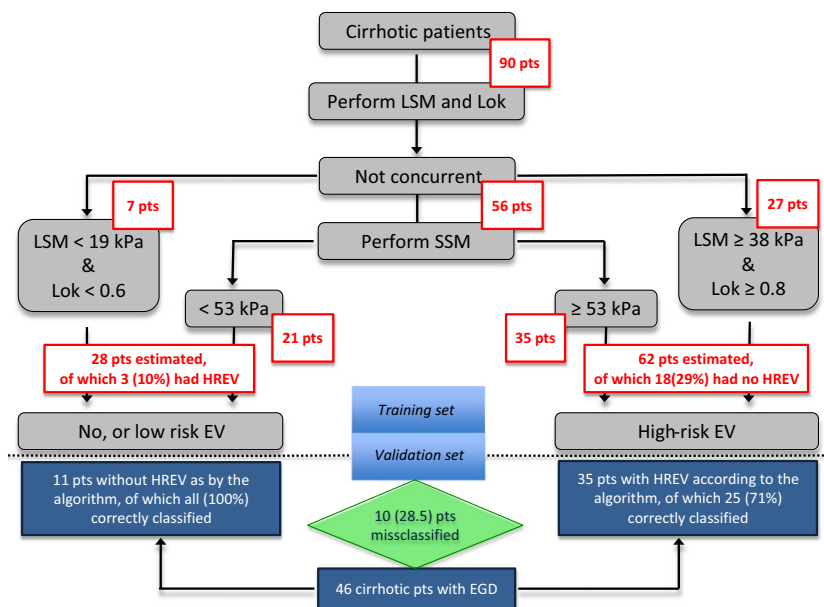


Fig. 2. Performance of the stepwise algorithm to classify patients in the training and validation group.

accurately predict either LEV, or CSPH. In the works of Kim et al. (31, 47) it was shown that for increasing values of LSPS, the risk of having/developing high-risk varices in HBV related cirrhosis also increases. The cut-off values used to stratify the patients were 6.5 and 9.5 respectively. The threshold value was further challenged by Berzigotti *et al.* [32] in a cohort of cirrhotic with various aetiologies, proposing an alternate value of 3.21 for predicting the presence of varices of any grade. In our cohort of patients (also because of multiple aetiologies), we found the value of 4.23 as having a good sensitivity (0.93), moderate specificity (0.63) and the best accuracy (AUROC = 0.818) for predicting the presence of high-risk EVs. In our validation population, LSPS correctly classified 72% of patients.

Oesophageal varices risk score was also proposed by Berzigotti [32] and combines the same variables (LSM, spleen size and platelets count) into a more elaborate way. In their population – in which the prevalence of EV was 31.6% and of large EV of 11.9%, EVRS ≥ 0.20 , predicted the presence of EV with good accuracy, both in the training set (AUROC: 0.9, Se: 70.3%, Sp: 76.5%) and the validation one (75% correctly classified). In our training population, EVRS showed an AUROC of 0.797 and for a value ≥ 0.4 predicted HREV with good Se (0.82) but moderate Sp (0.63), while in the validation set correctly classified 78% of patients.

The stepwise algorithm we are proposing, we consider it clinically logic, easy to use and applicable in everyday clinical practice and in any patient with cirrhosis. Lok score consists only in lab tests used on the regular basis in the follow-up of cirrhotic patients, and the use of Fibroscan is widening. Recording of SSM only

adds 5 min to the LSM examination time and can be easily performed by a trained nurse or a physician using ultrasound guidance. The algorithm showed its non-inferiority in comparison with LSPS and EVRS in both training and validation set. Although the algorithm offers a certain diagnostic gain (24% in the training set and 18% in the validation one), it seems that it would be more valuable if used as a rule-out option, since in the training set the probability to find HREV in patients classified as ‘negative’ is only 10%, while in the validation set it reached 0%. Before recommending its use, the algorithm needs to be independently validated.

As a drawback of our study (and a possible explanation for the low AUROC values obtained), we should also mention the high prevalence of grade 2 and 3 varices in our population: 44.4% in the training set and 41.3% in the validation one. This may be as a result of the limited resource settings of our health system, which may limit general access to the health services and, therefore, the patients are in more advance stages at presentation. This reality also explains the inclusion of patients with history of decompensation in this study.

In fact, the prevalence of varices was high in both training and validation set (80% and 76% respectively) and this is the reason why we chose not to test the algorithms’ performance to detect varices of any grade. The analysis we made on this (data not presented) show only a modest gain in diagnostic accuracy (one patient more correctly classified) as compared with HREV.

In conclusion, in compensated cirrhotic patients (especially if HCV related or with previous decompensation), this stepwise algorithm combining Lok score, liver and spleen stiffness can predict with high sensitivity the

presence of high-risk EV. Because of its good NPV, it could be used to select patients unlikely to have HREV and who eventually may benefit from more distanced further endoscopic evaluation.

Acknowledgements

The authors would like to thank Mrs Anca Maniu, Ms Anca Bugariu and Ms Adelina Horhat for their help in patient and data management.

Financial support: This work was financed by Cluj-Napoca University of Medicine and Pharmacy through the internal research grant nr 27020/7/15.11.2011.

Conflict of interest: The authors do not have any disclosures to report.

References

- Jensen DM. Endoscopic screening for varices in cirrhosis: findings, implications, and outcomes. *Gastroenterology* 2002; **122**: 1620–30.
- Merli M, Nicolini G, Angeloni S, et al. Incidence and natural history of small esophageal varices in cirrhotic patients. *J Hepatol* 2003; **38**: 266–72.
- Garcia-Tsao G, Sanyal AJ, Grace ND, Carey W and The Practice Guidelines Committee of the American Association for the Study of Liver Diseases, The practice parameters committee of the American College of Gastroenterology. Prevention and management of gastroesophageal varices and variceal hemorrhage in cirrhosis. *Hepatology* 2007; **46**: 922–38.
- de Franchis R. Revising consensus in portal hypertension: report of the Baveno V consensus workshop on methodology of diagnosis and therapy in portal hypertension. *J Hepatol* 2010; **53**: 762–8.
- D'Amico G, Garcia-Tsao G, Pagliaro L. Natural history and prognostic indicators of survival in cirrhosis: a systematic review of 118 studies. *J Hepatol* 2006; **44**: 217–31.
- D'Amico G, Pasta L, Morabito A, et al. Competing risks and prognostic stages of cirrhosis: a 25-year inception cohort study of 494 patients. *Aliment Pharmacol Ther* 2014; **39**: 1180–93.
- Friedrich-Rust M, Ong MF, Martens S, et al. Performance of transient elastography for the staging of liver fibrosis: a meta-analysis. *Gastroenterology* 2008; **134**: 960–74.
- Lupsor Platon M, Stefanescu H, Feier D, Maniu A, Badea R. Performance of unidimensional transient elastography in staging chronic hepatitis C. Results from a cohort of 1,202 biopsied patients from one single center. *J Gastrointest Liver Dis* 2013; **22**: 157–66.
- Verginoli J, Foucher J, Terreboune E, et al. Noninvasive tests for fibrosis and liver stiffness predict 5-year outcomes of patients with chronic hepatitis C. *Gastroenterology* 2011; **140**: 1970–9.
- Foucher J, Chanteloup E, Verginoli J, et al. Diagnosis of cirrhosis by transient elastography (FibroScan): a prospective study. *Gut* 2006; **55**: 403–8.
- Robic MA, Procopet B, Metivier S, et al. Liver stiffness accurately predicts portal hypertension related complications in patients with chronic liver disease: a prospective study. *J Hepatol* 2011; **55**: 1017–24.
- Bureau C, Metivier S, Peron JM, et al. Transient elastography accurately predicts presence of significant portal hypertension in patients with chronic liver disease. *Aliment Pharmacol Ther* 2008; **27**: 1261–8.
- Vizzutti F, Arena U, Romanelli RG, et al. Liver stiffness measurement predicts severe portal hypertension in patients with HCV-related cirrhosis. *Hepatology* 2007; **45**: 1290–7.
- Wai CT, Greenon JL, Fontana RJ, et al. A simple noninvasive index can predict both significant fibrosis and cirrhosis in patients with chronic hepatitis C. *Hepatology* 2003; **38**: 518–26.
- Lok AS, Ghany MG, Goodman ZD, et al. Predicting cirrhosis in patients with hepatitis C based on standard laboratory tests: results of the HALT-C cohort. *Hepatology* 2005; **42**: 282–92.
- Castera L, Le Bail B, Roudot-Thoraval F, et al. Early detection in routine clinical practice of cirrhosis and oesophageal varices in chronic hepatitis C: comparison of transient elastography (FibroScan) with standard laboratory tests and non-invasive scores. *J Hepatol* 2009; **50**: 59–68.
- Sebastiani G, Tempesta D, Fattovich G, et al. Prediction of oesophageal varices in hepatic cirrhosis by simple serum non-invasive markers: results of a multicenter, large-scale study. *J Hepatol* 2010; **53**: 630–8.
- Sebastiani G. Non-invasive assessment of liver fibrosis in chronic liver diseases: implementation in clinical practice and decisional algorithms. *World J Gastroenterol* 2009; **15**: 2190–203.
- Castera L, Sebastiani G, Le Bail B, et al. Prospective comparison of two algorithms combining non-invasive methods for staging liver fibrosis in chronic hepatitis C. *J Hepatol* 2010; **52**: 191–8.
- Stefanescu H, Grigorescu M, Lupsor M, et al. Spleen stiffness measurement using Fibroscan for the noninvasive assessment of esophageal varices in liver cirrhosis patients. *J Gastroenterol Hepatol* 2011a; **26**: 164–70.
- Colecchia A, Montrone L, Scaiola E, et al. Measurement of spleen stiffness to evaluate portal hypertension and the presence of esophageal varices in patients with HCV-related cirrhosis. *Gastroenterology* 2012; **143**: 646–54.
- Singh S, Eaton JE, Murad MH, et al. Accuracy of spleen stiffness measurement in detection of esophageal varices in patients with chronic liver disease: systematic review and meta-analysis. *Clin Gastroenterol Hepatol* 2013; **12**: 935–45.e4.
- Stefanescu H, Grigorescu M, Lupsor M, et al. A new and simple algorithm for the noninvasive assessment of esophageal varices in cirrhotic patients using serum fibrosis markers and transient elastography. *J Gastrointest Liver Dis* 2011b; **20**: 57–64.
- Arena U, Lupsor Platon M, Stasi C, et al. Liver stiffness is influenced by a standardized meal in patients with chronic hepatitis C virus at different stages of fibrotic evolution. *Hepatology* 2013; **58**: 65–72.
- Berzigotti A, de Gottardi A, Vukotic R, et al. Effect of meal ingestion on liver stiffness in patients with cirrhosis and portal hypertension. *PLoS ONE* 2013a; **8**: e58742.
- Ziol M, Handra-Luca A, Kettaneh A, et al. Noninvasive assessment of liver fibrosis by measurement of stiffness in patients with chronic hepatitis C. *Hepatology* 2005; **41**: 48–54.

27. Castera L, Forns X, Alberti A. Non-invasive evaluation of liver fibrosis using transient elastography. *J Hepatol* 2008; **48**: 835–47.
28. Kettaneh A, Marcellin P, Douvin C, *et al.* Features associated with success rate and performance of FibroScan measurements for the diagnosis of cirrhosis in HCV patients: a prospective study of 935 patients. *J Hepatol* 2007; **46**: 628–34.
29. Boursier J, Zarski JP, de Ledinghen V, *et al.* Determination of reliability criteria for liver stiffness evaluation by transient elastography. *Hepatology* 2013; **57**: 1182–91.
30. Gianini EG, Zaman A, Kreil A, *et al.* Platelet count/spleen diameter ratio for the noninvasive diagnosis of esophageal varices: results of a multicenter, prospective, validation study. *Am J Gastroenterol* 2006; **101**: 2511–9.
31. Kim BK, Han KH, Park JY, *et al.* A liver stiffness measurement-based, noninvasive prediction model for high-risk esophageal varices in B-viral liver cirrhosis. *Am J Gastroenterol* 2010; **105**: 1382–90.
32. Berzigotti A, Seijo S, Arena U, *et al.* Elastography, spleen size, and platelet count identify portal hypertension in patients with compensated cirrhosis. *Gastroenterology* 2013b; **144**: 102–11.
33. Fluss R, Faraggi D, Reiser B. Estimation of the Youden index and its associated cutoff point. *Biom J* 2005; **47**: 458–72.
34. Kazemi F, Kettaneh A, N'Kontchou G, *et al.* Liver stiffness measurement selects patients with cirrhosis at risk of bearing large esophageal varices. *J Hepatol* 2006; **45**: 230–5.
35. Nguyen-Khac E, Saint-Leger P, Tramier B, *et al.* Noninvasive diagnosis of large esophageal varices by Fibroscan: strong influence of cirrhosis etiology. *Alcohol Clin Exp Res* 2010; **34**: 1146–53.
36. Bosch J. Predictions from a hard liver. *J Hepatol* 2006; **45**: 174–7.
37. Lemoine M, Katsahian S, Ziolk M, *et al.* Liver stiffness measurement as a predictive tool of clinically significant portal hypertension in patients with compensated hepatitis C virus or alcohol-related cirrhosis. *Aliment Pharmacol Therap* 2008; **28**: 1102–10.
38. Shi KQ, Fan YC, Pan ZZ, *et al.* Transient elastography: a meta-analysis of diagnostic accuracy in evaluation of portal hypertension in chronic liver disease. *Liver Int* 2013; **33**: 62–71.
39. Talwalkar JA, Yin M, Venkatesh S, *et al.* Feasibility of *in vivo* MR elastographic splenic stiffness measurements in the assessment of portal hypertension. *Am J Roentgenol* 2009; **193**: 122–7.
40. Ronot M, Lambert S, Elkrief L, *et al.* Assessment of portal hypertension and high-risk oesophageal varices with liver and spleen three-dimensional multifrequency MR elastography in liver cirrhosis. *Eur Radiol* 2014; **24**: 1394–402.
41. Furuichi Y, Moriyasu F, Taira J, *et al.* Noninvasive diagnostic method for idiopathic portal hypertension based on measurements of liver and spleen stiffness by ARFI elastography. *J Gastroenterol* 2013; **48**: 1061–8.
42. Bota S, Sporea I, Sirli R, *et al.* Spleen assessment by acoustic radiation force impulse elastography (ARFI) for prediction of liver cirrhosis and portal hypertension. *Med Ultrason* 2010; **12**: 213–7.
43. Stefanescu H, Procopet B, Lupsor Platon M, Bureau C. Is there any place for spleen stiffness measurement in portal hypertension? *Am J Gastroenterol* 2013; **108**: 1660–1.
44. Sharma P, Kirnake V, Tyagi P, *et al.* Spleen stiffness in patients with cirrhosis in predicting esophageal varices. *Am J Gastroenterol* 2013; **108**: 1101–7.
45. Calvaruso V, Bronte F, Conte E, *et al.* Modified spleen stiffness measurement by transient elastography is associated with presence of large oesophageal varices in patients with compensated hepatitis C virus cirrhosis. *J Viral Hepatitis* 2013; **20**: 867–74.
46. Giannini E, Botta F, Borro P, *et al.* Platelet count/spleen diameter ratio: proposal and validation of a non-invasive parameter to predict the presence of esophageal varices in patients with liver cirrhosis. *Gut* 2003; **52**: 1200–5.
47. Kim BK, Kim DY, Han KH, *et al.* Risk assessment of esophageal variceal bleeding in B-viral liver cirrhosis by a liver stiffness measurement-based model. *Am J Gastroenterol* 2011; **106**: 1654–62.

Supporting information

Additional Supporting Information may be found in the online version of this article:

Table S1. Baseline characteristics of patients in the training and validation groups. When not otherwise specified, for each variable means (\pm standard deviation) or medians (range) are provided, based on their normal/abnormal distribution as depicted by Shapiro–Wilk test.

Table S2. Performance of the stepwise algorithm in the training group: subgroup analysis according to aetiology and history of previous decompensation.

HEPATOLOGY

Spleen stiffness measurement using fibroscan for the noninvasive assessment of esophageal varices in liver cirrhosis patientsHoria Stefanescu,^{*,†} Mircea Grigorescu,^{*} Monica Lupsor,[†] Bogdan Procopet,^{*} Anca Maniu[†] and Radu Badea[†]Departments of ^{*}Hepatology and [†]Medical Imaging, 3rd Medical Clinic, University of Medicine and Pharmacy, Cluj-Napoca, Romania**Key words**

esophageal varices, liver cirrhosis, noninvasive, spleen stiffness, transient elastography.

Accepted for publication 9 March 2010.

Correspondence

Horia Stefanescu, 3rd Medical Clinic, Iuliu Hatieganu University of Medicine and Pharmacy, 19-21 Croitorilor Street, 400162, Cluj-Napoca, Romania. Email: hstefanescu@umfcluj.ro

This work was funded by the Romanian Authority for Scientific Research through the 2007–2013 National Program for Research, Development and Innovation [grants PNCDI2-PC nr 41-071/2007 and 12-131/2008].

Abstract**Background and Aim:** Splenomegaly is a common finding in liver cirrhosis that should determine changes in the spleen's density because of portal and splenic congestion and/or because of tissue hyperplasia and fibrosis. These changes might be quantified by elastography, so the aim of the study was to investigate whether spleen stiffness measured by transient elastography varies as liver disease progresses and whether this would be a suitable method for the noninvasive evaluation of the presence of esophageal varices.**Patients and Methods:** One hundred and ninety-one patients (135 liver cirrhosis, 39 chronic hepatitis and 17 healthy controls) were evaluated by transient elastography for measurements of spleen and liver stiffness. Cirrhotic patients also underwent upper endoscopy for the diagnosis of esophageal varices.**Results:** Spleen stiffness showed higher values in liver cirrhosis patients as compared with chronic hepatitis and with controls: 60.96 vs 34.49 vs 22.01 KPa ($P < 0.0001$). In the case of liver cirrhosis, spleen stiffness was significantly higher in patients with varices as compared with those without (63.69 vs 47.78 KPa, $P < 0.0001$), 52.5 KPa being the best cut-off value, with an area under the receiver operating characteristic of 0.74. Using both liver and spleen stiffness measurement we correctly predicted the presence of esophageal varices with 89.95% diagnostic accuracy.**Conclusion:** Spleen stiffness can be assessed using transient elastography, its value increasing as the liver disease progresses. In liver cirrhosis patients spleen stiffness can predict the presence, but not the grade of esophageal varices. Esophageal varices' presence can be better predicted if both spleen and liver stiffness measurements are used.**Introduction**

Liver cirrhosis (LC) is the final evolutive stage of any chronic liver disease and its outcomes are modulated by the degree and the consequences of portal hypertension (PH). Unfortunately, clinical investigation of PH is mainly invasive and implies either hepatic vein catheterization and hepatic vein pressure gradient (HVPG) measurement, or endoscopy for esophageal varices (EV) screening and grading. It was previously demonstrated that a HVPG value higher than 10 mmHg predicts the presence of EV, while a value higher than 12 mmHg is predictive for variceal bleeding.¹

Many efforts have been made to find a noninvasive surrogate marker for PH or for the presence or grade of EV, but until now, only a few biochemical markers (aspartate aminotransferase [AST] to platelets ratio index) or mixed indexes (platelets count to spleen diameter ratio) have been demonstrated to be partially correlated with the presence of EV.^{2,3}

Splenomegaly is a common finding in liver cirrhosis and one should expect also changes in the spleen's density, because of tissue hyperplasia and fibrosis^{4,5} and/or because of portal and splenic congestion due to the splanchnic hyperdynamic state.⁶ These changes may be quantified by elastography. Until now, magnetic resonance elastography (MRE) was used with encouraging results in this respect.⁷

Fibroscan uses the principle of one-dimension transient elastography (TE) for the assessment of tissue stiffness. TE was used in chronic liver diseases and was proven to accurately predict liver fibrosis in a variety of clinical conditions^{8–12} and in some studies correlated also with the severity of PH and the presence of esophageal varices.^{13–16} Fibroscan recently started to be used for the assessment of spleen stiffness in cirrhotic patients.^{17,18}

The aim of this study was to investigate whether spleen stiffness, assessed by TE, is a useful tool for grading chronic liver diseases and to compare its performance in predicting the presence

and size of esophageal varices in liver cirrhosis patients with other validated noninvasive approaches (liver stiffness measurement and platelet count to spleen size ratio).

Methods

Patients

One hundred and ninety-one patients were prospectively included in the study: 137 had liver cirrhosis, 37 had HCV chronic hepatitis and 17 were healthy controls.

Controls were selected according to the following criteria: no history of liver disease, negative hepatitis B virus (HBV) and hepatitis C virus (HCV) serology, insignificant alcohol intake, normal ultrasound and laboratory work-up.

All chronic hepatitis (CH) patients had positive serum HCV-RNA and different stages of severity, as shown by the interpretation of fibrosis stage on liver biopsy specimens according to the METAVIR score: F1-32.4%, F2-37.8% and F3-29.7%.

All cirrhotic patients had either HCV, or alcohol-induced liver disease. The majority of them were previously diagnosed by clinical, biochemical and imaging methods, while in a few cases the diagnosis had been histologically proven (HCV infected patients that turned out to have F4 METAVIR fibrosis stage on liver biopsy). Among them, 64.9% were classified as Child-Pugh A, 28.4% as Child-Pugh B and 6.8% as Child-Pugh C class.

All patients underwent transient elastography of both the liver and spleen for the assessment of liver stiffness (LSM) and spleen stiffness (SSM). LC patients were evaluated by upper endoscopy for the assessment of esophageal varices. Routine biological parameters were recorded for every patient according to the follow-up protocol of each condition.

The study was designed to respect all ethical guidelines issued by the 2000 revision (Edinburgh) of the 1975 Declaration of Helsinki. All patients were enrolled for the study after signing an informed consent that was previously revised and approved, together with the study protocol, by the Ethical Committee of the Cluj-Napoca University of Medicine and Pharmacy.

Liver and spleen stiffness measurement

Liver and spleen stiffness measurements were performed using TE (FibroScan, Echosens, Paris, France). The medium probe was used for all patients. For the liver stiffness measurement we used the same technical background and examination procedure as the one that was previously described.⁹ The results were expressed in kilopascals (kPa). Ten successful measurements were carried out on each patient. The success rate was calculated as the number of validated measurements divided by the number of total measurements. The median value of 10 successful measurements was kept as a representative of the liver stiffness, according to the manufacturer's recommendations and previous evidence: interquartile range (IQR) lower than 30% of the median value and success rate of at least 60%.^{19,20}

For assessing the spleen stiffness (SSM) we changed the standard procedure, by having the patient in supine position with his left arm in maximum abduction and by placing the transducer in the left intercostal spaces, usually on the posterior axillary line. The same quality thresholds as for LSM were used (IQR < 30%,

success rate \geq 60%). All stiffness measurements were performed by an experienced operator, with more than 500 examinations of patients with chronic liver diseases.

We used ultrasonography to depict the spleen parenchyma and to choose the right place for SS measurement and to measure the spleen diameters, perimeter and surface for each patient, as well.

Upper endoscopy

All LC patients underwent upper endoscopy, using a flexible EVIS EXERA video gastroscope (Olympus Europa Medical Systems, Hamburg, Germany). Esophageal varices were graded according to their size as follows: (i) grade 1: small, straight esophageal varices; (ii) grade 2: enlarged, tortuous varices occupying less than one third of the lumen; and (iii) grade 3: large, coil-shaped esophageal varices occupying more than one third of the lumen.

Statistical analysis

The statistical analysis was performed using the SPSS software version 15.0 (SPSS Inc. Chicago, IL, USA). The elastographic data were expressed as median values. The distribution of liver and spleen stiffness values in the various classes of patients and on different variceal grades was visually inspected through box plots. The continuous variables were presented as median values and range (minimum and maximum values). The data were compared using the Mann-Whitney *U*-test and the χ^2 test for continuous and categorical variables, respectively. The differences between more than two independent groups were tested by the Kruskal-Wallis test. The relationships between the parameters were characterized using the Spearman correlation coefficients.

The diagnostic performance of LSM and SSM was assessed using sensitivity (Se), specificity (Sp), positive predictive value (PPV), negative predictive value (NPV), accuracy, likelihood ratios (LR) and receiver operating characteristic (ROC) curves. The ROC curve is a plot of sensitivity versus 1-specificity for all possible cutoff values. The most commonly used index of accuracy is the area under the ROC curve (AUROC), with values close to 1 indicating higher diagnostic accuracy. Optimal cutoffs for liver and spleen stiffness were chosen so that the sum of sensitivity and specificity would be maximal; positive and negative predictive values were computed for these values.

Results

The clinical, biological and ultrasonographical characteristics of patients according to their diagnosis are shown in Table 1.

Overall analysis of spleen stiffness in the study population

In 12 patients (three from the CH group and nine from the LC group) no valid SSM recordings could be obtained (success rate = 0) and in another 16 patients (three controls, seven with CH and six with LC) we obtained a success rate < 60%. We tried to analyze the causes that lead to SSM failure, focusing on the spleen size and body mass index and therefore our initial analysis comes from all 191 patients. The main factors influencing the SSM

Table 1 Baseline characteristics of patients

Characteristics of patients	Median (range) or number (%)			<i>P</i>
	Controls	Chronic hepatitis	Cirrhosis	
<i>n</i> (%)	17 (8.9%)	37 (19.4%)	137 (71.7%)	
Male	5 (29.4%)	19 (51.3%)	77 (56.2%)	0.054
Female	12 (70.6%)	18 (48.7%)	60 (43.8%)	
Age (years)	28 (25–33)	46 (18–61)	56 (31–76)	< 0.0001
BMI (kg/m ²)	22.38 (18.07–28.02)	24.7 (19.33–35.19)	26.36 (17.21–36.3)	< 0.0001
AST (U/L)	28 (11–42)	47.5 (22–115)	78 (20–468)	< 0.0001
ALT (U/L)	32 (16–41)	75 (15–249)	60 (11–356)	< 0.0001
Total Bilirubin (mg/dL)	0.71 (0.28–0.98)	0.72 (0.34–1.96)	1.47 (0.44–33.57)	< 0.001
GGT (U/L)	33 (26–75)	32 (17–394)	32 (13–1888)	< 0.0001
ALP (U/L)	184 (132–256)	184 (110–307)	291 (115–996)	< 0.0001
Platelet count (109/L)	187 (156–297)	179 (112–315)	107 (28–393)	< 0.0001
INR	0.99 (0.86–1.26)	1.01 (0.83–1.25)	1.24 (0.85–2.56)	< 0.0001
Spleen-LD (mm)	98.66 (74.3–127.84)	109 (77.02–141.1)	141.1 (80–222)	< 0.0001
Spleen-TD (mm)	45.65 (37.56–63.7)	52.7 (31.2–87.1)	69 (22.7–114.2)	< 0.0001
Spleen Area (cm ²)	38.4 (25.5–52.79)	44.69 (25.69–85.7)	77.85 (27.7–190.72)	< 0.0001
PSR (N/mL/mm)	1940 (1460–2800)	1790 (910–3490)	700 (150–1550)	< 0.001

ALT, alanine aminotransferase; ALP, alkaline phosphatase; AST, aspartate aminotransferase; BMI, body mass index; GGT, gamma-glutamyl-transpeptidase; INR, international normalised ratio; PSR, platelets count to spleen diameter ratio; spleen-LD, spleen longitudinal diameter; spleen-TD, spleen transversal diameter.

Table 2 Main factors that influence the success of spleen stiffness measurement (data are expressed as medians and ranges)

Patients	SR 0%	SR 1–59%	SR ≥ 60%	<i>P</i>
<i>n</i> (%)	12 (6.3)	16 (8.3)	163 (85.4)	
Characteristics				
BMI (kg/m ²)	25.51 (22.86–34.63)	25.46 (17.21–34.19)	25.55 (18.07–36.3)	0.67
Spleen-LD (mm)	109 (80–135)	108 (77–160)	131 (74–222)	0.004
Spleen-SD (mm)	55 (40–69)	60 (37–98)	65 (23–114)	0.08
Spleen area (cm ²)	41 (29–67)	50 (26–111)	73 (26–191)	0.0001

BMI, body mass index; spleen-LD, spleen longitudinal diameter; spleen-TD, spleen transversal diameter; SR, success rate.

success rate are synthesized in Table 2. When analyzing the performance of SSM in predicting the presence of EV, only patients with a success rate ≥ 60% were included and therefore only 122 liver cirrhosis patients were studied further.

Spleen stiffness increased in LC patients when compared with CH ones and with controls, as shown in Figure 1. The median values for SSM in each subgroup were as follows: controls: 17.8 kPa (ranged between 6.9 and 42.08 kPa), CH patients: 33.8 kPa (13–64 kPa), with 54.2 kPa in the LC group (23.4–75 kPa), with an overall *P*-value < 0.0001. The increment was also significant between the two groups, with *P*-value of 0.001 and < 0.0001, respectively.

Noninvasive assessment of esophageal varices in liver cirrhosis patients

All LC patients were screened for the presence of esophageal varices. Following upper endoscopy evaluation, 15.1% of LC patients showed no esophageal varices (V0); 40.9% had grade 1 esophageal varices (V1); 30.8% grade 2 (V2) and 13.2% grade 3 varices (V3). According to the presence of esophageal varices, the LC patients were split into two groups: those with no varices (EV

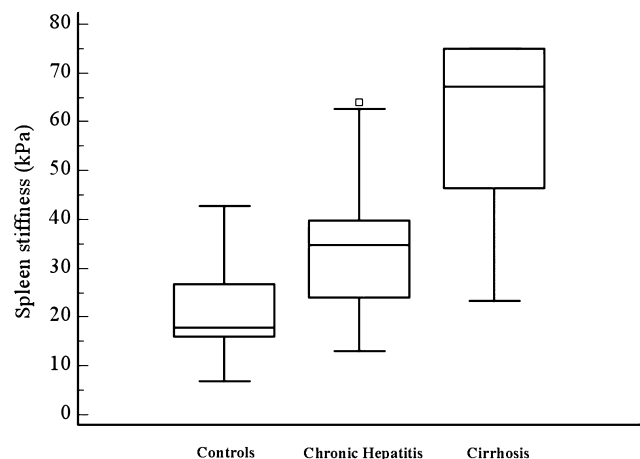


Figure 1 Box plots of spleen stiffness values for controls, chronic hepatitis and cirrhosis patients. The top of the bottom of the boxes are the first and third quartiles, respectively. The length of the box thus represents the interquartile range within which 50% of the values were located. The line through the middle of each box represents the median. The error shows the minimum and maximum values (range).

Table 3 Comparison between the variations of SSM, LSM and PSR in cirrhotic patients according to the presence or absence of esophageal varices (EV) (data are expressed as medians and ranges)

Variable	Patients		P
	EV absent	EV present	
SSM	46.05 (23.7–75)	72 (23.4–75)	0.001
PSR	1210 (550–2130)	650 (150–1990)	0.01
LSM	26.3 (9.9–40.3)	38.4 (12–75)	0.003

EV, esophageal varices; LSM, liver stiffness measurement; PSR, platelets count to spleen diameter ratio; SSM, spleen stiffness measurement.

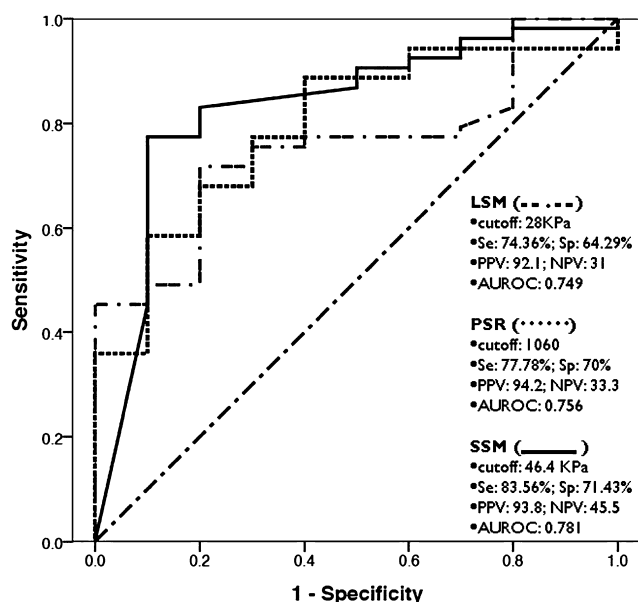


Figure 2 Receiver operating characteristic (ROC) curve representation of platelet count/spleen size ratio (PSR), liver stiffness measurement (LSM) and spleen stiffness measurement (SSM) in distinguishing liver cirrhosis (LC) patients with or without esophageal varices (EV).

absent) and those with varices (EV present). The spleen and liver stiffness, as well as the platelet count/spleen size ratio (PSR) were evaluated and compared in these two groups.

Platelet count to spleen size ratio

Platelet count/spleen size ratio was significantly higher in patients presenting EV compared with those without ($P = 0.01$, Table 2). The best cutoff value in our dataset was 1067 for the prediction of EV, with a diagnostic accuracy of this value of 75.34% and an AUROC of 0.756 (Table 3, Fig. 2).

Liver stiffness

Liver stiffness values constantly increased as the EV grade increased, with significant differences between V0 and any other subgroup $P = 0.021$ (V0–V1); 0.003 (V0–V2); 0.018 (V0–V3).

When comparing V1 with V2 and V3, respectively, no significant difference was observed $P = 0.921$ (V1–V2); 0.730 (V1–V3); 0.992 (V2–V3). On the whole, the median LSM value of patients with EV, regardless of their grade – 38.4 kPa (12–75 kPa), was significantly higher than that of patients with no EV – 26.3 kPa (9.9–40.3 kPa), $P = 0.003$.

For an LSM value higher than 28 kPa we managed to predict the presence of esophageal varices in LC patients with 71.70% diagnostic accuracy, the area under the ROC curve being 0.749. The detailed diagnostic performance and AUROC analysis of LSM in predicting EV is shown in Table 3 and Figure 2.

Spleen stiffness

The median value of SSM for patients with no varices (V0) was 46.05 kPa (ranging from 23.7 to 75 kPa), 63.15 kPa (23.4–75 kPa) for patients with grade 1 varices (V1), 63.91 kPa (34.8–75 kPa) for patients with grade 2 varices (V2) and 64.9 kPa (33.3–75 kPa) for grade 3 varices patients. No significant difference could be observed between V1, V2, V3 subgroups, but when comparing patients with no varices to those with esophageal varices, regardless of grade, a strong significant difference was noted ($P < 0.001$). A detailed view of these data can be found in Table 4 and in Figure 3.

For an SSM value higher than 46.4 kPa we managed to predict the presence of esophageal varices in LC patients with 80.45% diagnostic accuracy, the AUROC being 0.781. The detailed diagnostic performance and AUROC analysis of SSM in predicting EV is shown in Table 3 and in Figure 2.

In our liver cirrhosis population, SSM was significantly correlated with LSM (moderate/good positive Spearman analysis): overall $r = 0.424$, $P < 0.0001$; LC patients with no EV $r = 0.587$, $P = 0.027$; LC patients with EV $r = 0.412$, $P < 0.001$. Simultaneously, the SSM exhibited a moderate/poor negative correlation with PSR when looking at the entire LC population ($r = -0.314$, $P < 0.003$), but this was not significant when looking at the absent EV subgroup: $r = -0.423$, $P = 0.223$, or at the EV present subgroup: $r = -0.220$, $P = 0.098$.

Combined analysis of SSM and LSM in predicting esophageal varices in LC patients

Further on, we attempted to appreciate the performance of SSM combined with LSM in predicting the presence of EV in cirrhotic patients. We imagined a ‘step by step’ approach for selecting patients with high susceptibility for developing EV: we moved along the LSM ROC curve so as to choose a cutoff value of high sensitivity – 19 kPa (Se 92.21%), and then on the SSM ROC so as to choose a high specificity value for the presence of EV – 55 kPa (Sp 78.57%). Using these LSM and SSM values, we managed to predict the presence of esophageal varices in liver cirrhosis patients with a diagnostic accuracy of 88.52% (Table 4).

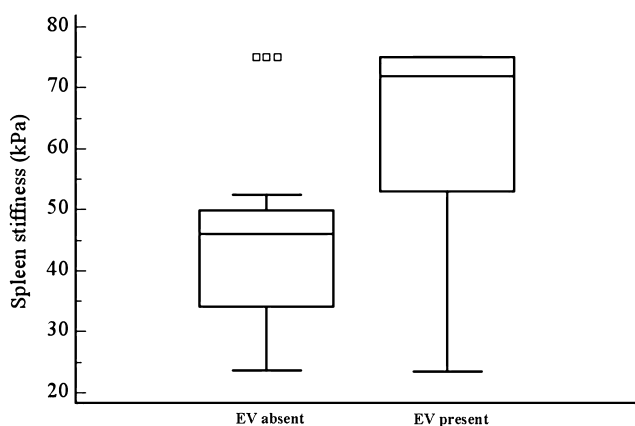
Discussion

Noninvasive assessment of portal hypertension has become an issue of growing importance over the past years. Although HVPG measurement and endoscopy are considered the standard of care in patients suffering from liver cirrhosis, alternative surrogate

Table 4 Comparative analysis of platelets to spleen size ratio, spleen stiffness, liver stiffness and combination of both in predicting the presence of esophageal varices in liver cirrhosis patients

	PSR	LSM	SSM	LSM+SSM
Cutoff value	≤ 1068	> 28	> 46.4	LSM > 19 kPa SSM > 55 kPa
Se (%)	77.78	74.36	83.56	92.85
Sp (%)	70	64.29	71.43	40
+LR	2.59	2.08	2.92	1.547
-LR	0.32	0.40	0.23	0.178
PPV	94.2	92.1	93.8	94.54
NPV	33.3	31.0	45.5	33.33
Diagnostic accuracy (%)	75.34	71.73	80.45	88.52

LR, likelihood ratio; LSM, liver stiffness measurement; NPV, negative predictive value; PPV, positive predictive value; PSR, platelets count to spleen diameter ratio; SSM, spleen stiffness measurement.

**Figure 3** Box plots showing the increment of spleen stiffness measurement (SSM) in liver cirrhosis (LC) patients with esophageal varices (EV) as compared with those without.

markers are being imagined for the appreciation of the severity of disease, the presence of complications, or the response to treatment. Until now, the liver stiffness and platelet count to spleen size ratio have been proposed and validated as predictors for the EV. Although splenomegaly is common in liver cirrhosis, this finding was considered only in terms of size, and not as a complex change. The splenomegaly developing in the context of liver cirrhosis is commonly ascribed to blood congestion, but older studies demonstrated that it cannot be considered only as a consequence of increased portal pressure and augmented resistance to splenic vein outflow.²¹ Surprisingly, no relationship could be found between the spleen size and the degree of esophageal varices.²² Multiple studies demonstrated pooling of blood in the red pulp, intraparenchymal arterial aneurysms,²³ and other multiple histopathologic changes, which evolve towards diffuse fibrosis of the spleen,²⁴ more likely because of endothelin overexpression and changes in the balance of endothelin receptors.²⁵ Association with viral liver cirrhosis suggests an immunologic pathway.²⁶ In patients who underwent liver transplantation, despite the important decrease of the outflow resistance of the splenic vein, only a slight decrease in spleen size could be observed, probably due to persistence of the hyperplastic

component.²⁷ So, in our view, it is only logical to presume that the increment in size should determine changes in the spleen's density as well, which is a physical parameter that may be quantified by elastography. We used transient elastography to measure the spleen stiffness and we were trying to demonstrate that SSM is a useful tool for grading chronic liver disease and to compare its performance in predicting the presence of EV in liver cirrhosis patients with other validated noninvasive approaches.

Recently spleen stiffness was identified as a potential surrogate marker for portal hypertension. A study²⁸ that examined whether MRE could accurately measure portal hypertension in 35 patients with varying degrees of chronic liver disease and 12 healthy volunteers, found a highly significant correlation between liver and spleen stiffness in patients with portal hypertension. As far as the SSM using transient elastography is concerned, only two reports have been presented so far. The first one¹⁷ showed an important increase of SSM values in LC patients compared with controls and the strong correlation of SSM with a previously proven surrogate marker for PH (platelet/spleen size ratio) in the same group of patients. The other one,¹⁸ adding SSM to the usual LSM evaluation of chronic liver disease patients, and using two different thresholds, managed to increase the Se and PPV of TE in detecting liver cirrhosis and the presence of EV; it concluded that SSM is independent from LSM and its assessment increases the accuracy of TE as a noninvasive diagnostic tool for cirrhosis and PH. Our data clearly suggest that in the natural history of chronic liver disease, starting from the healthy liver and reaching chronic hepatitis and finally liver cirrhosis, there is a significant increase in spleen stiffness; furthermore, in the case of liver cirrhosis we managed to find a cutoff value (46.4 kPa) with a good AUROC (0.781), which is predictive for the presence of esophageal varices and which correlated with other noninvasive markers for EV (LSM and PSR). We also showed that the spleen stiffness is a variable that can easily be acquired in chronic liver disease patients, provided the spleen is large enough to 'fit' into the acquisition window. Although it is widely accepted that obesity is one of the factors strongly associated with failure of liver stiffness measurement, in our population (having only a moderately increased median BMI), we demonstrated (Table 2) that the spleen longitudinal diameter and spleen area were significantly lower in patients with SSM failure, suggesting that the most important success factor is the access to the spleen.

The relationship between liver stiffness and portal hypertension and/or esophageal varices was the subject of several studies analyzing LSM as a marker for the grade of esophageal varices. These studies found in some situations a good correlation^{29,30} or no correlation at all,¹⁶ or looked at LSM from the HVPG point of view.^{13–16} LSM was found to be a good predictor, having the area under the ROC curve varying from 0.76 to 0.84 in some studies.^{16,19,30} Depending on the cutoff value used (13.9 kPa, 17.6 kPa or 21.3 kPa, respectively) the sensitivity for predicting the presence of EV decreased from 95% down to 79%, and the specificity increased from 43% up to 70%. Using a higher cutoff value (30.5 kPa), it was possible to predict large EV (\geq grade 2) with an acceptable sensitivity and specificity (76% and 80%, respectively), but the positive predictive value did not exceed 54%. These results were critically analyzed in a review³¹ that noticed some important aspects: the evaluation of the EV grade is subjective, and none of the above cited studies mentioned data on the quality of endoscopic evaluation; the cutoff value of LS for predicting EV is still a matter of debate since the results were not prospectively validated on independent cohorts; and the specificity and positive predictive values reported so far are too low to allow their use in current clinical practice.

Our data on this issue are even more confusing. For a higher cutoff value (28 kPa), the AUROC in our study is only 0.749. Nevertheless, the diagnostic accuracy is acceptable (71.73%) and the Se and Sp as well (74.36% and 64.29%, respectively). It is worth mentioning that the PPV was 92.1% for the presence of EV, but unfortunately we did not manage to distinguish between different EV grades. Our unsatisfactory performance may be explained by three possible factors: (i) the subjective assessment of the size of esophageal varices on endoscopy; (ii) the unequal distribution of patients according to the EV grade, leading to differently sized subgroups of patients; and (iii) the fact that the endoscopic and LSM evaluation were not always concurrent, since we enrolled some patients presenting for their cirrhosis follow-up, which did not necessarily include endoscopy. Taking into account the so-far available data, it can be concluded that liver stiffness alone is not reliable enough to be used as a screening method to detect the EV grade in liver cirrhosis patients, so as to avoid unnecessary endoscopies,³² which is a strong argument for the initiation of new studies on the subject.

It has been proven that a platelet count to spleen diameter ratio higher than 909 is a good predictor of the presence of esophageal varices in LC patients.³ These data were further validated in a prospective multicenter trial³³ that showed for the proposed cutoff value a very good sensitivity and diagnostic accuracy (91.5% and 86%, respectively) but a modest specificity (67%). However, a recent independent study³⁴ using the same cutoff value found a negative predictive value of only 73% and a positive predictive value of 74%, concluding that PSR with a cutoff value of 909 may not be sufficiently accurate in predicting the presence of esophageal varices. Our findings seem to favor the latter conclusion, since despite the relatively good AUROC and diagnostic accuracy (see Fig. 2 and Table 4) the NPV reached only 33%. However, our best cutoff value was 1068 (Se = 77.78% and Sp = 70%) while the proposed value (909) in our patients showed a Se of only 66.67% and a similar Sp.

As a drawback of our study and as a preliminary conclusion on spleen stiffness measurement, we must state that the results we

obtained seem to be influenced by the intrinsic characteristics of the machine (FibroScan). As described earlier, the upper SSM limit reached the highest value measurable by the device (75 kPa) in each group of LC patients, regardless of their variceal status or the grade of their varices. Thus, we have to face a significant interpolation between the patient groups. If the FibroScan had measured values beyond 75 kPa, we would possibly have obtained better figures after analyzing the data.

We believe that using TE to measure both liver and spleen stiffness ensures a better prediction of the presence of esophageal varices. We propose a simple TE algorithm: first perform a liver stiffness measurement; if higher than 19 kPa, consider liver cirrhosis with clinically significant PH (EV present). Next measure the spleen stiffness as well; if higher than 55 kPa, it is highly probable to find esophageal varices at endoscopy (diagnostic accuracy of 88.5%). Table 4 clearly shows the high PPV of this approach (94.54%) and its satisfactory -LR (0.178), suggesting that a patient with a LSM < 19 kPa and SSM < 55 kPa is unlikely to have esophageal varices. Of course, there is still the case of the patients with LSM > 19 kPa and SSM < 55 kPa, whose esophageal varices status cannot be predicted with sufficient accuracy and who have a strong indication for gastroscopy. However, before making any recommendations, these findings need further and extensive internal and external validation.

This is the first extensive report on this issue, although performed on a limited number of cases. However, we may safely conclude that the spleen stiffness can be assessed using transient elastography, the main factor influencing the measurement being the spleen size. Spleen stiffness increases as the liver disease worsens, evolving from the normal liver to chronic hepatitis and to liver cirrhosis. In liver cirrhosis patients SSM, similarly to LSM, can predict the presence, but not the grade of esophageal varices, with good diagnostic accuracy. Using a combined approach (both liver and spleen stiffness measurement) we can obtain a better discrimination and a higher diagnostic accuracy in predicting the presence of esophageal varices in this category of patients.

References

- 1 Bosch J, Garcia-Pagan JC, Berzigotti A, Abraldes JG. Measurement of portal pressure and its role in the management of chronic liver disease. *Semin. Liver Dis.* 2006; **26**: 348–62.
- 2 Wai CT, Greenon JL, Fontana RJ *et al.* A simple noninvasive index can predict both significant fibrosis and cirrhosis in patients with chronic hepatitis C. *Hepatology* 2003; **38**: 518–26.
- 3 Giannini E, Botta F, Borro P *et al.* Platelet count/spleen diameter ratio: proposal and validation of a non-invasive parameter to predict the presence of esophageal varices in patients with liver cirrhosis. *Gut* 2003; **52**: 1200–5.
- 4 Bolognesi M, Boscato N. Spleen and liver cirrhosis: relationship between spleen enlargement and portal hypertension in patients with liver cirrhosis. In: Chen TM, ed. *New Developments in Liver Cirrhosis Research*. Hauppauge, NY: Nova Science Publishers, 2006; 49–67.
- 5 Bolognesi M, Merkel C, Sacerdoti D, Nava V, Gatta A. The role of spleen enlargement in cirrhosis with portal hypertension. *Dig. Liver Dis.* 2002; **34**: 144–50.
- 6 Kuddus RH, Nalesnik MA, Subbotin VM, Rao AS, Gandhi CR. Enhanced synthesis and reduced metabolism of endothelin 1 (ET-1)

- by hepatocytes—an important mechanism of increased endogenous levels of ET-1 in liver cirrhosis. *J. Hepatol.* 2000; **33**: 725–32.
- 7 Yin M, Talwalkar JA, Glaser KJ. A preliminary assessment of hepatic fibrosis with magnetic resonance elastography. *Clin. Gastroenterol. Hepatol.* 2007; **5**: 1207–13.e2.
 - 8 Sandrin L, Fourquet B, Hasquenoph JM *et al.* Transient elastography: a new noninvasive method for assessment of hepatic fibrosis. *Ultrasound. Med. Biol.* 2003; **29**: 1705–13.
 - 9 Zioli M, Handra-Luca A, Kettaneh A *et al.* Noninvasive assessment of liver fibrosis by measurement of stiffness in patients with chronic hepatitis C. *Hepatology* 2005; **41**: 48–54.
 - 10 Foucher J, Chanteloup E, Vergniol J *et al.* Diagnosis of cirrhosis by transient elastography (FibroScan): a prospective study. *Gut* 2006; **55**: 403–8.
 - 11 Ganne-Carrie N, Zioli M, de Ledinghen V *et al.* Accuracy of liver stiffness measurement for the diagnosis of cirrhosis in patients with chronic liver diseases. *Hepatology* 2006; **44**: 1511–17.
 - 12 Lupsor M, Badea R, Stefanescu H *et al.* Analysis of histopathological changes that influence liver stiffness in chronic hepatitis C. Results from a cohort of 324 patients. *J. Gastrointest. Liver Dis.* 2008; **17**: 155–63.
 - 13 Carrion JA, Navasa M, Bosch J, Bruguera M, Gilibert R, Forns X. Transient elastography for diagnosis of advanced fibrosis and portal hypertension in patients with hepatitis C recurrence after liver transplantation. *Liver Transpl.* 2006; **12**: 1791–8.
 - 14 Bureau C, Metivier S, Peron JM *et al.* Prospective assessment of liver stiffness for the non-invasive prediction of portal hypertension (abstract). *J. Hepatol.* 2007; **46**: S34.
 - 15 Lemoine M, Katsahian S, Nahon P *et al.* Liver stiffness measurement is correlated with hepatic venous pressure gradient in patients with uncomplicated alcoholic and/or HCV related cirrhosis (abstract). *Hepatology* 2006; **44**: 204A.
 - 16 Vizzutti F, Arena U, Romanelli RG *et al.* Liver stiffness measurement predicts severe portal hypertension in patients with HCV-related cirrhosis. *Hepatology* 2007; **45**: 1290–7.
 - 17 Stefanescu H, Lupsor M, Grigorescu M, Procopet B, Maniu A, Badea R. Transient elastography of the spleen as non-invasive assessment of portal hypertension in liver cirrhosis patients. Poster abstract nr 63, Proceedings of EASL Monothematic Conference Portal Hypertension: Advances in Knowledge, Evaluation and Management, Budapest, 2009, p. 130.
 - 18 Di Marco V, Bronte F, Calvaruso V *et al.* Fibrospleen: measuring spleen stiffness by transient elastography increases accuracy of staging liver fibrosis and of portal hypertension in chronic viral hepatitis (abstract). *Dig. Liver Dis.* 2009; **41**: A38.
 - 19 Castera L, Forns X, Alberti A. Non-invasive evaluation of liver fibrosis using transient elastography. *J. Hepatol.* 2008; **48**: 835–47.
 - 20 Kettaneh A, Marcellin P, Douvin C *et al.* Features associated with success rate and performance of fibroscan measurements for the diagnosis of cirrhosis in HCV patients: a prospective study of 935 patients. *J. Hepatol.* 2007; **46**: 628–34.
 - 21 Merkel C, Gatta A, Arnaboldi L, Zuin R. Splenic haemodynamics and portal hypertension in patients with liver cirrhosis and spleen enlargement. *Clin. Physiol.* 1985; **5**: 531–9.
 - 22 Sheth SG, Amarapurkar DN, Chopra KB, Mani SA, Mehta PJ. Evaluation of splenomegaly in portal hypertension. *J. Clin. Gastroenterol.* 1996; **22**: 28–30.
 - 23 Kreef L, Williams RA. Arterio-venography of the portal system. *Br. Med. J.* 1964; **2**: 1500–3.
 - 24 Manenti A, Botticelli A, Gibertini G, Botticelli L. Experimental congestive splenomegaly: histological observations in rats. *Pathologica* 1993; **85**: 721–4.
 - 25 Pinzani M, Milani S, De Franco R, Grappone C, Caligiuri A, Gentilini A. Endothelin 1 is overexpressed in human cirrhotic liver and exerts multiple effects on activated stellate cells. *Gastroenterology* 1996; **110**: 534–48.
 - 26 Gibson PR, Gibson RN, Dithfield MR, Donlan JD. Splenomegaly—an insensitive sign of portal hypertension. *Aust. N. Z. J. Med.* 1990; **20**: 326–45.
 - 27 Bolognesi M, Sacerdoti D, Bombonato G *et al.* Changes in portal flow after liver transplantation: effect on hepatic arterial resistance indices and role of spleen size. *Hepatology* 2002; **35**: 601–8.
 - 28 Talwalkar J. Evaluation of fibrosis and portal hypertension: non-invasive assessment. Oral presentation abstract, Proceedings of EASL Monothematic Conference Portal Hypertension: Advances in Knowledge, Evaluation and Management, Budapest, 2009, p. 47.
 - 29 Castera L, LeBail B, Roudot-Thoraval F *et al.* Early detection in routine clinical practice of cirrhosis and oesophageal varices in chronic hepatitis C: Comparison of transient elastography (FibroScan) with standard laboratory tests and non-invasive scores. *J. Hepatol.* 2009; **50**: 59–68.
 - 30 Kazemi F, Kettaneh A, N'Kontchou G *et al.* Liver stiffness measurement selects patients with cirrhosis at risk of bearing large esophageal varices. *J. Hepatol.* 2006; **45**: 230–5.
 - 31 Bosch J. Predictions from a hard liver. *J. Hepatol.* 2006; **45**: 174–7.
 - 32 Bureau C, Metivier S, Peron JM *et al.* Transient elastography accurately predicts presence of significant portal hypertension in patients with chronic liver disease. *Aliment. Pharmacol. Ther.* 2008; **27**: 1261–8.
 - 33 Gianini EG, Zaman A, Kreil A *et al.* Platelet count/spleen diameter ratio for the noninvasive diagnosis of esophageal varices: results of a multicenter, prospective, validation study. *Am. J. Gastroenterol.* 2006; **101**: 2511–19.
 - 34 Schwartzberg E, Meyer T, Golla V, Sahdala NP, Min AD. Utilization of platelet count spleen diameter ratio in predicting the presence of esophageal varices in patients with cirrhosis. *J. Clin. Gastroenterol.* 2010; **44**: 146–50.

Bidimensional shear wave ultrasound elastography with supersonic imaging to predict presence of oesophageal varices in cirrhosis

We read with great interest the manuscript by Jansen et al.,¹ recently published in *Liver International*. In keeping with their findings, we also hold liver and spleen elastography (L/S-2D-SWE) as important tools for the non-invasive assessment of cirrhotic patients. In their work, Jansen¹ did not assess the prediction of complications of CSPH, like presence of oesophageal varices (EV). The Baveno VI consensus states that EV may be ruled-out when liver stiffness (measured by transient elastography) is <20 kPa and concurrently platelet (PLT) count >150 × 10³/mL.² New elastography technologies, embedded in conventional ultrasound scanners, such as 2D-SWE with Aixplorer® Supersonic Imagine (2D SWE.SSI) are appealing, but have not been tested in connection with the Baveno VI recommendations.

For this reason, we prospectively tested the role of L/S-2D-SWE.SSI in ruling out EVs in a cohort of 73 compensated cirrhotic patients and approved by the Ethical Committee of our hospital (93/2013/U/Sper). Forty-four out of 73 patients (60.27%) had EV.

L-2D-SWE, S-2D-SWE and PLT had a modest accuracy to predict the presence of EV when tested individually, showing AUCs of 0.753 (95% CI: 0.623-0.883), 0.747 (95% CI: 0.617-0.876) and 0.773 (95% CI: 0.648-0.898), at best cut-off values of 19 kPa, 38 kPa and 100 × 10³/mL, respectively.

In the settings of Baveno VI recommendations, L-2D-SWE.SSI (<20 kPa) and PLT (>150 × 10³) ruled-out EV with 68.50% accuracy (80% PPV; 95.45% specificity). Adopting instead our own cut-off values (L-2D-SWE.SSI < 19 kPa; PLT > 100 × 10³), EV were ruled-out with 76.71% overall accuracy (87.50% PPV and 95.45% specificity).

Considering a stepwise approach (L-2D SWE.SSI < 19 and PLT > 100 × 10³ = no EV; L-2D-SWE.SSI > 19 and PLT < 100 × 10³ = EV probable), 34 patients remained in the grey zone (L-2D-SWE.SSI < 19 and PLT < 100 × 10³ or L-2D-SWE.SSI > 19 and PLT > 100 × 10³). S-2D-SWE.SSI (</≥ 38 kPa) was used to further classify these patients falling in the grey zone. With this refined algorithm, EV were ruled-out with 83.07% accuracy (77.8% PPV; 84.6% specificity; 86.8% NPV; 80.8% sensitivity) and 54/73 (74%) endoscopies could have been spared overall.

These data confirm the conclusion of Jansen et al.,¹ pointing out L/S-2D-SWE as a robust clinical tool for the management of cirrhotic

patients. Although both sets of results still need external validations, L/S-2D-SWE.SSI appears to be a promising non-invasive technique for the assessment of CSPH and EVs in patients with compensated advanced chronic liver diseases. The best cut-off values to be used in the Baveno VI algorithm are still to be agreed and validated in the instance of newer shear-wave elastography machines.

CONFLICT OF INTEREST

The authors do not have any disclosures to report.

FUNDING INFORMATION

HS was financed by European Commission, through the FP7-PEOPLE(Marie Curie)-2013-IAPP project "CLEVER" (Grant Agreement No.: 612273).

Horia Stefanescu^{1,2} 

Giulia Allegretti¹

Veronica Salvatore¹

Fabio Piscaglia¹ 

¹Unit of Internal Medicine, Department of Medical and Surgical Sciences, University of Bologna, Bologna, Italy

²Hepatology Unit, Regional Institute of Gastroenterology and Hepatology, Cluj Napoca, Romania

REFERENCES

- Jansen C, Bogs C, Verlinden W, et al. Shear-wave elastography of the liver and spleen identifies clinically significant portal hypertension: a prospective multi-center study. *Liver Int.* 2017;37:396-405.
- de Franchis R, Baveno VI Faculty. Expanding consensus in portal hypertension: report of the Baveno VI Consensus Workshop: stratifying risk and individualizing care for portal hypertension. *J Hepatol.* 2015;63:743-752.



Development and prognostic relevance of a histologic grading and staging system for alcohol-related liver disease

Carolin Lackner^{1,*,&§}, Rudolf E. Stauber^{2,§}, Susan Davies^{3,&}, Helmut Denk^{1,&},
Hans Peter Dienes^{4,&}, Viviane Gnemmi^{5,&}, Maria Guido^{6,&}, Rosa Miquel^{7,&},
Valerie Paradis^{8,9,10,&}, Peter Schirmacher^{11,&}, Luigi Terracciano^{12,&}, Andrea Berghold¹³,
Gudrun Pregartner¹³, Lukas Binder², Philipp Douschan², Florian Rainer², Stephan Sygulla¹,
Marion Jager¹⁴, Pierre-Emmanuel Rautou¹⁴, Andreea Bumbu^{15,16}, Adelina Horhat^{15,16},
Ioana Rusu^{17,&}, Horia Stefanescu^{15,16}, Sönke Detlefsen^{18,19,&}, Aleksander Krag^{19,20},
Maja Thiele^{19,20}, Helena Cortez-Pinto²¹, Christophe Moreno²², Annette S.H. Gouw^{23,&§},
Dina G. Tiniakos^{24,25,&§}

¹Institute of Pathology, Medical University of Graz, Austria; ²Division of Gastroenterology and Hepatology, Department of Internal Medicine, Medical University of Graz, Graz, Austria; ³Department of Histopathology, Cambridge University Hospitals NHS Foundation Trust, Cambridge, United Kingdom; ⁴Department of Pathology, Medical University of Vienna, Vienna, Austria; ⁵Université Lille, Canther, Inserm, UMR-S 1277, CHU Lille, Service de Pathologie, Lille, France; ⁶Department of Medicine - DIMED, University of Padova, Padova, Italy; ⁷Liver Histopathology Laboratory, Institute of Liver Studies, King's College Hospital, London, United Kingdom; ⁸Assistance Publique-Hôpitaux de Paris, Service d'Anatomie et de Cytologie Pathologiques, Hôpital Universitaire Beaujon, France; ⁹Université Paris Diderot, CNRS, Centre de Recherche sur l'Inflammation (CRI), Paris, France; ¹⁰Département Hospitalo-Universitaire (DHU) UNITY, Clichy, France; ¹¹Institute of Pathology, University Hospital Heidelberg, Heidelberg, Germany; ¹²Anatomic Pathology Institute, Humanitas University Research Hospital, Rozzano (Milano), Italy; ¹³Institute for Medical Informatics, Statistics and Documentation, Medical University of Graz, Graz, Austria; ¹⁴Université de Paris, AP-HP, Hôpital Beaujon, Service d'Hépatologie, DMU DIGEST, Centre de Référence des Maladies Vasculaires du Foie, FILFOIE, ERN RARE-LIVER, Centre de recherche sur l'inflammation, Inserm, UMR 1149, Paris, France; ¹⁵Liver Unit, Regional Institute of Gastroenterology and Hepatology, Cluj-Napoca, Romania; ¹⁶Liver Research Club, Cluj-Napoca, Romania; ¹⁷University of Medicine and Pharmacy "Iuliu Hatieganu", Cluj-Napoca, Romania; ¹⁸Department of Pathology, Odense University Hospital, Odense C, Denmark; ¹⁹Department of Clinical Research, Faculty of Health Sciences, University of Southern Denmark, Odense C, Denmark; ²⁰Department of Gastroenterology and Hepatology and OPEN, Odense Patient data Explorative Network, Odense University Hospital, Odense C, Denmark; ²¹Clínica Universitária de Gastroenterologia, Laboratório de Nutrição, Faculdade de Medicina, Universidade de Lisboa, Portugal; ²²Department of Gastroenterology, Hepatopancreatology and Digestive Oncology, CUB Hôpital Erasme, Université Libre de Bruxelles, Bruxelles, Belgium; ²³Dept. of Pathology and Medical Biology, University Medical Center Groningen, Groningen, Netherlands; ²⁴Transitional and Clinical Research Institute, Newcastle University, Newcastle upon Tyne NE2 4HH, UK; ²⁵Department of Pathology, Aretaieio Hospital, Medical School, National & Kapodistrian University of Athens, Athens 11528, Greece

Background & Aims: The SALVE Histopathology Group (SHG) developed and validated a grading and staging system for the clinical and full histological spectrum of alcohol-related liver disease (ALD) and evaluated its prognostic utility in a multinational cohort of 445 patients.

Methods: SALVE grade was described by semiquantitative scores for steatosis, activity (hepatocellular injury and lobular neutrophils) and cholestasis. The histological diagnosis of steatohepatitis due to ALD (histological ASH, hASH) was based on the presence of hepatocellular ballooning and lobular neutrophils. Fibrosis staging was adapted from the Clinical Research Network staging system for non-alcoholic fatty liver disease and the Laennec staging system and reflects the pattern and extent of

ALD fibrosis. There are 7 SALVE fibrosis stages (SFS) ranging from no fibrosis to severe cirrhosis.

Results: Interobserver κ -value for each grading and staging parameter was >0.6 . In the whole study cohort, long-term outcome was associated with activity grade and cholestasis, as well as cirrhosis with very broad septa (severe cirrhosis) ($p < 0.001$ for all parameters). In decompensated ALD, adverse short-term outcome was associated with activity grade, hASH and cholestasis ($p = 0.038, 0.012$ and 0.001 , respectively), whereas in compensated ALD, hASH and severe fibrosis/cirrhosis were associated with decompensation-free survival ($p = 0.011$ and 0.001 , respectively). On multivariable analysis, severe cirrhosis emerged as an independent histological predictor of long-term survival in the whole study cohort. Severe cirrhosis and hASH were identified as independent predictors of short-term survival in decompensated ALD, and also as independent predictors of decompensation-free survival in compensated ALD.

Conclusion: The SALVE grading and staging system is a reproducible and prognostically relevant method for the histological assessment of disease activity and fibrosis in ALD.

Lay summary: Patients with alcohol-related liver disease (ALD) may undergo liver biopsy to assess disease severity. We

Keywords: Alcohol-related liver disease; prognosis; grading; staging; cholestasis.
Received 8 July 2020; received in revised form 18 April 2021; accepted 11 May 2021;
available online 11 June 2021

* Corresponding author. Address: Institute of Pathology, Medical University of Graz, Neue Stiftingtalstraße 6, 8010 Graz, Austria; Tel.: +43 316 385 71739, fax: +43 316 385 79000.

E-mail address: karoline.lackner@medunigraz.at (C. Lackner).

§ C. Lackner and R. E. Stauber share first authorship.

§ A. S. H. Gouw and D. G. Tiniakos share senior authorship.

& Members of the SALVE Histopathology Group.

<https://doi.org/10.1016/j.jhep.2021.05.029>



developed a system to classify ALD under the microscope by grading ALD activity and staging the extent of liver scarring. We validated the prognostic performance of this system in 445 patients from 4 European centers.

© 2021 The Authors. Published by Elsevier B.V. on behalf of European Association for the Study of the Liver. This is an open access article under the CC BY license (<http://creativecommons.org/licenses/by/4.0/>).

Introduction

Alcohol abuse is a major global health concern, being a frequent cause of chronic liver disease, cirrhosis, hepatocellular carcinoma and indication for liver transplantation. Alcohol-related liver disease (ALD) shows a spectrum of liver pathology ranging from steatosis to steatohepatitis and fibrosis.¹ For the sake of clarity, steatohepatitis related to ALD² is referred to as histological alcoholic steatohepatitis (hASH) in this manuscript, to differentiate it from non-alcoholic steatohepatitis and it is not synonymous with the clinical scenario of alcoholic hepatitis.

Clinically, steatosis is associated with few, if any, symptoms and has a low risk of progression, whereas hASH is a major driver of fibrogenesis and disease progression. In turn, progression can be associated with clinical abnormalities, development of cirrhosis and hepatocellular carcinoma. Severe symptoms may be due to decompensation of cirrhosis and/or clinical alcoholic hepatitis the latter being associated with 3-month mortality rates of 20–50%.^{2,3} As clinical ALD classifications may correspond poorly with histology,⁴ EASL Clinical Practice Guidelines for the Management of ALD recommend liver biopsy in cases where the diagnosis of ALD is uncertain in both clinical practice and clinical trials.²

Standardized and reproducible assessment of disease activity and fibrosis is a prerequisite for histology-based patient stratification, prognosis and monitoring of treatment effects. Several histological grading and staging systems have been developed for use in chronic liver disease including non-alcoholic fatty liver disease (NAFLD)^{5,6} and viral hepatitis.^{7,8} Although ALD is among the most frequent of liver diseases and its morphological features are well described, few proposals for specific grading and staging systems have been made¹ and a universally accepted system for the full clinical spectrum of ALD is currently lacking.

As ALD and NAFLD show histological overlap, some have proposed applying NAFLD grading and staging systems for ALD,⁹ but several prognostically relevant ALD features, like cholestasis, Mallory-Denk bodies (MDB) and megamitochondria, are not considered in NAFLD grading.¹⁰ Further, the vast majority of patients with ALD have cirrhosis at first presentation¹¹ in contrast to patients with NAFLD in whom it is infrequent.¹² Histological substages of cirrhosis^{13,14} and the extent of pericellular fibrosis (PCF)¹⁵ are prognostically relevant in ALD but are not reflected in current NAFLD staging systems. Finally, ALD is associated with fibro-obliteration of hepatic veins, perivenular fibrosis and sclerosing hyaline necrosis, all predictors of progression and adverse prognosis which are rare in NAFLD.^{16,17}

A group of European liver pathologists, members of the EASL-endorsed consortium for the Study of Alcohol-related LiVer disease in Europe (SALVE), comprising the SALVE Histopathology Group (SHG), convened to design a morphological grading and staging system valid for the whole clinical spectrum of the disease and evaluated its prognostic utility.

Patients and methods

Study cohort

A previously described retrospective cohort with clinical and histologically confirmed ALD, the Graz cohort,¹¹ was used to design the morphological grading and staging system and to assess interobserver variation. The prognostic utility of the grading and staging system was then evaluated in the Graz cohort and 3 additional cohorts from SALVE centres in Odense (Odense University Hospital, Denmark), Paris (Hôpital Beaujon, Clichy, France), and Cluj-Napoca (Regional Institute of Gastroenterology and Hepatology, Cluj-Napoca, Romania). Patients in the Graz cohort underwent liver biopsy for diagnosis and/or staging of liver disease. The Paris and Cluj cohorts included consecutive patients undergoing liver biopsy for suspicion of clinical alcoholic hepatitis. The Odense cohort included patients from a prospective diagnostic study on patients with compensated ALD in Southern Denmark.^{18,19} Patients received standard of care or, if needed, intensive care support.

Follow-up data on survival and liver transplantation were available for all patients. Length of survival and cause of death were documented based on data from hospitals, family practitioners and national death registries. Data on abstinence during follow-up were available in 323 out of 445 patients. In addition, data on liver-related events were collected in the subgroup of patients with compensated ALD. All studies received approval by the local Ethics Committees of all centres. Informed consent was obtained in accordance with the Declaration of Helsinki.

Design of the SALVE grading and staging system

The SALVE grading and staging system was based on (i) characteristic morphological features of ALD, (ii) previously reported independent prognostic parameters of grade^{15,20,21} and stage,^{11,14,22} and (iii) at least substantial interobserver agreement as documented in the literature or according to the results of studies by the SHG (described below). For the Graz cohort, morphological evaluations were carried out by members of the SHG in consensus using a multiheaded microscope. Scanned liver biopsy slides of the Cluj-Napoca, Paris and Odense patients were scored in consensus by groups of at least 3 SHG pathologists using the “share screen” option on a digital platform. One SHG pathologist (CL) attended all virtual scoring sessions to ensure homogeneity of histological evaluation. The observers were unaware of the clinical data.

All studied samples were routinely stained with hematoxylin-eosin and either chromotrope aniline blue or Sirius red.

SALVE grading

A semiquantitative evaluation method was defined using numerical scores for macrovesicular steatosis (0-3), hepatocellular ballooning (0-2), MDB (0-2), and lobular neutrophils (0-2). Ballooning was defined as hepatocellular enlargement (at least 2x the size of normal hepatocytes), rounded cellular shape and rarefied cytoplasm (cytoplasmic clarification). Cholestasis was specified as hepatocellular, canalicular, or ductular cholestasis and scored as absent (0) or present (1). The SHG evaluated 30 cases on digitized slides for the assessment of interobserver variation.

Parameters with substantial interobserver agreement ($\kappa > 0.6$) namely steatosis, ballooning, MDB, lobular neutrophils, canalicular and ductular cholestasis were selected as

descriptors of SALVE Grade defined by scores for steatosis (0-3), activity (0-4), canalicular (0-1) and ductular cholestasis (0-1) (Fig. S1). Because ballooning and MDB scores showed a strong correlation (Spearman's rho = 0.9), the higher score of either feature rather than their sum was considered, to avoid over-estimation of hepatocellular injury. The activity range of 0-4 was based on cellular injury and inflammation as the sum of scores for ballooning or MDB and lobular neutrophils. The definition of ASH¹ was based on ballooning and neutrophil scores of ≥1 each and cases with activity scores of 3 and 4, or in some cases 2, were diagnosed with hASH. The SALVE grading system is shown in Box 1.

SALVE staging

Fibrosis stages were described based on a combination of the NASH Clinical Research Network (CRN)⁵ and the Laennec systems¹⁴ with some modifications. The SALVE staging system details 7 SALVE fibrosis stages (SFS) comprising 4 pre-cirrhotic (SFS 0, 1, 2, and 3), similar to the CRN, and 3 cirrhotic stages (SFS 4A, 4B, and 4C), similar to Laennec. For some clinical settings, and also within trials, the presence of severe pericellular fibrosis (PCF) may be included, as described below and in Table 1. Morphological aspects of staging are also illustrated in Table 1 and Figs S2, S3 and S4.

Box 1. SALVE grading.

Steatosis (S) grade: Macrovesicular steatosis*; % parenchymal involvement
Score 0: <5%
Score 1: 5-33%
Score 2: 34-66%
Score 3: >66%
Activity (A) grade: Sum of scores for hepatocellular and lobular inflammation
Hepatocellular injury (ballooning (B) or Mallory-Denk bodies (MDB))**
Score 0: None-rare
Score 1: Few [§]
Score 2: Many ^{§§}
Lobular neutrophils (LN)
Score 0: None-rare
Score 1: Few [§]
Score 2: Many ^{§§} and/or satellitosis [%]
Cholestasis type
Canalicular cholestasis (CC)
Score 0: None
Score 1: Present
Ductular cholestasis (DC)
Score 0: None
Score 1: Present
SALVE grade is described by itemization of each of the component scores:
S 0-3, A (B/MDB 0-2 + LN 0-2), CC 0-1, DC 0-1

SALVE, Consortium for the Study of Alcohol-related LiVer disease in Europe.

*Lipid vacuoles in the cytoplasm of hepatocytes larger than the hepatocellular nucleus.

**If scores for ballooning and Mallory-Denk bodies are unequal the higher score is applied.

[§]Feature is appreciated after a reasonable search and is present in few microscopic fields.

^{§§}Feature is frequent and easy to find without searching and present in many microscopic fields.

[%]Neutrophils surrounding ballooned hepatocytes.

SALVE fibrosis stage 1 (SFS 1) comprises 2 distinct morphological patterns: Typically, centrilobular regions are affected by PCF occasionally extending to intermediate lobular areas (Fig. S2B). Alternatively, there may be predominantly portal-based fibrosis with periportal extension (Fig. S2C).¹⁰ SFS 2 is defined by coexisting centrilobular PCF and periportal fibrosis (Fig. S2D). In SFS 3 portal-based dense fibrous septa develop, linking portal tracts, portal tracts and central veins as well as central veins. This may be accompanied by variable degrees of PCF (see below for when PCF predominates) (SFS 3) (Fig. S2E,F). The cirrhosis stage SFS 4 is characterized by destruction of lobular architecture and development of parenchymal nodules surrounded by septa, the thickness of which are used for sub-classification. Septa may be dense and thin (SFS 4A; Fig. S3A,B), broad (SFS 4B; Fig. S3C,D) or very broad (SFS 4C; Fig. S3E,F). The assessment of septal thickness was based on the dimension of the smallest distinct parenchymal nodule as detailed in Table 1.

Expanded SALVE fibrosis staging in consideration of severe forms of pericellular fibrosis

In ALD, PCF can be the predominant pattern of fibrosis, present at all stages and therefore SFS 1, 3, and 4A-C can be further classified as outlined below and in Table 1.

In SFS1 cases, the designation *SFS 1P* may be used to indicate the presence of centrilobular PCF only (Fig. S2B). In some cases of SFS 3, SFS 3P denotes that severe PCF may assume a septum-like configuration (centro-central septal PCF) (Fig. S4A) or involve entire hepatic lobules but with preservation of porto-central relations (Figs S2E and S4B). In this setting obliterative venous lesions are frequently noted, and a few dense septa may be seen. In SFS 4AP severe PCF is present, destroying portal-central relations resulting in indistinct parenchymal nodules (Fig. S3B). SFS 4B and 4C with severe PCF and indistinct parenchymal nodules may be referred to as *SFS 4BP* (Fig. S3D) or *4CP* (Fig. S3F), respectively.

An algorithm was designed to facilitate and standardize the staging procedure (Fig. 1). Two groups of observers of the SHG independently assessed SFS of the first consecutive 140 cases of the Graz cohort using the SALVE Staging Algorithm for interobserver studies.

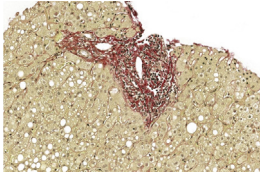
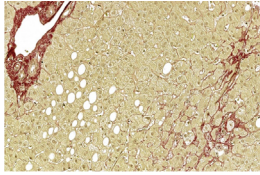
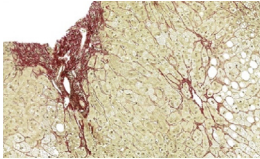

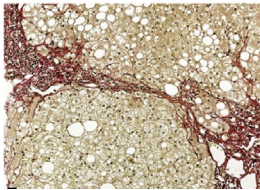
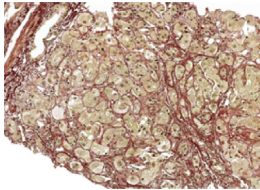
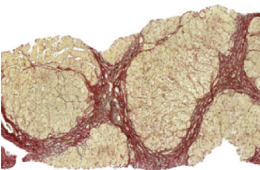
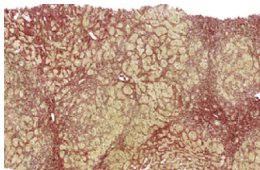
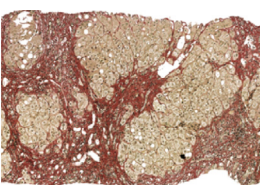
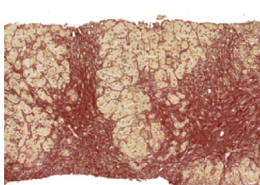
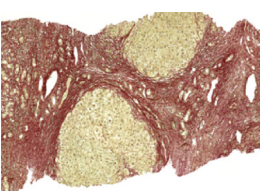
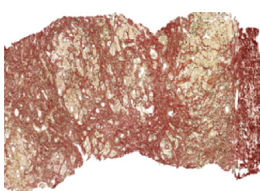
Assessment of venous lesions of ALD

Perivenular fibrosis, sclerosing hyaline necrosis and fibro-obliteration of hepatic veins are presumed to be of prognostic relevance. Therefore, their presence was evaluated by 5 SHG observers in 140 cases of the Graz cohort.

Statistical analyses

Continuous variables were reported as median (Q1, Q3), whereas categorical data are presented as relative frequencies. Liver-related mortality at short-term (90 days) or long-term (end of follow-up) was defined as death due to liver failure, complications of cirrhosis or HCC. Patients with non-liver-related death and those undergoing liver transplantation during follow-up were censored and counted as non-event. Decompensation-free survival was defined as absence of liver-related events (new-onset jaundice, ascites, portal hypertensive bleeding, hepatic encephalopathy) or liver-related death during follow-up. The effect of prognostic variables on survival was analysed by the Kaplan-Meier method and compared by log-rank tests performing Bonferroni correction for pairwise comparisons. The association of clinical, biochemical, and histological variables

Table 1. SALVE staging.

SFS	Description	Morphological changes ^a	Examples	
0	No fibrosis	Fibrosis is absent		
1	Mild fibrosis	Periportal fibrosis only or PCF ^b in zone(s) 3 ± 2 SFS 1P^c: PCF in zone(s) 3 ± 2 only		
2	Moderate fibrosis	Periportal fibrosis and PCF in zone(s) 3 ± 2		
3	Severe fibrosis	≥1 complete septum ^d bridging portal tracts and/or central veins, ±PCF SFS 3P^c: Panlobular PCF and/or complete septal PCF ± few dense septa ± venous lesions		
4A	Cirrhosis thin septa	≥1 parenchymal nodule ^e , thin septa ^f , ± 1 broad septum ^g , ±PCF SFS 4AP^c: Severe PCF ^h in >50% of parenchyma, indistinct parenchymal nodules ⁱ		
4B	Cirrhosis broad septa	Parenchymal nodules, >1 broad septum, ± 1 very broad septum ^j , ±PCF SFS 4BP^c: Severe PCF in >50% of parenchyma		
4C	Cirrhosis very broad septa	Parenchymal nodules, >1 very broad septum, ±PCF SFS 4CP^c: Severe PCF in >50% of parenchyma		

PCF, pericellular fibrosis; SALVE, Consortium for the Study of Alcohol-related LiVer disease in Europe; SFS, SALVE Fibrosis Stage.

^aDescription of the full range of topographical abnormal fibrosis including the degree of both dense septal and pericellular fibrosis.

^bPericellular fibrosis: Collagen fibers surrounding single or small groups of hepatocytes.

^cOPTIONAL, the presence of pericellular fibrosis as a dominant fibrosis type may be classified as “P” substage.

^dComplete septum: Fibrous band consisting mainly of collagen fibers resembling septa in viral hepatitis or septal PCF crossing biopsy diameter and linking portal tracts, portal tracts and central veins, or central veins.

^eParenchymal nodule without evidence of portal-central relations surrounded by dense septa.

^fThin septum: Dense septum, <50% of diameter of smallest parenchymal nodule.

^gBroad septum: Dense septum, ≥50% of the diameter of smallest parenchymal nodule but not thicker.

^hPCF evaluated at **LOW magnification** (20x or 40x total magnification).

ⁱParenchymal areas of indistinct nodular shape dissected by severe PCF.

^jVery broad septum: Dense septum, wider than the diameter of smallest parenchymal nodule.

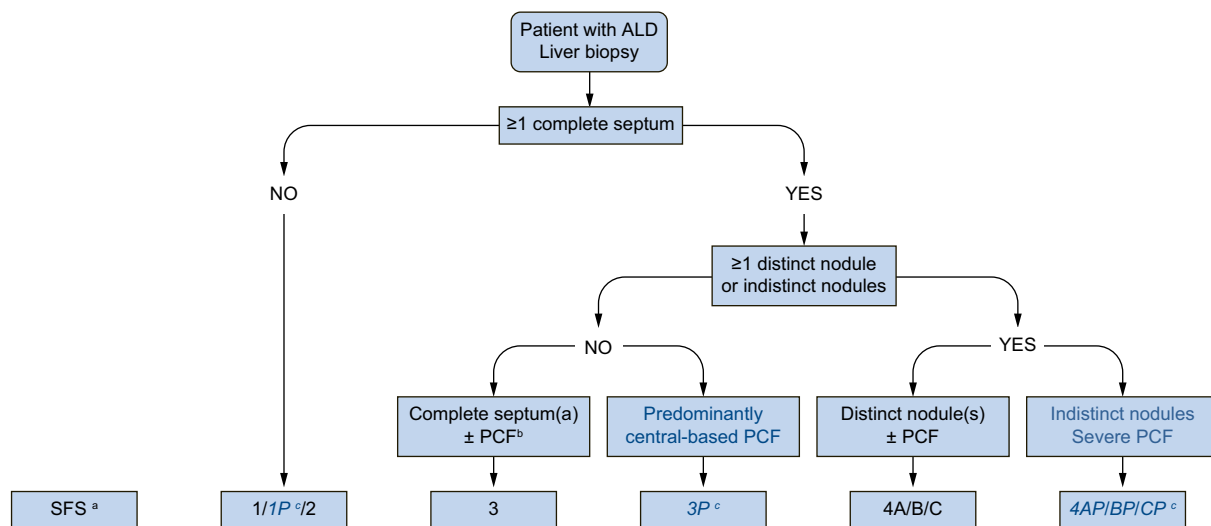


Fig. 1. SALVE staging algorithm. ALD, alcohol-related liver disease; PCF, pericellular fibrosis; SALVE, Consortium for the Study of Alcohol-related LiVer disease in Europe; SFS, SALVE fibrosis stage; ^aOptional stages to indicate presence of PCF as the predominant fibrosis type. For further details regarding definitions please see Table 1 footnote.

with survival was analysed by univariable and multivariable Cox regression. Multicollinearity was assessed with variance inflation factors (VIF). Statistical analyses were performed using SPSS Statistics Version 26 (SPSS Inc., Chicago, IL, USA) or R version 3.6.1. A *p* value of <0.05 was considered significant.

Results

Clinical, biochemical, demographical, and histological characteristics of the study cohort

The whole study cohort consisted of 445 patients representing the entire clinical spectrum of ALD. Subgroup analysis was performed in patients with (i) compensated ALD defined by lack of clinical symptoms and no evidence of cirrhosis on ultrasonography or biochemistry (n = 159), (ii) decompensated ALD characterized by bilirubin levels >3 mg/dl and/or signs of decompensation (new-onset jaundice, ascites, hepatic encephalopathy, portal hypertensive gastrointestinal bleeding) (n = 286), and (iii) decompensated ALD and hASH (n = 181). Twenty-eight patients died from non-liver-related causes. Twenty-two patients underwent liver transplantation during follow-up (6 patients within 90 days from liver biopsy). Clinical, biochemical, and demographic characteristics of the study cohorts are shown in Table 2.

Histological characteristics of the study cohort are compiled in Table S1. Median biopsy length was 25 mm in transcutaneous and 27 mm in transjugular biopsies. Decompensated patients more often had severe cirrhosis (SFS 4C). In addition, all cirrhotic stages with severe PCF (SFS 4AP, 4BP and 4CP) were more frequent in decompensated than in compensated patients. Individuals with decompensated disease had higher activity grade and presence of hASH than patients with compensated ALD. Canalicular cholestasis was infrequent and ductular cholestasis was nearly absent in compensated patients, but they were present in approximately 57% and 27% of those with decompensation, respectively.

Parameters of SALVE grading and staging in interobserver studies

Substantial interobserver agreement was found for steatosis, ballooning, MDBs, lobular neutrophils, canalicular and ductular

cholestasis, whereas agreement was moderate for the interpretation of hepatocellular cholestasis. Interobserver agreement for interpretation of the 7 SFS as well as the SFS with severe PCF was substantial (Table 3).

Association of SALVE grading with survival

Kaplan-Meier analysis in the whole study cohort revealed no prognostic utility for steatosis grade (data not shown). The association of SALVE activity grade with survival is shown in Fig. 2A. High activity (grade 2-4) was associated with significantly shorter survival (*p* <0.001 vs. grade 0-1). An association with shorter survival was also seen for patients with hASH compared to those without hASH (*p* <0.001; Fig. S5). Survival of patients with canalicular or ductular cholestasis was significantly shorter than that of individuals without cholestasis (both *p* <0.001, significance level *p* = 0.016) (Fig. 2B).

Patients with decompensated ALD and activity grade 2-4, hASH or canalicular and/or ductular cholestasis had significantly higher 90-day mortality than patients with activity grade 0-1, no hASH or no cholestasis (*p* = 0.038, 0.012 or 0.001, respectively) (Fig. S6A-C). In the subgroup of decompensated patients with hASH, canalicular and/or ductular cholestasis was associated with lower 90-day survival compared to those without cholestasis (*p* = 0.029) (Fig. S7).

In patients with compensated ALD, activity grade 2-4 or hASH was associated with a higher incidence of liver-related events during follow-up than activity grade 0-1 or no hASH (*p* = 0.011, respectively) (Fig. S8A-B).

Association of SALVE staging with survival

SFS staging was aggregated in a 5-tiered system based on relation to survival: no fibrosis (SFS 0), mild and moderate fibrosis (SFS 1 and 2), severe fibrosis (SFS 3), cirrhosis with thin or broad septa (SFS 4A and 4B), and cirrhosis with very broad septa (severe cirrhosis; SFS 4C). On Kaplan-Meier analysis the respective 10-year survival probabilities of patients were 100%, 89%, 65%, 43% and 32% (Fig. 3A).

Table 2. Clinical, biochemical and demographic characteristics of the study cohorts.

Centre	Graz (n = 172)	Cluj-Napoca (n = 92)	Paris (n = 75)	Odense (n = 106)
Period of enrolment	1995-2009	2016-2019	2011-2019	2013-2016
Decompensated ALD, %	69	100	100	0
Age, years	49 (41-57)	51 (43-57)	54 (48-59)	56 (49-62)
BMI	25 (22-29)	26 (22-30)	26 (22-30)	26 (23-28)
Sex female, %	31	27	20	26
AST, U/L	45 (26-77)	140 (99-188)	146 (96-197)	39 (27-55)
ALT, U/L	28 (16-54)	44 (27-57)	41 (31-67)	30 (21-43)
GGT, U/L	148 (62-327)	332 (207-642)	272 (134-667)	103 (47-238)
Alkaline phosphatase, U/L	160 (109-226)	463 (322-573)	164 (122-234)	96 (76-125)
Bilirubin, mg/dl	2.6 (1.1-8.5)	8.1 (4.0-19.5)	11.1 (6.7-19.4)	0.6 (0.4-0.9)
INR	1.22 (1.03-1.57)	1.93 (1.65-2.29)	1.82 (1.58-2.36)	1.0 (0.9-1.1)
Creatinine, mg/dl	0.9 (0.8-1.1)	0.7 (0.6-0.8)	0.7 (0.6-1.0)	0.8 (0.7-0.9)
Albumin, g/dl	3.5 (2.9-4.3)	2.8 (2.5-3.1)	2.0 (1.8-2.4)	4.1 (3.8-4.3)
Platelet count, G/L	138 (94-231)	110 (78-162)	127 (73-173)	227 (163-297)
Leucocyte count, G/L	6.8 (5.3-10.8)	9.8 (7.2-13.0)	9.9 (7.0-15.2)	6.7 (5.4-9.2)
MCV, fl	100 (94-105)	102 (97-108)	not reported	95 (91-101)
Sodium, mmol/L	138 (135-141)	136 (133-139)	132 (128-136)	139 (138-141)
Variceal bleeding, %	15	16	not reported	0
Hepatic encephalopathy, %	21	37	31	0
Ascites, %	44	84	88	0
MELD	14 (9-20)	22 (19-26)	23 (19-27)	6 (6-8)
Child-Pugh score	8 (6-10)	10 (8-12)	12 (11-13)	5 (5-5)
Route of biopsy, n (percutaneous/transjugular)	164/8	0/92	0/75	106/0
Length of biopsy core, mm	18 (12-27)	21 (16-28)	37 (28-50)	33 (27-40)
Survival, years	4.1 (0.9-8.8)	1.6 (0.4-3.5)	0.5 (0.1-1.4)	4.0 (3.5-4.9)
90-day mortality, %	9	23	27	0
5-year mortality, %	34	49	44	5

ALT, alanine aminotransferase; AST, aspartate aminotransferase; GGT, gamma glutamyltransferase; INR, international normalized ratio; MCV, mean corpuscular volume; MELD, model for end-stage liver disease.

Data are given as median (IQR).

Long-term mortality was significantly higher for patients with severe cirrhosis vs. pre-cirrhotic stages and vs. lesser cirrhosis ($p < 0.001$ and $p = 0.003$, significance level $p = 0.016$). In contrast, severe cirrhosis showed only a trend in relation to short-term outcome ($p = 0.162$) in patients with decompensated disease and also in the subgroup of decompensated patients with hASH ($p = 0.070$) (Fig. S9). In compensated ALD, severe fibrosis/cirrhosis was related to the development of liver-related events on long-term follow-up ($p < 0.001$) (Fig. 3B).

Association of the pericellular fibrosis type with outcome, inflammation, and venous lesions

Stages with severe PCF (SFS 3P, 4AP, 4BP, 4CP) had significantly worse long-term outcome than the respective SFS stages without severe PCF (SFS 3, 4A, 4B, 4C) ($p = 0.042$) (Fig. S10).

Severe PCF was associated with ballooning/MDB, cholestasis and lobular neutrophils (Chi-square test, $p < 0.001$ for all parameters). In the Graz cohort, venous lesions were assessed and associated with severe PCF although no association of any of the venous lesions with long- or short-term prognosis was found.

Independent predictors of survival and liver-related events

Clinical, biochemical and histological variables associated with long- or short-term survival on univariable Cox regression are detailed in Table S2. On multivariable Cox regression, sex, model for end-stage liver disease (MELD), platelet count, hepatic encephalopathy, and severe cirrhosis emerged as independent predictors of long-term liver-related mortality (Table 4). In a subgroup of patients in whom follow-up data on abstinence were available ($n = 323$), sex, MELD, hepatic encephalopathy,

Table 3. Interobserver variation in scoring of histological features of SALVE grade and stage (Graz cohort).

Item	Scoring system	Kappa value
Steatosis	Score 0: <5%; 1: 5-33%; 2: 34-66%; 3: >66%	0.88 ^a
Hepatocellular ballooning	Score 0: none, 1: few; 2: many	0.66 ^a
Mallory-Denk bodies	Score 0: none, 1: few; 2: many	0.78 ^a
Lobular neutrophils	Score 0: none, 1: few, 2: many and/or satellitosis	0.67 ^a
Hepatocellular cholestasis	0: none, 1: present	0.33 ^b
Canalicular cholestasis	0: none, 1: present	0.65 ^b
Ductular cholestasis	0: none, 1: present	0.66 ^b
SFS (all substages)	0, 1/1P, 2, 3/3P, 4A/4AP, 4B/4BP, 4C/4CP	0.69 ^c
SFS (main stages)	0, 1, 2, 3, 4A, 4B, 4C	0.80 ^c
Pericellular fibrosis	0, 1	0.69 ^c

SALVE, Consortium for the Study of Alcohol-related LiVer disease in Europe; SFS, SALVE fibrosis stage.

^aKendall's W, 10 raters, 27-29 observations.

^bFleiss' Kappa, 10 raters, 28-29 observations.

^cCohen's Kappa, 2 rater groups, 138 observations.

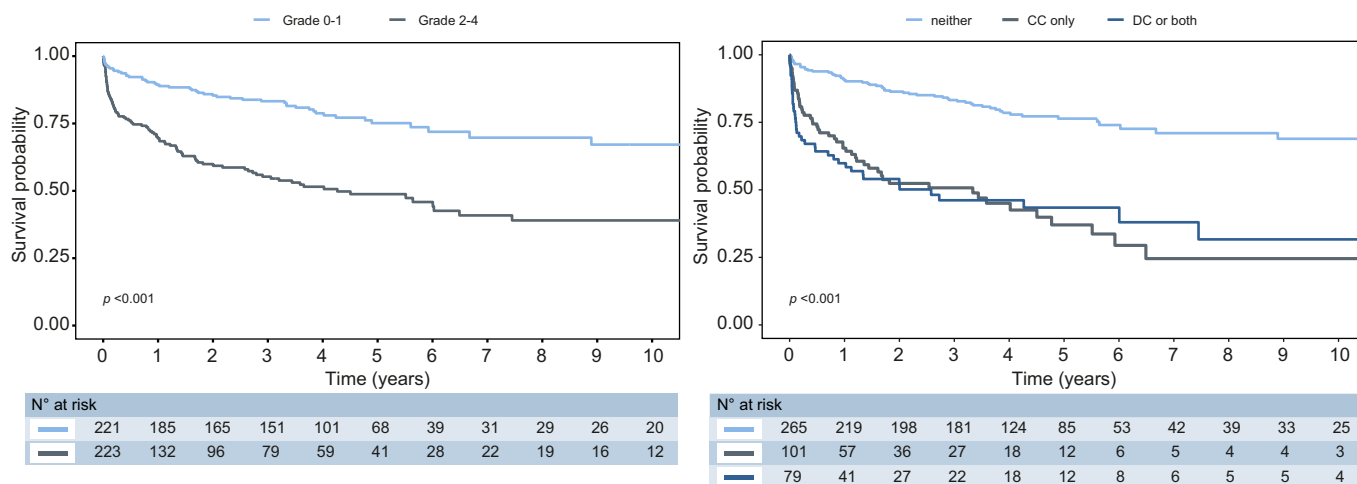


Fig. 2. Kaplan-Meier plots of long-term survival by SALVE grade (whole cohort, n = 445). (A) Effect of activity grade on survival: 0-1, no or mild activity; 2-4, high activity; $p < 0.001$ (log-rank test). (B) Effect of CC and DC on survival; $p < 0.001$ (log-rank test). CC, canalicular cholestasis; DC, ductular cholestasis; SALVE, Consortium for the Study of Alcohol-related LiVer disease in Europe.

abstinence, and severe cirrhosis were independent predictors of long-term liver-related mortality.

In decompensated ALD, MELD, hepatic encephalopathy, hASH, and severe cirrhosis were independent predictors of short-term (90-day) liver-related mortality. In the subgroup of decompensated patients with hASH, MELD, hepatic encephalopathy, and severe cirrhosis independently predicted 90-day liver-related death.

In patients with compensated ALD, decompensation-free survival was independently predicted by MELD, albumin, hASH, severe cirrhosis, and abstinence during follow-up.

Discussion

The aim of our study was to design and validate an ALD-specific histological grading and staging system that has hitherto been

lacking. This study presents the SALVE grading and staging system, a robust histological method with substantial interobserver agreement and clear associations to clinical outcomes in ALD.

While none of the grading features have been identified as independent prognostic factors for long-term outcome in previous studies,^{11,23} ballooning, MDBs or lobular neutrophils have been described as independent predictors of short-term mortality in patients with decompensated ALD.^{15,20,24} The association of hASH with short-term outcome in decompensated patients in our study confirms these results. Histological diagnosis of hASH in patients with decompensated ALD is clinically important to identify those with worse prognosis. Furthermore, in those with decompensation and hASH, short-term prognosis is predicted by clinical factors along with severe cirrhosis. The results emphasize the clinical utility of liver biopsy in these high-risk situations.

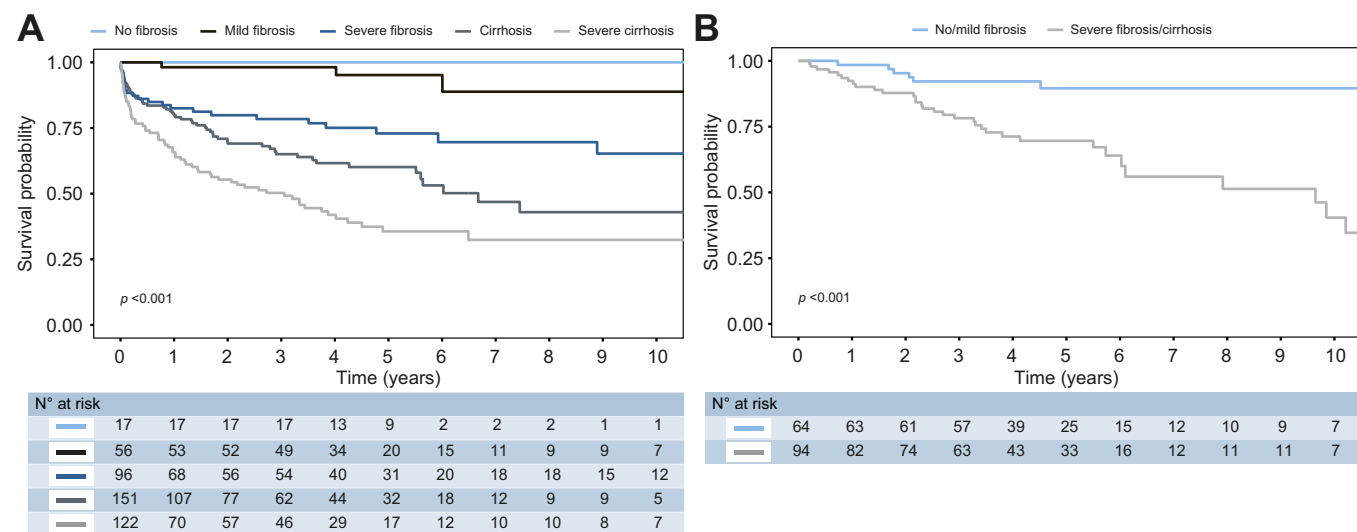


Fig. 3. Kaplan-Meier plots of long-term outcome by SFS. (A) Effect of SFS tiers on long-term survival (whole cohort, n = 445): no fibrosis, SFS 0; mild fibrosis, SFS 1-2; severe fibrosis, SFS 3; cirrhosis, SFS 4A-4B; severe cirrhosis, SFS 4C; $p < 0.001$ (log-rank test). (B) Effect of SFS on decompensation-free survival during follow-up (compensated ALD, n = 159): no/mild fibrosis, SFS 0-2; severe fibrosis/cirrhosis, SFS 3-4; $p < 0.001$ (log-rank test). ALD, alcohol-related liver disease; SALVE, Consortium for the Study of Alcohol-related LiVer disease in Europe; SFS, SALVE fibrosis stage.

Table 4. Clinical, biochemical and histological predictors of outcome in patients with ALD.

Variable	Hazard ratio (95% CI)	p value
Predictors of long-term liver-related mortality in the whole cohort (n = 445)		
Severe cirrhosis (SFS 4C)	1.88 (1.32-2.68)	<0.001
Male sex	0.68 (0.47-0.97)	0.036
MELD	1.11 (1.08-1.13)	<0.001
Platelet count	0.997 (0.995--0.999)	0.014
Hepatic encephalopathy	1.58 (1.09-2.27)	0.015
<i>Entered variables: severe cirrhosis (SFS 4C), hASH, ductular cholestasis, sex, MELD, WBC, platelet count, hepatic encephalopathy. Maximal VIF = 2.17.</i>		
Predictors of 90-day liver-related mortality in patients with decompensated ALD (n = 286)		
Severe cirrhosis (SFS 4C)	2.21 (1.24-3.96)	0.008
hASH present	1.98 (1.02-3.85)	0.043
MELD	1.19 (1.14-1.24)	<0.001
Hepatic encephalopathy	2.44 (1.38-4.30)	0.002
<i>Entered variables: severe cirrhosis (SFS 4C), hASH, ductular cholestasis, sex, MELD, WBC, hepatic encephalopathy. Maximal VIF = 1.64.</i>		
Predictors of 90-day liver-related mortality in decompensated patients with hASH (n = 181)		
Severe cirrhosis (SFS 4C)	2.16 (1.11-4.18)	0.023
MELD	1.19 (1.13-1.26)	<0.001
Hepatic encephalopathy	2.28 (1.20-4.35)	0.012
<i>Entered variables: severe cirrhosis (SFS 4C), canalicular cholestasis, sex, MELD, WBC, platelet count, hepatic encephalopathy. Maximal VIF = 1.51.</i>		
Predictors of decompensation-free survival in patients with compensated ALD (n = 159)		
Severe cirrhosis (SFS 4C)	3.26 (1.38-7.69)	0.007
hASH present	2.80 (1.32-5.96)	0.008
MELD	1.22 (1.05-1.42)	0.011
Albumin	0.44 (0.22-0.91)	0.026
Abstinence during follow-up	0.33 (0.12-0.91)	0.032
<i>Entered variables: severe cirrhosis (SFS 4C), hASH, age, MELD, albumin, abstinence during follow-up. Maximal VIF = 1.32.</i>		

Multivariable Cox regression.

ALD, alcohol-related liver disease; hASH, histological steatohepatitis due to ALD; MELD, model for end-stage liver disease; SALVE, Consortium for the Study of Alcohol-related Liver disease in Europe; SFS, SALVE fibrosis stage; VIF, variance inflation factor; WBC, white blood cell count.

Cholestasis is a distinct feature of severe ALD, which is not described in NAFLD.^{1,25} Ballooning-associated obstruction of bile radicles,²⁶ as well as impaired bile formation and transport in hepatocytes,²⁷ may be involved in canalicular cholestasis. Defective bile secretion via canalicular transporters and/or decreased bile flow have been implicated in sepsis-associated cholestasis.^{28,29} Bacterial infection and sepsis-associated immune paralysis are frequent in advanced ALD and often fatal complications triggering acute-on-chronic liver failure.³⁰ Ductular cholestasis has been associated with evolving (subclinical) sepsis and thus may indicate infection at an early stage.^{15,20,24} Both canalicular and ductular cholestasis convey prognostic information in the whole study cohort, in the decompensated subgroup as well as in decompensated patients with hASH. This supports similar results of others^{29,31} and underscores the prognostic utility of morphological cholestasis as an integral factor of SALVE grading.

Since most patients with ALD exhibit severe fibrosis or cirrhosis at first diagnosis, any stepwise staging method should allow sub-classification into prognostically meaningful categories. Based on the SALVE staging system and Kaplan-Meier analyses, 2 cirrhosis substages with different mortality risk could be defined. Patients with severe cirrhosis (SFS 4C) had worse outcome than patients with lesser grades of cirrhosis (SFS 4A and 4B). Moreover, severe cirrhosis emerged as an independent histological predictor for both long- and short-term survival in the whole study cohort, in subgroups of patients with symptomatic/decompensated disease as well as in patients with hASH. Our data are thus in line with results from

earlier studies, indicating the prognostic utility of cirrhosis substaging in chronic liver disease.^{14,32}

PCF can be a striking feature in ALD. Interestingly, in contrast to SFS with predominant septal fibrosis, (like SFS 3 or 4A/B/C), severe PCF (SFS 3P or 4AP/BP/CP) was associated with morphological features of liver injury, inflammation, fibro-obliterative venous lesions, cholestasis, and significantly shorter long-term outcome. The PCF pattern may indicate active disease and ongoing fibrogenesis. It may represent an immature type of fibrosis because it lacks elastic fibres and clusterin, a potent inhibitor of matrix-degrading metalloproteinases³³ present in mature scar tissue.³⁴ Data from rodent models of cirrhosis suggest that recent fibrous septa are readily degraded whereas older septa rich in elastin are more resistant.³⁵ Therefore, it could be speculated that PCF is more sensitive to degradation than dense fibrotic septa. Regression of PCF observed in a paired biopsy on follow-up could indicate decreased or resolved liver injury in phases of abstinence or medical intervention and could be useful to trace early anti-fibrotic treatment effects to monitor the evolution of fibrosis. Specific stages – SFS 3P, 4AP, 4BP and 4CP – were introduced in the SALVE staging system as an option to identify cases in which PCF is the predominant fibrosis type and to define these stages, which are not currently represented in other staging systems. If applied with the help of the staging algorithm, interrater agreement is substantial.

Our study has some limitations related to its retrospective design. Although a large panel of expert hepatopathologists reached substantial interobserver agreement, the proposed system should also be validated in a general pathology setting.

In conclusion, the SALVE histopathology group developed and validated an ALD-specific grading and staging system based on a large cohort of patients representing the whole clinical spectrum of ALD. This histological system integrates features of disease activity and fibrosis in a prognostic context. The large patient number has enabled us to evaluate the applicability and prognostic utility of SALVE grading and staging in clinically important subgroups, with compensated and decompensated disease, as well as in patients with histological ASH. Activity scores can be used to define the severity of injury and inflammation and to diagnose steatohepatitis and may, along with SALVE stage, help guide patient management.

Abbreviations

ALD, alcohol-related liver disease; hASH, histological steatohepatitis due to ALD; MDB, Mallory-Denk body; PCF, pericellular fibrosis; SALVE, Consortium for the Study of Alcohol-related LiVer disease in Europe; SFS, SALVE fibrosis stage; SHG, SALVE Histopathology Group.

Financial support

The authors received no financial support to produce this manuscript.

Conflicts of interest

The authors declare no conflicts of interest that pertain to this work.

Please refer to the accompanying ICMJE disclosure forms for further details.

Authors' contributions

CL, RES, HCP, CM, ASHG, DT: study design, data evaluation, manuscript writing and final review; CL, SD, HD, HPD, VG, MG, RM, VP, PS, LT, IR, SD, SS, ASHG, DT: review of histologic slides and final review; CL, RES, AB, GP: data management, statistical analysis and final review; RES, LB, PD, FR, PER, MJ, HS, AB, AH, MT, AK: patient recruitment, data collection and final review.

Data availability statement

The data that support the findings of this study are available from the corresponding author, upon reasonable request.

Acknowledgement

The authors thank Drs. Elizabeth M. Brunt and Ian R. Wanless for fruitful discussion of the ALD-specific staging system.

Supplementary data

Supplementary data to this article can be found online at <https://doi.org/10.1016/j.jhep.2021.05.029>.

References

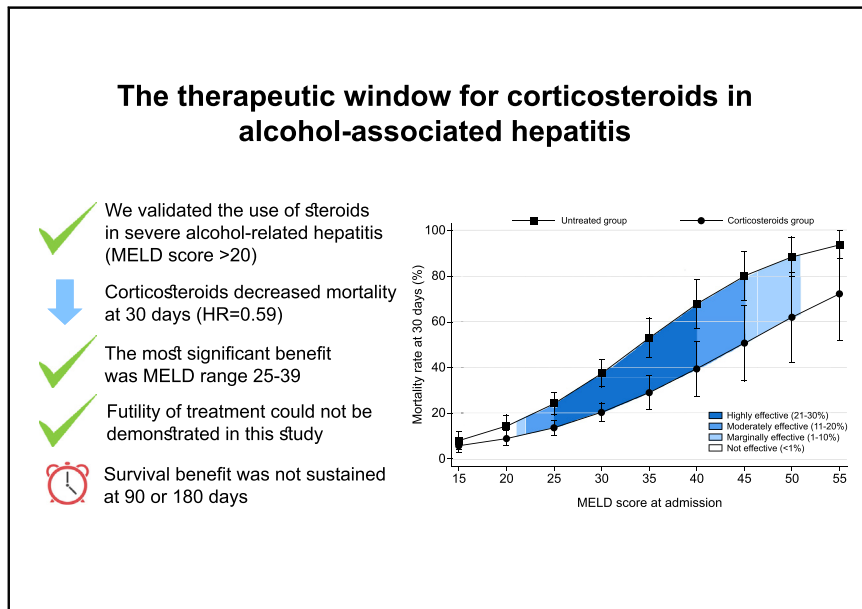
Author names in bold designate shared co-first authorship

- [1] Yip WW, Burt AD. Alcoholic liver disease. *Semin Diagn Pathol* 2006;23:149–160.
- [2] European Association for the Study of the Liver. EASL Clinical Practice Guidelines: Management of Alcohol-Related Liver Disease. *J Hepatol* 2018;69:154–181.
- [3] Lucey MR, Mathurin P, Morgan TR. Alcoholic hepatitis. *N Engl J Med* 2009;360:2758–2769.
- [4] Shen NT, Salajegheh A, Brown Jr RS. A call to standardize definitions, data collection, and outcome assessment to improve care in alcohol-related liver disease. *Hepatology* 2019;70:1038–1044.
- [5] Kleiner DE, Brunt EM, Van Natta M, Behling C, Contos MJ, Cummings OW, et al. Design and validation of a histological scoring system for nonalcoholic fatty liver disease. *Hepatology* 2005;41:1313–1321.
- [6] Bedossa P, FLIP Pathology Consortium. Utility and appropriateness of the fatty liver inhibition of progression (FLIP) algorithm and steatosis, activity, and fibrosis (SAF) score in the evaluation of biopsies of nonalcoholic fatty liver disease. *Hepatology* 2014;60:565–575.
- [7] Ishak K, Baptista A, Bianchi L, Callea F, De Groote J, Gudat F, et al. Histological grading and staging of chronic hepatitis. *J Hepatol* 1995;22:696–699.
- [8] Bedossa P, Poinard T. An algorithm for the grading of activity in chronic hepatitis C. The METAVIR Cooperative Study Group. *Hepatology* 1996;24:289–293.
- [9] Lefkowitz JH. Morphology of alcoholic liver disease. *Clin Liver Dis* 2005;9:37–53.
- [10] Brunt EM, Neuschwander-Tetri BA, Burt AD. Fatty liver disease: alcoholic and non-alcoholic. In: Burt AD, Portmann B, Ferrel L, editors. *MacSween's Pathology of the Liver*. Edinburgh: Churchill Livingstone; 2012. p. 293–359.
- [11] **Lackner C, Spindelboeck W**, Haybaeck J, Douschan P, Rainer F, Terracciano L, et al. Histological parameters and alcohol abstinence determine long-term prognosis in patients with alcoholic liver disease. *J Hepatol* 2017;66:610–618.
- [12] Goh GB, Pagadala MR, Dasarathy J, Unalp-Arida A, Sargent R, Hawkins C, et al. Clinical spectrum of non-alcoholic fatty liver disease in diabetic and non-diabetic patients. *BBA Clin* 2014;3:141–145.
- [13] Tsochatzis E, Bruno S, Isgro G, Hall A, Theocharidou E, Manousou P, et al. Collagen proportionate area is superior to other histological methods for sub-classifying cirrhosis and determining prognosis. *J Hepatol* 2014;60:948–954.
- [14] Kim SU, Oh HJ, Wanless IR, Lee S, Han KH, Park YN. The Laennec staging system for histological sub-classification of cirrhosis is useful for stratification of prognosis in patients with liver cirrhosis. *J Hepatol* 2012;57:556–563.
- [15] Altamirano J, Miquel R, Katoonizadeh A, Abraldes JG, Duarte-Rojo A, Louvet A, et al. A histologic scoring system for prognosis of patients with alcoholic hepatitis. *Gastroenterology* 2014;146:1231–1239.e1-6.
- [16] Burt AD, MacSween RN. Hepatic vein lesions in alcoholic liver disease: retrospective biopsy and necropsy study. *J Clin Pathol* 1986;39:63–67.
- [17] Nakano M, Worner TM, Lieber CS. Perivascular fibrosis in alcoholic liver injury: ultrastructure and histologic progression. *Gastroenterology* 1982;83:777–785.
- [18] Thiele M, Detlefsen S, Sevelsted Moller L, Madsen BS, Fuglsang Hansen J, Fiaglia AD, et al. Transient and 2-dimensional shear-wave elastography provide comparable assessment of alcoholic liver fibrosis and cirrhosis. *Gastroenterology* 2016;150:123–133.
- [19] Thiele M, Madsen BS, Hansen JF, Detlefsen S, Antonsen S, Krag A. Accuracy of the enhanced liver fibrosis test vs FibroTest, elastography, and indirect markers in detection of advanced fibrosis in patients with alcoholic liver disease. *Gastroenterology* 2018;154:1369–1379.
- [20] Katoonizadeh A, Laleman W, Verslype C, Wilmer A, Maleux G, Roskams T, et al. Early features of acute-on-chronic alcoholic liver failure: a prospective cohort study. *Gut* 2010;59:1561–1569.
- [21] Spahr L, Rubbia-Brandt L, Genevay M, Hadengue A, Giostra E. Early liver biopsy, intraparenchymal cholestasis, and prognosis in patients with alcoholic steatohepatitis. *BMC Gastroenterol* 2011;11:115.
- [22] Altamirano J, Bataller R. Alcoholic liver disease: pathogenesis and new targets for therapy. *Nat Rev Gastroenterol Hepatol* 2011;8:491–501.
- [23] Masson S, Emmerson I, Henderson E, Fletcher EH, Burt AD, Day CP, et al. Clinical but not histological factors predict long-term prognosis in patients with histologically advanced non-decompensated alcoholic liver disease. *Liver Int* 2014;34:235–242.
- [24] Mookerjee RP, Lackner C, Stauber R, Stadlbauer V, Deheragoda M, Aigelsreiter A, et al. The role of liver biopsy in the diagnosis and prognosis of patients with acute deterioration of alcoholic cirrhosis. *J Hepatol* 2011;55:1103–1111.
- [25] Tiniakos DG. Liver biopsy in alcoholic and non-alcoholic steatohepatitis patients. *Gastroenterol Clin Biol* 2009;33:930–939.
- [26] McGill DB. Steatosis, cholestasis, and alkaline phosphatase in alcoholic liver disease. *Am J Dig Dis* 1978;23:1057–1060.
- [27] Jones A, Selby PJ, Viner C, Hobbs S, Gore ME, McElwain TJ. Tumour necrosis factor, cholestatic jaundice, and chronic liver disease. *Gut* 1990;31:938–939.

- [28] Geier A, Fickert P, Trauner M. Mechanisms of disease: mechanisms and clinical implications of cholestasis in sepsis. *Nat Clin Pract Gastroenterol Hepatol* 2006;3:574–585.
- [29] Lefkowitz JH. Bile ductular cholestasis: an ominous histopathologic sign related to sepsis and "cholangitis lenta. *Hum Pathol* 1982;13:19–24.
- [30] Wasmuth HE, Kunz D, Yagmur E, Timmer-Stranghoner A, Vidacek D, Siewert E, et al. Patients with acute on chronic liver failure display "sepsis-like" immune paralysis. *J Hepatol* 2005;42:195–201.
- [31] Nissenbaum M, Chedid A, Mendenhall C, Gartside P. Prognostic significance of cholestatic alcoholic hepatitis. *VA Cooperative Study Group #119. Dig Dis Sci* 1990;35:891–896.
- [32] Kim MY, Cho MY, Baik SK, Park HJ, Jeon HK, Im CK, et al. Histological subclassification of cirrhosis using the Laennec fibrosis scoring system correlates with clinical stage and grade of portal hypertension. *J Hepatol* 2011;55:1004–1009.
- [33] Jeong S, Ledee DR, Gordon GM, Itakura T, Patel N, Martin A, et al. Interaction of clusterin and matrix metalloproteinase-9 and its implication for epithelial homeostasis and inflammation. *Am J Pathol* 2012;180:2028–2039.
- [34] Aigelsreiter A, Janig E, Sostaric J, Pichler M, Unterthor D, Halasz J, et al. Clusterin expression in cholestasis, hepatocellular carcinoma and liver fibrosis. *Histopathology* 2009;54:561–570.
- [35] Pellicoro A, Ramachandran P, Iredale JP. Reversibility of liver fibrosis. *Fibrogenesis Tissue Repair* 2012;5:S26.

Identification of optimal therapeutic window for steroid use in severe alcohol-associated hepatitis: A worldwide study

Graphical abstract



Authors

Juan Pablo Arab, Luis Antonio Díaz, Natalia Baeza, ..., Patrick S. Kamath, Ashwani K. Singal, Ramon Bataller

Correspondence

jparab@uc.cl (J.P. Arab).

Lay summary

Alcohol-associated hepatitis is a condition where the liver is severely inflamed as a result of excess alcohol use. It is associated with high mortality and it is not clear whether the most commonly used treatments (corticosteroids) are effective, particularly in patients with very severe liver disease. In this worldwide study, the use of corticosteroids was associated with increased 30-day, but not 90- or 180-day, survival. The maximal benefit was observed in patients with an MELD score (a marker of severity of liver disease; higher scores signify worse disease) between 25-39. However, this benefit was lost in patients with the most severe liver disease (MELD score higher than 51).

Highlights

- We validated the use of corticosteroids for patients with severe alcohol-associated hepatitis defined by an MELD score >20.
- The use of corticosteroids was associated with increased 30-day survival.
- The maximum benefit of corticosteroids was seen in patients with MELD scores between 25-39.
- A MELD score >51 can be used to define futility of corticosteroid treatment in patients with severe AH.
- The survival benefit was not sustained at 90 or 180 days.



Identification of optimal therapeutic window for steroid use in severe alcohol-associated hepatitis: A worldwide study

Juan Pablo Arab^{1,*}, Luis Antonio Díaz^{1,†}, Natalia Baeza¹, Francisco Idalsoaga¹, Eduardo Fuentes-López², Jorge Arnold^{1,3}, Carolina A. Ramírez⁴, Dalia Morales-Arreaez⁵, Meritxell Ventura-Cots⁵, Edilmar Alvarado-Tapias⁵, Wei Zhang⁶, Virginia Clark⁶, Douglas Simonetto⁷, Joseph C. Ahn⁷, Seth Buryska⁷, Tej I. Mehta^{8,9}, Horia Stefanescu¹⁰, Adelina Horhat¹⁰, Andreea Bumbu¹⁰, Winston Dunn¹¹, Bashar Attar¹², Rohit Agrawal¹³, Zohaib Syed Haque¹², Muhammad Majeed¹², Joaquín Cabezas^{14,15}, Inés García-Carrera^{14,15}, Richard Parker¹⁶, Berta Cuyàs¹⁷, Maria Poca¹⁷, German Soriano¹⁷, Shiv K. Sarin¹⁸, Rakhi Maiwall¹⁸, Prasun K. Jalal¹⁹, Saba Abdulsada¹⁹, María Fátima Higuera-de la Tijera²⁰, Anand V. Kulkarni²¹, P Nagaraja Rao²¹, Patricia Guerra Salazar²², Lubomir Skladaný^{23,24}, Natália Bystrianska^{23,24}, Veronica Prado²⁵, Ana Clemente-Sanchez^{5,26,27}, Diego Rincón^{26,27}, Tehseen Haider²⁸, Kristina R. Chacko²⁸, Fernando Cairo²⁹, Marcela de Sousa Coelho²⁹, Gustavo A. Romero³⁰, Florencia D. Pollarsky³⁰, Juan Carlos Restrepo³¹, Susana Castro-Sanchez³¹, Luis G. Toro³², Pamela Yaquich³³, Manuel Mendizabal³⁴, Maria Laura Garrido³⁵, Adrián Narvaez³⁶, Fernando Bessone³⁷, Julio Santiago Marcelo³⁸, Diego Piombino³⁹, Melisa Dirchwolf⁴⁰, Juan Pablo Arancibia⁴¹, José Altamirano⁴², Won Kim⁴³, Roberta C. Araujo⁴⁴, Andrés Duarte Rojo⁵, Victor Vargas⁴⁵, Pierre-Emmanuel Rautou^{46,47,48}, Tazime Issoufaly^{46,47,48}, Felipe Zamarripa⁴⁹, Aldo Torre⁵⁰, Michael R. Lucey⁵¹, Philippe Mathurin⁵², Alexandre Louvet⁵², Guadalupe García-Tsao⁵³, José Alberto González⁵⁴, Elizabeth Verna⁵⁵, Robert S. Brown⁵⁶, Juan Pablo Roblero⁵⁷, Juan G. Abraldes⁵⁸, Marco Arrese¹, Vijay H. Shah⁷, Patrick S. Kamath⁷, Ashwani K. Singal⁸, Ramon Bataller⁵

¹Department of Gastroenterology, Escuela de Medicina, Pontificia Universidad Católica de Chile, Santiago, Chile; ²Department of Health Sciences, Facultad de Medicina, Pontificia Universidad Católica de Chile, Santiago, Chile; ³Servicio Medicina Interna, Hospital El Pino, Santiago, Chile; ⁴Departamento de Anestesiología, Clínica Las Condes, Santiago, Chile; ⁵Center for Liver Diseases, Division of Gastroenterology, Hepatology and Nutrition, University of Pittsburgh Medical Center, PA, USA; ⁶Division of Gastroenterology and Hepatology, University of Florida, Gainesville, FL, USA; ⁷Division of Gastroenterology and Hepatology, Mayo Clinic, Rochester, MN, USA; ⁸Division of Gastroenterology and Hepatology, Department of Medicine, University of South Dakota Sanford School of Medicine, Sioux Falls, SD, USA; ⁹The Johns Hopkins Hospital, Department of Interventional Radiology, Baltimore, MD, USA; ¹⁰Regional Institute of Gastroenterology and Hepatology, Cluj-Napoca, Romania; ¹¹University of Kansas Medical Center, KS, USA; ¹²Division of Gastroenterology & Hepatology, Cook County Health and Hospital Systems, Chicago, Illinois, USA; ¹³Division of Gastroenterology and Hepatology, University of Illinois, Chicago, Illinois, USA; ¹⁴Gastroenterology and Hepatology Department, University Hospital Marques de Valdecilla, Santander, Spain; ¹⁵Research Institute Valdecilla (IDIVAL), Santander, Spain; ¹⁶Leeds Liver Unit, St James's University Hospital, Leeds Teaching Hospitals NHS Trust, Leeds, UK; ¹⁷Department of Gastroenterology, Hospital de la Santa Creu i Sant Pau, CIBERehd, Barcelona, Spain; ¹⁸Institute of Liver and Biliary Sciences, New Delhi, India; ¹⁹Department of Gastroenterology and Hepatology, Baylor College of Medicine, Houston, TX, USA; ²⁰Servicio de Gastroenterología, Hospital General de México, Universidad Nacional Autónoma de México, Mexico; ²¹Department of Hepatology, Asian Institute of Gastroenterology, Hyderabad, India; ²²Instituto de Gastroenterología Boliviano-Japonés, Cochabamba, Bolivia; ²³Division of Hepatology, Gastroenterology and Liver Transplantation, Department of Internal Medicine II, Slovak Medical University, Slovak Republic; ²⁴F. D. Roosevelt University Hospital, Banská Bystrica, Slovak Republic; ²⁵Centre Hospitalier de Luxembourg, Luxembourg; ²⁶Liver Unit, Department of Digestive Diseases Hospital General Universitario Gregorio Marañón Madrid, Spain; ²⁷CIBERehd Centro de Investigación Biomédica en Red de Enfermedades Hepáticas y Digestivas Madrid, Spain; ²⁸Division of Gastroenterology and Hepatology, Montefiore Medical Center, Bronx, NY, USA; ²⁹Liver Transplant Unit, Hospital El Cruce, Florencio Varela, Buenos Aires, Argentina; ³⁰Sección Hepatología, Hospital de Gastroenterología Dr. Carlos Bonorino Udaondo, Buenos Aires, Argentina; ³¹Unidad de Hepatología del Hospital Pablo Tobon Uribe, Grupo de Gastrohepatología de la Universidad de Antioquia, Medellín, Colombia; ³²Hepatology and Liver Transplant Unit, Hospitales de San Vicente Fundación de Medellín y Rionegro, Colombia; ³³Departamento de Gastroenterología, Hospital San Juan de Dios, Santiago, Chile; ³⁴Hepatology and Liver Transplant Unit, Hospital Universitario Austral, Buenos Aires, Argentina; ³⁵Hospital Central San Luis, San Luis, Argentina; ³⁶Liver Unit, Hospital Italiano de Buenos Aires,

Keywords: alcohol; alcoholic hepatitis; alcohol-associated liver disease; alcoholic liver disease; cirrhosis; steroids; corticosteroids; MELD; Maddrey discriminant function. Received 3 February 2021; received in revised form 18 May 2021; accepted 3 June 2021; available online 21 June 2021

* Corresponding author. Address: Departamento de Gastroenterología, Escuela de Medicina, Pontificia Universidad Católica de Chile, Marcoleta 367, 8330024 Santiago, Chile. E-mail address: jparab@uc.cl (J.P. Arab).

[†] Authors share first authorship.

<https://doi.org/10.1016/j.jhep.2021.06.019>



ELSEVIER

Buenos Aires, Argentina; ³⁷Hospital Provincial del Centenario, Universidad Nacional de Rosario, Rosario, Argentina; ³⁸Hospital de Emergencias, Villa el Salvador, Peru; ³⁹Servicio de Medicina Interna del Hospital de Emergencias Dr Clemente Álvarez de Rosario, Santa Fe, Argentina; ⁴⁰Unidad de Hígado, Hospital Privado de Rosario, Rosario, Argentina; ⁴¹Departamento de Gastroenterología y Hepatología, Clínica Santa María, Santiago, Chile; ⁴²Department of Internal Medicine, Hospital Quironsalud, Barcelona, Spain; ⁴³Division of Gastroenterology and Hepatology, Department of Internal Medicine, Seoul Metropolitan Government Seoul National University Boramae Medical Center, Seoul National University College of Medicine, Seoul, South Korea; ⁴⁴Gastroenterology Division, Ribeirão Preto Medical School, University of São Paulo, 14048-900 Ribeirão Preto, SP, Brazil; ⁴⁵Liver Unit, Hospital Vall d'Hebron, Universitat Autònoma Barcelona, CIBEREHD, Barcelona, Spain; ⁴⁶Université de Paris, Centre de recherche sur l'inflammation, Inserm, U1149, CNRS, ERL8252, F-75018 Paris, France; ⁴⁷Service d'Hépatologie, DHU Unity, DMU Digest, Hôpital Beaujon, AP-HP, Clichy, France; ⁴⁸Centre de Référence des Maladies Vasculaires du Foie, French Network for Rare Liver Diseases (FILFOIE), European Reference Network on Hepatological Diseases (ERN RARE-LIVER); ⁴⁹Gastroenterology, Juarez Hospital, Mexico City, Mexico; ⁵⁰Gastroenterology Department, Instituto Nacional de Ciencias Médicas y Nutrición "Salvador Zubirán", Mexico City, Mexico; ⁵¹Division of Gastroenterology and Hepatology, University of Wisconsin School of Medicine and Public Health, Madison, WI, USA; ⁵²Hôpital Claude Huriez, Services des Maladies de l'Appareil Digestif, CHRU Lille, and Unité INSERM 995, Lille, France; ⁵³Section of Digestive Diseases, Yale University School of Medicine/VA-CT Healthcare System, New Haven/West Haven, USA; ⁵⁴Gastroenterology Department, Hospital Universitario "Dr José E González" Universidad Autónoma de Nuevo León, Monterrey, Mexico; ⁵⁵Division of Digestive and Liver Diseases, Department of Medicine and Center for Liver Disease and Transplantation, Columbia University Irving Medical Center, New York, NY, USA; ⁵⁶Division of Gastroenterology and Hepatology, Weill Cornell Medical College, New York, NY; ⁵⁷Sección Gastroenterología, Hospital Clínico Universidad de Chile, Escuela de Medicina Universidad de Chile, Santiago, Chile; ⁵⁸Division of Gastroenterology, Liver Unit, University of Alberta, Edmonton, Canada

Background & Aims: Corticosteroids are the only effective therapy for severe alcohol-associated hepatitis (AH), defined by a model for end-stage liver disease (MELD) score >20. However, there are patients who may be too sick to benefit from therapy. Herein, we aimed to identify the range of MELD scores within which steroids are effective for AH.

Methods: We performed a retrospective, international multi-center cohort study across 4 continents, including 3,380 adults with a clinical and/or histological diagnosis of AH. The main outcome was mortality at 30 days. We used a discrete-time survival analysis model, and MELD cut-offs were established using the transform-the-endpoints method.

Results: In our cohort, median age was 49 (40–56) years, 76.5% were male, and 79% had underlying cirrhosis. Median MELD at admission was 24 (19–29). Survival was 88% (87–89) at 30 days, 77% (76–78) at 90 days, and 72% (72–74) at 180 days. A total of 1,225 patients received corticosteroids. In an adjusted-survival-model, corticosteroid use decreased 30-day mortality by 41% (hazard ratio [HR] 0.59; 0.47–0.74; $p < 0.001$). Steroids only improved survival in patients with MELD scores between 21 (HR 0.61; 0.39–0.95; $p = 0.027$) and 51 (HR 0.72; 0.52–0.99; $p = 0.041$). The maximum effect of corticosteroid treatment (21–30% survival benefit) was observed with MELD scores between 25 (HR 0.58; 0.42–0.77; $p < 0.001$) and 39 (HR 0.57; 0.41–0.79; $p < 0.001$). No corticosteroid benefit was seen in patients with MELD >51. The type of corticosteroids used (prednisone, prednisolone, or methylprednisolone) was not associated with survival benefit ($p = 0.247$).

Conclusion: Corticosteroids improve 30-day survival only among patients with severe AH, especially with MELD scores between 25 and 39.

Lay summary: Alcohol-associated hepatitis is a condition where the liver is severely inflamed as a result of excess alcohol use. It is associated with high mortality and it is not clear whether the most commonly used treatments (corticosteroids) are effective, particularly in patients with very severe liver disease. In this worldwide study, the use of corticosteroids was associated with increased 30-day, but not 90- or 180-day, survival. The maximal benefit was observed in patients with an MELD score (a marker of severity of liver disease; higher scores signify worse disease)

between 25–39. However, this benefit was lost in patients with the most severe liver disease (MELD score higher than 51).

© 2021 European Association for the Study of the Liver. Published by Elsevier B.V. All rights reserved.

Introduction

Alcohol use disorder (AUD) is one of the leading risk factors for disability and death worldwide¹ and constitutes the seventh leading risk factor for premature death and disability.² Every year, 2.8 million people die as a result of alcohol consumption. Although excessive alcohol consumption is frequent, AUD is usually underdiagnosed. A total of 5.1% of adults have AUD, affecting 8.6% of men and 1.7% of women.³ Alcohol consumption explains half of the cirrhosis cases worldwide, and approximately 35% of patients with AUD will develop chronic liver disease.⁴ Alcohol-associated hepatitis (AH) constitutes an acute and severe form of alcohol-associated liver disease (ALD) and its global incidence is increasing. Evidence from the Caucasian and Hispanic population suggests an AH incidence from 10% to 35% in patients with ALD.^{5–8} The mortality rate associated with an AH episode is approximately 30–40% at 90 days.⁵ Consequently, several efforts have been made to predict disease severity and identify patients who will benefit from corticosteroids. The current models used to predict short-term mortality include the Maddrey's modified discriminant function (mDF),⁹ the model for end-stage liver disease (MELD) score,^{10–12} the ABIC score,¹³ and the Glasgow AH score.¹⁴ The Lille score helps to reassess prognosis and identify corticosteroid non-responders.¹⁵ The use of the MELD score at baseline along with the Lille score on day 7 has demonstrated the best performance to predict 2-month and 6-month mortality.¹⁶ However, the best predictor of survival at 90 days is the ability to maintain alcohol abstinence.¹⁷ There is currently no model that can be used to determine futility of treatment, *i.e.* the characteristics of a patient in whom the outcome will be poor despite treatment.

Several pharmacological treatments have been assessed for severe AH during the last decades. Despite conflicting evidence, corticosteroids are considered the first-line of pharmacological therapy⁹ and are recommended by clinical guidelines.^{18–20} One of the largest randomized clinical trials (STOPAH, 2015)²¹ demonstrated a non-significant reduction in 30-day mortality

in patients with severe AH. However, this benefit was shown in patients predominantly with MELD scores <30 and was lost at 90-day and 1-year follow-up.²¹ Those results have been consistently observed in 2 systematic reviews.^{22,23} As a limitation, most of these studies have included only 1 country or region, and ALD is known to be modulated by genetic and environmental factors.¹⁸ Studies including multinational cohorts, which could be applicable worldwide, are lacking.

Additionally, corticosteroids have been associated with a higher risk of complications, including bacterial, viral, and fungal infections, gastrointestinal bleeding, and metabolic complications, among others. Currently, more centers are performing early liver transplantation for severe AH and severe infections secondary to the use of corticosteroids may preclude some patients from this possibility. Thus, it becomes even more relevant to define the specific subgroup of patients who will benefit from corticosteroids and those for whom the intervention will not improve outcomes. Moreover, it remains unclear whether there is a ceiling beyond which corticosteroids will cease to confer a benefit. Therefore, we aimed to evaluate the range of MELD scores associated with therapeutic benefit in a multinational cohort of patients with severe AH.

Materials and methods

Study design and participants

We conducted a retrospective registry-based study of patients admitted to the hospital with severe AH. We defined severe AH using the National Institute on Alcohol Abuse and Alcoholism clinical criteria as: i) increase of total bilirubin levels >3 mg/dl (>50 $\mu\text{mol/L}$), aspartate aminotransferase (AST) >50 IU/ml but <400 IU/L, AST/alanine aminotransferase (ALT) ratio >1.5; ii) absence of other causes of liver disease; iii) consumption of >2 drinks per day (40 g) in women and >3 drinks per day (50–60 g) in men; iv) excessive alcohol consumption for more than 5 years continuously or interrupted; and v) <60 days of abstinence before the onset of jaundice.²⁴ Liver biopsy was obtained when the diagnosis of AH was in question (possible AH) and according to local practice in centers with access to and experience with transjugular liver biopsy. We included all patients meeting the above criteria, clinical (probable AH) or histological (definite AH), independent of the use of steroids during the course of disease. We excluded patients aged <18 year-old, pregnant women and those with AST and/or ALT levels above 400 IU/ml. Patients meeting any of the following criteria were also excluded: i) alcohol abstinence for >60 days before clinical presentation; ii) presence of drug-induced liver injury, ischemic hepatitis, biliary duct obstruction, viral hepatitis, autoimmune hepatitis, or Wilson disease; iii) hepatocellular carcinoma beyond Milan criteria; iv) extrahepatic neoplasia with a life expectancy of less than 6 months; or v) history of severe extrahepatic disease (e.g., chronic kidney failure requiring hemodialysis, heart disease [NYHA class ≥ 3], and lung disease [mMRC class ≥ 3] conferring a life expectancy of less than 6 months). We included a total of 53 centers from 17 countries on 4 continents. The median number of patients included per center was 34 [13–80].

Data collection

We retrospectively collected data from the collaborators of each center. We performed a retrospective review of the records of patients hospitalized with the diagnosis of severe AH (from January 2009 to January 2019). The centers were invited through the Engage Platform from ALD special interest group from the

American Association for the Study of Liver Diseases. We collected laboratory results at admission, as well as the type of steroids and length of use. We recorded the MELD and mDF scores at admission and during hospitalization, mortality and causes of death at 30 days. The data collected was recorded in a confidential electronic case report form. The electronic database was managed by the main researchers of the study through the RedCap platform. We requested an informed consent waiver at each participating center or leveraging from previous consortia (InTeam, GLOBAL), and de-identified data was analyzed.

Statistical analysis

The primary outcome was 30-day mortality in patients with severe AH, treated or not with corticosteroids, and the MELD therapeutic window that correlates with treatment benefit. The secondary outcomes were complications resulting from the use of corticosteroids in patients with severe AH, and the clinical differences between the steroids used. Categorical variables were summarized using frequencies and percentages. We assessed normality distribution in continuous data using the Kolmogorov-Smirnov test. Continuous variables with normal distribution were described with mean and standard deviation. Variables without a normal distribution were summarized using the median and interquartile ranges. Analyses were completed using the chi-square test for categorical variables, the Student's *t* test for normally distributed continuous variables and non-parametric tests in the case of continuous variables that are not normally distributed.

We used discrete-time survival models specified in terms of discrete-time hazard to estimate the risk of death at 30 days. In this model, the beginning and the end of each time analysis interval are the same for all patients.²⁵ This survival model can be estimated through dichotomous response regressions once the database structure has been transformed into a person-period type.²⁶ The estimation of the discrete-time hazard was performed via logistic regression models, obtaining hazards as predicted probabilities. A multivariable logistic regression model was used to adjust for baseline differences in socio-demographics and clinical variables and for potential confounders. To relax a constant effect assumption of the regression models, we added an interaction term between the time and MELD score. Wald's test was applied to assess the statistical significance of the interaction term added to the logistic regression model. Furthermore, a post-estimation analysis was performed to obtain the predicted probabilities of mortality at 30 days for different MELD scores according to steroid use. Regarding the comparisons between steroid use groups, the hazard ratio (HR) was estimated for different MELD scores, establishing their cut-offs. The *transform-the-endpoints method* was used for estimation since it produces asymmetric confidence intervals at 95% and guaranteed that they were entirely positive.²⁷ STATA software reports transformed confidence intervals based on the *transform-the-endpoints method* for standard parametric and semi-parametric survival models.²⁸ All analyses were performed with STATA software version 16 (StataCorp, College Station, Texas).

Results

Baseline characteristics of the cohort

We included 3,380 patients from 53 centers in 17 countries on 4 continents. The median age in our cohort was 49 (40–56) years old and 76.5% were male. The most frequent ethnicities were

Caucasian (45.3%), Hispanic or Latino (17.1%), Asian (14.3%), and Indian (13.4%). Seventy-nine percent of patients had a prior history of cirrhosis. The median MELD score and mDF at admission were 24 (19–29) and 54 (37–81), respectively. At admission, patients presented with median bilirubin of 12.2 (5.9–22.6) mg/dl, International normalized ratio of 2.0 (1.5–2.0), and albumin 2.6 (2.0–3.0) g/dl. The median creatinine at admission was 0.9 (0.6–1.3) mg/dl and 3.3% of patients required dialysis during hospitalization. Table 1 summarizes the main characteristics of the global cohort, and differences in patients according to use of steroids.

Among patients in whom follow-up information was available, the estimated survival was 88.1% (95% CI 87.2–88.9) at 30 days, 77% (95% CI 75.9–78.1) at 90 days, and 72.4% (95% CI 71.6–73.7) at 180 days. Only 56 of patients underwent liver transplantation during the follow-up period. The main attributed causes of death were multi-organ failure (25.6%), infections (17.4%), liver failure (11.4%), acute kidney injury (9.7%), and gastrointestinal bleeding (9.7%) (Fig. S1), although the majority had more than 1 cause of death.

Use of corticosteroids among the cohort

A total of 1,225 patients were treated with corticosteroids (43.5% of the global cohort when patients with missing data were excluded). The median MELD score, mDF, and bilirubin at the onset of corticosteroid treatment were 25 (21–29), 62 (46–85), and 15.2 (8.4–23.9) mg/dl, respectively. The median MELD scores at 30, 90 and 180 days were 20 (15–26), 16 (11–22), and 14 (10–20), respectively. There were no significant differences in MELD score

between steroid-treated and untreated groups at 30-, 90-, and 180-day follow-up (Fig. 1A and Fig. S2A). Serum bilirubin was significantly higher in patients treated with corticosteroids; the decrease in serum bilirubin at day 7 was also higher in the steroid-treated group (Fig. 1B and Fig. S2B). The most frequent corticosteroids administered were prednisone (53.2%), prednisolone (31.3%), and methylprednisolone (11.9%). The median time of use of corticosteroids was 20.1 (7–28) days.

Impact of corticosteroid use on survival and identification of the optimal therapeutic window

Thirty-day mortality was 10.1% (95% CI 8.9–11.4) in the corticosteroids group vs. 12.8% (11.6–14.1) in the untreated group ($p = 0.238$). The 90-day mortality was 21.0% (95% CI 19.1–23.1) in the corticosteroids group and 20.1% (95% CI 18.4–21.9) in the untreated group; 180-day mortality was 24.5% (95% CI 22.1–27.1) in the corticosteroids group and 26.4% (95% CI 23.7–29.4) in the untreated group. Due to the baseline differences between both groups, we analyzed the data adjusting for age, gender, ethnicity, cirrhosis, dialysis, and MELD score. On adjusted analysis, the use of corticosteroids decreased the relative risk of 30-day mortality by 41% (HR 0.59; 95% CI 0.47–0.74; $p < 0.001$) (Fig. 2); however, there were no significant differences at 90 (HR 0.92; 95% CI 0.33–2.56; $p = 0.871$) or 180 days (HR 0.14; 95% CI 0.01–1.48; $p = 0.102$) (Fig. S3). Additionally, the therapeutic benefit in reducing 30-day mortality was only observed when steroids were used in patients with MELD scores between 21 (HR 0.61; 95% CI 0.39–0.95; $p = 0.027$) and 51 (HR 0.72; 95% CI 0.52–0.99; $p = 0.041$) (Fig. 2). Importantly, considering the upper limit of the 95% CI of the HR,

Table 1. Baseline characteristics of patients according to the use of corticosteroids.

Characteristics	Global (N = 3,380)	Non-corticosteroid group (n = 1,592)	Corticosteroid group (n = 1,225)	p value ^a
Age (y) [†]	49 (40–56)	49 (42–57)	47 (39–55)	0.003
Men (%)	76.5	75.5	71.2	0.010
Ethnicity (%)				<0.001
Caucasian	45.3	43.7	59.5	
Hispanic or Latino	17.1	17.1	25.0	
Asian	14.3	27.6	1.5	
Indian	13.4	3.4	3.4	
Black	4.8	2.7	4.0	
Mestizo	3.1	3.2	4.4	
American-Indian	0.6	0.8	0.7	
Other	1.4	1.5	1.5	
Cirrhosis (%)	79.1	76.7	79.5	0.238
MELD at admission [†]	24 (19–29)	22 (18–29)	25 (21–31)	<0.001
mDF at admission [†]	54 (37–81)	45 (27–68)	63 (46–90)	<0.001
Laboratory testing:				
AST (IU/L) [†]	142 (96–216)	142 (94–220)	148 (110–214)	0.230
ALT (IU/L) [†]	48 (32–80)	48 (32–78)	50 (33–79)	0.323
GGT (IU/L) [†]	268 (118–530)	266 (116–566)	285 (132–513)	0.887
Alkaline phosphatase (IU/L) [†]	172 (122–260)	167 (115–249)	189 (131–292)	0.015
Total bilirubin (mg/dl) [†]	12.2 (5.9–22.6)	9.4 (4.7–19.3)	16.4 (8.9–25.9)	<0.001
INR [†]	2.0 (1.5–2.0)	1.8 (1.4–2.0)	2.0 (1.8–2.1)	<0.001
Creatinine (mg/dl) [†]	0.9 (0.6–1.3)	0.9 (0.7–1.5)	0.9 (0.6–1.4)	0.273
Sodium (mEq/L) [†]	133 (129–137)	133 (129–137)	130 (130–137)	0.737
Albumin (g/dl) [†]	2.6 (2.0–3.0)	2.7 (2.1–3.0)	2.7 (2.0–3.0)	0.371
Dialysis* (%)	3.4	5.7	1.4	<0.001
Liver transplant (%)	3.3	3.0	4.1	0.266

Comparisons were performed using Chi-square test for categorical variables, the Student's *t* test for normally distributed continuous variables and non-parametric tests in the case of continuous variables that are not normally distributed. Patients in the global cohort who had missing data were excluded from the multivariable logistic regression model. GGT, gamma-glutamyltransferase; INR, international normalized ratio; mDF, Maddrey's modified discriminant function; MELD, model for end-stage liver disease.

^ap value for non-corticosteroid vs. corticosteroid group.

[†]Median and interquartile range [25–75].

*At least twice in the last week.

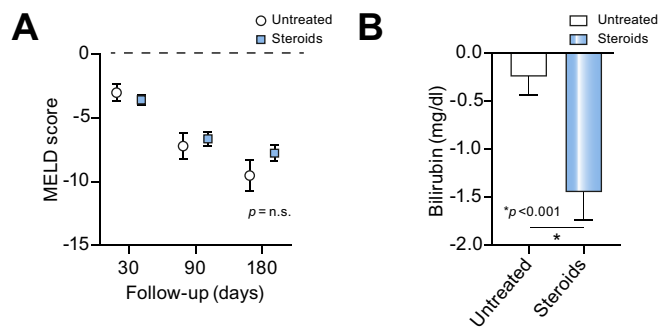


Fig. 1. Impact of steroid use in terms of severity at 30, 90 and 180 days. (A), Changes in MELD score between admission and 30, 90 and 180 days according to steroid use. (B), Change in serum bilirubin between admission and by day 7 according to steroid use. The groups were compared with the Mann-Whitney *U* test, and a *p* value < 0.05 was considered significant. MELD, model for end-stage liver disease; n.s., not significant.

the maximum effect of corticosteroids (21–30% survival benefit) was observed in patients with MELD scores between 25 (HR 0.58; 95% CI 0.42–0.77; $p < 0.001$) and 39 (HR 0.57; 95% CI 0.41–0.79; $p < 0.001$). Moderate benefit (11–20% survival benefit) was observed with MELD between 22–24 and 40–44 (Fig. 2). There was no significant association between survival and the type of corticosteroid used (prednisone, prednisolone, or methylprednisolone) ($p = 0.247$). Different MELD cut-offs and 95% CIs for 30-day patient mortality are described in Fig. 3.

We evaluated the response to treatment with the Lille model at day 7 (according to the validated cut-off value < 0.45). We stratified patients into 3 groups according to MELD score at admission (less than 25, between 25–39, and 40 or more)(Fig. S4). In patients with MELD scores of 25 or less, 70.9% of the group without corticosteroids had response criteria, compared to 62.8% of treated patients from the corticosteroids group ($p = 0.006$). Inversely, in patients with MELD scores over 40, the treatment response was higher in the corticosteroids group (44.2% vs. 21.8%, $p = 0.018$). There were no differences in

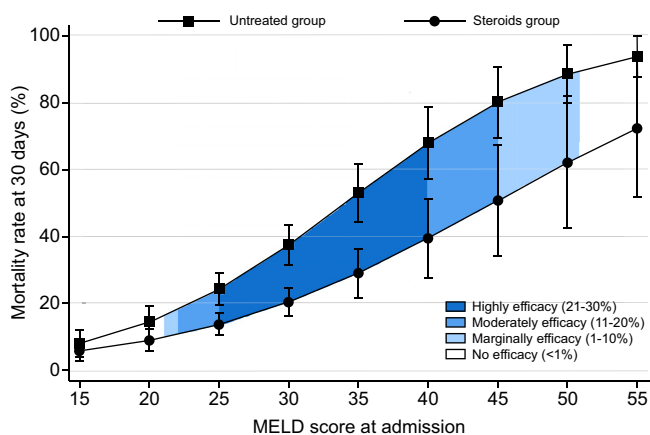


Fig. 2. Predictive model of 30-day survival adjusted by age, gender, ethnicity, cirrhosis, dialysis, and MELD score. The curves represent mortality per use of steroids and severity (MELD score). A discrete-time hazard was estimated at 30 days using an adjusted multivariable logistic regression. We added an interaction term between the time and the MELD score. Efficacy was defined based on the upper limit of the 95% CI of the hazard ratio. The hazard ratio was 0.59, 95% CI 0.47–0.74, $p < 0.001$. MELD, model for end-stage liver disease.

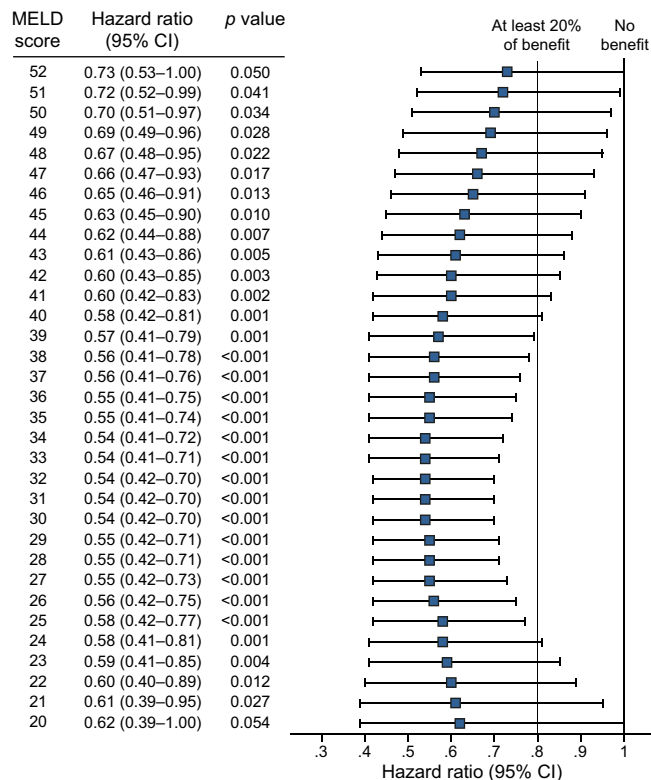


Fig. 3. Forest plot of the predictive model of 30-day survival adjusted by age, gender, ethnicity, cirrhosis, dialysis, and MELD score. A hazard ratio less than 1 represents a survival benefit with corticosteroids treatment. The transform-the-endpoints method was used to estimate the hazard ratio for different MELD scores. A *p* value < 0.05 was considered statistically significant. MELD, model for end-stage liver disease.

response to treatment in patients with MELD scores between 25–39 (36.4% in the group without corticosteroids and 39% in the corticosteroids group; $p = 0.482$).

Complications of corticosteroid use

The most frequent reason for discontinuing corticosteroid treatment was non-variceal gastrointestinal bleeding (78%), infections (15.7%), variceal bleeding (3.4%), and acute kidney injury (3%). At the end of follow-up, there were no differences in mortality rate due to documented infections between corticosteroids and untreated groups (18.4% vs. 19.5%, respectively; $p = 0.709$). The observed mortality due to acute kidney injury was higher in the untreated group than the corticosteroids group (14.2% vs. 5.4%, respectively; $p < 0.001$)(Fig. 4).

Discussion

Severe AH is a life-threatening condition, with high short-term mortality.¹⁸ Corticosteroids constitute the first-line therapy for patients with severe AH (MELD > 20), despite conflicting data on their benefit.^{18–20} However, it is unclear whether there is an upper limit of MELD score beyond which corticosteroids will cease to confer a benefit. In this large retrospective, multicenter cohort study, we demonstrated that: i) the use of corticosteroids decreases 30-day mortality in severe AH by 41%, but does not reduce mortality at 90 or 180 days; ii) using an MELD score > 20 to initiate treatment with corticosteroids for severe AH is valid; iii) steroid therapy is beneficial in patients with severe AH

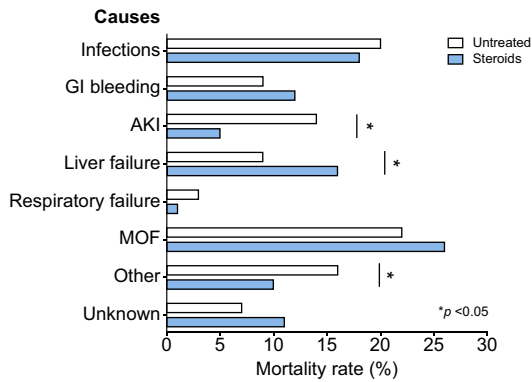


Fig. 4. Principal causes of death according to corticosteroid use at 180 days of follow-up. Comparisons were performed using the chi-square test. A *p* value <0.05 was considered statistically significant. AKI, acute kidney injury; GI bleeding, gastrointestinal bleeding; MOF, multiple organ failure.

with MELD scores between 21 and 51 points. Interestingly, corticosteroids confer their maximum survival benefit (of at least 20–30%) in patients with MELD scores between ≥ 25 and 39; and vi) there is a moderate benefit (10–20% survival benefit) with steroid therapy in patients with MELD scores between 22–24 and 40–44.

One of the main strengths of our study is its global nature. We included 3,380 patients from 17 countries and 4 continents, including 7 different ethnicities (especially Caucasian, Hispanic, Asian-Pacific Islander, and South Asian). This is arguably the largest and ethnically most heterogeneous cohort in this field. Nearly half of the cohort included in the multivariable analysis (43.5%) were treated with corticosteroids; treated patients had more severe liver disease at baseline, evidenced by a higher MELD score and mDF. Thus, only after appropriate adjustment for disease severity and baseline characteristics could the real benefit of corticosteroids be assessed. Prednisone was the most frequently used therapy, and the median time of therapy was 3 weeks (20.1 days). Our cohort is quite different from previous studies. First, a large percentage of prior studies were carried out in the 70s and 80s, most had a low number of patients, and the intensive care support for patients with severe AH was not what we currently have today.^{9,29–38} In these studies, there were important differences in corticosteroid dosage, with doses up to 3 grams of methylprednisolone in 1 study.³⁶ Therefore, most of the initial systematic reviews yielded contradictory conclusions.^{39–42} Three prior studies with 131, 101, and 61 patients demonstrated a short-term benefit with corticosteroid use.^{43,44} In 2015, the STOPAH study demonstrated that the use of prednisolone in patients with severe AH was associated with a non-significant decrease in mortality at 28 days; however, there was no significant effect on mortality at 90-day or 1-year follow-up. That study included 1,103 patients from the UK, with a mean MELD lower than our cohort (21.2 ± 6.2).²¹ These results have also been supported by recent systematic reviews.^{22,45} In 2019, a Cochrane systematic review that included 16 studies (from 1977 to 2015) with a total of 1,884 participants concluded that corticosteroids confer no clear benefit over placebo with respect to all-cause mortality at 3 months in patients with severe AH. However, there is great heterogeneity in the included studies (severity of AH, corticosteroid dose, presence of cirrhosis), many of them with a high-risk of bias or unclear risk of bias.²³ Although the STOPAH trial suggested short-term benefits, it

raised concerns regarding the benefit of corticosteroids in the most severe stages of AH and in different ethnicities. That is, it is unclear from current studies whether there is a level of disease severity beyond which steroids are ineffective or futile in patients with AH.

Based on previous data, there is no robust evidence of a possible disease severity window in which steroids are most effective. In fact, the STOPAH study suggested a narrow therapeutic window (mean MELD score of 21.2 ± 6.2).²¹ In the current study, we demonstrated the short-term benefit of corticosteroids even with higher MELD scores, and the highest effect was observed in patients with MELD scores between 25 (HR 0.58; 95% CI 0.42–0.77; *p* <0.001) and 39 (HR 0.57; 95% CI 0.41–0.79; *p* <0.001), expanding the therapeutic window suggested by the STOPAH study. Different preparations of corticosteroids are used in various countries, depending on availability. We demonstrated in this study that prednisone was as effective as prednisolone, confirming its benefit in patients with severe AH.

Corticosteroid therapy has several adverse effects, including an increased risk of severe infections, upper gastrointestinal bleeding, hyperglycemia, or decompensation of diabetes mellitus, psychological disturbances, and adrenal insufficiency, among others.⁴⁶ All of these conditions increase morbidity, mortality, length of hospital stay, and healthcare costs. Thus, it becomes even more relevant to abstain or suspend corticosteroid treatment when the risks outweigh the benefits. Infections are the most important adverse effect in severe AH. Two previous studies reported a higher risk of severe infections with the use of prednisolone.^{21,46} A recent systematic review showed that corticosteroid use does not increase mortality from bacterial infections, but it can increase the risk of fungal infections.⁴⁷ Other systematic reviews did not show that corticosteroids increase severe adverse effects; however, the evidence is not strong.⁴⁸ In our study, even with prolonged use of corticosteroids, only 17.4% of the cohort died due to infections, with no differences in the infection rate between treated and untreated patients.

Our retrospective cohort study includes a vast number of patients, ethnicities, and centers. However, our study suffers from the limitations of any retrospective cohort study, including the extensive variability regarding the indication of steroid use and the absence of all the desired variables for all patients. Further, of the 3,380 patients included, only 45% completed follow-up to 180 days, reducing the sample size for long-term outcome analysis. Also, identifying cut-offs based on repeated confidence intervals has limitations since this could disadvantage groups with smaller sample size. The causes of death and the numbers of organ failures could not be clearly ascertained from the data. It was also unclear whether all infections were captured in the database, given the lower prevalence than in other studies. Based on these limitations, the indication for steroids in patients with high MELD (over 40) must be analyzed individually, balancing the benefit and the risk of infections.

In conclusion, our study confirms that corticosteroid use increases 30-day, but not 90- or 180-day, survival in patients with severe AH. The maximum benefit of corticosteroid therapy was observed in patients with MELD scores between 25 and 39; futility of corticosteroid treatment was observed in patients with MELD scores >51 . The benefit of multiple investigational agents is currently being investigated in clinical trials. Until the benefit of these agents is demonstrated, it seems reasonable to use

corticosteroids in patients with severe AH and MELD scores between 21–51 in the absence of contraindications.

Abbreviations

AH, alcohol-associated hepatitis; ALD, alcohol-associated liver disease; AST, aspartate aminotransferase; AUD, alcohol use disorder; HR, hazard ratio; mDF, Maddrey's modified discriminant function; MELD, model for end-stage liver disease.

Financial support

Juan Pablo Arab and Marco Arrese receive support from the Chilean government through the Fondo Nacional de Desarrollo Científico y Tecnológico (FONDECYT 1200227 to JPA and 1191145 to MA) and the Comisión Nacional de Investigación Científica y Tecnológica (CONICYT, AFB170005, CARE Chile UC). Ramón Bataller is recipient of NIAAA U01AA021908 and U01AA020821. Dalia Morales Arraez, Meritxell Ventura Cots, and Ana Clemente-Sanchez are recipients of a scholarship grant for study extension abroad, sponsored by the Spanish Association for the Study of the Liver (AEEH). Vijay Shah is supported by NIH AA26974-01 grant. Patrick S. Kamath has received grant support through NIH AA26974-01. Manuel Mendizabal received support from the National Cancer Institute, Argentina (DI-2018-19-APN-INC#MS). Andreea Bumbu, Adelina Horhat and Horia Stefanescu are supported by the Romanian Executive Unit for Scientific Research (UEFISCDI) through the PN-III-P1-1.1-TE-2016-1196 grant awarded to HS.

Conflict of interest

The authors declare no conflicts of interest that pertain to this work.

Please refer to the accompanying ICMJE disclosure forms for further details.

Authors' contributions

JPA, AKS, and RB conceived and designed the study; all authors collected the data, contributed to data analysis and interpretation; JPA, LAD, NB, FI, EF, JA, CAR, JPR, JGA, MA, VHS, PSK, AKS, and RB performed final analysis and drafted the manuscript; all the authors participated in drafting the article and revising it critically for important intellectual content; and all the authors gave final approval of the version submitted.

Data availability statement

The datasets generated and analyzed during the current study are not publicly available but are available from the corresponding author on reasonable request.

Supplementary data

Supplementary data to this article can be found online at <https://doi.org/10.1016/j.jhep.2021.06.019>.

References

Author names in bold designate shared co-first authorship

- [1] Lopez AD, Williams TN, Levin A, Tonelli M, Singh JA, Burney PGJ, et al. Remembering the forgotten non-communicable diseases. *BMC Med* 2014;12:200.
- [2] GBD 2016 Alcohol Collaborators. Alcohol use and burden for 195 countries and territories, 1990–2016: a systematic analysis for the Global Burden of Disease Study 2016. *Lancet* 2018;392:1015–1035.
- [3] World Health Organization. Global Status Report on Alcohol and Health 2018. World Health Organization; 2019.
- [4] Arab JP, Bataller R, Roblero JP. Are we really taking care of alcohol-related liver disease in Latin America? *Clin Liver Dis* 2020;16:91–95.
- [5] Jmelnitzky A. Alcoholic hepatitis: epidemiologic nature and severity of the clinical course in Argentina. *Acta Gastroenterol Latinoam* 1987;17:287–297.
- [6] Christoffersen P, Nielsen K. Histological changes in human liver biopsies from chronic alcoholics. *Acta Pathol Microbiol Scand A* 1972;80:557–565.
- [7] **Trabut J-B, Plat A**, Thepot V, Fontaine H, Vallet-Pichard A, Nalpas B, et al. Influence of liver biopsy on abstinence in alcohol-dependent patients. *Alcohol Alcohol* 2008;43:559–563.
- [8] Naveau S, Giraud V, Borotto E, Aubert A, Capron F, Chaput JC. Excess weight risk factor for alcoholic liver disease. *Hepatology* 1997;25:108–111.
- [9] Maddrey WC, Boitnott JK, Bedine MS, Weber Jr FL, Mezey E, White Jr RI. Corticosteroid therapy of alcoholic hepatitis. *Gastroenterology* 1978;75:193–199.
- [10] Dunn W, Jamil LH, Brown LS, Wiesner RH, Kim WR, Menon KVN, et al. MELD accurately predicts mortality in patients with alcoholic hepatitis. *Hepatology* 2005;41:353–358.
- [11] Ruf AE, Kremers WK, Chavez LL, Descalzi VI, Podesta LG, Villamil FG. Addition of serum sodium into the MELD score predicts waiting list mortality better than MELD alone. *Liver Transpl* 2005;11:336–343.
- [12] Kamath PS, Wiesner RH, Malinchoc M, Kremers W, Therneau TM, Kosberg CL, et al. A model to predict survival in patients with end-stage liver disease. *Hepatology* 2001;33:464–470.
- [13] Dominguez M, Rincón D, Abraldez JG, Miquel R, Colmenero J, Bellot P, et al. A new scoring system for prognostic stratification of patients with alcoholic hepatitis. *Am J Gastroenterol* 2008;103:2747–2756.
- [14] Forrest EH, Evans CDJ, Stewart S, Phillips M, Oo YH, McAvoy NC, et al. Analysis of factors predictive of mortality in alcoholic hepatitis and derivation and validation of the Glasgow alcoholic hepatitis score. *Gut* 2005;54:1174–1179.
- [15] Louvet A, Naveau S, Abdelnour M, Ramond M-J, Diaz E, Fartoux L, et al. The Lille model: a new tool for therapeutic strategy in patients with severe alcoholic hepatitis treated with steroids. *Hepatology* 2007;45:1348–1354.
- [16] **Louvet A, Labreuche J**, Artru F, Boursier J, Kim DJ, O'Grady J, et al. Combining data from liver disease scoring Systems better predicts outcomes of patients with alcoholic hepatitis. *Gastroenterology* 2015;149:398–406.e8; quiz e16–7.
- [17] **Altamirano J, López-Pelayo H**, Michelena J, Jones PD, Ortega L, Ginès P, et al. Alcohol abstinence in patients surviving an episode of alcoholic hepatitis: prediction and impact on long-term survival. *Hepatology* 2017;66:1842–1853.
- [18] Arab JP, Roblero JP, Altamirano J, Bessone F, Chaves Araujo R, Higuera-De la Tijera F, et al. Alcohol-related liver disease: clinical practice guidelines by the Latin American association for the study of the liver (ALEH). *Ann Hepatol* 2019;18:518–535.
- [19] Crabb DW, Im GY, Szabo G, Mellinger JL. Diagnosis and treatment of alcohol-associated liver diseases: 2019 practice guidance from the American association for the study of liver diseases. *Hepatology* [Internet] 2020. Available from: <https://aasldpubs.onlinelibrary.wiley.com/doi/abs/10.1002/hep.30866>.
- [20] European Association for the Study of the Liver. Electronic address: easloffice@easloffice.eu, European association for the study of the liver. EASL clinical practice guidelines: management of alcohol-related liver disease. *J Hepatol* 2018;69:154–181.
- [21] Thursz MR, Richardson P, Allison M, Austin A, Bowers M, Day CP, et al. Prednisolone or pentoxifylline for alcoholic hepatitis. *N Engl J Med* 2015;372:1619–1628.
- [22] Singh S, Murad MH, Chandar AK, Bongiorno CM, Singal AK, Atkinson SR, et al. Comparative effectiveness of pharmacological interventions for severe alcoholic hepatitis: a systematic review and network meta-analysis. *Gastroenterology* 2015;149:958–70.e12.
- [23] Pavlov CS, Varganova DL, Casazza G, Tsochatzis E, Nikolova D, Gluud C. Glucocorticosteroids for people with alcoholic hepatitis. *Cochr Database Syst Rev* 2019;4:CD001511.
- [24] Crabb DW, Bataller R, Chalasani NP, Kamath PS, Lucey M, Mathurin P, et al. Standard definitions and common data elements for clinical trials in patients with alcoholic hepatitis: recommendation from the NIAAA alcoholic hepatitis consortia. *Gastroenterology* 2016;150:785–790.
- [25] Rabe-Hesketh S, Skrondal A. Multilevel and Longitudinal Modeling Using Stata. Second Edition. Stata Press; 2008.

- [26] Austin PC. A tutorial on multilevel survival analysis: methods, models and applications. *Int Stat Rev* 2017;85:185–203.
- [27] Cummings P. *Analysis of Incidence Rates*. CRC Press; 2019.
- [28] Cummings P. Estimating adjusted risk ratios for matched and unmatched data: an update. *Stata J* 2011;11:290–298.
- [29] Helman RA, Temko MH, Nye SW, Fallon HJ. Alcoholic hepatitis. Natural history and evaluation of prednisolone therapy. *Ann Intern Med* 1971;74:311–321.
- [30] Porter HP, Simon FR, Pope 2nd CE, Volwiler W, Fenster LF. Corticosteroid therapy in severe alcoholic hepatitis. A double-blind drug trial. *N Engl J Med* 1971;284:1350–1355.
- [31] Campra JL, Hamlin Jr EM, Kirshbaum RJ, Olivier M, Redeker AG, Reynolds TB. Prednisone therapy of acute alcoholic hepatitis. Report of a controlled trial. *Ann Intern Med* 1973;79:625–631.
- [32] Blitzer BL, Mutchnick MG, Joshi PH, Phillips MM, Fessel JM, Conn HO. Adrenocorticosteroid therapy in alcoholic hepatitis. A prospective, double-blind randomized study. *Am J Dig Dis* 1977;22:477–484.
- [33] Lesesne HR, Bozymski EM, Fallon HJ. Treatment of alcoholic hepatitis with encephalopathy. Comparison of prednisolone with caloric supplements. *Gastroenterology* 1978;74:169–173.
- [34] Shumaker JB, Resnick RH, Galambos JT, Makopour H, Iber FL. A controlled trial of 6-methylprednisolone in acute alcoholic hepatitis. With a note on published results in encephalopathic patients. *Am J Gastroenterol* 1978;69:443–449.
- [35] Depew W, Boyer T, Omata M, Redeker A, Reynolds T. Double-blind controlled trial of prednisolone therapy in patients with severe acute alcoholic hepatitis and spontaneous encephalopathy. *Gastroenterology* 1980;78:524–529.
- [36] Theodossi A, Eddleston AL, Williams R. Controlled trial of methylprednisolone therapy in severe acute alcoholic hepatitis. *Gut* 1982;23:75–79.
- [37] Bories P, Guedj JY, Mirouze D, Yousfi A, Michel H. Treatment of acute alcoholic hepatitis with prednisolone. 45 patients. *Presse Med* 1987;16:769–772.
- [38] Carithers Jr RL, Herlong HF, Diehl AM, Shaw EW, Combes B, Fallon HJ, et al. Methylprednisolone therapy in patients with severe alcoholic hepatitis. A randomized multicenter trial. *Ann Intern Med* 1989;110:685–690.
- [39] Imperiale TF, McCullough AJ. Do corticosteroids reduce mortality from alcoholic hepatitis? A meta-analysis of the randomized trials. *Ann Intern Med* 1990;113:299–307.
- [40] Hofer T, McMahon L. Corticosteroids and alcoholic hepatitis. *Hepatology* 1991;13:199–201.
- [41] Daures JP, Peray P, Bories P, Blanc P, Yousfi A, Michel H, et al. [Corticoid therapy in the treatment of acute alcoholic hepatitis. Results of a meta-analysis]. *Gastroenterol Clin Biol* 1991;15:223–228.
- [42] Christensen E, Gluud C. Glucocorticoids are ineffective in alcoholic hepatitis: a meta-analysis adjusting for confounding variables. *Gut* 1995;37:113–118.
- [43] Mendenhall CL, Anderson S, Garcia-Pont P, Goldberg S, Kiernan T, Seeff LB, et al. Short-term and long-term survival in patients with alcoholic hepatitis treated with oxandrolone and prednisolone. *N Engl J Med* 1984;311:1464–1470.
- [44] Phillips M, Curtis H, Portmann B, Donaldson N, Bomford A, O'Grady J. Antioxidants versus corticosteroids in the treatment of severe alcoholic hepatitis—a randomised clinical trial. *J Hepatol* 2006;44:784–790.
- [45] Louvet A, Thursz MR, Kim DJ, Labreuche J, Atkinson SR, Sidhu SS, et al. Corticosteroids reduce risk of death within 28 Days for patients with severe alcoholic hepatitis, compared with pentoxifylline or placebo—a meta-analysis of individual data from controlled trials. *Gastroenterology* 2018;155. 458–468.e8.
- [46] Vergis N, Atkinson SR, Knapp S, Maurice J, Allison M, Austin A, et al. In patients with severe alcoholic hepatitis, prednisolone increases susceptibility to infection and infection-related mortality, and is associated with high circulating levels of bacterial DNA. *Gastroenterology* 2017;152. 1068–1077.e4.
- [47] Hmoud BS, Patel K, Bataller R, Singal AK. Corticosteroids and occurrence of and mortality from infections in severe alcoholic hepatitis: a meta-analysis of randomized trials. *Liver Int* 2016;36:721–728.
- [48] Pavlov CS, Varganova DL, Casazza G, Tsochatzis E, Nikolova D, Gluud C. Glucocorticosteroids for people with alcoholic hepatitis (Cochrane review). *Cochrane Database Syst Rev* 2017 Nov 2;11(11):CD001511. <https://doi.org/10.1002/14651858.CD001511.pub3>.

The EFSUMB Guidelines and Recommendations for the Clinical Practice of Elastography in Non-Hepatic Applications: Update 2018

Die EFSUMB-Leitlinien und Empfehlungen für die klinische Praxis der Elastografie bei nichthepatischen Anwendungen: Update 2018

Authors

Adrian Săftoiu¹, Odd Helge Gilja², Paul S. Sidhu³, Christoph F. Dietrich⁴, Vito Cantisani⁵, Dominique Amy⁶, Michael Bachmann-Nielsen⁷, Flaviu Bob⁸, Jörg Bojunga⁹, Marko Brock¹⁰, Fabrizio Calliada¹¹, Dirk André Clevert¹², Jean-Michel Correas¹³, Mirko D'Onofrio¹⁴, Caroline Ewertsen⁷, André Farrokh¹⁵, Daniela Fodor¹⁶, Pietro Fusaroli¹⁷, Roald Flesland Havre², Michael Hocke¹⁸, André Ignee⁴, Christian Jenssen¹⁹, Andrea Sabine Klauser²⁰, Christian Kollmann²¹, Maija Radzina²², Kumar V. Ramnarine²³, Luca Maria Sconfienza²⁴, Carolina Solomon²⁵, Ioan Sporea²⁶, Horia Ștefănescu²⁷, Mickael Tanter²⁸, Peter Vilmann²⁹

Affiliations

- 1 Research Center of Gastroenterology and Hepatology Craiova, University of Medicine and Pharmacy Craiova, Romania
- 2 National Centre for Ultrasound in Gastroenterology, Haukeland University Hospital, Bergen, and Department of Clinical Medicine, University of Bergen, Norway
- 3 Department of Radiology, King's College London, King's College Hospital, United Kingdom of Great Britain and Northern Ireland
- 4 Medizinische Klinik 2, Caritas-Krankenhaus, Bad Mergentheim, Germany
- 5 Radiological, Pathological and Oncological Sciences Department, University Sapienza, Rome, Italy
- 6 Radiology Department, Breast Center, Aix-en-Provence, France
- 7 Department of Radiology, Copenhagen-University-Hospital, Rigshospitalet, Copenhagen OE, Denmark
- 8 Nephrology Department, University of Medicine and Pharmacy "Victor Babeș" Timișoara, Romania
- 9 Med. Klinik I, Department of Endocrinology Universitätsklinikum, Frankfurt am Main, Germany
- 10 Department of Urology, Marien Hospital Herne, Ruhr-University Bochum, Germany
- 11 Department of Radiology, Policlinico San Matteo, University of Pavia, Pavia, Italy
- 12 Department of Clinical Radiology, University of Munich-Grosshadern Campus, Munich, Germany
- 13 Service de Radiologie adultes, Hôpital Necker, Université Paris Descartes, Paris, France
- 14 Department of Radiology, G.B. Rossi University Hospital, University of Verona, Verona, Italy
- 15 Department of Breast Imaging and Interventions, University Hospital Schleswig-Holstein Campus Kiel, Germany
- 16 2nd Medical Clinic, "Iuliu Hațieganu" University of Medicine and Pharmacy Cluj-Napoca, Romania
- 17 Gastroenterology Unit, Department of Medical and Surgical Sciences, University of Bologna/Hospital of Imola, Italy
- 18 Internal Medicine II, Klinikum Meiningen, Germany
- 19 Klinik für Innere Medizin, Krankenhaus Märkisch Oderland Strausberg/Wriezen, Germany
- 20 Universitätsklinik für Radiologie/Medizinische Universität Innsbruck, Austria
- 21 Center for Medical Physics & Biomedical Engineering, Medical University of Vienna, Austria
- 22 Radiology Research Laboratory, Riga Stradins University, Medical faculty, University of Latvia, Diagnostic Radiology Institute, Paula Stradina Clinical University Hospital, Riga, Latvia
- 23 Medical Physics Department, Guy's and St Thomas' NHS Foundation Trust, London, and University of Leicester, Leicester, United Kingdom of Great Britain and Northern Ireland
- 24 IRCCS Istituto Ortopedico Galeazzi, Milano Italy and Department of Biomedical Sciences for Health, University of Milano, Italy
- 25 Radiology Department, "Iuliu Hațieganu" University of Medicine and Pharmacy Cluj-Napoca, Emergency Clinical County Hospital, Cluj-Napoca, Romania
- 26 Department of Gastroenterology and Hepatology, University of Medicine and Pharmacy "Victor Babeș" Timișoara, Romania
- 27 Hepatology Unit, Regional Institute of Gastroenterology and Hepatology, Cluj-Napoca, Romania

All authors contributed equally to the manuscript.

28 Physics for Medicine Paris Institute, INSERM, CNRS, ESPCI
Paris, France

29 Endoscopy Department, Copenhagen University Hospital
Herlev, Denmark

Key words

ultrasound elastography, guideline, EFSUMB

received 22.08.2018

accepted 10.03.2019

Bibliography

DOI <https://doi.org/10.1055/a-0838-9937>

Published online: June 25, 2019

Ultraschall in Med 2019; 40: 425–453

© Georg Thieme Verlag KG, Stuttgart · New York

ISSN 0172-4614

Correspondence

Prof. Adrian Saftoiu

Research Center in Gastroenterology and Hepatology,
University of Medicine and Pharmacy Craiova, Macinului 1,
200640 Craiova, Romania

Tel.: ++40/7 44 82 33 55

Fax: ++40/2 51/31 02 87

adrian.saftoiu@umfvcv.ro

ABSTRACT

This manuscript describes the use of ultrasound elastography, with the exception of liver applications, and represents an update of the 2013 EFSUMB (European Federation of Societies for Ultrasound in Medicine and Biology) Guidelines and Recommendations on the clinical use of elastography.

ZUSAMMENFASSUNG

Diese Arbeit beschreibt den Einsatz der Ultraschall-Elastografie mit Ausnahme der Leberanwendungen und ist eine Aktualisierung der Leitlinien und Empfehlungen der EFSUMB (European Federation of Societies for Ultrasound in Medicine and Biology) von 2013 zum klinischen Einsatz der Elastografie.

ABBREVIATIONS

SE	strain elastography
SWE	shear wave elastography
pSWE	point shear wave elastography
TE	transient elastography
IQR	interquartile range
IQR/M	interquartile range/median
ARFI	acoustic radiation force impulse
BIRADS	Breast Imaging Reporting and Data System
TIRADS	Thyroid Imaging Reporting and Data System
TI	thermal index
MI	mechanical index
SR	strain ratio
SH	strain histogram
EFSUMB	European Federation of Societies for Ultrasound in Medicine and Biology
ECMUS	European Committee of Medical Ultrasound Safety
WFUMB	World Federation for Ultrasound in Medicine and Biology
LoE	levels of evidence
GoR	grades of recommendation

1. Introduction

This manuscript describes the use of ultrasound elastography, with the exception of liver applications, and represents an update of the 2013 EFSUMB (European Federation of Societies for Ultra-

sound in Medicine and Biology) Guidelines and Recommendations on the clinical use of elastography. A taskforce comprising 32 EFSUMB members was established in 2017 to draft a manuscript derived and updated from the previous EFSUMB guidelines on elastography: part 1 (Basic Principles and Technology) and part 2 (Clinical Applications) [1, 2]. For each recommendation levels of evidence (LoE) and grades of recommendation (GoR) were also included to show the clinical role and value of elastography in various non-liver applications. These were assigned according to the Oxford Centre for Evidence-based Medicine criteria (<http://www.cebm.net/oxford-centre-evidencebased-medicine-levels-evidence-march-2009/>). A consensus opinion was established by vote as follows: strong consensus (>95%), broad consensus (>80%), with approval, disapproval or abstaining from each participant. The manuscript was prepared initially by e-mail communication and was discussed in a consensus meeting in Frankfurt am Main, Germany, during February 2018.

2. Training

EFSUMB maintains a policy to attain high quality in all aspects of ultrasound education and to promote excellent professional standards in the practice of elastography. EFSUMB has defined three levels of competence, defined in the document on minimal training requirements [3], and these training levels also apply to the application of elastography. To ensure high-quality scanning and the lowest possible intra-operator variability, EFSUMB recommends that ultrasound elastography should be performed by operators that have passed competence Level 1. This is particularly relevant to the evaluation of focal lesions present in various

organs as these lesions must be first assessed by B-mode and Doppler ultrasound [4]. However, it is possible to train dedicated personnel to selectively perform elastography, e. g. for the thyroid gland [5]. Nevertheless, there has to be an appreciation of the difference between acquisition and interpretation of elastography, as the latter also requires knowledge of the patient's clinical history, hematological and biochemical parameters, and other comparative imaging findings. Furthermore, experience in ultrasonography is important as this influences the ability to perform shear wave measurements, particularly in obese patients [6]. For all ultrasound operators it is important to follow international guidelines, obtain adequate knowledge and training, and to perform elastography in accordance with national medico-legal regulations.

RECOMMENDATION 1

The operator should obtain adequate knowledge and training in ultrasonography and elastographic methods and perform the examination within the medico-legal framework of the specific country (LoE 5, GoR C) (For 20, Abstain 0, Against 0).

3. Terminology

Terminology of ultrasound elastography has been widely accepted [1, 7]. In the following, we briefly refer to the distinction between strain elastography (SE) and shear wave elastography (SWE), which includes acoustic radiation force impulse (ARFI) based techniques and transient elastography (TE). All available ultrasound elastography methods employ ultrasound to measure the internal tissue shear deformations resulting from an applied force but the type of force is important. If the force varies slowly relative to the shear propagation time to the depth of interest, as is the case for transducer palpation or physiological motion, it is considered quasi-static. The signal processing within the scanner for all current commercial ultrasound elastography methods begins with the measurement of tissue displacement as a function of spatial position and time, which is performed using cross-correlation tracking, Doppler, or other signal processing. The various elastography methods differ importantly according to what they do with these displacement data, to create an elastogram or elasticity measurement.

According to the EFSUMB guidelines, there are two options for the property displayed [8, 9]:

- Display tissue strain or strain rate, calculated from the spatial gradient of displacement or velocity respectively, as in SE. SE is a type of quasistatic elastography, because the applied force varies slowly, while the acquired images are qualitative for tissue properties.
- Display shear wave speed, calculated by using the time varying displacement data to measure the arrival time of a shear wave at various locations. There are a number of such methods, which are grouped under the heading SWE, and include transient elastography (TE), point shear wave elastography (pSWE)

and multidimensional SWE (2D-SWE and 3D-SWE). These are based on either a transient shear deformation induced by a controlled applied force (TE) or by quantification of tissue displacement induced by acoustic radiation force impulse (ARFI) [8, 9].

Most SE ultrasound systems do have an indicator (quality index) displayed in real time, indicating that the degree of compressions/decompressions is appropriate to generate repeatable and reproducible SE images [7 – 11]. The pressure and direction of compressions can be changed by the examiner, especially for external ultrasound procedures, with the compressions/decompressions needed by most systems being less than 2%. Quality factors for the shear wave speed estimate are available also for the 2D-SWE techniques. For ARFI-based techniques, an approach similar to that of TE has been employed to assess the quality of the measurement, including the interquartile range (IQR) values (i. e. the difference between the 75th and 25th percentile) and IQR/median. Assessment is considered reliable when the IQR is less than 30% of the median [8, 9]. The values obtained for SWE vary between different machines and are not interchangeable.

For more terminology and quality assurance details, refer to the EFSUMB and WFUMB guidelines on the use of elastography [1, 2, 7 – 11].

4. Safety

Elastography needs a “push” to the organ of interest that can be produced either mechanically or acoustically and may be quasi-static or dynamic. Different techniques are commercially available for the measurement of elastic values for an increasingly wide range of clinical applications. It is essential to know the principle of each of the techniques and how it is applied to understand the implications for patient safety [1 – 3]. A possible risk depends on the technology or type of elastography used and its anatomical application.

4.1 Methods

Techniques which utilize a mechanically induced force to generate SE, strain rate imaging, TE and time harmonic elastography (which uses external vibrations at multiple frequencies to create compound shear wave speed maps) share the same output issues as conventional B-mode ultrasound examination [1]. Therefore, applications of TE measuring quantitative stiffness data were demonstrated to be feasible for children to assess not only liver stiffness data [12, 13] but also spleen stiffness measurement [14] with no increased risk. Also, there is new evidence that patients with cardiac pacemakers or implantable cardioverter defibrillators, have a low potential to be harmed by TE applications [15, 16].

Acoustically induced techniques which require push pulses (known as ARFI imaging, ARFI quantification, pSWE, SWE [2]) on the other hand operate with higher output (higher TI and MI values) [17, 18]. The safety profile is comparable with pulse-wave Doppler mode and the acoustic output will depend on the applied sequence and repetition of pushing and tracking pulses.

A certain amount of energy is required to displace the tissue, even a few microns, using acoustic radiation force to generate shear waves within the tissue (longer pulses of up to 1000 μ s are needed, as compared to short pulses up to 2 μ s for diagnostic ultrasound) [8, 9]. The number of push pulses and repetitions during the measurement determine the amount of energy deposited in the tissue. Simulations have revealed a possible temperature rise of about 5 degrees Celsius if bone is present or sensitive tissues such as the eye and a fetus are involved with the temperature maximum at the focus [19–21]. Also, tracking beams, repeated with high frequencies, use pulse pressures close to the upper Food and Drug Administration limit ($MI \leq 1.9$) to ensure a sufficient signal-to-noise ratio for reliable detection [22]. During ARFI imaging, the displayed indices (MI and TI) may be underestimated.

RECOMMENDATION 2

To comply with safety, the ALARA (as low as reasonably achievable) principle should be applied when using ultrasound elastography (LoE 2b, GoR B) (For 18, Abstain 2, Against 0).

RECOMMENDATION 3

Caution is recommended for shear wave elastography using long pulse sequences, particularly when exposing sensitive tissues (LoE 2b, GoR B) (For 19, Abstain 1, Against 0).

5. Breast

5.1 Background

Breast elastography is used for differentiating benign focal lesions from suspicious focal lesions – benign lesions have low stiffness, while malignant lesions have high stiffness. Both strain and shear wave methods have been evaluated for improving the generally high sensitivity and specificity of the Breast Imaging Reporting and Data System (BIRADS) and it is recommended that they are used as add-ons to the regular B-mode examination.

5.2 Methods

5.2.1 Strain elastography

SE images in breast ultrasound may be evaluated visually using the Tsukuba score (also known as the Itoh or Ueno score) [23], semi-quantitatively using strain ratio (SR) or strain histograms (SH) [24] or by the lesion size on elastography divided by the lesion size on B-mode ultrasound (E/B ratio) [25]. An optimal elastogram includes the glandular tissue, the surrounding fat, and the lesion [11].

The Tsukuba score is a five-point visual scale, where the lesion is scored according to the extent of stiff tissue. A lesion not stiffer

than the surrounding tissue is designated as 1, a value of 2 or 3 is assigned to lesions with increasing proportions of stiff tissue, a value of 4 is assigned to a lesion that is stiffer throughout, and 5 indicates that the stiffness extends beyond the margins of the mass seen on B-mode. The best cut-off point for discriminating benign from suspicious masses has been shown to be a score between 3 and 4 [26–28]. It has been shown that SE, in addition to B-mode ultrasound, increases the specificity of the examination (up to 97%) and helps to avoid unnecessary biopsies [29].

Anechoic lesions with liquid content show a typical three-layered echo-pattern in SE, called the Blue Green Red (BGR) sign.

5.2.2 Shear wave elastography

For SWE, findings are measured in m/s but may also be reported in kPa depending on the system used. As for SE the optimal image should include the lesion, fat and the glandular tissue. Malignant tumors tend to be more heterogeneous and stiffer than benign tumors. Often the stiffness seems to be most marked at the periphery of the mass and may demonstrate such high values that the system is unable to record a measurement.

5.3 Clinical Applications

5.3.1 Evaluation of breast masses

An early study using SR in 99 nonpalpable benign and malignant breast masses established an optimal cut-off of 2.24 and stated that the higher the SR, the higher the risk of malignancy [30]. The cut-off for SR has since been evaluated in several studies with different systems and is incomparable between different vendors, as seen in other organ applications. In a recent meta-analysis [31], the accuracy of SR was evaluated based on 9 studies (2087 tumors) with a sensitivity of 0.88 and a specificity of 0.83. The E/B ratio (ratio of the lesion size with SE to the lesion size with B-mode ultrasound) increases with increasing tumor grading, with low grade tumors having a ratio close to 1 [11].

In the BE1 multicenter study SWE results were studied retrospectively and several parameters were examined. One finding of the study was that the addition of SWE resulted in some BIRADS 3 lesions appearing stiffer and potentially allowed for an upgrade to a 4a mass, requiring a biopsy. If SWE had been included and used in this way, the overall sensitivity and specificity would have increased to 98.6% and 78.5% versus 97.2% and 61.1% for B-mode ultrasound alone [32]. Increasing stiffness has also been shown to correlate with increasing tumor grading [33–36].

In cysts with pure liquid, no signals are obtained from the shear waves and the lesion is seen as black. However, in cysts with a higher viscosity shear wave signals may be obtained depicting the cyst as having a low stiffness.

5.3.2 Evaluation of axillary lymph nodes

Both SWE and SE have been used in the evaluation of axillary lymph nodes, with one study reporting a sensitivity and specificity of 82.8% and 69.6%, respectively, using SWE to distinguish between benign and malignant lymph nodes using a cut-off of 1.44 m/s [37]. Using SE, the sensitivity was 60% and the specificity was 79.6% for the diagnosis of malignancy [38]. Another study

compared the AUROC for elastography with the AUROC for conventional B-mode ultrasound. The values were 62 % and 92 %, respectively, and no significant improvement was shown when elastography was added to B-mode ultrasound (AUC: 93 %) [39].

5.3.3 Prognosis

The key factors for prognostic information are provided by histological and pathological analysis, based on cancer sub-typing and also immuno-histochemical analysis. Univariate analysis has demonstrated a significant correlation between stiffness of a breast cancer and prognostic factors. For SWE, studies reported an increased stiffness for cancer grading of more malignant tumors, larger lesion size, tumor and lympho-vascular invasion in invasive breast cancer. Triple-negative carcinomas (testing negative for oestrogen, progesterone and HER2 receptors), which are often evaluated with BIRADS 3 on B-mode ultrasound, are quite difficult to assess in clinical practice. SWE is reported to show increased stiffness in these cases and can lead to the correct assessment [33–35, 40].

A study reporting the analysis of 396 breast cancers showed that SWE is an independent predictor of lymph node metastasis when using E-mean (mean elasticity values for a defined region of interest) as a descriptor. When the breast cancer had E-mean < 50 kPa, only 7 % of the lymph nodes were metastatic, whereas 41 % of the lymph nodes were positive when E-mean was higher than 150 kPa [41].

5.3.4 Efficacy of neoadjuvant therapy

The tumor response to neoadjuvant chemotherapy may be evaluated with different imaging modalities. In a study with a small sample size of 15 patients, the possibility of predicting response to neoadjuvant chemotherapy with SE was reported [42]. However, larger studies for SE using commercially available systems are not available. A significant correlation between response to treatment and the decrease in heterogeneity and tumor stiffness has been reported [43, 44]. Currently, imaging methods other than elastography should be used in the evaluation of tumor response to neoadjuvant chemotherapy.

5.4 Limitations and artifacts

Pre-compression with the transducer should be avoided as this increases the stiffness of all tissues. Normal fatty tissue has E-mean values ranging from 5–10 kPa (using SWE) if the scale is from 0–180, although the color scale may be changed. If the color changes according to these values, the pre-compression should be adjusted [45].

RECOMMENDATION 4

Ultrasound elastography could be used to increase diagnostic confidence in the characterization of a breast lesion (LoE 2a, GoR B) (For 20, Abstain 0, Against 0).

RECOMMENDATION 5

A BIRADS 3 lesion appearing stiffer on breast ultrasound elastography should be considered for biopsy (LoE 2a, GoR b) (For 20, Abstain 0, Against 0).

6. Prostate

6.1 Background

The screening standard for prostate abnormalities has been the combination of digital rectal examination and the serum prostate specific antigen (PSA) level. However, PSA screening leads to a substantial number of unnecessary biopsies in patients with no or indolent cancer who do not need immediate treatment [46] and has a high false-negative rate (17–21 %) [47]. Saturation biopsy (up to 40 cores) can rule out prostate cancer, but has many limitations, including cost and morbidity, and over-diagnosis of microscopic tumor foci [48]. SE and SWE assessment and identification of stiff prostatic tissue with a transrectal ultrasound approach can be useful as described in previous elastography guidelines [1].

6.2 Methods

6.2.1 Strain elastography

Hypochoic stiff lesions of the prostate are suspicious for malignancy [49]. Slight compressions are induced using the transrectal transducer. The use of an inflatable balloon has been suggested to improve the standardization of compressions. The elastography box should cover the entire gland and the surrounding tissues, but avoid the bladder. Semi-quantitative information can be derived by measuring the SR between two regions of interest.

Using stepwise scanning of the prostate from base to apex, SE allows detection of stiff regions and provides stiffness comparisons between lesions and the adjacent prostatic tissue. Most studies report a significant improvement in prostate cancer identification with SE, including guidance for targeted biopsies [50–53]. However, there are still controversies and one recent study reported the inability to differentiate prostate cancer from chronic prostatitis [54]. The sensitivity, specificity, negative predictive value, positive predictive value, and accuracy for identifying cancer index lesions for focal therapy were 58.8 %, 43.3 %, 54.1 %, 48.1 %, and 51.6 %, respectively [55]. Though improvement in biopsy guidance is reported in many studies [53, 56, 57], others did not confirm this result [58].

6.2.2 Shear wave elastography

Unlike SE, SWE requires no compression on the rectal wall [59]. Optimized settings include maximizing penetration and setting up an appropriate scale. The image can cover the entire gland in the transverse section when the prostate is not markedly enlarged. Otherwise, each side of the prostate is imaged separately from base to apex for review and measurements of elastography values. For each plane, the transducer is maintained in a steady

position until the image stabilizes. Hypoechoic stiff lesions are suspicious for malignancy. The ratio between the mean elasticity values of two regions can be calculated.

In young healthy subjects the entire prostate exhibits a uniform low stiffness appearance with low elasticity values [60, 61]. In benign prostate hyperplasia, the peripheral zone remains homogeneous with low stiffness, while the central and transition zones become heterogeneous and stiff, particularly when there are calcifications. Typical benign peripheral lesions have a similar stiffness as the surrounding normal parenchyma, while cancers are stiff [60, 61]. The best cut-off stiffness value to maximize the negative predictive value for malignant lesions was found to be 35 and 37 kPa in two studies with 2D-SWE [57, 58] with a sensitivity, specificity, PPV and NPV of 63 %, 91 %, 69.4 %, and 91 %, respectively. The SWE ratio provided additional information as it considers the increased stiffness of the peripheral zone from calcification and chronic prostatitis. The ratio showing the best accuracy to differentiate between the nodule and the adjacent peripheral gland for benign and malignant lesions was 1.5 ± 0.9 and 4.0 ± 1.9 , respectively ($p < 0.002$) [61].

6.3 Clinical applications

Several studies indicate that elastography provides useful additional information to conventional transrectal ultrasound for prostate cancer detection. Applications that have been more extensively investigated include the characterization of abnormal areas, the detection of lesions not seen with any previous imaging technique and biopsy targeting. Additionally, elastography could be combined with other imaging techniques in the same examination to address the heterogeneous growth pattern of prostate cancer. Improvement in detection and prediction of cancer was seen during multiparametric ultrasound when elastography is used as a triage test followed by contrast-enhanced ultrasound or as an adjunct during image fusion of magnetic resonance imaging and transrectal ultrasound [62–65].

6.4 Limitations and artifacts

Both techniques suffer from intrinsic limitations: not all cancers are stiff and not all stiff lesions are cancers (particularly in the presence of calcifications and fibrosis). The transrectal technique carries an intrinsic risk of inadvertently applying excess pre-compression because of the end fire arrangement of the transducer.

Limitations of SE include the non-uniform force over the gland and intra- and inter-operator dependency. 2D-SWE has additional limitations such as a slower frame rate and the small elasticity box which only allows examination of half the gland at a time.

RECOMMENDATION 6

Transrectal ultrasound elastography of the prostate could be used to identify suspicious target regions for biopsy in order to increase the diagnostic yield of biopsy (LoE 2b, GoR b) (For 20, Abstain 0, Against 0).

7. Thyroid

7.1 Background

Chronic thyroiditis and malignant tumors increase diffuse or focal thyroid stiffness [66]. Elastography is emerging as a potential indicator for these abnormalities and may provide additional information to support clinical decision-making.

7.2 Classification systems – TIRADS

Accurate estimation of the malignancy risk by ultrasound could help to select thyroid nodules with a high risk of cancer for fine needle aspiration and biopsy (FNAB). More recently, an assessment concept called “grading system” or “reporting system” termed “Thyroid Imaging Reporting and Data System” or TIRADS has emerged, allowing thyroid nodules to be classified into categories related to their ultrasound patterns [66–74].

7.3 Methods

SE is the initial method which has been implemented on most commercially available ultrasound systems, thus evidence is quite consolidated on this topic, with a number of studies and meta-analyses being published [75–81]. More recently, SWE has become available for thyroid evaluation with multiple studies reported [82–85].

7.4 Clinical applications

7.4.1 Strain elastography

Two different methods of assessing SE outcome have been reported, namely semi-quantitative scoring systems involving five, four, or two color patterns respectively [86–88] and SR, which compares the strain values of the nodule to those of the surrounding thyroid parenchyma (parenchyma-to-nodule ratio) or the surrounding muscles (muscle-to-nodule ratio) [4, 89]. Although no consensus has been reached about the cut-off values to use for SR (as low as 1.5 for benign nodules and as high as 5 for malignant nodules have been suggested), it has been shown that the SR has a lower inter-observer variability and is more easily learned than simple color patterns [4]. Importantly, most studies on SE were performed in selected populations with a high prevalence of malignant nodules. It has been shown that SE has a lower sensitivity and specificity in a low-risk population [4, 90]. Furthermore, tumors other than papillary carcinomas may have an unexpectedly low stiffness [4, 91, 92]. In patients with coexistent diffuse thyroid disease, the role of SE in detecting malignant nodules has still not been validated [4]. The most recent meta-analysis [81] included 13 studies on SE performed from 2007 to 2016, with sensitivities ranging from 48 % [93] to 97 % [94] and specificities ranging from 64 % [95] to 100 % [94]. The pooled sensitivity and specificity of the meta-analysis was 84 % (95 % CI, 76 %–90 %) and 90 % (95 % CI, 85 %–94 %), respectively, with pooled accuracy of 94 % (95 % CI, 91 %–96 %).

7.4.2 SWE

The mean SW elasticity for malignant thyroid nodules is 19.60–52.18 kPa with a reported cut-off value of 26.6–65 kPa [96–

104]. For benign nodules the mean elasticity is lower at 15.3–28 kPa [96–104]. Studies included nodules from 2–71 mm and most were papillary carcinomas. Therefore, cut-off values have a wide range and a single threshold cannot be established [82, 83, 85]. The sensitivity for SWE has been reported as 63.8–93.8%, and the specificity as 50–88.2% [96, 97, 100, 102, 104–106]. The most recent meta-analysis [82] included 14 studies and 2851 thyroid nodules with cut-off values ranging from 26.6 to 85.2 kPa. It concluded that 2D-SWE has a fairly good diagnostic accuracy although the sensitivity and specificity are average. Studies using ARFI indicated that it enables the evaluation of tissue stiffness and the mean SWE velocity for malignant nodules is 3.13–3.9 m/s [96, 107–111] with a cut-off value 2.15–3.77 m/s [96, 107–111]. Interestingly, a recent meta-analysis [81] showed that SE and SWE are not significantly different in terms of sensitivity (SWE pooled sensitivity = 79% [95% CI, 73%–84%]) but SE is superior to SWE in terms of specificity (SWE pooled specificity = 87% [95% CI, 79%–92%]) and accuracy (SWE pooled accuracy = 83% [95% CI, 80%–86%]).

7.5 Limitations and artifacts

The thyroid is among the most extensively investigated non-liver application after the breast. Nevertheless, the relevance in the malignant/benign differential diagnosis remains unclear. Recent American Thyroid Association and Korean guidelines do not consider stiffness as an indicator of malignancy. However, elastography was recently mentioned by both the French TIRADS and the EU-TIRADS as a complementary imaging tool [70, 112]. Thus, elastography should not replace B-mode US assessment but should be used as a complementary tool for assessing nodules for fine-needle aspiration, especially due to its high negative predictive value (only 3% false-positive results) [70].

RECOMMENDATION 7

Ultrasound elastography of the thyroid could be used as part of nodule characterization, particularly with use of semi-quantitative methods (LoE 2A, GoR A) (For 17, Abstain 3, Against 0).

8. Pancreas

8.1 Background

Elastographic properties of the pancreas may be studied with a transabdominal approach, as well as with an endoscopic or intra-operative ultrasound approach. Pancreatic transabdominal ultrasound elastography requires clear visualization of the gland (which is not always possible with external ultrasound), whereas endoscopic ultrasound (EUS) is a minimally invasive technique that provides high-resolution images of the pancreas, with the close vicinity of the transducer and the pancreas avoiding artifacts (fat, gas, etc.).

8.2 Methods

For the elastographic assessment of the pancreatic parenchyma and focal pancreatic lesions, SWE [7, 113–133] as well as SE [7, 119, 120, 123, 124, 131, 134–177] may be used. Transabdominal elastography can be performed both by using SE with qualitative and semiquantitative information, and SWE with qualitative and quantitative data. EUS can be performed currently only with SE techniques with qualitative and semi-quantitative evaluation [178]. For the semi-quantitative approach, both SR and SH can be used in order to obtain an estimate of the elasticity [153].

The normal pancreas has a uniform intermediate stiffness throughout the head, body, and tail [123, 124, 129, 130, 132]. Embryologically, the pancreas develops from two primordia, a dorsal and a ventral part. With SE, elasticity properties seem to be almost similar in the two parts of a healthy pancreas with a homogeneous low stiffness appearance [158]. Studies in normal volunteers affirmed that the mean wave velocity value obtained in a healthy pancreas with the ARFI technique is approximately 1.40 m/s [114].

8.3 Clinical applications

8.3.1 Effect of aging, gender, anatomical segment, and other variables

With advancing age, pancreatic elasticity may decrease as has been shown consistently for SE [134] and SWE [121, 129, 131]. Data on the influence of gender, body mass index (BMI), and pancreatic echogenicity are not consistent, with most studies demonstrating no significant influence of these variables on shear wave velocity [113, 116, 121, 129, 131]. One study using SE with SH analysis showed lower mean strain values in patients with a hyper-echoic pancreas and higher BMI [134]. In another study shear wave velocity was significantly lower in men compared to women [129].

8.3.2 Acute pancreatitis

The consistency of the pancreatic parenchyma usually becomes stiffer in acute pancreatitis as compared to the healthy pancreas, which is identifiable with SE and SWE, including ARFI [116]. Necrosis is identified as a low stiffness area. However, studies using elastographic techniques in patients with acute pancreatitis are conflicting [116, 130, 179, 180]. One prospective study failed to find significant differences in pancreatic shear wave velocities between patients with acute pancreatitis and healthy volunteers [130]. Three other studies showed significantly higher pancreatic shear wave velocities in patients with acute pancreatitis compared to persons with a normal pancreas [116, 179, 180]. In one of these studies, shear wave velocities of patients with acute pancreatitis were higher than in chronic pancreatitis patients [179]. Another prospective study compared transabdominal ARFI imaging with B-mode ultrasound and computed tomography (CT) at hospital admission for the diagnosis of acute pancreatitis. SWE was more accurate (100%) for the diagnosis of acute pancreatitis than CT (76%) and B-mode ultrasound (53.4%). The authors were able to identify segmental involvement of the pancreas as well as parenchymal necrosis [180].

8.3.3 Chronic pancreatitis

Qualitative SE displays the pancreatic parenchyma in chronic pancreatitis with a heterogeneous colored (honeycombed) pattern, with predominantly stiffer strands. Nevertheless, differential diagnosis between chronic pancreatitis and pancreatic tumor can be challenging during elastography because both diseases have a similar stiffness. Therefore, elastography alone is not able to distinguish chronic pancreatitis from malignant tumors [164].

Both SWE and SE may be used to assess pancreatic fibrosis and chronic pancreatitis and in particular to grade the severity of fibrosis (based on simple scoring systems with 4 grades) and chronic pancreatitis [115–117, 122–124, 127, 131, 136, 138, 142, 146, 151, 164, 167, 169, 170, 179, 181–185]. In patients with chronic pancreatitis, pancreatic shear wave velocities [116, 124, 127, 131, 186], SR [148] and SH [146] are significantly higher than in healthy volunteers or patients with a normal pancreatic parenchyma. Several studies have shown a significant correlation between SWE [117, 123, 184] and semi-quantitative SE [138, 167, 169, 185] and histological pancreatic fibrosis stage. Moreover, SWE [122, 124, 169] and SR [141] are significantly correlated with stages of chronic pancreatitis derived from EUS-based criteria for the diagnosis of chronic pancreatitis. Another recent study showed significantly higher pancreatic SWE velocities in patients with clinical markers of severe disease (disease duration > 10 years, chronic analgesic treatment, lower body weight) [127]. A direct relationship between the SR of pancreatic parenchyma and low stiffness peripancreatic tissue and the probability of pancreatic exocrine insufficiency was shown in a study using EUS-SE [136]. Another study reported an inverse correlation between preoperative SW velocity and postoperative exocrine function in patients undergoing pancreatic resection [117].

EUS elastography might be helpful in identifying patients with autoimmune pancreatitis, due to the unique appearance of diffuse stiff tissue with an elastographic pattern visible both in the mass lesion and in the adjacent pancreatic parenchyma, with mainly stiff color signals that were evenly spread over the head and the body of the pancreas [161, 187].

8.3.4 Preoperative indications

Recently, elastography has been used prior to pancreatic surgery to examine the gland stiffness in order to assess the risk of surgical complications. Evaluation of pancreatic stiffness might be an objective index to estimate pancreatic fibrosis and predict the risk of postoperative pancreatic fistula. Data from several studies suggest that SWE [115, 117, 184, 188] and SE [138, 170, 185] may be used for this purpose. In particular, a pancreatic parenchyma with a low stiffness as determined by semi-quantitative SE [138, 170] or SWE [117] proved to be an independent predictor of postoperative pancreatic fistula.

8.3.5 Pancreatic ductal adenocarcinoma and other solid pancreatic neoplasms

In pancreatic ductal adenocarcinoma (PDAC), shear wave velocities are significantly higher than in normal pancreatic parenchyma

obtained in healthy subjects [116, 125, 133] as well as in pancreatic parenchyma surrounding the tumor [125]. Shear wave velocities measured in PDAC usually exceed 3 m/s [116, 125, 126, 133]. However, there is a significant overlap of SWE velocities between malignant solid lesions, benign solid lesions, and chronic pancreatitis [116, 126]. One study demonstrated a significantly higher difference between the SWE velocities of malignant lesions and surrounding pancreatic parenchyma compared to the difference values between benign lesions and surrounding parenchyma [126]. No large prospective comparative studies evaluating the accuracy of SWE for the characterization of solid pancreatic lesions are available.

More evidence is available on the clinical value of EUS-SE for the differential diagnosis of solid pancreatic lesions [172, 189–192]. An early study described EUS elastography patterns in healthy subjects, in diffuse chronic pancreatitis and in focal pancreatic lesions [139]. All malignant pancreatic tumors and serous cystadenomas showed a honeycomb pattern of medium stiffness, and were well delineated against healthy parenchyma. However, this pattern was also observed in half of the chronic pancreatitis patients, so that the specificity of the method was reported at only about 60%, attributed to fibrotic structures producing similar mechanical properties in cancer and chronic pancreatitis [139, 164]. Therefore, elastography is not sufficient to contribute to the early diagnosis of pancreatic carcinoma in chronic pancreatitis [139, 164].

Qualitative [137, 139, 163, 164, 193–195] and semi-quantitative SE approaches (SR, SH analysis) [135, 142–144, 149, 150, 152–156, 175, 177, 196–199] have been used for the differential diagnosis of benign and malignant focal pancreatic masses, with both showing high overall accuracy. Computer-aided diagnosis techniques might improve the accuracy for the differential diagnosis of focal pancreatic masses, with artificial neural networks being used most often [154, 156]. Several multicenter studies [155, 156, 194] and other prospective studies [135, 149, 150, 152, 177, 197, 198] consistently showed a very high sensitivity (over 90%), but considerably lower specificity and negative predictive values for the diagnosis of benign versus malignant focal pancreatic masses. These findings have been summarized in meta-analyses, affirming the very high sensitivity (95%–99%) and negative predictive value of EUS-SE, but limited specificity (64%–76%) and positive predictive value to diagnose pancreatic malignancy [172, 189–192]. Significant differences in favor of qualitative or semi-quantitative assessment techniques have not been observed in meta-analyses. Therefore, there is expert consensus that SE cannot replace a cytopathological diagnosis of focal pancreatic disease [162, 200, 201]. Combining several EUS-based advanced tools of tissue characterization may provide the best results in differential diagnosis of focal pancreatic lesions [135, 143, 144, 149, 202–205]. Nevertheless, when EUS-guided sampling is negative or inconclusive, suspicious findings with elastography and contrast-enhanced techniques will influence further clinical decisions by indicating repeat sampling or direct referral to surgery. On the other hand, the finding of a solid pancreatic lesion with elastographic properties of low stiffness and without hypo-enhancement in contrast-enhanced EUS is nearly always predictive for the benign nature of the lesion. Since the negative

predictive value of EUS-FNA for the diagnosis of a malignant solid pancreatic lesion is only 72% [203–207], such a finding may prevent potentially nondiagnostic or risky procedures [195, 207].

8.3.6 Cystic pancreatic tumors

Elastography can have a role in pancreatic cystic lesions, both with SE and with SWE, in particular with ARFI. SWE has been shown to be accurate for the differentiation between serous and mucinous cystic pancreatic lesions [133, 208–212]. Serous cystadenomas are filled with serous fluid exhibiting similar physical properties as water, while numerous and dense septa together with a fibrous scar can be present in a mucinous cystadenoma. Therefore, the microcystic serous cystadenoma appears as a very stiff lesion with EUS-SE [139, 164, 196]. With ARFI, shear wave velocity in serous cystadenoma is infinitely high and numerical values cannot be obtained. Due to the more complex fluid content, shear wave velocities in mucinous cystic lesions are very high, but numerical values may be obtained in most cases [133, 208–212].

8.4 Limitations and artifacts

EUS-elastography suffers from technical limitations and artifacts. Some issues are common with transabdominal ultrasound, such as the need to obtain a close proximity to the target and to avoid anatomical planes allowing slip movements anterior to or within the imaged region [1]. In particular, large vessels in the imaged area represent the main reason for shear stress damping. Issues peculiar to EUS are essentially caused by the small size of the transducer providing a limited stress source to image the region of interest. In addition, it is very difficult to standardize the pressure exerted by the echoendoscope tip to the gastrointestinal wall, resulting in variability of the color mapping. Lastly, respiration and heartbeat-induced movements of the target lesion may cause a complete lack of color signal within the region of interest. As far as the color mapping of EUS elastography is concerned, disadvantages include subjective differences in color vision and image categories that may not correspond well to pathology [194]. The selection of frames for the SR or SH measurements is user-dependent. In addition, unrepresentative elastograms or reference tissues with a different distance to the stress source may result in method bias [213]. For these reasons, finding an optimal cut-off for differentiating pancreatic tumors from benign disease has been challenging.

RECOMMENDATION 8

Transabdominal and endoscopic ultrasound elastography may be used as additional imaging tools for the diagnosis and grading of chronic pancreatitis (LoE 2b, GoR B) (For 20, Abstain 0, Against 0).

RECOMMENDATION 9

Endoscopic ultrasound elastography could be used as a complementary imaging tool for the characterization of solid

pancreatic lesions. However, it cannot decisively differentiate focal pancreatitis from pancreatic carcinoma (LoE 2a, GoR B) (For 20, Abstain 0, Against 0).

RECOMMENDATION 10

When a combination of endoscopic ultrasound elastography with contrast studies suggests pancreatic cancer despite a negative or inconclusive biopsy, repeated sampling or surgery should be considered (LoE 2b, GoR B) (For 12, Abstain 7, Against 1).

9. GastroIntestinal Tract

9.1 Background

The gastrointestinal tract wall may be visualized by ultrasound as a layered structure consisting of typically 5 layers [214, 215]. When examining the intestine, it is preferable to use frequencies above 7.5 MHz to enable optimal visualization of wall layers, thickened bowel wall and focal lesions. This also applies for SE and SWE.

9.2 Methods

SE and SWE are the methods used for elasticity imaging and measurements in bowel examinations. Studies investigating elastography of bowel wall lesions are predominantly based on SE.

9.2.1 Image interpretation and evaluation

Pathological lesions that increase wall thickness are most relevant for SE and SWE. This is because the bowel wall is a thin structure on ultrasound imaging that has natural peristalsis and allows considerable movement on both the serosa and the luminal sides. This tends to add artifacts to strain imaging and makes a targeted SWE or SE measurement more difficult and user-dependent. The bowel wall may become thickened in both neoplastic and inflammatory disease, predominantly in Crohn's disease (CD). In particular, SE has been applied in order to clinically distinguish fibrotic from inflammatory lesions in CD and to distinguish rectal adenoma from adenocarcinoma.

9.3 Clinical applications

9.3.1 Distinction between fibrous and inflammatory strictures in Crohn's disease

Several studies on CD in animal models and human specimens conclude that stiffness is associated with the presence of fibrotic strictures. Some studies indicate that SE and SWE elastography can differentiate fibrosis from inflammatory lesions [216–218]. A study compared SE in terminal ileum stenosis in CD reporting a higher visual score of tissue stiffness in fibrosis using magnetic resonance (MR) enterography as a reference [219]. Another ex vivo study on bowel specimens from CD and neoplastic lesions

also showed that higher stiffness was present in both CD lesions and in adenocarcinoma, but not in adenomas [220].

The results from seven small series were included in a systematic review of 154 CD lesions in 129 patients [221], suggesting that stiffness was significantly higher in fibrotic stenosis. Nevertheless, the systematic review mentions “inhomogeneous and scarcely comparable” endpoints, as authors used either absolute strain values or a strain ratio with various anatomic structures for comparison (mesenteric fat surrounding the bowel wall or abdominal wall muscles). In a study of ten patients, SE using the mean strain in the bowel wall of affected and unaffected bowel segments pre-, intra- and postoperatively found significant differences in strain values in affected and unaffected segments which correlated well with the histological distribution of connective tissue and collagen content [222]. Also, the strain measurements had an acceptable intraclass correlation coefficient (ICC) in the three examinations. A study of 23 consecutive patients undergoing surgery for CD [223] found excellent differentiation of patients with severe ileal fibrosis by histology but also by using SR (including an excellent inter-rater agreement). Conflicting findings are reported in a prospective study on SE in 26 patients undergoing surgery for stricturing CD. On preoperative ultrasound, the SR did not correlate with histological scoring of fibrosis or inflammation [224]. Strain imaging of bowel lesions in CD may predict the response to anti-inflammatory treatment. In a prospective study of 30 patients with CD, the five patients who needed surgery had significantly higher SR measurements at baseline and there was a significant negative correlation between the SR at baseline and wall thickness following 52 weeks of anti-tumor necrosis factor (TNF) therapy [225]. SWE should not be used as a method to distinguish fibrotic from inflammatory lesions in CD based on current evidence.

9.3.2 Characterization and staging of rectal tumors

The differentiation and staging of rectal tumors can be performed using SE as an add-on to B-mode endoscopic rectal ultrasound (ERUS). Thus, SE may improve the staging of rectal cancer and differentiate adenoma from adenocarcinoma, when compared to ERUS alone and with MR imaging (with high interobserver agreement of recorded videos and images) [226–228]. Another group found good correlation between diffusion-weighted MR imaging which is associated with fibrosis, and SWE of malignant rectal tumors [229]. Another study assessed the performance of ERUS for rectal tumors using SWE using an 8 MHz endorectal transducer, finding that the tumor stiffness measurements corresponded accurately to the pathological tumor T-stage and diagnostic accuracy of tumor staging improved from 76.7 % to 93.3 % [230].

RECOMMENDATION 11

Ultrasound strain elastography can be used to characterize bowel wall lesions in Crohn's disease (LoE 3b, GoRC) (For 19, Abstain 1, Against 0).

RECOMMENDATION 12

Ultrasound elastography may improve the staging of rectal cancer when used as an add-on to endoscopic rectal ultrasound and magnetic resonance imaging (LoE 2b, GoRC) (For 17, Abstain 3, Against 0).

10. Spleen

10.1 Background

Spleen stiffness measurement is an elastography technique used to assess the severity of chronic liver disease, mainly in conjunction with liver stiffness measurements for the evaluation of liver fibrosis or portal hypertension-related complications. Various SWE techniques have been investigated to predict the presence of clinically significant portal hypertension, esophageal varices or to predict long-term prognosis.

10.2 Methodology

Spleen elastography should be performed after at least 3 hours of fasting and after at least 10 minutes of rest [231, 232], with the patient in dorsal decubitus and with the left arm in maximal adduction [233]. The transducer should be placed between the left intercostal spaces in an area with a good ultrasound window needed for TE [234], or at least 2 cm below the capsule for non-TE techniques [235, 236], with the measurement preferably being performed at the inferior pole [237].

10.3. Clinical applications

a) Assessment of liver fibrosis

Using spleen stiffness as a surrogate marker for staging liver fibrosis, two studies [238, 239] demonstrated a pooled sensitivity and specificity for detecting significant fibrosis (F2) and cirrhosis (F4) of 0.70 and 0.87 and 0.77 and 0.82, respectively with an AUROC of 0.88 and 0.85, respectively [22].

b) Assessment of clinically significant portal hypertension

Spleen stiffness correlates well with the hepatic vein portal gradient and has an excellent diagnostic accuracy (AUROC = 0.92) for clinically significant portal hypertension, irrespective of the technique used [240], with TE showing a better correlation with the hepatic vein portal gradient than measuring liver stiffness [234]. For values ≥ 46 kPa, the AUROC for clinically significant portal hypertension varies from 0.846 to 0.966, with good sensitivity (0.77–0.88) and specificity (0.79–0.91) [234, 241].

For pSWE, the overall correlation with the hepatic vein portal gradient is similar and better than for liver stiffness measurements [242], but for values > 10 mmHg, the association is weaker [242, 243]. However, for pSWE, the plotted sensitivity is higher than for other techniques (0.98 vs. 0.62–0.83), while the specificity is lower (0.78 vs. 0.89–0.93), thus raising the possibility of the heterogeneity and variability of this technique [240, 244].

As for 2D-SWE, the diagnostic accuracy varied significantly, as AUROC analysis shows: 0.63 (for a cut-off value of 34 kPa) [245], 0.725 [235] or 0.84 [237]. Despite the fact that the last two studies recommend different cut-off values to rule-in (≥ 40 or 35.6 kPa) or out (≤ 22.7 or 21.7 kPa) clinically significant portal hypertension, the diagnostic accuracy remains low for the study by Procopet et al. [235] (12/40 correctly classified), but satisfactory for the study by Jansen et al. [237] (66/111 patients correctly classified). However, if a combined approach is used (both spleen and liver stiffness measured), only 11/109 patients (89.9% accuracy) are misclassified [237].

c) Assessment of oesophageal varices

TE of splenic stiffness has a good accuracy to detect the presence of oesophageal varices (80.4%), but it is unable to differentiate the grade [233]. Values ≤ 40 kPa were proposed to rule-out oesophageal varices, while values ≥ 55 kPa were suggested to rule them in [234]. In a meta-analysis, the pooled sensitivity and specificity to detect varices was satisfactory (0.76 and 0.78, respectively), while the sensitivity is better (0.86 vs. 0.69) for the detection of varices needing treatment [246]. A modified calculation algorithm for TE was proposed, so that values > 75 kPa could be measured, which proved to be the sole independent predictor of the need to treat [247]. Therefore, a dedicated transducer and calculation algorithm were developed, showing better performance compared with the original algorithm and with liver stiffness [248].

For pSWE, the sensitivity and specificity for detecting oesophageal varices varies from 0.31 and 0.79 [249] up to 0.95 and 0.92 [243]. However, the pooled performance for detecting the need to treat appears to be lower than for TE [246], although the analysis did not take into account a report which showed very good positive and negative predictive values: 0.97 and 0.89, respectively [243].

With 2D-SWE, [245] there is no discrimination between patients with and without varices needing treatment. In a much larger cohort, however, the AUROC for detecting oesophageal varices of any grade was 0.8, while the probability is only 10% for patients with compensated cirrhosis if the spleen stiffness is lower than 25.6 kPa (10). If 2D-SWE SSM (≤ 38 kPa) is used in a step-wise approach alongside liver stiffness (≤ 19 kPa) and platelet count ($\leq 100 \times 10^3$), the oesophageal varices can be ruled-out with 83% accuracy and 74% of unnecessary endoscopies could be eliminated [248].

d) Assessment of prognosis and response to therapy

Spleen stiffness can also predict liver-related complications, as the only independent predictor of decompensation besides the MELD score (if higher than 54 kPa), in a cohort of compensated hepatitis C virus (HCV) cirrhosis, during a 2-year follow-up period [250]. No data is available regarding the role of spleen stiffness in monitoring the response to non-selective beta-blockers. Spleen stiffness (assessed by pSWE) seems to decrease after TIPS placement [251, 252], suggesting that spleen stiffness could be an additional tool to evaluate TIPS efficiency.

Small series also suggest that successful antiviral therapy of HCV cirrhosis induces a small reduction of spleen stiffness during follow-up, which is not always significant and it is not as important or as persistent as liver stiffness reduction [253, 254], reflecting more likely a reduction of hepatic inflammation.

e) Miscellaneous

Spleen stiffness was also used to assess patients with non-cirrhotic portal hypertension. In extrahepatic portal vein obstruction, spleen stiffness increases and is higher in patients with a history of bleeding [255]. In patients with idiopathic portal sinusoidal disease, spleen stiffness is markedly increased, in contrast to quasi-normal liver stiffness values [256, 257]. Furthermore, a combination could be used in children with biliary atresia before or after Kasai portoenterostomy to predict outcome or to monitor subsequent liver disease and portal hypertension [258, 259]. Spleen stiffness by TE was also positively correlated with the grade of bone-marrow fibrosis in patients with primary myelofibrosis, suggesting that this could be a simple noninvasive method to monitor disease progression [260].

10.4 Limitations and artifacts

TE can be performed in only 85–90% of cases, mainly because of high BMI, presence of ascites, lung or colonic gas interposition, or transverse spleen diameter < 4 cm [233, 234, 247]. An additional 12–21% of patients reach the maximum value (75 kPa) measured by the conventional machine [233, 247], hence the applicability of TE is approximately 70%. The applicability of 2D-SWE is similar and appears to be related to a higher BMI and smaller spleen size [261]. As for pSWE, the applicability is higher (up to 97%) [242], but the reproducibility is influenced by small spleen size and central obesity [244].

RECOMMENDATION 13

Ultrasound elastography of the spleen can be used as an additional noninvasive method to assess portal hypertension (LoE 2b, GoR B) (For 20, Abstain 0, Against 0).

11. Kidney

11.1 Background

Renal elastography has been used for the noninvasive assessment of chronic kidney disease (CKD), particularly for the early stages when renal function is not yet significantly affected, or for disease monitoring [262]. The hypothesis that the development of glomerular and interstitial fibrosis should lead to stiffness changes is supported by experimental findings in a rat model of CKD [263].

11.2 Methods & confounding factors

11.2.1 Strain elastography

SE can only be used for superficial kidneys, usually renal transplants, mainly a qualitative technique that supposes uniform deformation of the tissue of interest, with a limited role due to the depth of the organ, the difficulty to apply reproducible homogeneous external deformation and the inability to achieve absolute stiffness measurements [264].

11.2.2 Shear wave elastography

TE allows quantitative evaluation of the tissue stiffness and has been widely used for liver fibrosis estimation [2, 265], but the volume of tissue involved in the measurement is at a fixed depth and has a length of 40 mm, making this technique unsuitable for renal stiffness estimation.

The inter-operator agreement of pSWE used in transplanted kidneys obtained in different studies was fair or moderate with the ICC ranging between 0.31 [268] and 0.47 [269]. In studies performed in native kidneys, the reproducibility of the method was strong, with ICCs between 0.60 [270] and 0.71 [271]. The inter-operator agreement obtained in the elastographic assessment of the kidneys (native and transplant) was lower compared to studies of liver stiffness (ICCs are over 0.80), because of confounding factors. Currently, there are few studies available using 2D SWE techniques in the assessment of the kidneys [272, 273].

11.3 Clinical applications

11.3.1 Normal kidney stiffness

A limited number of studies (most of them using pSWE) report normal kidney stiffness, and are different depending on the type of pSWE device used. In adult native kidneys, normal cortical stiffness values range from 2.15 to 2.54 m/s with one system [114, 270, 271, 277–279] compared to 1.23 to 1.54 m/s with a different system [280]. In 9–16-year-old children, higher pSWE stiffness values were found, ranging from 3.00 to 3.33 m/sec (mean 3.13 ± 0.09 m/s, corresponding approximately to 29.4 kPa). In a study performed in healthy people aged 18–30, 31–50, 51–65, and above 65 years, pSWE was 2.94 ± 0.60 , 2.26 ± 0.82 , 2.48 ± 0.8 and 1.82 ± 0.63 m/s, respectively [277]. In the same study, a statistically significant difference was found between women and men. Surprisingly, normal kidney stiffness was found to exhibit an inverse, statistically significant relationship with patient age ($p = 0.0003$). Using pSWE, similar values were found in a small series of normal volunteers with superficial kidneys, with a cortical average stiffness of 15.4 ± 2.5 kPa [281]. The stiffness of the renal medulla was found to be lower than the cortical stiffness [272], except for in one study using pSWE [278].

11.3.2 Kidney stiffness for the assessment of renal pathology

In renal transplantation, serum creatinine levels and estimated Glomerular Filtration Rate (eGFR) are poor predictors of the severity of histological lesions. A noninvasive test that could provide diagnosis and/or prognosis early on to avoid repeated biopsies and to allow early targeted therapeutic intervention could improve pa-

tient management. Several studies report a correlation between renal stiffness and fibrosis or renal function. In experimental models of glomerulosclerosis, the cortical stiffness was correlated to the degree of renal dysfunction [263]. In humans, this correlation remains highly variable in both native and transplanted kidneys. Some authors reported a correlation between renal stiffness and fibrosis or renal function with several techniques [270, 278, 282–285].

In other studies, the correlation between CKD stages and kidney stiffness was negative, as shear wave velocity was found to decrease with increasing stages of CKD [270, 286] or decreasing eGFR [287, 288]. The cut-off values of renal stiffness proposed by different studies could only predict advanced stages of CKD. In the remaining studies, no correlation was found between renal stiffness and the degree of CKD or interstitial fibrosis and tubular atrophy, even in diabetic CKD [270, 272, 278, 288–294]. The renal perfusion changes might impact renal stiffness and explain some discrepancies between results [284], as intrarenal blood flow is decreased with the progression of fibrosis. Thus, renal blood flow decrease could be the cause of the decrease of stiffness with the progression of CKD, and could have a bigger influence on stiffness compared to renal fibrosis.

Additional preliminary applications include stiffness assessment in the case of reflux nephropathy and tumor. In a study of 28 children, CKD degree increased SWE values mainly in the kidney involved with vesicoureteral reflux (6.57 ± 0.96 m/s) but also in the contralateral kidney (4.09 ± 0.97 m/s) while the normal value in the pediatric population without renal disease was 3.13 ± 0.09 m/s [295]. The increased stiffness even in the contralateral kidney may result from increased glomerular filtration and minimal fibrosis. Renal elastography might also play a role in the detection and characterization of renal masses, improving the identification of ill-defined lesions and providing information about tumor stiffness [296].

11.4 Limitations and artifacts

Anatomical confounding factors include renal anisotropy, blood perfusion and hydronephrosis. The effect of anisotropy has been demonstrated in muscle and kidney elastography due to their spatial organization [275, 276]. When shear wave propagation is parallel to the renal tubules and interlobular arteries (and the ultrasound beam is perpendicular to these structures), the velocity of the shear waves is increased [262]. Elasticity measurements performed in the perpendicular direction to the long axis of the pyramids exhibit higher values for all renal compartments. Renal perfusion strongly affects renal elastography, with a drop in the medulla ranging from 44% to 72.7% in renal artery occlusion, and an increase over 500% in renal vein thrombosis [276]. Hydronephrosis also results in a renal elasticity increase, with a correlation between urinary tract pressure and cortical stiffness varying from 119% to 137% between 5 and 40 mmHg [276]. Additional confounding factors include the type of technology and effect of transmit frequency, attenuation of transmit pulse (deteriorating signal-to-noise ratio). Using ARFI, the shear wave velocity was reduced by 27% when the depth increased from 2–3 cm to 6–7 cm (2.95 ± 0.41 m/s and 2.16 ± 0.61 m/s, respectively) [277].

Measurement depth influences the reproducibility of the method, a lower reproducibility being found in patients with deep kidneys, either native kidneys at a depth more than 4 cm or transplanted kidneys.

RECOMMENDATION 14

No current recommendation can be given for the application of ultrasound elastography in native kidneys (LoE 2b, GoR B) (For 10, Abstain 0, Against 0).

RECOMMENDATION 15

Ultrasound renal elastography can be used as an additional tool for the diagnosis of chronic allograft nephropathy (LoE 2b, GoR B) (For 9, Abstain 1, Against 0).

12. Lymph nodes

12.1 Background

Noninvasive discrimination of malignant and benign lymph nodes is important for further diagnostic and clinical decision-making. Whereas contrast-enhanced ultrasound is not recommended for the assessment of lymph nodes [297], elastography has a better diagnostic performance [298], with evidence for the examination of superficial lymph nodes and mediastinal lymph nodes. Superficial lymph nodes have been investigated by percutaneous US using SE and SWE. Mediastinal lymph nodes have been investigated by endoscopic ultrasound using only SE.

12.2 Methods

SE is the method most frequently described, as the technique is more widely available on most commercial systems, with more consolidated evidence with a number of single research studies and two meta-analyses published. More recently, SWE has been evaluated with one meta-analysis published.

12.3 Clinical applications

12.3.1 Differential diagnosis of lymphadenopathy

Assessment of superficial lymph nodes using SE presents conflicting data. Two recent meta-analyses demonstrated a high accuracy in differentiating between benign and malignant lymph nodes. The first meta-analysis included 578 patients with 936 lymph nodes with a sensitivity of the scoring and SR measurements of 76 % and 83 %, respectively [299]. The second meta-analysis included 545 patients with 835 lymph nodes and indicated a sensitivity of the elasticity scoring and SR measurements of 74 % and 88 %, with a specificity of 88 % and 91 %, respectively [300].

A meta-analysis including 481 patients with 647 lymph nodes evaluated the role of SWE in superficial lymph nodes. SWE for the discrimination of malignant and benign lymph nodes achieved a

sensitivity of 81 % and specificity of 85 % [301]. The latest meta-analysis regarding the value of EUS elastography for the differentiation of malignant and benign lymph nodes included 6 studies with 368 patients and 431 lymph node, with SE demonstrating a sensitivity of 88 %, and a specificity of 85 % [302]. Newer studies including patients investigated by endobronchial ultrasound (EBUS) had similar performance [303, 304].

12.3.2 Preoperative Assessment of Lymph Nodes in Patients with Known Primary Cancer

With preoperative lymph node assessment for metastatic involvement, no systematic review is available. Two studies investigated SWE in the prediction of metastatic involvement from thyroid cancer. A retrospective analysis [305] found that using the Mean Elastic Modulus with a cut-off set to 29 kPa led to 66.67 % sensitivity and 72.62 % specificity, 78 % PPV, 64.71 % NPV and 0.748 AUC, whereas the combination with B-mode ultrasound lead to 98.04 % sensitivity, 45.45 % specificity, 73.53 % PPV, 93.75 % NPV and 0.811 AUROC. Other authors found that the best SWE parameter for predicting metastatic involvement was the maximum value of elasticity with the cut-off set to 40 kPa, leading to 80 % sensitivity, 93.1 % specificity and 0.918 AUC [306].

12.4 Limitations and artifacts

Elastography is unlikely to be suitable for a differential diagnosis, but is more likely to be useful for targeting malignant lymph nodes for fine needle aspiration if multiple lymph nodes are present [307]. It cannot be assumed that the entire lymph node is involved in malignancy, but may range from a few undetectable cells to involvement of a small area. Only a limited number of studies with small sample sizes are available and invariably have a selection bias [308, 309]. Some malignant lymph nodes cannot be discriminated by tissue stiffness alone, as is the case with the lymph nodes of lymphoma [310]. There is no standardization of the technique particularly in SE, making study comparisons difficult [311]. Often with lymph node imaging in EUS, there is a relative depletion of surrounding tissue as a normal reference for SR calculation, including the gastrointestinal wall advocated as the standard comparison for tissue reference [309].

RECOMMENDATION 16

High-frequency transcutaneous and endoscopic ultrasound elastography can be used as additional tools for the differentiation between benign and malignant lymph nodes (LoE 2a GoR B) (For 20, Abstain 0, Against 0).

RECOMMENDATION 17

Ultrasound elastography can be used for identifying the most suspicious lymph nodes and/or suspicious areas within the lymph node to be targeted for sampling (LoE 5, GoR D) (For 19, Abstain 1, Against 0).

13. MusculoSkeletal

13.1 Background

In comparison with the previous guidelines, there has been an increase in studies regarding musculoskeletal (MSK) elastography [2].

13.2 Methods

Published data concerning the use of SE, ARFI imaging, and SWE for elastographic evaluation of the MSK structures, especially for tendons, muscles and nerves, are available.

13.3 Clinical applications

13.3.1 Tendons

In SE the healthy Achilles tendon is mostly rigid (86.7 – 93 % of the tendon has high stiffness) [312, 313] and there is an increase in stiffness with age [314]. Using SWE, different values of shear wave velocity or elastic modulus were obtained depending on the machine used, tendon position, or plane of imaging [113, 315, 316]. In Achilles tendinopathy the SR (comparing tendon with Kager's fat) is higher and the tendon becomes less stiff [317]. SE proved to be superior to B-mode ultrasound (sensitivity 99 %, specificity 78 %, accuracy 95 %) [318], underlining the ability of SE to detect pathology before the appearance of the B-mode ultrasound morphologic changes [319, 320]. No differences between athletes and controls nor between the dominant and non-dominant leg were found in SE evaluation of the patellar tendon [321]. With age, a significant decrease in shear wave velocity values was detected, with SWE having the capacity to detect aging tendons before morphologic abnormalities were observed on B-mode ultrasound [322, 323].

For lateral epicondylitis the addition of SE to B-mode ultrasound findings improves the sensitivity for detecting tendon pathology [324, 325]. Using B-mode ultrasound in combination with SE resulted in a better correlation with histologic results. In the rotator cuff, SE can detect small partial tears of the supraspinatus tendon [326]. In patients with tendinopathy, a significant decrease in the shear wave velocity of the supraspinatus muscle was observed [327]. Currently, no observations monitoring tendon healing are available in longitudinal studies.

13.3.2 Muscle

Using SE, the normal relaxed muscle appears as an inhomogeneous mosaic of intermediate or increased stiffness with scattered less stiff and stiffer areas, especially at the boundaries of the muscle [328, 329]. In SWE the normal relaxed muscle has a lower shear wave velocity (which increases during contraction) and the boundary fascia or aponeurosis show intermediate shear wave velocity [330].

Physiological factors (age, sex, muscle performance, fatigue, or training) and pathological changes (trauma, degeneration, or neuromuscular disease) influence muscle elasticity [331 – 337]. Normal and abnormal ranges of shear wave velocity of various

muscles are available [327, 333, 336, 338] but the results are limited, without establishing any reference values.

SWE for the evaluation of muscle stiffness in various neurologic conditions (Parkinson disease, chronic stroke, cerebral palsy, multiple sclerosis or Duchenne dystrophy) is a reliable quantitative imaging technique for diagnosis, treatment decisions and follow-up and may be an alternative to electromyography [333, 338 – 342].

In inflammatory myopathies SE demonstrated that the involved muscles become stiffer, and significant correlations with histological findings were obtained [328, 343]. Acute muscle and fascial tears show a lower shear wave velocity [330], but no prospective studies have been published.

13.3.3 Ligaments and fascia

Using SWE in patients with adhesive capsulitis, the coracohumeral ligament proved to be stiffer in the symptomatic shoulder [344]. The increased stiffness of the transverse carpal ligament evaluated on SE may be one of the causes for carpal tunnel syndrome [345]. The plantar fascia becomes less stiff with age and in subjects with plantar fasciitis abnormality is seen when using ARFI imaging (pixel intensity), SE or SWE even in the absence of pathological findings on B-mode ultrasound examination [346 – 350], suggesting a role of elastography in the diagnosis of early stages of plantar fasciitis.

13.3.4 Nerves

Median nerve strain is significantly lower in patients with carpal tunnel syndrome than in controls [351], and the perineural area surrounding the median nerve is stiffer than in healthy volunteers [352]. The SE can be used to follow up the median nerve recovering after carpal tunnel release [353] or after local corticosteroid injection [354] but does not have the capability to categorize the severity. The combined use of B-mode ultrasound and SE has been suggested [355].

Using pSWE the shear wave velocity of the median nerve was 3.857 m/s in patients with carpal tunnel syndrome and 2.542 m/s in the control group ($p < 0.05$) [356]. Using 2D-SWE the mean shear modulus of the median nerve was 66.7 kPa in patients and 32.0 kPa in the control group ($p < 0.001$) [357]. Both methods have high sensitivity and specificity for carpal tunnel syndrome diagnosis and are highly reproducible. The increased stiffness was attributed to nerve fibrosis or edema.

The elasticity of the tibial nerve in diabetic patients is reduced compared with a control group and decreased further after developing diabetic peripheral neuropathy [358 – 360].

The joints and limb position and the patients' age should be taken into consideration during a nerve ultrasound examination [361].

13.4 Practical points

SE is an operator-dependent technique, with a recommendation to record several (at least 3) compression-relaxation cycles as cine-loops and then select the best elastograms for evaluation. The examination transducer should be perpendicular to the tissue

to avoid anisotropy, as the B-mode ultrasound appearance influences the quality of the elastogram.

The use of standoff devices for SE of the superficial structures does not influence the elastogram (a minimum 3 mm distance between transducer and lesion being necessary) [362], but the inclusion of gel within the region of interest should be avoided (may mask minimal differences in tendon stiffness) [329].

The SWE examination of muscles and tendons should be performed with the lightest transducer pressure. The dimension of the region of interest does not influence the mean elastic modulus [363].

The transducer must be oriented longitudinally to the muscle fibers in order to achieve accurate and reliable SWE measurements. The shear waves propagate faster in contracted tendons and muscles and along the long axis of tendons [330]. The ligaments should be examined in the same position as the corresponding joints [344].

13.5 Limitations and artifacts

When a solid structure is delimited by an incompressible shell, SE analysis of the internal structure is limited (the eggshell effect) [364]. Cystic masses characteristically have a mosaic of all levels of stiffness. Low stiffness lines may appear at the interfaces between tissues (due to tissue shifting), around calcifications, behind bone or at the superficial edge of a homogeneous lesion. Fluctuant changes at the borders of the Achilles tendon in an axial elastogram can be seen due to varying contact with the skin [365].

A limitation of SWE is depth of penetration. Superficial structures may be better visualized by applying a 5 mm layer of coupling ultrasound gel as standoff. SWE examination is influenced by the transducer pressure and angle, and the shear modulus depends on the orientation of the transducer relative to the examined structures [330, 366].

RECOMMENDATION 18

Ultrasound elastography can be used as a supplementary tool to increase confidence in diagnosing tendinopathy, particularly for Achilles tendinopathy, for evaluating muscle stiffness and for plantar fasciitis (LoE 2b GoR B) (For 19, Abstain 1, Against 0).

RECOMMENDATION 19

Ultrasound elastography can be used for the diagnosis and follow-up of carpal tunnel syndrome and diabetic peripheral neuropathy (LoE 2b, GoR B) (For 19, Abstain 1, Against 0).

14. Testis

14.1 Background

Traditionally the presence of a focal lesion in the testis was addressed by removing the testis for histological examination, on the premise that nearly all of these lesions are malignant. However, access to modern ultrasound technology has rendered this approach obsolete, and as many as 80% of incidentally discovered lesions are benign [367]. The use of newer contrast-enhanced ultrasound and elastography techniques [368], combined as multiparametric ultrasound [369], has resulted in a more cautious approach to incidental focal testicular lesions [370]. The use of elastography to assess the stiffness of abnormal areas of the testis to ascertain stiffness as a sign of underlying malignancy is an attractive proposition to add to the overall multiparametric assessment.

14.2 Methods

14.2.1 Strain elastography

SE has been the most employed technique for the assessment of testicular lesions [371–375]. Early studies, predominantly retrospective, have commented on the possibility of differentiating malignant from benign lesions with certainty using SE and SR. However, these findings have not been confirmed in recent studies, with specificities between 25.0% and 37.5% in differentiating benign from malignant lesions [375–377]. A number of case series detailing the use of SE and SR (some in combination with contrast-enhanced ultrasound) have described the findings in Leydig cell tumors [378], epidermoid cysts, hematoma, lymphoma, focal infarction, capillary hemangioma, adrenal rest cells [379–384] and in extra-testicular lesions [385], without comparison between the findings of these different lesions.

14.2.2 SWE

There is limited information regarding the use of SWE in the evaluation of testicular lesions. Investigation of the role of SWE in the overall assessment of background parenchyma has suggested that values may be elevated in the case of testicular microlithiasis [386], infertility [387], undescended testis [388]. It also has the potential to differentiate seminomas from non-seminomatous lesions [389] and has been evaluated in burnt-out tumors [390]. No prospective study reporting the differences in SWE in focal testicular lesions has been published.

14.3 Clinical applications

The use of all forms of elastography in the assessment of focal testicular lesions is promising, with tissue stiffness confirmed with both SE and SWE techniques, but with overlap in findings between benign and malignant neoplasms. The current status would allow elastography to be an adjunct to the overall ultrasound examination rather than a standalone technique.

14.4 Limitations and artifacts

For testicular lesions, the values obtained for SWE vary between different machines and are not interchangeable [391]. The prob-

lems associated with the areas of fibrosis adjacent to the tunica albuginea hamper the assessment of focal lesions adjacent to this region [392]. Measurements using SWE between the center and peripheral zones differ and the point of measurement requires standardization [393, 394].

RECOMMENDATION 20

Ultrasound elastography for the evaluation of focal testicular lesions can only be recommended in conjunction with other ultrasound techniques, as there is overlap between benign and malignant neoplasms (LoE 3A GoR B) (For 19, Abstain 1, Against 0).

15. Vascular

15.1 Background

It is well established that ageing and atherosclerotic disease increases arterial stiffness [395]. Elastography biomarkers are emerging as potential indicators for diseases such as stroke, hypertension, diabetes mellitus and cardiovascular disease, and may provide additional information to support clinical decision-making.

15.2 Methods

The majority of studies are based on SE. Early studies used intravascular ultrasound and more recent studies have focused on noninvasive techniques including SWE. These techniques have been compared with alternative imaging techniques, histology, clinical outcome measures and/or in experimental phantoms and simulations.

15.3 Clinical applications

15.3.1 Strain elastography

Plaque characterization is a challenging, clinically important application for which evidence of clinical benefit is growing [396]. Evidence from animal and human studies [397–403] typically associates vulnerable plaque with regions of high strain. The potential to detect and age thrombus has been demonstrated in animal models [404, 405]. A clinical application to differentiate acute from chronic deep vein thrombosis (DVT) has been demonstrated in humans [406–408], and a systematic review concluded that elastography imaging is a feasible adjunct to current first-line imaging for DVT [409]. However, at least one recent study was not able to differentiate acute DVT from subacute DVT [410]. Other potential vascular applications include cardiac, abdominal aorta and the use of elastography biomarkers for disease [411–414].

15.3.2 SWE

The feasibility of quantifying Young's modulus in arteries has been demonstrated in human [415], ex-vivo animal [416, 417] and phantom [418–420] studies. Identification of the vulnerable car-

otid plaque is emerging as a promising clinical application. Phantom studies have demonstrated the feasibility of Young's modulus estimates but highlight errors due to the requirement for a different wave propagation model than used by current commercial systems [418–421]. Nevertheless, human studies show good reproducibility and potential clinical benefit [422–426], with evidence that Young's modulus of carotid plaque correlates with qualitative (Gray-Weale scale) appearance [422, 425, 426] and quantitative (grayscale median) B-mode ultrasound measurements [422, 426], and helps to provide improved diagnostic performance of carotid plaque vulnerability [422, 426]. Studies found a lower mean Young's modulus for vulnerable plaque, although values differ (50 kPa vs. 79 kPa [426]; 62 kPa vs. 88 kPa [422]; 81 kPa vs. 115 kPa [425]). Evidence is limited for other vascular applications such as cardiac [427–429] and DVT [430, 431].

15.4 Limitations and artifacts

Vascular imaging is challenging due to the small heterogeneous tissue size, the dynamic environment resulting from pulsatile blood flow, thin vessel walls, non-linear tissue elasticity and shear wave propagation model assumptions which may not be valid due to the potential for Lamb wave propagation in vessel walls [415, 418]. Studies should report the shear wave velocity or calculation used to convert velocity to Young's modulus as future scanners may implement different models of wave propagation. Vascular applications are promising, especially for the assessment of carotid plaque, where larger, multicenter studies are required to validate initial findings, establish cut-off values and optimize methodologies.

RECOMMENDATION 21

Vascular ultrasound elastography is an area of active research. However, it cannot currently be recommended for clinical decision-making (LoE 5, GoR C) (For 20, Abstain 0, Against 0).

16. Intraoperative

16.1 Background

All surgical disciplines make use of preoperative imaging to visualize a pathology for improved surgical planning.

16.2 Methods

Improved ultrasound technology has resulted in high-frequency small transducers with better resolution including 3 D ultrasound, contrast-enhanced ultrasound and elastography.

16.3 Clinical applications

The utility of intraoperative ultrasound is less obvious. The advantages include intraoperative navigation without ionizing radiation exposure or relevant workflow interruption, assessment of the extent of resection, and organ shift monitoring and compensation (most important for the brain). Disadvantages for ultrasound elas-

tography include organ deformity intraoperatively due to a number of factors including tumor resection sequelae and post-interventional swelling. The use of intraoperative elastography has been reported for the liver [8, 9, 432–435], brain [436–443], pancreas [115, 185], prostate [444], lung [445] and other organs [446].

RECOMMENDATION 22

Intraoperative ultrasound elastography is an area of active research. However, it cannot be currently recommended for clinical decision-making (LoE 5, GoR C) (For 20, Abstain 0, Against 0).

Conflict of interest

Odd Helge Gilja: Advisory Board/Consultant fee from: AbbVie, Bracco, GE Healthcare, Samsung, and Takeda
Paul S. Sidhu: Speaker honoraria, Bracco, Siemens, Samsung, Hitachi, GE and Philips
Christoph F. Dietrich: Speaker honoraria, Bracco, Hitachi, GE, Mindray, Supersonic, Pentax, Olympus, Fuji, Boston Scientific, AbbVie, Falk Foundation, Novartis, Roche; Advisory, Board Member, Hitachi, Mindray, Siemens; Research grant, GE, Mindray, SuperSonic
Vito Cantisani: Speaker honoraria, Canon/Toshiba, Bracco, Samsung
Dominique Amy: Speaker honoraria, Hitachi, Supersonic, EpiSonica
Marco Brock: Speaker honoraria, Hitachi
Fabrizio Calliada: Speaker honoraria, Bracco, Hitachi, Shenshen Mindray
Dirk Andre Clevert: Speaker honoraria, Siemens, Samsung, GE, Bracco, Philips; Advisory Board, Siemens, Samsung, Bracco, Philips
Jean-Michel Correias: Speaker honoraria, Hitachi-Aloka, Canon/Toshiba, Philips, Supersonic, Bracco, Guerbet; Research collaboration, Bracco Sonocap, Guerbet NsSafe and Secure protocols
Mirko D'Onofrio: Speaker honoraria, Siemens, Bracco, Hitachi; Advisory Board Siemens, Bracco
Andre Farrokh: Speaker honoraria, Hitachi
Pietro Fusaroli: Speaker honoraria, Olympus
Roald Flesland Havre: Speaker honoraria, GE Healthcare, Conference participation support from Pharmacosmos, Ultrasound equipment from Samsung Medison
André Ignee: Speaker honoraria: Siemens, Canon/Toshiba, Hitachi, Boston Scientific, Bracco, Supersonic, Abbvie
Christian Jenssen: Speaker honoraria, Bracco, Hitachi, Canon/Toshiba, Falk Foundation, Covidien; Research grant, Novartis
Maija Radzina: Speaker honoraria, Bracco, Canon/Toshiba
Luca Sconfienza: Travel grants from Bracco Imaging Italia Srl, Esaote SPA, Abiogen SPA, Fidia Middle East. Speaker honoraria from Fidia Middle East
Ioan Sporea: Speaker honoraria, Philips, GE, Canon/Toshiba; Advisory Board Member, Siemens; Congress participation support, Siemens
Mickael Tanter: Speaker honoraria, Supersonic; Co Founder and shareholder, Supersonic; Research collaboration, Supersonic
Peter Vilmann: Speaker honoraria, Pentax, Norgine; Advisory Board, Boston Scientific; Consultancy MediGlobe
The following members declared no conflicts of interest: Adrian Săftoiu, Michael Bachmann Nielsen, Flaviu Bob, Jörg Bojunga, Caroline Ewertsen, Michael Hocke, Andrea Klauer, Christian Kollmann, Kumar V Ramnarine, Carolina Solomon, Daniela Fodor, Horia Ștefănescu

Acknowledgement

The authors thank the EFSUMB secretary Lynne Rudd for her never-ending support of the EFSUMB guidelines. We also thank the following companies for funding a consensus meeting of the authors held in Frankfurt in February 2018, at which we agreed the recommendations made in this paper: bk/Ultrasound, Echosens, Esaote SpA, GE Healthcare, Hitachi, Medical Systems, Philips Healthcare, Shenzhen Mindray Bio-medical Electronics Co., Ltd, Siemens Healthineers, SuperSonic and Canon/Toshiba Medical. Representatives of these companies were in attendance at this meeting, to assist with product technical information, but did not take part in forming the manuscript or the recommendations.

References

- [1] Bamber J, Cosgrove D, Dietrich CF et al. EFSUMB Guidelines and Recommendations on the Clinical Use of Ultrasound Elastography. Part 1: Basic Principles and Technology. *Ultraschall in Der Medizin* 2013; 34: 169–184
- [2] Cosgrove D, Piscaglia F, Bamber J et al. EFSUMB Guidelines and Recommendations on the Clinical Use of Ultrasound Elastography. Part 2: Clinical Applications. *Ultraschall in Der Medizin* 2013; 34: 238–253
- [3] Education and Practical Standards Committee ErFoSfUiMaB. Minimum training recommendations for the practice of medical ultrasound. *Ultraschall in Med* 2006; 27: 79–105
- [4] Cosgrove D, Barr R, Bojunga J et al. WFUMB Guidelines and Recommendations on the Clinical Use of Ultrasound Elastography: Part 4. Thyroid. *Ultrasound Med Biol* 2017; 43: 4–26
- [5] Tatar IG, Kurt A, Yilmaz KB et al. The learning curve of real time elastosonography: a preliminary study conducted for the assessment of malignancy risk in thyroid nodules. *Med Ultrason* 2013; 15: 278–284
- [6] Grădinaru-Tașcău O, Sporea I, Bota S et al. Does experience play a role in the ability to perform liver stiffness measurements by means of super-sonic shear imaging (SSI)? *Med Ultrason* 2013; 15: 180–183
- [7] Shiina T, Nightingale KR, Palmeri ML et al. WFUMB guidelines and recommendations for clinical use of ultrasound elastography: Part 1: basic principles and terminology. *Ultrasound Med Biol* 2015; 41: 1126–1147
- [8] Dietrich CF, Bamber J, Berzigotti A et al. EFSUMB Guidelines and Recommendations on the Clinical Use of Liver Ultrasound Elastography, Update 2017 (Long Version). *Ultraschall in Der Medizin* 2017; 38: E16–E47
- [9] Dietrich CF, Bamber J, Berzigotti A et al. EFSUMB Guidelines and Recommendations on the Clinical Use of Liver Ultrasound Elastography, Update 2017 (Short Version). *Ultraschall in Der Medizin* 2017; 38: 377–394
- [10] Ferraioli G, Filice C, Castera L et al. WFUMB guidelines and recommendations for clinical use of ultrasound elastography: Part 3: liver. *Ultrasound Med Biol* 2015; 41: 1161–1179
- [11] Barr RG, Nakashima K, Amy D et al. WFUMB guidelines and recommendations for clinical use of ultrasound elastography: Part 2: breast. *Ultrasound Med Biol* 2015; 41: 1148–1160
- [12] Stenzel M, Mentzel HJ. Ultrasound elastography and contrast-enhanced ultrasound in infants, children and adolescents. *Eur J Radiol* 2014; 83: 1560–1569
- [13] Goldschmidt I, Streckenbach C, Dingemann C et al. Application and limitations of transient liver elastography in children. *J Pediatr Gastroenterol Nutr* 2013; 57: 109–113
- [14] Goldschmidt I, Brauch C, Poynard T et al. Spleen stiffness measurement by transient elastography to diagnose portal hypertension in children. *J Pediatr Gastroenterol Nutr* 2014; 59: 197–203

- [15] Peralta L, Molina FS, Melchor J et al. Transient Elastography to Assess the Cervical Ripening during Pregnancy: A Preliminary Study. *Ultraschall in Med* 2017; 38: 395–402
- [16] Friedrich-Rust M, Schoelzel F, Linzbach S et al. Safety of transient elastography in patients with implanted cardiac rhythm devices. *Dig Liver Dis* 2017; 49: 314–316
- [17] Tabaru M, Yoshikawa H, Azuma T et al. Experimental study on temperature rise of acoustic radiation force elastography. *J Med Ultrason* (2001) 2012; 39: 137–146
- [18] Herman BA, Harris GR. Models and regulatory considerations for transient temperature rise during diagnostic ultrasound pulses. *Ultrasound Med Biol* 2002; 28: 1217–1224
- [19] Liu Y, Herman BA, Soneson JE et al. Thermal safety simulations of transient temperature rise during acoustic radiation force-based ultrasound elastography. *Ultrasound Med Biol* 2014; 40: 1001–1014
- [20] Palmeri ML, Nightingale KR. On the thermal effects associated with radiation force imaging of soft tissue. *IEEE Trans Ultrason Ferroelectr Freq Control* 2004; 51: 551–565
- [21] Skurczynski MJ, Duck FA, Shipley JA et al. Evaluation of experimental methods for assessing safety for ultrasound radiation force elastography. *Br J Radiol* 2009; 82: 666–674
- [22] Deng Y, Palmeri ML, Rouze NC et al. Evaluating the Benefit of Elevated Acoustic Output in Harmonic Motion Estimation in Ultrasonic Shear Wave Elasticity Imaging. *Ultrasound Med Biol* 2018; 44: 303–310
- [23] Itoh A, Ueno E, Tohno E et al. Breast disease: clinical application of US elastography for diagnosis. *Radiology* 2006; 239: 341–350
- [24] Carlsen JF, Ewertsen C, Sletting S et al. Strain histograms are equal to strain ratios in predicting malignancy in breast tumours. *PLoS One* 2017; 12: e0186230
- [25] Grajo JR, Barr RG. Strain elastography for prediction of breast cancer tumour grades. *J Ultrasound Med* 2014; 33: 129–134
- [26] Hatzung G, Grunwald S, Zygmunt M et al. Sonoelastography in the diagnosis of malignant and benign breast lesions: initial clinical experiences. *Ultraschall in Med* 2010; 31: 596–603
- [27] Cho N, Jang M, Lyou CY et al. Distinguishing benign from malignant masses at breast US: combined US elastography and color doppler US-influence on radiologist accuracy. *Radiology* 2012; 262: 80–90
- [28] Wojcinski S, Farrok A, Weber S et al. Multicenter study of ultrasound real-time tissue elastography in 779 cases for the assessment of breast lesions: improved diagnostic performance by combining the BI-RADS®-US classification system with sonoelastography. *Ultraschall in Med* 2010; 31: 484–491
- [29] Sadigh G, Carlos RC, Neal CH et al. Ultrasonographic differentiation of malignant from benign breast lesions: a meta-analytic comparison of elasticity and BIRADS scoring. *Breast Cancer Res Treat* 2012; 133: 23–35
- [30] Cho N, Moon WK, Kim HY et al. Sonoelastographic strain index for differentiation of benign and malignant nonpalpable breast masses. *J Ultrasound Med* 2010; 29: 1–7
- [31] Sadigh G, Carlos RC, Neal CH et al. Accuracy of quantitative ultrasound elastography for differentiation of malignant and benign breast abnormalities: a meta-analysis. *Breast Cancer Res Treat* 2012; 134: 923–931
- [32] Berg WA, Cosgrove DO, Doré CJ et al. Shear-wave elastography improves the specificity of breast US: the BE1 multinational study of 939 masses. *Radiology* 2012; 262: 435–449
- [33] Evans A, Whelehan P, Thomson K et al. Invasive breast cancer: relationship between shear-wave elastographic findings and histologic prognostic factors. *Radiology* 2012; 263: 673–677
- [34] Chang JM, Park IA, Lee SH et al. Stiffness of tumours measured by shear-wave elastography correlated with subtypes of breast cancer. *Eur Radiol* 2013; 23: 2450–2458
- [35] Choi WJ, Kim HH, Cha JH et al. Predicting prognostic factors of breast cancer using shear wave elastography. *Ultrasound Med Biol* 2014; 40: 269–274
- [36] Berg WA, Mendelson EB, Cosgrove DO et al. Quantitative Maximum Shear-Wave Stiffness of Breast Masses as a Predictor of Histopathologic Severity. *Am J Roentgenol* 2015; 205: 448–455
- [37] Tamaki K, Tamaki N, Kamada Y et al. Non-invasive evaluation of axillary lymph node status in breast cancer patients using shear wave elastography. *Tohoku J Exp Med* 2013; 231: 211–216
- [38] Wojcinski S, Dupont J, Schmidt W et al. Real-time ultrasound elastography in 180 axillary lymph nodes: elasticity distribution in healthy lymph nodes and prediction of breast cancer metastases. *BMC Med Imaging* 2012; 12: 35
- [39] Park YM, Fornage BD, Benveniste AP et al. Strain elastography of abnormal axillary nodes in breast cancer patients does not improve diagnostic accuracy compared with conventional ultrasound alone. *Am J Roentgenol* 2014; 203: 1371–1378
- [40] Youk JH, Gweon HM, Son EJ et al. Shear-wave elastography of invasive breast cancer: correlation between quantitative mean elasticity value and immunohistochemical profile. *Breast Cancer Res Treat* 2013; 138: 119–126
- [41] Evans A, Rauchhaus P, Whelehan P et al. Does shear wave ultrasound independently predict axillary lymph node metastasis in women with invasive breast cancer? *Breast Cancer Res Treat* 2014; 143: 153–157
- [42] Falou O, Sadeghi-Naini A, Prematilake S et al. Evaluation of neoadjuvant chemotherapy response in women with locally advanced breast cancer using ultrasound elastography. *Transl Oncol* 2013; 6: 17–24
- [43] Evans A, Armstrong S, Whelehan P et al. Can shear-wave elastography predict response to neoadjuvant chemotherapy in women with invasive breast cancer? *Br J Cancer* 2013; 109: 2798–2802
- [44] Lee SH, Chang JM, Han W et al. Shear-Wave Elastography for the Detection of Residual Breast Cancer After Neoadjuvant Chemotherapy. *Ann Surg Oncol* 2015; 22 (Suppl. 3): S376–S384
- [45] Tanter M, Bercoff J, Athanasiou A et al. Quantitative assessment of breast lesion viscoelasticity: initial clinical results using supersonic shear imaging. *Ultrasound Med Biol* 2008; 34: 1373–1386
- [46] Kelloff GJ, Choyke P, Coffey DS et al. Challenges in clinical prostate cancer: role of imaging. *Am J Roentgenol* 2009; 192: 1455–1470
- [47] Singh H, Canto EI, Shariat SF et al. Predictors of prostate cancer after initial negative systematic 12 core biopsy. *J Urol* 2004; 171: 1850–1854
- [48] Ashley RA, Inman BA, Routh JC et al. Reassessing the diagnostic yield of saturation biopsy of the prostate. *Eur Urol* 2008; 53: 976–981
- [49] Onur R, Littrup PJ, Pontes JE et al. Contemporary impact of transrectal ultrasound lesions for prostate cancer detection. *J Urol* 2004; 172: 512–514
- [50] Pallwein L, Mitterberger M, Struve P et al. Real-time elastography for detecting prostate cancer: preliminary experience. *BJU Int* 2007; 100: 42–46
- [51] Salomon G, Köllerman J, Thederan I et al. Evaluation of prostate cancer detection with ultrasound real-time elastography: a comparison with step section pathological analysis after radical prostatectomy. *Eur Urol* 2008; 54: 1354–1362
- [52] Brock M, von Bodman C, Sommerer F et al. Comparison of real-time elastography with grey-scale ultrasonography for detection of organ-confined prostate cancer and extra capsular extension: a prospective analysis using whole mount sections after radical prostatectomy. *BJU Int* 2011; 108: E217–222
- [53] Brock M, von Bodman C, Palisaar RJ et al. The impact of real-time elastography guiding a systematic prostate biopsy to improve cancer detection rate: a prospective study of 353 patients. *J Urol* 2012; 187: 2039–2043

- [54] Kapoor A, Mahajan G, Sidhu BS. Real-time elastography in the detection of prostate cancer in patients with raised PSA level. *Ultrasound Med Biol* 2011; 37: 1374–1381
- [55] Walz J, Marcy M, Pianna JT et al. Identification of the prostate cancer index lesion by real-time elastography: considerations for focal therapy of prostate cancer. *World J Urol* 2011; 29: 589–594
- [56] Aigner F, Pallwein L, Junker D et al. Value of real-time elastography targeted biopsy for prostate cancer detection in men with prostate specific antigen 1.25 ng/ml or greater and 4.00 ng/ml or less. *J Urol* 2010; 184: 913–917
- [57] Aboumarzouk OM, Ogston S, Huang Z et al. Diagnostic accuracy of transrectal elastosonography (TRES) imaging for the diagnosis of prostate cancer: a systematic review and meta-analysis. *BJU Int* 2012; 110: 1414–1423; discussion 1423
- [58] Kamoi K, Okihara K, Ochiai A et al. The utility of transrectal real-time elastography in the diagnosis of prostate cancer. *Ultrasound Med Biol* 2008; 34: 1025–1032
- [59] Bercoff J, Tanter M, Muller M et al. The role of viscosity in the impulse diffraction field of elastic waves induced by the acoustic radiation force. *IEEE Trans Ultrason Ferroelectr Freq Control* 2004; 51: 1523–1536
- [60] Barr RG, Memo R, Schaub CR. Shear wave ultrasound elastography of the prostate: initial results. *Ultrasound Q* 2012; 28: 13–20
- [61] Correas JM, Tissier AM, Khairoune A et al. Ultrasound elastography of the prostate: state of the art. *Diagn Interv Imaging* 2013; 94: 551–560
- [62] Aigner F, Schäfer G, Steiner E et al. Value of enhanced transrectal ultrasound targeted biopsy for prostate cancer diagnosis: a retrospective data analysis. *World J Urol* 2012; 30: 341–346
- [63] Brock M, Eggert T, Löttenberg B et al. Value of real-time elastography to guide the systematic prostate biopsy in men with normal digital rectal exam. *Aktuelle Urol* 2013; 44: 40–44
- [64] Brock M, Löttenberg B, Roghmann F et al. Impact of real-time elastography on magnetic resonance imaging/ultrasound fusion guided biopsy in patients with prior negative prostate biopsies. *J Urol* 2015; 193: 1191–1197
- [65] Brock M, Roghmann F, Sonntag C et al. Fusion of Magnetic Resonance Imaging and Real-Time Elastography to Visualize Prostate Cancer: A Prospective Analysis using Whole Mount Sections after Radical Prostatectomy. *Ultraschall in Med* 2015; 36: 355–361
- [66] Friedrich-Rust M, Meyer G, Dauth N et al. Interobserver agreement of Thyroid Imaging Reporting and Data System (TIRADS) and strain elastography for the assessment of thyroid nodules. *PLoS One* 2013; 8: e77927
- [67] Ito Y, Amino N, Yokozawa T et al. Ultrasonographic evaluation of thyroid nodules in 900 patients: comparison among ultrasonographic, cytological, and histological findings. *Thyroid* 2007; 17: 1269–1276
- [68] Tae HJ, Lim DJ, Baek KH et al. Diagnostic value of ultrasonography to distinguish between benign and malignant lesions in the management of thyroid nodules. *Thyroid* 2007; 17: 461–466
- [69] Haugen BR, Alexander EK, Bible KC et al. 2015 American Thyroid Association Management Guidelines for Adult Patients with Thyroid Nodules and Differentiated Thyroid Cancer: The American Thyroid Association Guidelines Task Force on Thyroid Nodules and Differentiated Thyroid Cancer. *Thyroid* 2016; 26: 1–133
- [70] Russ G, Bonnema SJ, Erdogan MF et al. European Thyroid Association Guidelines for Ultrasound Malignancy Risk Stratification of Thyroid Nodules in Adults: The EU-TIRADS. *Eur Thyroid J* 2017; 6: 225–237
- [71] Kwak JY, Han KH, Yoon JH et al. Thyroid imaging reporting and data system for US features of nodules: a step in establishing better stratification of cancer risk. *Radiology* 2011; 260: 892–899
- [72] Horvath E, Majlis S, Rossi R et al. An ultrasonogram reporting system for thyroid nodules stratifying cancer risk for clinical management. *J Clin Endocrinol Metab* 2009; 94: 1748–1751
- [73] Park JY, Lee HJ, Jang HW et al. A proposal for a thyroid imaging reporting and data system for ultrasound features of thyroid carcinoma. *Thyroid* 2009; 19: 1257–1264
- [74] Yoon JH, Lee HS, Kim EK et al. Malignancy Risk Stratification of Thyroid Nodules: Comparison between the Thyroid Imaging Reporting and Data System and the 2014 American Thyroid Association Management Guidelines. *Radiology* 2016; 278: 917–924
- [75] Cantisani V, Grazhdani H, Drakonaki E et al. Strain US Elastography for the Characterization of Thyroid Nodules: Advantages and Limitation. *Int J Endocrinol* 2015; 2015: 908575
- [76] Cantisani V, Maceroni P, D'Andrea V et al. Strain ratio ultrasound elastography increases the accuracy of colour-Doppler ultrasound in the evaluation of Thy-3 nodules. A bi-centre university experience. *Eur Radiol* 2016; 26: 1441–1449
- [77] Cantisani V, Grazhdani H, Ricci P et al. Q-elastosonography of solid thyroid nodules: assessment of diagnostic efficacy and interobserver variability in a large patient cohort. *Eur Radiol* 2014; 24: 143–150
- [78] Ghajrzadeh M, Sodagari F, Shakiba M. Diagnostic accuracy of sonoelastography in detecting malignant thyroid nodules: a systematic review and meta-analysis. *Am J Roentgenol* 2014; 202: W379–W389
- [79] Razavi SA, Hadduck TA, Sadigh G et al. Comparative effectiveness of elastographic and B-mode ultrasound criteria for diagnostic discrimination of thyroid nodules: a meta-analysis. *Am J Roentgenol* 2013; 200: 1317–1326
- [80] Sun J, Cai J, Wang X. Real-time ultrasound elastography for differentiation of benign and malignant thyroid nodules: a meta-analysis. *J Ultrasound Med* 2014; 33: 495–502
- [81] Hu X, Liu Y, Qian L. Diagnostic potential of real-time elastography (RTE) and shear wave elastography (SWE) to differentiate benign and malignant thyroid nodules: A systematic review and meta-analysis. *Medicine (Baltimore)* 2017; 96: e8282
- [82] Nattabi HA, Sharif NM, Yahya N et al. Is Diagnostic Performance of Quantitative 2D-Shear Wave Elastography Optimal for Clinical Classification of Benign and Malignant Thyroid Nodules?: A Systematic Review and Meta-analysis. *Acad Radiol* 2017. (Epub ahead of print)
- [83] Tian W, Hao S, Gao B et al. Comparing the Diagnostic Accuracy of RTE and SWE in Differentiating Malignant Thyroid Nodules from Benign Ones: a Meta-Analysis. *Cell Physiol Biochem* 2016; 39: 2451–2463
- [84] Lin P, Chen M, Liu B et al. Diagnostic performance of shear wave elastography in the identification of malignant thyroid nodules: a meta-analysis. *Eur Radiol* 2014; 24: 2729–2738
- [85] Zhan J, Jin JM, Diao XH et al. Acoustic radiation force impulse imaging (ARFI) for differentiation of benign and malignant thyroid nodules – A meta-analysis. *Eur J Radiol* 2015; 84: 2181–2186
- [86] Rago T, Vitti P. Role of thyroid ultrasound in the diagnostic evaluation of thyroid nodules. *Best Pract Res Clin Endocrinol Metab* 2008; 22: 913–928
- [87] Rago T, Vitti P. Potential value of elastosonography in the diagnosis of malignancy in thyroid nodules. *Q J Nucl Med Mol Imaging* 2009; 53: 455–464
- [88] Rago T, Scutari M, Santini F et al. Real-time elastosonography: useful tool for refining the presurgical diagnosis in thyroid nodules with indeterminate or nondiagnostic cytology. *J Clin Endocrinol Metab* 2010; 95: 5274–5280
- [89] Ciledag N, Arda K, Aribas BK et al. The utility of ultrasound elastography and MicroPure imaging in the differentiation of benign and malignant thyroid nodules. *Am J Roentgenol* 2012; 198: W244–W249
- [90] Vidal-Casariago A, López-González L, Jiménez-Pérez A et al. Accuracy of ultrasound elastography in the diagnosis of thyroid cancer in a low-risk population. *Exp Clin Endocrinol Diabetes* 2012; 120: 635–638
- [91] Hong Y, Liu X, Li Z et al. Real-time ultrasound elastography in the differential diagnosis of benign and malignant thyroid nodules. *J Ultrasound Med* 2009; 28: 861–867

- [92] Unlütürk U, Erdoğan MF, Demir O et al. Ultrasound elastography is not superior to grayscale ultrasound in predicting malignancy in thyroid nodules. *Thyroid* 2012; 22: 1031–1038
- [93] Zhan J, Diao XH, Chai QL et al. Comparative study of acoustic radiation force impulse imaging with real-time elastography in differential diagnosis of thyroid nodules. *Ultrasound Med Biol* 2013; 39: 2217–2225
- [94] Rago T, Santini F, Scutari M et al. Elastography: new developments in ultrasound for predicting malignancy in thyroid nodules. *J Clin Endocrinol Metab* 2007; 92: 2917–2922
- [95] Kagoya R, Monobe H, Tojima H. Utility of elastography for differential diagnosis of benign and malignant thyroid nodules. *Otolaryngol Head Neck Surg* 2010; 143: 230–234
- [96] He YP, Xu HX, Li XL et al. Comparison of Virtual Touch Tissue Imaging & Quantification (VTIQ) and Toshiba shear wave elastography (T-SWE) in diagnosis of thyroid nodules: Initial experience. *Clin Hemorheol Microcirc* 2017; 66: 15–26
- [97] Wang F, Chang C, Gao Y et al. Does Shear Wave Elastography Provide Additional Value in the Evaluation of Thyroid Nodules That Are Suspicious for Malignancy? *J Ultrasound Med* 2016; 35: 2397–2404
- [98] Swan KZ, Nielsen VE, Bibby BM et al. Is the reproducibility of shear wave elastography of thyroid nodules high enough for clinical use? A methodological study. *Clin Endocrinol (Oxf)* 2017; 86: 606–613
- [99] Bardet S, Ciappuccini R, Pellot-Barakat C et al. Shear Wave Elastography in Thyroid Nodules with Indeterminate Cytology: Results of a Prospective Bicentric Study. *Thyroid* 2017; 27: 1441–1449
- [100] Liu Z, Jing H, Han X et al. Shear wave elastography combined with the thyroid imaging reporting and data system for malignancy risk stratification in thyroid nodules. *Oncotarget* 2017; 8: 43406–43416
- [101] Dobruch-Sobczak K, Gumińska A, Bakula-Zalewska E et al. Shear wave elastography in medullary thyroid carcinoma diagnostics. *J Ultrason* 2015; 15: 358–367
- [102] Dobruch-Sobczak K, Zalewska EB, Gumińska A et al. Diagnostic Performance of Shear Wave Elastography Parameters Alone and in Combination with Conventional B-Mode Ultrasound Parameters for the Characterization of Thyroid Nodules: A Prospective, Dual-Center Study. *Ultrasound Med Biol* 2016; 42: 2803–2811
- [103] Wang D, He YP, Zhang YF et al. The diagnostic performance of shear wave speed (SWS) imaging for thyroid nodules with elasticity modulus and SWS measurement. *Oncotarget* 2017; 8: 13387–13399
- [104] Duan SB, Yu J, Li X et al. Diagnostic value of two-dimensional shear wave elastography in papillary thyroid microcarcinoma. *Onco Targets Ther* 2016; 9: 1311–1317
- [105] Liu MJ, Men YM, Zhang YL et al. Improvement of diagnostic efficiency in distinguishing the benign and malignant thyroid nodules via conventional ultrasound combined with ultrasound contrast and elastography. *Oncol Lett* 2017; 14: 867–871
- [106] Wang F, Chang C, Chen M et al. Does Lesion Size Affect the Value of Shear Wave Elastography for Differentiating Between Benign and Malignant Thyroid Nodules? *J Ultrasound Med* 2018; 37: 601–609
- [107] Liu BJ, Lu F, Xu HX et al. The diagnosis value of acoustic radiation force impulse (ARFI) elastography for thyroid malignancy without highly suspicious features on conventional ultrasound. *Int J Clin Exp Med* 2015; 8: 15362–15372
- [108] Liu BJ, Zhao CK, Xu HX et al. Quality measurement on shear wave speed imaging: diagnostic value in differentiation of thyroid malignancy and the associated factors. *Oncotarget* 2017; 8: 4848–4959
- [109] Zhou H, Yue WW, Du LY et al. A Modified Thyroid Imaging Reporting and Data System (mTI-RADS) For Thyroid Nodules in Coexisting Hashimoto's Thyroiditis. *Sci Rep* 2016; 6: 26410
- [110] Pandey NN, Pradhan GS, Manchanda A et al. Diagnostic Value of Acoustic Radiation Force Impulse Quantification in the Differentiation of Benign and Malignant Thyroid Nodules. *Ultrason Imaging* 2017; 39: 326–336
- [111] Liu BJ, Li DD, Xu HX et al. Quantitative Shear Wave Velocity Measurement on Acoustic Radiation Force Impulse Elastography for Differential Diagnosis between Benign and Malignant Thyroid Nodules: A Meta-analysis. *Ultrasound Med Biol* 2015; 41: 3035–3043
- [112] Russ G. Risk stratification of thyroid nodules on ultrasonography with the French TI-RADS: description and reflections. *Ultrasonography* 2016; 35: 25–38
- [113] Arda K, Ciledag N, Aktas E et al. Quantitative assessment of normal soft-tissue elasticity using shear-wave ultrasound elastography. *Am J Roentgenol* 2011; 197: 532–536
- [114] Gallotti A, D'Onofrio M, Pozzi Mucelli R. Acoustic Radiation Force Impulse (ARFI) technique in ultrasound with Virtual Touch tissue quantification of the upper abdomen. *Radiol Med* 2010; 115: 889–897
- [115] D'Onofrio M, Tremolada G, De Robertis R et al. Prevent Pancreatic Fistula after Pancreatoduodenectomy: Possible Role of Ultrasound Elastography. *Dig Surg* 2018; 35: 164–170
- [116] Goertz RS, Schuderer J, Strobel D et al. Acoustic radiation force impulse shear wave elastography (ARFI) of acute and chronic pancreatitis and pancreatic tumour. *Eur J Radiol* 2016; 85: 2211–2216
- [117] Harada N, Ishizawa T, Inoue Y et al. Acoustic radiation force impulse imaging of the pancreas for estimation of pathologic fibrosis and risk of postoperative pancreatic fistula. *J Am Coll Surg* 2014; 219: 887–894. e885
- [118] He Y, Wang H, Li XP et al. Pancreatic Elastography From Acoustic Radiation Force Impulse Imaging for Evaluation of Diabetic Microangiopathy. *Am J Roentgenol* 2017; 209: 775–780
- [119] Hirooka Y, Kuwahara T, Irisawa A et al. JSUM ultrasound elastography practice guidelines: pancreas. *J Med Ultrason (2001)* 2015; 42: 151–174
- [120] Kawada N, Tanaka S. Elastography for the pancreas: Current status and future perspective. *World J Gastroenterol* 2016; 22: 3712–3724
- [121] Kawada N, Tanaka S, Uehara H et al. Potential use of point shear wave elastography for the pancreas: a single center prospective study. *Eur J Radiol* 2014; 83: 620–624
- [122] Kuwahara T, Hirooka Y, Kawashima H et al. Usefulness of shear wave elastography as a quantitative diagnosis of chronic pancreatitis. *J Gastroenterol Hepatol* 2018; 33: 756–761
- [123] Kuwahara T, Hirooka Y, Kawashima H et al. Quantitative evaluation of pancreatic tumour fibrosis using shear wave elastography. *Pancreatol* 2016; 16: 1063–1068
- [124] Llamaza-Torres CJ, Fuentes-Pardo M, Álvarez-Higuera FJ et al. Usefulness of percutaneous elastography by acoustic radiation force impulse for the non-invasive diagnosis of chronic pancreatitis. *Rev Esp Enferm Dig* 2016; 108: 450–456
- [125] Onoyama T, Koda M, Fujise Y et al. Utility of virtual touch quantification in the diagnosis of pancreatic ductal adenocarcinoma. *Clin Imaging* 2017; 42: 64–67
- [126] Park MK, Jo J, Kwon H et al. Usefulness of acoustic radiation force impulse elastography in the differential diagnosis of benign and malignant solid pancreatic lesions. *Ultrasonography* 2014; 33: 26–33
- [127] Pozzi R, Parzanese I, Baccarin A et al. Point shear-wave elastography in chronic pancreatitis: A promising tool for staging disease severity. *Pancreatol* 2017; 17: 905–910
- [128] Sağlam D, Bilgili MC, Kara C et al. Acoustic Radiation Force Impulse Elastography in Determining the Effects of Type 1 Diabetes on Pancreas and Kidney Elasticity in Children. *Am J Roentgenol* 2017; 209: 1143–1149
- [129] Stumpf S, Jaeger H, Graeter T et al. Influence of age, sex, body mass index, alcohol, and smoking on shear wave velocity (p-SWE) of the pancreas. *Abdom Radiol (NY)* 2016; 41: 1310–1316

- [130] Xie J, Zou L, Yao M et al. A Preliminary Investigation of Normal Pancreas and Acute Pancreatitis Elasticity Using Virtual Touch Tissue Quantification (VTQ) Imaging. *Med Sci Monit* 2015; 21: 1693–1699
- [131] Yashima Y, Sasahira N, Isayama H et al. Acoustic radiation force impulse elastography for noninvasive assessment of chronic pancreatitis. *J Gastroenterol* 2012; 47: 427–432
- [132] Zaro R, Lupsor-Platon M, Cheviet A et al. The pursuit of normal reference values of pancreas stiffness by using Acoustic Radiation Force Impulse (ARFI) elastography. *Med Ultrason* 2016; 18: 425–430
- [133] D'Onofrio M, De Robertis R, Crosara S et al. Acoustic radiation force impulse with shear wave speed quantification of pancreatic masses: A prospective study. *Pancreatol* 2016; 16: 106–109
- [134] Chantarojanasiri T, Hirooka Y, Kawashima H et al. Age-related changes in pancreatic elasticity: When should we be concerned about their effect on strain elastography? *Ultrasonics* 2016; 69: 90–96
- [135] Chantarojanasiri T, Hirooka Y, Kawashima H et al. Endoscopic ultrasound in diagnosis of solid pancreatic lesions: Elastography or contrast-enhanced harmonic alone versus the combination. *Endosc Int Open* 2017; 5: E1136–E1143
- [136] Dominguez-Muñoz JE, Iglesias-García J, Castiñeira Alvarino M et al. EUS elastography to predict pancreatic exocrine insufficiency in patients with chronic pancreatitis. *Gastrointest Endosc* 2015; 81: 136–142
- [137] Dyrła P, Gil J, Florek M et al. Elastography in pancreatic solid tumours diagnoses. *Prz Gastroenterol* 2015; 10: 41–46
- [138] Harada N, Yoshizumi T, Maeda T et al. Preoperative Pancreatic Stiffness by Real-time Tissue Elastography to Predict Pancreatic Fistula After Pancreaticoduodenectomy. *Anticancer Res* 2017; 37: 1909–1915
- [139] Hirche TO, Ignee A, Barreiros AP et al. Indications and limitations of endoscopic ultrasound elastography for evaluation of focal pancreatic lesions. *Endoscopy* 2008; 40: 910–917
- [140] Iglesias García JJ, Lariño Noia J, Alvarez Castro A et al. Second-generation endoscopic ultrasound elastography in the differential diagnosis of solid pancreatic masses. Pancreatic cancer vs. inflammatory mass in chronic pancreatitis. *Rev Esp Enferm Dig* 2009; 101: 723–730
- [141] Iglesias-García J, Domínguez-Muñoz JE, Castiñeira-Alvarino M et al. Quantitative elastography associated with endoscopic ultrasound for the diagnosis of chronic pancreatitis. *Endoscopy* 2013; 45: 781–788
- [142] Iglesias-García J, Larino-Noia J, Abdulkader I et al. Quantitative endoscopic ultrasound elastography: an accurate method for the differentiation of solid pancreatic masses. *Gastroenterology* 2010; 139: 1172–1180
- [143] Iglesias-García J, Lindkvist B, Lariño-Noia J et al. Differential diagnosis of solid pancreatic masses: contrast-enhanced harmonic (CEH-EUS), quantitative-elastography (QE-EUS), or both? *United European Gastroenterol J* 2017; 5: 236–246
- [144] Iordache S, Costache MI, Popescu CF et al. Clinical impact of EUS elastography followed by contrast-enhanced EUS in patients with focal pancreatic masses and negative EUS-guided FNA. *Medical Ultrasonography* 2016; 18: 18–24
- [145] Itokawa F, Itoi T, Sofuni A et al. EUS elastography combined with the strain ratio of tissue elasticity for diagnosis of solid pancreatic masses. *J Gastroenterol* 2011; 46: 843–853
- [146] Janssen J, Papavassiliou I. Effect of aging and diffuse chronic pancreatitis on pancreas elasticity evaluated using semiquantitative EUS elastography. *Ultraschall in Med* 2014; 35: 253–258
- [147] Kawada N, Tanaka S, Uehara H et al. Alteration of strain ratio evaluated by transabdominal ultrasound elastography may predict the efficacy of preoperative chemoradiation performed for pancreatic ductal carcinoma: preliminary results. *Hepatogastroenterology* 2014; 61: 480–483
- [148] Kim SY, Cho JH, Kim YJ et al. Diagnostic efficacy of quantitative endoscopic ultrasound elastography for differentiating pancreatic disease. *J Gastroenterol Hepatol* 2017; 32: 1115–1122
- [149] Kongkam P, Lakananurak N, Navichareon P et al. Combination of EUS-FNA and elastography (strain ratio) to exclude malignant solid pancreatic lesions: A prospective single-blinded study. *J Gastroenterol Hepatol* 2015; 30: 1683–1689
- [150] Opačić D, Rustemović N, Kalauz M et al. Endoscopic ultrasound elastography strain histograms in the evaluation of patients with pancreatic masses. *World J Gastroenterol* 2015; 21: 4014–4019
- [151] Rana SS, Dambalkar A, Chhabra P et al. Is pancreatic exocrine insufficiency in celiac disease related to structural alterations in pancreatic parenchyma? *Ann Gastroenterol* 2016; 29: 363–366
- [152] Rustemović N, Kalauz M, Grubelić Ravić K et al. Differentiation of Pancreatic Masses via Endoscopic Ultrasound Strain Ratio Elastography Using Adjacent Pancreatic Tissue as the Reference. *Pancreas* 2017; 46: 347–351
- [153] Săftoiu A, Vilmann P. Differential diagnosis of focal pancreatic masses by semiquantitative EUS elastography: between strain ratios and strain histograms. *Gastrointest Endosc* 2013; 78: 188–189
- [154] Săftoiu A, Vilmann P, Gorunescu F et al. Neural network analysis of dynamic sequences of EUS elastography used for the differential diagnosis of chronic pancreatitis and pancreatic cancer. *Gastrointest Endosc* 2008; 68: 1086–1094
- [155] Săftoiu A, Vilmann P, Gorunescu F et al. Accuracy of endoscopic ultrasound elastography used for differential diagnosis of focal pancreatic masses: a multicenter study. *Endoscopy* 2011; 43: 596–603
- [156] Săftoiu A, Vilmann P, Gorunescu F et al. Efficacy of an Artificial Neural Network-Based Approach to Endoscopic Ultrasound Elastography in Diagnosis of Focal Pancreatic Masses. *Clinical Gastroenterology and Hepatology* 2012; 10: U84–U167
- [157] Cui XW, Chang JM, Kan QC et al. Endoscopic ultrasound elastography: Current status and future perspectives. *World J Gastroenterol* 2015; 21: 13212–13224
- [158] Dietrich CF. Elastography, the new dimension in ultrasonography. *Praxis (Bern 1994)* 2011; 100: 1533–1542
- [159] Dietrich CF, Barr RG, Farrokhi A et al. Strain Elastography – How To Do It? *Ultrasound Int Open* 2017; 3: E137–E149
- [160] Dietrich CF, Cantisani V. Current status and perspectives of elastography. *Eur J Radiol* 2014; 83: 403–404
- [161] Dietrich CF, Hirche TO, Ott M et al. Real-time tissue elastography in the diagnosis of autoimmune pancreatitis. *Endoscopy* 2009; 41: 718–720
- [162] Dietrich CF, Săftoiu A, Jenssen C. Real time elastography endoscopic ultrasound (RTE-EUS), a comprehensive review. *Eur J Radiol* 2014; 83: 405–414
- [163] Hocke M, Ignee A, Dietrich CF. Advanced endosonographic diagnostic tools for discrimination of focal chronic pancreatitis and pancreatic carcinoma—elastography, contrast enhanced high mechanical index (CEHMI) and low mechanical index (CELMI) endosonography in direct comparison. *Z Gastroenterol* 2012; 50: 199–203
- [164] Janssen J, Schlörer E, Greiner L. EUS elastography of the pancreas: feasibility and pattern description of the normal pancreas, chronic pancreatitis, and focal pancreatic lesions. *Gastrointest Endosc* 2007; 65: 971–978
- [165] Azemoto N, Kumagi T, Koizumi M et al. Diagnostic Challenge in Pancreatic Sarcoidosis using Endoscopic Ultrasonography. *Intern Med* 2018; 57: 231–235
- [166] Chantarojanasiri T, Hirooka Y, Kawashima H et al. Endoscopic ultrasound in the diagnosis of acinar cell carcinoma of the pancreas: contrast-enhanced endoscopic ultrasound, endoscopic ultrasound elastography, and pathological correlation. *Endosc Int Open* 2016; 4: E1223–E1226
- [167] Itoh Y, Itoh A, Kawashima H et al. Quantitative analysis of diagnosing pancreatic fibrosis using EUS-elastography (comparison with surgical specimens). *J Gastroenterol* 2014; 49: 1183–1192

- [168] Jafri M, Sachdev AH, Khanna L et al. The Role of Real Time Endoscopic Ultrasound Guided Elastography for Targeting EUS-FNA of Suspicious Pancreatic Masses: A Review of the Literature and A Single Center Experience. *JOP* 2016; 17: 516–524
- [169] Kuwahara T, Hirooka Y, Kawashima H et al. Quantitative diagnosis of chronic pancreatitis using EUS elastography. *J Gastroenterol* 2017; 52: 868–874
- [170] Kuwahara T, Hirooka Y, Kawashima H et al. Usefulness of endoscopic ultrasonography-elastography as a predictive tool for the occurrence of pancreatic fistula after pancreatoduodenectomy. *J Hepatobiliary Pancreat Sci* 2017; 24: 649–656
- [171] Lee TH, Cho YD, Cha SW et al. Endoscopic ultrasound elastography for the pancreas in Korea: a preliminary single center study. *Clin Endosc* 2013; 46: 172–177
- [172] Pei Q, Zou X, Zhang X et al. Diagnostic value of EUS elastography in differentiation of benign and malignant solid pancreatic masses: a meta-analysis. *Pancreatol* 2012; 12: 402–408
- [173] Popescu A, Ciocalteu AM, Gheonea DI et al. Utility of endoscopic ultrasound multimodal examination with fine needle aspiration for the diagnosis of pancreatic insulinoma – a case report. *Current health sciences journal* 2012; 38: 36–40
- [174] Rana SS, Sharma R, Guleria S et al. Endoscopic ultrasound (EUS) elastography and contrast enhanced EUS in groove pancreatitis. *Indian J Gastroenterol* 2018; 37: 70–71
- [175] Schrader H, Wiese M, Ellrichmann M et al. Diagnostic value of quantitative EUS elastography for malignant pancreatic tumours: relationship with pancreatic fibrosis. *Ultraschall in Med* 2012; 33: E196–E201
- [176] Soares JB, Iglesias-García J, Goncalves B et al. Interobserver agreement of EUS elastography in the evaluation of solid pancreatic lesions. *Endosc Ultrasound* 2015; 4: 244–249
- [177] Rustemovic N, Opacic D, Ostojic Z et al. Comparison of elastography methods in patients with pancreatic masses. *Endosc Ultrasound* 2014; 3: S4
- [178] Saftoiu A, Vilman P. Endoscopic ultrasound elastography – a new imaging technique for the visualization of tissue elasticity distribution. *J Gastrointest Liver Dis* 2006; 15: 161–165
- [179] Mateen MA, Muheet KA, Mohan RJ et al. Evaluation of ultrasound based acoustic radiation force impulse (ARFI) and eSie touch sonoelastography for diagnosis of inflammatory pancreatic diseases. *JOP* 2012; 13: 36–44
- [180] Goya C, Hamidi C, Hattapoglu S et al. Use of acoustic radiation force impulse elastography to diagnose acute pancreatitis at hospital admission: comparison with sonography and computed tomography. *J Ultrasound Med* 2014; 33: 1453–1460
- [181] Domínguez-Muñoz JE. Predicting Pancreatic Exocrine Insufficiency With EUS Elastography. *Gastroenterol Hepatol (N Y)* 2016; 12: 511–512
- [182] Uchida H, Hirooka Y, Itoh A et al. Feasibility of tissue elastography using transcutaneous ultrasonography for the diagnosis of pancreatic diseases. *Pancreas* 2009; 38: 17–22
- [183] Friedrich-Rust M, Schlueter N, Smaczny C et al. Non-invasive measurement of liver and pancreas fibrosis in patients with cystic fibrosis. *J Cyst Fibros* 2013; 12: 431–439
- [184] Sugimoto M, Takahashi S, Kojima M et al. What is the nature of pancreatic consistency? Assessment of the elastic modulus of the pancreas and comparison with tactile sensation, histology, and occurrence of postoperative pancreatic fistula after pancreaticoduodenectomy. *Surgery* 2014; 156: 1204–1211
- [185] Hatano M, Watanabe J, Kushihata F et al. Quantification of pancreatic stiffness on intraoperative ultrasound elastography and evaluation of its relationship with postoperative pancreatic fistula. *Int Surg* 2015; 100: 497–502
- [186] D'Onofrio M, Crosara S, De Robertis R et al. Elastography of the pancreas. *Eur J Radiol* 2014; 83: 415–419
- [187] Dong Y, D'Onofrio M, Hocke M et al. Autoimmune pancreatitis: Imaging features. *Endosc Ultrasound* 2018; 7: 196–203
- [188] Lee TK, Kang CM, Park MS et al. Prediction of postoperative pancreatic fistulas after pancreatotomy: assessment with acoustic radiation force impulse elastography. *J Ultrasound Med* 2014; 33: 781–786
- [189] Hu DM, Gong TT, Zhu Q. Endoscopic ultrasound elastography for differential diagnosis of pancreatic masses: a meta-analysis. *Dig Dis Sci* 2013; 58: 1125–1131
- [190] Mei M, Ni J, Liu D et al. EUS elastography for diagnosis of solid pancreatic masses: a meta-analysis. *Gastrointest Endosc* 2013; 77: 578–589
- [191] Li X, Xu W, Shi J et al. Endoscopic ultrasound elastography for differentiating between pancreatic adenocarcinoma and inflammatory masses: a meta-analysis. *World J Gastroenterol* 2013; 19: 6284–6291
- [192] Ying L, Lin X, Xie ZL et al. Clinical utility of endoscopic ultrasound elastography for identification of malignant pancreatic masses: a meta-analysis. *J Gastroenterol Hepatol* 2013; 28: 1434–1443
- [193] Iglesias-García J, Larino-Noia J, Abdulkader I et al. EUS elastography for the characterization of solid pancreatic masses. *Gastrointest Endosc* 2009; 70: 1101–1108
- [194] Giovannini M, Thomas B, Erwan B et al. Endoscopic ultrasound elastography for evaluation of lymph nodes and pancreatic masses: A multi-center study. *World Journal of Gastroenterology* 2009; 15: 1587–1593
- [195] Ignee A, Jenssen C, Hocke M et al. Contrast-enhanced (endoscopic) ultrasound and endoscopic ultrasound elastography in gastrointestinal stromal tumours. *Endoscopic Ultrasound* 2017; 6: 55–60
- [196] Havre RF, Ødegaard S, Gilja OH et al. Characterization of solid focal pancreatic lesions using endoscopic ultrasonography with real-time elastography. *Scand J Gastroenterol* 2014; 49: 742–751
- [197] Dawwas MF, Taha H, Leeds JS et al. Diagnostic accuracy of quantitative EUS elastography for discriminating malignant from benign solid pancreatic masses: a prospective, single-center study. *Gastrointest Endosc* 2012; 76: 953–961
- [198] Mayerle J, Beyer G, Simon P et al. Prospective cohort study comparing transient EUS guided elastography to EUS-FNA for the diagnosis of solid pancreatic mass lesions. *Pancreatol* 2016; 16: 110–114
- [199] Figueiredo FA, da Silva PM, Monges G et al. Yield of Contrast-Enhanced Power Doppler Endoscopic Ultrasonography and Strain Ratio Obtained by EUS-Elastography in the Diagnosis of Focal Pancreatic Solid Lesions. *Endosc Ultrasound* 2012; 1: 143–149
- [200] Popescu A, Ciocalteu AM, Gheonea DI et al. Utility of endoscopic ultrasound multimodal examination with fine needle aspiration for the diagnosis of pancreatic insulinoma – a case report. *Curr Health Sci J* 2012; 38: 36–40
- [201] Deprez PH. EUS elastography: is it replacing or supplementing tissue acquisition? *Gastrointest Endosc* 2013; 77: 590–592
- [202] Săftoiu A, Iordache SA, Gheonea DI et al. Combined contrast-enhanced power Doppler and real-time sonoelastography performed during EUS, used in the differential diagnosis of focal pancreatic masses (with videos). *Gastrointest Endosc* 2010; 72: 739–747
- [203] Dumonceau JM, Deprez PH, Jenssen C et al. Indications, results, and clinical impact of endoscopic ultrasound (EUS)-guided sampling in gastroenterology: European Society of Gastrointestinal Endoscopy (ESGE) Clinical Guideline – Updated January 2017. *Endoscopy* 2017; 49: 695–714
- [204] Jenssen C, Hocke M, Fusaroli P et al. EFSUMB Guidelines on Interventional Ultrasound (INVUS), Part IV – EUS-guided interventions: General Aspects and EUS-guided Sampling (Short Version). *Ultraschall in Med* 2016; 37: 157–169
- [205] Jenssen C, Hocke M, Fusaroli P et al. EFSUMB Guidelines on Interventional Ultrasound (INVUS), Part IV – EUS-guided Interventions: General

- aspects and EUS-guided sampling (Long Version). *Ultraschall in Med* 2016; 37: E33–E76
- [206] Hewitt MJ, McPhail MJ, Possamai L et al. EUS-guided FNA for diagnosis of solid pancreatic neoplasms: a meta-analysis. *Gastrointest Endosc* 2012; 75: 319–331
- [207] Dietrich C, Sahai A, D'Onofrio M et al. Differential diagnosis of small solid pancreatic lesions. *Gastrointestinal Endoscopy* 2016; 84: 933–940
- [208] D'Onofrio M, Crosara S, Canestrini S et al. Virtual analysis of pancreatic cystic lesion fluid content by ultrasound acoustic radiation force impulse quantification. *J Ultrasound Med* 2013; 32: 647–651
- [209] D'Onofrio M, Gallotti A, Falconi M et al. Acoustic radiation force impulse ultrasound imaging of pancreatic cystic lesions: preliminary results. *Pancreas* 2010; 39: 939–940
- [210] D'Onofrio M, Gallotti A, Martone E et al. Solid appearance of pancreatic serous cystadenoma diagnosed as cystic at ultrasound acoustic radiation force impulse imaging. *JOP* 2009; 10: 543–546
- [211] D'Onofrio M, Gallotti A, Mucelli RP. Pancreatic mucinous cystadenoma at ultrasound acoustic radiation force impulse (ARFI) imaging. *Pancreas* 2010; 39: 684–685
- [212] D'Onofrio M, Gallotti A, Salvia R et al. Acoustic radiation force impulse (ARFI) ultrasound imaging of pancreatic cystic lesions. *Eur J Radiol* 2011; 80: 241–244
- [213] Havre RF, Waage JR, Gilja OH et al. Real-Time Elastography: Strain Ratio Measurements Are Influenced by the Position of the Reference Area. *Ultraschall in Med* 2011. (Epub ahead of print)
- [214] Nylund K, Ødegaard S, Hausken T et al. Sonography of the small intestine. *World J Gastroenterol* 2009; 15: 1319–1330
- [215] Nylund K, Maconi G, Hollerweger A et al. EFSUMB Recommendations and Guidelines for Gastrointestinal Ultrasound Part 1: Examination Techniques and Normal Findings (Long version). *Ultraschall in Der Medizin* 2017; 38: E1–E15
- [216] Kim K, Johnson LA, Jia C et al. Noninvasive ultrasound elasticity imaging (UEI) of Crohn's disease: animal model. *Ultrasound Med Biol* 2008; 34: 902–912
- [217] Stidham RW, Higgins PD. Imaging of intestinal fibrosis: current challenges and future methods. *United European Gastroenterol J* 2016; 4: 515–522
- [218] Dillman JR, Stidham RW, Higgins PD et al. US elastography-derived shear wave velocity helps distinguish acutely inflamed from fibrotic bowel in a Crohn disease animal model. *Radiology* 2013; 267: 757–766
- [219] Sconfienza LM, Cavallaro F, Colombi V et al. In-vivo Axial-strain Sonoelastography Helps Distinguish Acutely-inflamed from Fibrotic Terminal Ileum Strictures in Patients with Crohn's Disease: Preliminary Results. *Ultrasound Med Biol* 2016; 42: 855–863
- [220] Havre RF, Leh S, Gilja OH et al. Strain assessment in surgically resected inflammatory and neoplastic bowel lesions. *Ultraschall in Med* 2014; 35: 149–158
- [221] Pescatori LC, Mauri G, Savarino E et al. Bowel Sonoelastography in Patients with Crohn's Disease: A Systematic Review. *Ultrasound Med Biol* 2018; 44: 297–302
- [222] Baumgart DC, Müller HP, Grittner U et al. US-based Real-time Elastography for the Detection of Fibrotic Gut Tissue in Patients with Stricturing Crohn Disease. *Radiology* 2015; 275: 889–899
- [223] Fraquelli M, Branchi F, Cribiù FM et al. The Role of Ultrasound Elasticity Imaging in Predicting Ileal Fibrosis in Crohn's Disease Patients. *Inflamm Bowel Dis* 2015; 21: 2605–2612
- [224] Serra C, Rizzello F, Pratico C et al. Real-time elastography for the detection of fibrotic and inflammatory tissue in patients with stricturing Crohn's disease. *J Ultrasound* 2017; 20: 273–284
- [225] Orlando S, Fraquelli M, Coletta M et al. Ultrasound Elasticity Imaging predicts therapeutic outcomes of patients with Crohn's disease treated with anti-tumour necrosis factor antibodies. *J Crohns Colitis* 2018; 12: 63–70
- [226] Waage JE, Bach SP, Pfeffer F et al. Combined endorectal ultrasonography and strain elastography for the staging of early rectal cancer. *Colorectal Dis* 2015; 17: 50–56
- [227] Waage JE, Leh S, Røsler C et al. Endorectal ultrasonography, strain elastography and MRI differentiation of rectal adenomas and adenocarcinomas. *Colorectal Dis* 2015; 17: 124–131
- [228] Waage JE, Rafaelsen SR, Borley NR et al. Strain Elastography Evaluation of Rectal Tumours: Inter- and Intraobserver Reproducibility. *Ultraschall in Med* 2015; 36: 611–617
- [229] Rafaelsen SR, Vagn-Hansen C, Sørensen T et al. Elastography and diffusion-weighted MRI in patients with rectal cancer. *Br J Radiol* 2015; 88: 20150294
- [230] Chen LD, Wang W, Xu JB et al. Assessment of Rectal Tumours with Shear-Wave Elastography before Surgery: Comparison with Endorectal US. *Radiology* 2017; 285: 279–292
- [231] Arena U, Lupsor Platon M, Stasi C et al. Liver stiffness is influenced by a standardized meal in patients with chronic hepatitis C virus at different stages of fibrotic evolution. *Hepatology* 2013; 58: 65–72
- [232] Berzigotti A, De Gottardi A, Vukotic R et al. Effect of meal ingestion on liver stiffness in patients with cirrhosis and portal hypertension. *PLoS One* 2013; 8: e58742
- [233] Ștefănescu H, Grigorescu M, Lupșor M et al. Spleen stiffness measurement using Fibroscan for the noninvasive assessment of esophageal varices in liver cirrhosis patients. *J Gastroenterol Hepatol* 2011; 26: 164–170
- [234] Colecchia A, Montrone L, Scaioli E et al. Measurement of spleen stiffness to evaluate portal hypertension and the presence of esophageal varices in patients with HCV-related cirrhosis. *Gastroenterology* 2012; 143: 646–654
- [235] Procopet B, Berzigotti A, Abralde JG et al. Real-time shear-wave elastography: applicability, reliability and accuracy for clinically significant portal hypertension. *J Hepatol* 2015; 62: 1068–1075
- [236] Karlas T, Lindner F, Tröltzsch M et al. Assessment of spleen stiffness using acoustic radiation force impulse imaging (ARFI): definition of examination standards and impact of breathing maneuvers. *Ultraschall in Med* 2014; 35: 38–43
- [237] Jansen C, Bogs C, Verlinden W et al. Shear-wave elastography of the liver and spleen identifies clinically significant portal hypertension: A prospective multicentre study. *Liver Int* 2017; 37: 396–405
- [238] Samir AE, Dhyan M, Vij A et al. Shear-wave elastography for the estimation of liver fibrosis in chronic liver disease: determining accuracy and ideal site for measurement. *Radiology* 2015; 274: 888–896
- [239] Grgurevic I, Puljiz Z, Brnic D et al. Liver and spleen stiffness and their ratio assessed by real-time two dimensional-shear wave elastography in patients with liver fibrosis and cirrhosis due to chronic viral hepatitis. *Eur Radiol* 2015; 25: 3214–3221
- [240] Song J, Huang J, Huang H et al. Performance of spleen stiffness measurement in prediction of clinical significant portal hypertension: A meta-analysis. *Clin Res Hepatol Gastroenterol* 2018; 42: 216–226
- [241] Zykus R, Jonaitis L, Petrenkienė V et al. Liver and spleen transient elastography predicts portal hypertension in patients with chronic liver disease: a prospective cohort study. *BMC Gastroenterol* 2015; 15: 183
- [242] Takuma Y, Nouse K, Morimoto Y et al. Portal Hypertension in Patients with Liver Cirrhosis: Diagnostic Accuracy of Spleen Stiffness. *Radiology* 2016; 279: 609–619
- [243] Attia D, Schoenemeier B, Rodt T et al. Evaluation of Liver and Spleen Stiffness with Acoustic Radiation Force Impulse Quantification Elastography for Diagnosing Clinically Significant Portal Hypertension. *Ultraschall in Med* 2015; 36: 603–610

- [244] Balakrishnan M, Souza F, Muñoz C et al. Liver and Spleen Stiffness Measurements by Point Shear Wave Elastography via Acoustic Radiation Force Impulse: Intraobserver and Interobserver Variability and Predictors of Variability in a US Population. *J Ultrasound Med* 2016; 35: 2373–2380
- [245] Elkrief L, Rautou PE, Ronot M et al. Prospective comparison of spleen and liver stiffness by using shear-wave and transient elastography for detection of portal hypertension in cirrhosis. *Radiology* 2015; 275: 589–598
- [246] Singh S, Eaton JE, Murad MH et al. Accuracy of spleen stiffness measurement in detection of esophageal varices in patients with chronic liver disease: systematic review and meta-analysis. *Clin Gastroenterol Hepatol* 2014; 12: 935–945.e934
- [247] Calvaruso V, Bronte F, Conte E et al. Modified spleen stiffness measurement by transient elastography is associated with presence of large oesophageal varices in patients with compensated hepatitis C virus cirrhosis. *J Viral Hepat* 2013; 20: 867–874
- [248] Stefanescu H, Allegretti G, Salvatore V et al. Bidimensional shear wave ultrasound elastography with supersonic imaging to predict presence of oesophageal varices in cirrhosis. *Liver Int* 2017; 37: 1405
- [249] Bota S, Sporea I, Sirlu R et al. Can ARFI elastography predict the presence of significant esophageal varices in newly diagnosed cirrhotic patients? *Ann Hepatol* 2012; 11: 519–525
- [250] Colecchia A, Colli A, Casazza G et al. Spleen stiffness measurement can predict clinical complications in compensated HCV-related cirrhosis: a prospective study. *J Hepatol* 2014; 60: 1158–1164
- [251] Gao J, Ran HT, Ye XP et al. The stiffness of the liver and spleen on ARFI Imaging pre and post TIPS placement: a preliminary observation. *Clin Imaging* 2012; 36: 135–141
- [252] Novelli PM, Cho K, Rubin JM. Sonographic assessment of spleen stiffness before and after transjugular intrahepatic portosystemic shunt placement with or without concurrent embolization of portal systemic collateral veins in patients with cirrhosis and portal hypertension: a feasibility study. *J Ultrasound Med* 2015; 34: 443–449
- [253] Verlinden W, Bourgeois S, Gigase P et al. Liver Fibrosis Evaluation Using Real-time Shear Wave Elastography in Hepatitis C-Monoinfected and Human Immunodeficiency Virus/Hepatitis C-Coinfected Patients. *J Ultrasound Med* 2016; 35: 1299–1308
- [254] Pons M, Simón-Talero M, Millán L et al. Basal values and changes of liver stiffness predict the risk of disease progression in compensated advanced chronic liver disease. *Dig Liver Dis* 2016; 48: 1214–1219
- [255] Sharma P, Mishra SR, Kumar M et al. Liver and spleen stiffness in patients with extrahepatic portal vein obstruction. *Radiology* 2012; 263: 893–899
- [256] Furuichi Y, Moriyasu F, Taira J et al. Noninvasive diagnostic method for idiopathic portal hypertension based on measurements of liver and spleen stiffness by ARFI elastography. *J Gastroenterol* 2013; 48: 1061–1068
- [257] Seijo S, Reverter E, Miquel R et al. Role of hepatic vein catheterisation and transient elastography in the diagnosis of idiopathic portal hypertension. *Dig Liver Dis* 2012; 44: 855–860
- [258] Uchida H, Sakamoto S, Kobayashi M et al. The degree of spleen stiffness measured on acoustic radiation force impulse elastography predicts the severity of portal hypertension in patients with biliary atresia after portoenterostomy. *J Pediatr Surg* 2015; 50: 559–564
- [259] Colecchia A, Marasco G, Festi D. Are Noninvasive Methods Clinically Useful in Advanced, Decompensated Liver Cirrhosis When “Les Jeux Sont Faits”? *Radiology* 2016; 278: 304–305
- [260] Iurlo A, Cattaneo D, Giunta M et al. Transient elastography spleen stiffness measurements in primary myelofibrosis patients: a pilot study in a single centre. *Br J Haematol* 2015; 170: 890–892
- [261] Cassinotto C, Charrie A, Mouries A et al. Liver and spleen elastography using supersonic shear imaging for the non-invasive diagnosis of cirrhosis severity and oesophageal varices. *Dig Liver Dis* 2015; 47: 695–701
- [262] Correas JM, Anglicheau D, Joly D et al. Ultrasound-based imaging methods of the kidney-recent developments. *Kidney Int* 2016; 90: 1199–1210
- [263] Derieppe M, Delmas Y, Gennisson JL et al. Detection of intrarenal microstructural changes with supersonic shear wave elastography in rats. *Eur Radiol* 2012; 22: 243–250
- [264] Franchi-Abella S, Elie C, Correas JM. Ultrasound elastography: advantages, limitations and artefacts of the different techniques from a study on a phantom. *Diagn Interv Imaging* 2013; 94: 497–501
- [265] Ferraioli G, Tinelli C, Malfitano A et al. Performance of real-time strain elastography, transient elastography, and aspartate-to-platelet ratio index in the assessment of fibrosis in chronic hepatitis C. *Am J Roentgenol* 2012; 199: 19–25
- [266] Nightingale K, Bentley R, Trahey G. Observations of tissue response to acoustic radiation force: opportunities for imaging. *Ultrason Imaging* 2002; 24: 129–138
- [267] Sarvazyan AP, Rudenko OV, Nyborg WL. Biomedical applications of radiation force of ultrasound: historical roots and physical basis. *Ultrasound Med Biol* 2010; 36: 1379–1394
- [268] Syversveen T, Brabrand K, Midtvedt K et al. Assessment of renal allograft fibrosis by acoustic radiation force impulse quantification—a pilot study. *Transpl Int* 2011; 24: 100–105
- [269] Ozkan F, Yavuz YC, Inci MF et al. Interobserver variability of ultrasound elastography in transplant kidneys: correlations with clinical-Doppler parameters. *Ultrasound Med Biol* 2013; 39: 4–9
- [270] Guo LH, Xu HX, Fu HJ et al. Acoustic radiation force impulse imaging for noninvasive evaluation of renal parenchyma elasticity: preliminary findings. *PLoS One* 2013; 8: e68925
- [271] Bob F, Bota S, Sporea I et al. Kidney shear wave speed values in subjects with and without renal pathology and inter-operator reproducibility of acoustic radiation force impulse elastography (ARFI)—preliminary results. *PLoS One* 2014; 9: e113761
- [272] Grenier N, Poulain S, Lepreux S et al. Quantitative elastography of renal transplants using supersonic shear imaging: a pilot study. *Eur Radiol* 2012; 22: 2138–2146
- [273] Samir AE, Allegretti AS, Zhu Q et al. Shear wave elastography in chronic kidney disease: a pilot experience in native kidneys. *BMC Nephrol* 2015; 16: 119
- [274] Gennisson JL, Rénier M, Catheline S et al. Acoustoelasticity in soft solids: assessment of the nonlinear shear modulus with the acoustic radiation force. *J Acoust Soc Am* 2007; 122: 3211–3219
- [275] Gennisson JL, Deffieux T, Macé E et al. Viscoelastic and anisotropic mechanical properties of in vivo muscle tissue assessed by supersonic shear imaging. *Ultrasound Med Biol* 2010; 36: 789–801
- [276] Gennisson JL, Grenier N, Combe C et al. Supersonic shear wave elastography of in vivo pig kidney: influence of blood pressure, urinary pressure and tissue anisotropy. *Ultrasound Med Biol* 2012; 38: 1559–1567
- [277] Bota S, Bob F, Sporea I et al. Factors that influence kidney shear wave speed assessed by acoustic radiation force impulse elastography in patients without kidney pathology. *Ultrasound Med Biol* 2015; 41: 1–6
- [278] Asano K, Ogata A, Tanaka K et al. Acoustic radiation force impulse elastography of the kidneys: is shear wave velocity affected by tissue fibrosis or renal blood flow? *J Ultrasound Med* 2014; 33: 793–801
- [279] Bob F, Bota S, Sporea I et al. Relationship between the estimated glomerular filtration rate and kidney shear wave speed values assessed by acoustic radiation force impulse elastography: a pilot study. *J Ultrasound Med* 2015; 34: 649–654
- [280] Singh H, Panta OB, Khanal U et al. Renal Cortical Elastography: Normal Values and Variations. *J Med Ultrasound* 2017; 25: 215–220

- [281] Grenier N, Gennisson JL, Cornelis F et al. Renal ultrasound elastography. *Diagn Interv Imaging* 2013; 94: 545–550
- [282] Arndt R, Schmidt S, Loddenkemper C et al. Noninvasive evaluation of renal allograft fibrosis by transient elastography—a pilot study. *Transpl Int* 2010; 23: 871–877
- [283] Stock KF, Klein BS, Cong MT et al. ARFI-based tissue elasticity quantification and kidney graft dysfunction: first clinical experiences. *Clin Hemorheol Microcirc* 2011; 49: 527–535
- [284] Marticorena Garcia SR, Guo J, Dürr M et al. Comparison of ultrasound shear wave elastography with magnetic resonance elastography and renal microvascular flow in the assessment of chronic renal allograft dysfunction. *Acta Radiol* 2018; 59: 1139–1145
- [285] Grass L, Szekely N, Alrajab A et al. Point shear wave elastography (pSWE) using Acoustic Radiation Force Impulse (ARFI) imaging: a feasibility study and norm values for renal parenchymal stiffness in healthy children and adolescents. *Med Ultrason* 2017; 19: 366–373
- [286] Sasaki Y, Hirooka Y, Kawashima H et al. Measurements of renal shear wave velocities in chronic kidney disease patients. *Acta Radiol* 2018; 59: 884–890
- [287] He WY, Jin YJ, Wang WP et al. Tissue elasticity quantification by acoustic radiation force impulse for the assessment of renal allograft function. *Ultrasound Med Biol* 2014; 40: 322–329
- [288] Bob F, Grosu I, Sporea I et al. Ultrasound-Based Shear Wave Elastography in the Assessment of Patients with Diabetic Kidney Disease. *Ultrasound Med Biol* 2017; 43: 2159–2166
- [289] Syversveen T, Midtvedt K, Berstad AE et al. Tissue elasticity estimated by acoustic radiation force impulse quantification depends on the applied transducer force: an experimental study in kidney transplant patients. *Eur Radiol* 2012; 22: 2130–2137
- [290] Wang L, Xia P, Lv K et al. Assessment of renal tissue elasticity by acoustic radiation force impulse quantification with histopathological correlation: preliminary experience in chronic kidney disease. *Eur Radiol* 2014; 24: 1694–1699
- [291] Lee J, Oh YT, Joo DJ et al. Acoustic Radiation Force Impulse Measurement in Renal Transplantation: A Prospective, Longitudinal Study With Protocol Biopsies. *Medicine (Baltimore)* 2015; 94: e1590
- [292] Bob F, Grosu I, Sporea I et al. Is there a correlation between kidney shear wave velocity measured with VTQ and histological parameters in patients with chronic glomerulonephritis? A pilot study. *Med Ultrason* 2018; 1: 27–31
- [293] Early HM, Cheang EC, Aguilera JM et al. Utility of Shear Wave Elastography for Assessing Allograft Fibrosis in Renal Transplant Recipients: A Pilot Study. *J Ultrasound Med* 2018; 37: 1455–1465
- [294] Yoo MG, Jung DC, Oh YT et al. Usefulness of Multiparametric Ultrasound for Evaluating Structural Abnormality of Transplanted Kidney: Can We Predict Histologic Abnormality on Renal Biopsy in Advance? *Am J Roentgenol* 2017; 209: W139–W144
- [295] Bruno C, Caliaro G, Zaffanello M et al. Acoustic radiation force impulse (ARFI) in the evaluation of the renal parenchymal stiffness in paediatric patients with vesicoureteral reflux: preliminary results. *Eur Radiol* 2013; 23: 3477–3484
- [296] Clevert DA, Stock K, Klein B et al. Evaluation of Acoustic Radiation Force Impulse (ARFI) imaging and contrast-enhanced ultrasound in renal tumours of unknown etiology in comparison to histological findings. *Clin Hemorheol Microcirc* 2009; 43: 95–107
- [297] Sidhu PS. Ultrasound Collaboration across Europe: An EFSUMB success story in politically troubled times? *Ultraschall in Med* 2016; 37: 451–452
- [298] Tan S, Miao LY, Cui LG et al. Value of Shear Wave Elastography Versus Contrast-Enhanced Sonography for Differentiating Benign and Malignant Superficial Lymphadenopathy Unexplained by Conventional Sonography. *J Ultrasound Med* 2017; 36: 189–199
- [299] Ghajarzadeh M, Mohammadifar M, Azarkhish K et al. Sono-elastography for Differentiating Benign and Malignant Cervical Lymph Nodes: A Systematic Review and Meta-Analysis. *Int J Prev Med* 2014; 5: 1521–1528
- [300] Ying L, Hou Y, Zheng HM et al. Real-time elastography for the differentiation of benign and malignant superficial lymph nodes: a meta-analysis. *Eur J Radiol* 2012; 81: 2576–2584
- [301] Suh CH, Choi YJ, Baek JH et al. The diagnostic performance of shear wave elastography for malignant cervical lymph nodes: A systematic review and meta-analysis. *Eur Radiol* 2017; 27: 222–230
- [302] Xu W, Shi J, Zeng X et al. EUS elastography for the differentiation of benign and malignant lymph nodes: a meta-analysis. *Gastrointest Endosc* 2011; 74: 1001–1009; quiz 1115.e1001–1004
- [303] Mao XW, Yang JY, Zheng XX et al. Comparison of two quantitative methods of endobronchial ultrasound real-time elastography for evaluating intrathoracic lymph nodes. *Zhonghua Jie He He Hu Xi Za Zhi* 2017; 40: 431–434
- [304] Sun J, Zheng X, Mao X et al. Endobronchial Ultrasound Elastography for Evaluation of Intrathoracic Lymph Nodes: A Pilot Study. *Respiration* 2017; 93: 327–338
- [305] Jung WS, Kim JA, Son EJ et al. Shear wave elastography in evaluation of cervical lymph node metastasis of papillary thyroid carcinoma: elasticity index as a prognostic implication. *Ann Surg Oncol* 2015; 22: 111–116
- [306] You J, Chen J, Xiang F et al. The value of quantitative shear wave elastography in differentiating the cervical lymph nodes in patients with thyroid nodules. *J Med Ultrason (2001)* 2018; 45: 251–259
- [307] Janssen J, Dietrich CF, Will U et al. Endosonographic elastography in the diagnosis of mediastinal lymph nodes. *Endoscopy* 2007; 39: 952–957
- [308] Bhatia KS, Lee YY, Yuen EH et al. Ultrasound elastography in the head and neck. Part II. Accuracy for malignancy. *Cancer Imaging* 2013; 13: 260–276
- [309] Larsen MH, Frstrup C, Hansen TP et al. Endoscopic ultrasound, endoscopic sonoelastography, and strain ratio evaluation of lymph nodes with histology as gold standard. *Endoscopy* 2012; 44: 759–766
- [310] Łasecki M, Olchowcy C, Sokołowska-Dąbek D et al. Modified sonoelastographic scale score for lymph node assessment in lymphoma – a preliminary report. *J Ultrason* 2015; 15: 45–55
- [311] Dudea SM, Botar-Jid C, Dumitriu D et al. Differentiating benign from malignant superficial lymph nodes with sonoelastography. *Med Ultrason* 2013; 15: 132–139
- [312] De Zordo T, Chhem R, Smekal V et al. Real-time sonoelastography: findings in patients with symptomatic achilles tendons and comparison to healthy volunteers. *Ultraschall in Med* 2010; 31: 394–400
- [313] De Zordo T, Fink C, Feuchtner GM et al. Real-time sonoelastography findings in healthy Achilles tendons. *Am J Roentgenol* 2009; 193: W134–W138
- [314] Turan A, Teber MA, Yakut ZI et al. Sonoelastographic assessment of the age-related changes of the Achilles tendon. *Med Ultrason* 2015; 17: 58–61
- [315] Aubry S, Risson JR, Kastler A et al. Biomechanical properties of the calcaneal tendon in vivo assessed by transient shear wave elastography. *Skeletal Radiol* 2013; 42: 1143–1150
- [316] Chen XM, Cui LG, He P et al. Shear wave elastographic characterization of normal and torn achilles tendons: a pilot study. *J Ultrasound Med* 2013; 32: 449–455
- [317] Ooi CC, Schneider ME, Malliaras P et al. Diagnostic performance of axial-strain sonoelastography in confirming clinically diagnosed Achilles tendinopathy: comparison with B-mode ultrasound and color Doppler imaging. *Ultrasound Med Biol* 2015; 41: 15–25
- [318] Klausner AS, Miyamoto H, Tamegger M et al. Achilles tendon assessed with sonoelastography: histologic agreement. *Radiology* 2013; 267: 837–842

- [319] Balaban M, Idilman IS, Ipek A et al. Elastographic Findings of Achilles Tendons in Asymptomatic Professional Male Volleyball Players. *J Ultrasound Med* 2016; 35: 2623–2628
- [320] Ooi CC, Schneider ME, Malliaras P et al. Prevalence of morphological and mechanical stiffness alterations of mid Achilles tendons in asymptomatic marathon runners before and after a competition. *Skeletal Radiol* 2015; 44: 1119–1127
- [321] Ozcan AN, Tan S, Tangal NG et al. Real-time sonoelastography of the patellar and quadriceps tendons: pattern description in professional athletes and healthy volunteers. *Med Ultrason* 2016; 18: 299–304
- [322] Klauser AS, Pamminger M, Halpern EJ et al. Extensor tendinopathy of the elbow assessed with sonoelastography: histologic correlation. *Eur Radiol* 2017; 27: 3460–3466
- [323] De Zordo T, Lill SR, Fink C et al. Real-time sonoelastography of lateral epicondylitis: comparison of findings between patients and healthy volunteers. *Am J Roentgenol* 2009; 193: 180–185
- [324] Lacourpaille L, Nordez A, Hug F et al. Time-course effect of exercise-induced muscle damage on localized muscle mechanical properties assessed using elastography. *Acta Physiol (Oxf)* 2014; 211: 135–146
- [325] Klauser AS, Pamminger MJ, Halpern EJ et al. Sonoelastography of the Common Flexor Tendon of the Elbow with Histologic Agreement: A Cadaveric Study. *Radiology* 2017; 283: 486–491
- [326] Tudisco C, Bisicchia S, Stefanini M et al. Tendon quality in small unilateral supraspinatus tendon tears. Real-time sonoelastography correlates with clinical findings. *Knee Surg Sports Traumatol Arthrosc* 2015; 23: 393–398
- [327] Roskopf AB, Ehrmann C, Buck FM et al. Quantitative Shear-Wave US Elastography of the Supraspinatus Muscle: Reliability of the Method and Relation to Tendon Integrity and Muscle Quality. *Radiology* 2016; 278: 465–474
- [328] Botar-Jid C, Damian L, Duda SM et al. The contribution of ultrasonography and sonoelastography in assessment of myositis. *Med Ultrason* 2010; 12: 120–126
- [329] Drakonaki E. Ultrasound elastography for imaging tendons and muscles. *J Ultrason* 2012; 12: 214–225
- [330] Taljanovic MS, Gimber LH, Becker GW et al. Shear-Wave Elastography: Basic Physics and Musculoskeletal Applications. *Radiographics* 2017; 37: 855–870
- [331] Akagi R, Kusama S. Comparison Between Neck and Shoulder Stiffness Determined by Shear Wave Ultrasound Elastography and a Muscle Hardness Meter. *Ultrasound Med Biol* 2015; 41: 2266–2271
- [332] Andonian P, Viallon M, Le Goff C et al. Shear-Wave Elastography Assessments of Quadriceps Stiffness Changes prior to, during and after Prolonged Exercise: A Longitudinal Study during an Extreme Mountain Ultra-Marathon. *PLoS One* 2016; 11: e0161855
- [333] Brandenburg JE, Eby SF, Song P et al. Quantifying passive muscle stiffness in children with and without cerebral palsy using ultrasound shear wave elastography. *Dev Med Child Neurol* 2016; 58: 1288–1294
- [334] Dubois G, Kheireddine W, Vergari C et al. Reliable protocol for shear wave elastography of lower limb muscles at rest and during passive stretching. *Ultrasound Med Biol* 2015; 41: 2284–2291
- [335] Eby SF, Cloud BA, Brandenburg JE et al. Shear wave elastography of passive skeletal muscle stiffness: influences of sex and age throughout adulthood. *Clin Biomech (Bristol, Avon)* 2015; 30: 22–27
- [336] Koo TK, Guo JY, Cohen JH et al. Quantifying the passive stretching response of human tibialis anterior muscle using shear wave elastography. *Clin Biomech (Bristol, Avon)* 2014; 29: 33–39
- [337] Nakamura M, Hasegawa S, Umegaki H et al. The difference in passive tension applied to the muscles composing the hamstrings – Comparison among muscles using ultrasound shear wave elastography. *Man Ther* 2016; 24: 1–6
- [338] Du LJ, He W, Cheng LG et al. Ultrasound shear wave elastography in assessment of muscle stiffness in patients with Parkinson's disease: a primary observation. *Clin Imaging* 2016; 40: 1075–1080
- [339] Eby S, Zhao H, Song P et al. Quantitative Evaluation of Passive Muscle Stiffness in Chronic Stroke. *Am J Phys Med Rehabil* 2016; 95: 899–910
- [340] Lee SS, Spear S, Rymer WZ. Quantifying changes in material properties of stroke-impaired muscle. *Clin Biomech (Bristol, Avon)* 2015; 30: 269–275
- [341] Lacourpaille L, Hug F, Guével A et al. Non-invasive assessment of muscle stiffness in patients with Duchenne muscular dystrophy. *Muscle Nerve* 2015; 51: 284–286
- [342] Illomei G, Spinicci G, Locci E et al. Muscle elastography: a new imaging technique for multiple sclerosis spasticity measurement. *Neurol Sci* 2017; 38: 433–439
- [343] Song Y, Lee S, Yoo DH et al. Strain sonoelastography of inflammatory myopathies: comparison with clinical examination, magnetic resonance imaging and pathologic findings. *Br J Radiol* 2016; 89: 20160283
- [344] Wu CH, Chen WS, Wang TG. Elasticity of the Coracohumeral Ligament in Patients with Adhesive Capsulitis of the Shoulder. *Radiology* 2016; 278: 458–464
- [345] Miyamoto H, Miura T, Morizaki Y et al. Comparative study on the stiffness of transverse carpal ligament between normal subjects and carpal tunnel syndrome patients. *Hand Surg* 2013; 18: 209–214
- [346] Lee SY, Park HJ, Kwag HJ et al. Ultrasound elastography in the early diagnosis of plantar fasciitis. *Clin Imaging* 2014; 38: 715–718
- [347] Ríos-Díaz J, Martínez-Payá JJ, del Baño-Aledo ME et al. Sonoelastography of Plantar Fascia: Reproducibility and Pattern Description in Healthy Subjects and Symptomatic Subjects. *Ultrasound Med Biol* 2015; 41: 2605–2613
- [348] Sconfienza LM, Silvestri E, Orlandi D et al. Real-time sonoelastography of the plantar fascia: comparison between patients with plantar fasciitis and healthy control subjects. *Radiology* 2013; 267: 195–200
- [349] Wu CH, Chen WS, Wang TG. Plantar fascia softening in plantar fasciitis with normal B-mode sonography. *Skeletal Radiol* 2015; 44: 1603–1607
- [350] Miyamoto H, Siedentopf C, Kastlunger M et al. Intracarpal tunnel contents: evaluation of the effects of corticosteroid injection with sonoelastography. *Radiology* 2014; 270: 809–815
- [351] Yoshii Y, Tung WL, Ishii T. Measurement of Median Nerve Strain and Applied Pressure for the Diagnosis of Carpal Tunnel Syndrome. *Ultrasound Med Biol* 2017; 43: 1205–1209
- [352] Klauser AS, Miyamoto H, Martinoli C et al. Sonoelastographic Findings of Carpal Tunnel Injection. *Ultraschall in Med* 2015; 36: 618–622
- [353] Yoshii Y, Tung WL, Ishii T. Strain and Morphological Changes of Median Nerve After Carpal Tunnel Release. *J Ultrasound Med* 2017; 36: 1153–1159
- [354] Miyamoto H, Halpern EJ, Kastlunger M et al. Carpal tunnel syndrome: diagnosis by means of median nerve elasticity–improved diagnostic accuracy of US with sonoelastography. *Radiology* 2014; 270: 481–486
- [355] Tatar IG, Kurt A, Yavasoglu NG et al. Carpal tunnel syndrome: elastographic strain ratio and cross-sectional area evaluation for the diagnosis and disease severity. *Med Ultrason* 2016; 18: 305–311
- [356] Zhang C, Li M, Jiang J et al. Diagnostic Value of Virtual Touch Tissue Imaging Quantification for Evaluating Median Nerve Stiffness in Carpal Tunnel Syndrome. *J Ultrasound Med* 2017; 36: 1783–1791
- [357] Kantarci F, Ustabasioglu FE, Delil S et al. Median nerve stiffness measurement by shear wave elastography: a potential sonographic method in the diagnosis of carpal tunnel syndrome. *Eur Radiol* 2014; 24: 434–440
- [358] Dikici AS, Ustabasioglu FE, Delil S et al. Evaluation of the Tibial Nerve with Shear-Wave Elastography: A Potential Sonographic Method for the

Diagnosis of Diabetic Peripheral Neuropathy. *Radiology* 2017; 282: 494–501

- [359] Ishibashi F, Taniguchi M, Kojima R et al. Elasticity of the tibial nerve assessed by sonoelastography was reduced before the development of neuropathy and further deterioration associated with the severity of neuropathy in patients with type 2 diabetes. *J Diabetes Investig* 2016; 7: 404–412
- [360] Klauser AS, Miyamoto H, Bellmann-Weiler R et al. Sonoelastography: musculoskeletal applications. *Radiology* 2014; 272: 622–633
- [361] Greening J, Dilley A. Posture-induced changes in peripheral nerve stiffness measured by ultrasound shear-wave elastography. *Muscle Nerve* 2017; 55: 213–222
- [362] Klauser AS, Faschingbauer R, Jaschke WR. Is sonoelastography of value in assessing tendons? *Semin Musculoskelet Radiol* 2010; 14: 323–333
- [363] Kot BC, Zhang ZJ, Lee AW et al. Elastic modulus of muscle and tendon with shear wave ultrasound elastography: variations with different technical settings. *PLoS One* 2012; 7: e44348
- [364] Domenichini R, Pialat JB, Podda A et al. Ultrasound elastography in tendon pathology: state of the art. *Skeletal Radiol* 2017; 46: 1643–1655
- [365] Drakonaki EE, Allen GM, Wilson DJ. Ultrasound elastography for musculoskeletal applications. *Br J Radiol* 2012; 85: 1435–1445
- [366] Alfuraih AM, O'Connor P, Hensor E et al. The effect of unit, depth, and probe load on the reliability of muscle shear wave elastography: Variables affecting reliability of SWE. *J Clin Ultrasound* 2018; 46: 108–115
- [367] Carmignani L, Gadda F, Gazzano G et al. High incidence of benign testicular neoplasms diagnosed by ultrasound. *J Urol* 2003; 170: 1783–1786
- [368] Shah A, Lung PF, Clarke JL et al. Re: New ultrasound techniques for imaging of the indeterminate testicular lesion may avoid surgery completely. *Clin Radiol* 2010; 65: 496–497
- [369] Sidhu PS. Multiparametric Ultrasound (MPUS) Imaging: Terminology Describing the Many Aspects of Ultrasonography. *Ultraschall in Med* 2015; 36: 315–317
- [370] Huang DY, Sidhu PS. Focal testicular lesions: colour Doppler ultrasound, contrast-enhanced ultrasound and tissue elastography as adjuvants to the diagnosis. *Br J Radiol* 2012; 85 Spec No 1: S41–S53
- [371] Pozza C, Gianfrilli D, Fattorini G et al. Diagnostic value of qualitative and strain ratio elastography in the differential diagnosis of non-palpable testicular lesions. *Andrology* 2016; 4: 1193–1203
- [372] Goddi A, Sacchi A, Magistretti G et al. Real-time tissue elastography for testicular lesion assessment. *Eur Radiol* 2012; 22: 721–730
- [373] Auer T, De Zordo T, Dejaco C et al. Value of Multiparametric US in the Assessment of Intratesticular Lesions. *Radiology* 2017; 285: 640–649
- [374] Aigner F, De Zordo T, Pallwein-Prettner L et al. Real-time sonoelastography for the evaluation of testicular lesions. *Radiology* 2012; 263: 584–589
- [375] Schröder C, Lock G, Schmidt C et al. Real-Time Elastography and Contrast-Enhanced Ultrasonography in the Evaluation of Testicular Masses: A Comparative Prospective Study. *Ultrasound Med Biol* 2016; 42: 1807–1815
- [376] Marsaud A, Durand M, Raffaelli C et al. Elastography shows promise in testicular cancer detection. *Prog Urol* 2015; 25: 75–82
- [377] Grasso M, Blanco S, Raber M et al. Elasto-sonography of the testis: preliminary experience. *Arch Ital Urol Androl* 2010; 82: 160–163
- [378] Lock G, Schröder C, Schmidt C et al. Contrast-enhanced ultrasound and real-time elastography for the diagnosis of benign Leydig cell tumours of the testis – a single center report on 13 cases. *Ultraschall in Med* 2014; 35: 534–539
- [379] Jedrzejewski G, Ben-Skowronek I, Wozniak MM et al. Testicular adrenal rest tumours in boys with congenital adrenal hyperplasia: 3D US and elastography—do we get more information for diagnosis and monitoring? *J Pediatr Urol* 2013; 9: 1032–1037
- [380] Bernardo S, Konstantatou E, Huang DY et al. Multiparametric sonographic imaging of a capillary hemangioma of the testis: appearances on gray-scale, color Doppler, contrast-enhanced ultrasound and strain elastography. *J Ultrasound* 2016; 19: 35–39
- [381] Patel K, Sellars ME, Clarke JL et al. Features of testicular epidermoid cysts on contrast-enhanced sonography and real-time tissue elastography. *J Ultrasound Med* 2012; 31: 115–122
- [382] Patel KV, Huang DY, Sidhu PS. Metachronous bilateral segmental testicular infarction: multi-parametric ultrasound imaging with grey-scale ultrasound, Doppler ultrasound, contrast-enhanced ultrasound (CEUS) and real-time tissue elastography (RTE). *J Ultrasound* 2014; 17: 233–238
- [383] Yusuf G, Konstantatou E, Sellars ME et al. Multiparametric Sonography of Testicular Hematomas: Features on Grayscale, Color Doppler, and Contrast-Enhanced Sonography and Strain Elastography. *J Ultrasound Med* 2015; 34: 1319–1328
- [384] Fang C, Konstantatou E, Romanos O et al. Reproducibility of 2-Dimensional Shear Wave Elastography Assessment of the Liver: A Direct Comparison With Point Shear Wave Elastography in Healthy Volunteers. *J Ultrasound Med* 2017; 36: 1563–1569
- [385] Rafailidis V, Robbie H, Konstantatou E et al. Sonographic imaging of extra-testicular focal lesions: comparison of grey-scale, colour Doppler and contrast-enhanced ultrasound. *Ultrasound* 2016; 24: 23–33
- [386] Pedersen MR, Møller H, Osther PJS et al. Comparison of Tissue Stiffness Using Shear Wave Elastography in Men with Normal Testicular Tissue, Testicular Microlithiasis and Testicular Cancer. *Ultrasound Int Open* 2017; 3: E150–E155
- [387] Rocher L, Criton A, Gennisson JL et al. Testicular Shear Wave Elastography in Normal and Infertile Men: A Prospective Study on 601 Patients. *Ultrasound Med Biol* 2017; 43: 782–789
- [388] Ucar AK, Alis D, Samanci C et al. A preliminary study of shear wave elastography for the evaluation of unilateral palpable undescended testes. *Eur J Radiol* 2017; 86: 248–251
- [389] Dikici AS, Er ME, Alis D et al. Is There Any Difference Between Seminomas and Nonseminomatous Germ Cell Tumours on Shear Wave Elastography? A Preliminary Study. *J Ultrasound Med* 2016; 35: 2575–2580
- [390] Rocher L, Glas L, Bellin MF et al. Burned-Out Testis Tumours in Asymptomatic Infertile Men: Multiparametric Sonography and MRI Findings. *J Ultrasound Med* 2017; 36: 821–831
- [391] Trottmann M, Rübenthaler J, Marcon J et al. Differences of standard values of Supersonic shear imaging and ARFI technique – in vivo study of testicular tissue. *Clin Hemorheol Microcirc* 2016; 64: 729–733
- [392] De Zordo T, Stronegger D, Pallwein-Prettner L et al. Multiparametric ultrasonography of the testicles. *Nat Rev Urol* 2013; 10: 135–148
- [393] D'Anastasi M, Schneevogt BS, Trottmann M et al. Acoustic radiation force impulse imaging of the testes: a preliminary experience. *Clin Hemorheol Microcirc* 2011; 49: 105–114
- [394] Trottmann M, Marcon J, D'Anastasi M et al. Shear-wave elastography of the testis in the healthy man – determination of standard values. *Clin Hemorheol Microcirc* 2016; 62: 273–281
- [395] Zieman SJ, Melenovsky V, Kass DA. Mechanisms, pathophysiology, and therapy of arterial stiffness. *Arteriosclerosis, thrombosis, and vascular biology* 2005; 25: 932–943
- [396] Mahmood B, Ewertsen C, Carlsen J et al. Ultrasound Vascular Elastography as a Tool for Assessing Atherosclerotic Plaques – A Systematic Literature Review. *Ultrasound international open* 2016; 2: E106–E112
- [397] de Korte CL, Pasterkamp G, van der Steen AF et al. Characterization of plaque components with intravascular ultrasound elastography in human femoral and coronary arteries in vitro. *Circulation* 2000; 102: 617–623
- [398] de Korte CL, van der Steen AF. Intravascular ultrasound elastography: an overview. *Ultrasonics* 2002; 40: 859–865

- [399] Majdoulina Y, Ohayon J, Keshavarz-Motamed Z et al. Endovascular shear strain elastography for the detection and characterization of the severity of atherosclerotic plaques: in vitro validation and in vivo evaluation. *Ultrasound in medicine & biology* 2014; 40: 890–903
- [400] Schaar JA, De Korte CL, Mastik F et al. Characterizing vulnerable plaque features with intravascular elastography. *Circulation* 2003; 108: 2636–2641
- [401] Dahl JJ, Dumont DM, Allen JD et al. Acoustic radiation force impulse imaging for noninvasive characterization of carotid artery atherosclerotic plaques: a feasibility study. *Ultrasound in medicine & biology* 2009; 35: 707–716
- [402] Czernuszewicz TJ, Homeister JW, Caughey MC et al. Non-invasive in vivo characterization of human carotid plaques with acoustic radiation force impulse ultrasound: comparison with histology after endarterectomy. *Ultrasound in medicine & biology* 2015; 41: 685–697
- [403] Meshram NH, Varghese T, Mitchell CC et al. Quantification of carotid artery plaque stability with multiple region of interest based ultrasound strain indices and relationship with cognition. *Physics in medicine and biology* 2017; 62: 6341–6360
- [404] Emelianov SY, Chen X, O'Donnell M et al. Triplex ultrasound: elasticity imaging to age deep venous thrombosis. *Ultrasound in medicine & biology* 2002; 28: 757–767
- [405] Xie H, Kim K, Aglyamov SR et al. Staging deep venous thrombosis using ultrasound elasticity imaging: animal model. *Ultrasound in medicine & biology* 2004; 30: 1385–1396
- [406] Rubin JM, Xie H, Kim K et al. Sonographic elasticity imaging of acute and chronic deep venous thrombosis in humans. *Journal of ultrasound in medicine: official journal of the American Institute of Ultrasound in Medicine* 2006; 25: 1179–1186
- [407] Takimura H, Hirano K, Muramatsu T et al. Vascular elastography: a novel method to characterize occluded lower limb arteries prior to endovascular therapy. *Journal of endovascular therapy: an official journal of the International Society of Endovascular Specialists* 2014; 21: 654–661
- [408] Yi X, Wei X, Wang Y et al. Role of real-time elastography in assessing the stage of thrombus. *International angiology: a journal of the International Union of Angiology* 2017; 36: 59–63
- [409] Dharmarajah B, Sounderajah V, Rowland SP et al. Aging techniques for deep vein thrombosis: a systematic review. *Phlebology* 2015; 30: 77–84
- [410] Aslan A, Barutca H, Ayaz E et al. Is real-time elastography helpful to differentiate acute from subacute deep venous thrombosis? A preliminary study. *Journal of clinical ultrasound: JCU* 2018; 46: 116–121
- [411] Su Y, Liu W, Wang D et al. Evaluation of abdominal aortic elasticity by strain rate imaging in patients with type 2 diabetes mellitus. *Journal of clinical ultrasound: JCU* 2014; 42: 475–480
- [412] Zheng XZ, Yang B, Wu J. A comparison of the approaches to assess the abdominal aortic stiffness using M-mode ultrasonography, tissue tracking and strain rate imaging. *JNMA: journal of the Nepal Medical Association* 2013; 52: 500–504
- [413] Korshunov VA, Wang H, Ahmed R et al. Model-based vascular elastography improves the detection of flow-induced carotid artery remodeling in mice. *Scientific reports* 2017; 7: 12081
- [414] Ribbers H, Lopata RG, Holeyijn S et al. Noninvasive two-dimensional strain imaging of arteries: validation in phantoms and preliminary experience in carotid arteries in vivo. *Ultrasound in medicine & biology* 2007; 33: 530–540
- [415] Couade M, Pernot M, Prada C et al. Quantitative assessment of arterial wall biomechanical properties using shear wave imaging. *Ultrasound in medicine & biology* 2010; 36: 1662–1676
- [416] Widman E, Maksuti E, Amador C et al. Shear Wave Elastography Quantifies Stiffness in Ex Vivo Porcine Artery with Stiffened Arterial Region. *Ultrasound in medicine & biology* 2016; 42: 2423–2435
- [417] Guo Y, Wang Y, Chang EJ et al. Multidirectional Estimation of Arterial Stiffness Using Vascular Guided Wave Imaging with Geometry Correction. *Ultrasound Med Biol* 2018; 44: 884–896
- [418] Maksuti E, Bini F, Fiorentini S et al. Influence of wall thickness and diameter on arterial shear wave elastography: a phantom and finite element study. *Physics in medicine and biology* 2017; 62: 2694–2718
- [419] Maksuti E, Widman E, Larsson D et al. Arterial Stiffness Estimation by Shear Wave Elastography: Validation in Phantoms with Mechanical Testing. *Ultrasound in medicine & biology* 2016; 42: 308–321
- [420] Widman E, Maksuti E, Larsson D et al. Shear wave elastography plaque characterization with mechanical testing validation: a phantom study. *Physics in medicine and biology* 2015; 60: 3151–3174
- [421] Ramnarine KV, Garrard JW, Dexter K et al. Shear wave elastography assessment of carotid plaque stiffness: in vitro reproducibility study. *Ultrasound in medicine & biology* 2014; 40: 200–209
- [422] Ramnarine KV, Garrard JW, Kanber B et al. Shear wave elastography imaging of carotid plaques: feasible, reproducible and of clinical potential. *Cardiovascular ultrasound* 2014; 12: 49
- [423] Garrard JW, Ramnarine K. Shear-wave elastography in carotid plaques: comparison with grayscale median and histological assessment in an interesting case. *Ultraschall in der Medizin* 2014; 35: 1–3
- [424] Lei Z, Qiang Y, Tianning P et al. Quantitative assessment of carotid atherosclerotic plaque: Initial clinical results using ShearWave™ Elastography. *Int J Clin Exp Med* 2016; 9: 9347–9355
- [425] Lou Z, Yang J, Tang L et al. Shear Wave Elastography Imaging for the Features of Symptomatic Carotid Plaques: A Feasibility Study. *Journal of ultrasound in medicine: official journal of the American Institute of Ultrasound in Medicine* 2017; 36: 1213–1223
- [426] Garrard JW, Ummur P, Nduwayo S et al. Shear Wave Elastography May Be Superior to Greyscale Median for the Identification of Carotid Plaque Vulnerability: A Comparison with Histology. *Ultraschall in der Medizin* 2015; 36: 386–390
- [427] Couade M, Pernot M, Messas E et al. In vivo quantitative mapping of myocardial stiffening and transmural anisotropy during the cardiac cycle. *IEEE transactions on medical imaging* 2011; 30: 295–305
- [428] Pernot M, Couade M, Mateo P et al. Real-time assessment of myocardial contractility using shear wave imaging. *Journal of the American College of Cardiology* 2011; 58: 65–72
- [429] Strachinaru M, Bosch JG, van Dalen BM et al. Cardiac Shear Wave Elastography Using a Clinical Ultrasound System. *Ultrasound in medicine & biology* 2017; 43: 1596–1606
- [430] Bernal M, Gennisson JL, Flaud P et al. Shear wave elastography quantification of blood elasticity during clotting. *Ultrasound in medicine & biology* 2012; 38: 2218–2228
- [431] Mfoumou E, Tripette J, Blostein M et al. Time-dependent hardening of blood clots quantitatively measured in vivo with shear-wave ultrasound imaging in a rabbit model of venous thrombosis. *Thrombosis research* 2014; 133: 265–271
- [432] Kobayashi Y, Omichi K, Kawaguchi Y et al. Intraoperative real-time tissue elastography during laparoscopic hepatectomy. *HPB (Oxford)* 2018; 20: 93–99
- [433] Platz Batista da Silva N, Schauer M, Hornung M et al. Intraoperative dignity assessment of hepatic tumours using semi-quantitative strain elastography and contrast-enhanced ultrasound for optimisation of liver tumour surgery. *Clin Hemorheol Microcirc* 2016; 64: 735–745
- [434] Jung EM, Platz Batista da Silva N, Jung W et al. Is Strain Elastography (IO-SE) Sufficient for Characterization of Liver Lesions before Surgical Resection—Or Is Contrast Enhanced Ultrasound (CEUS) Necessary? *PLoS One* 2015; 10: e0123737
- [435] Kawaguchi Y, Tanaka N, Nagai M et al. Usefulness of Intraoperative Real-Time Tissue Elastography During Laparoscopic Hepatectomy. *J Am Coll Surg* 2015; 221: e103–e111

- [436] Sastry R, Bi WL, Pieper S et al. Applications of Ultrasound in the Resection of Brain Tumours. *J Neuroimaging* 2017; 27: 5–15
- [437] Chauvet D, Imbault M, Capelle L et al. In Vivo Measurement of Brain Tumour Elasticity Using Intraoperative Shear Wave Elastography. *Ultraschall in Med* 2016; 37: 584–590
- [438] Chan HW, Pressler R, Uff C et al. A novel technique of detecting MRI-negative lesion in focal symptomatic epilepsy: intraoperative Shear-Wave elastography. *Epilepsia* 2014; 55: e30–e33
- [439] Selbekk T, Brekken R, Indergaard M et al. Comparison of contrast in brightness mode and strain ultrasonography of glial brain tumours. *BMC Med Imaging* 2012; 12: 11
- [440] Ji S, Hartov A, Roberts D et al. Data assimilation using a gradient descent method for estimation of intraoperative brain deformation. *Med Image Anal* 2009; 13: 744–756
- [441] Joldes GR, Wittek A, Couton M et al. Real-time prediction of brain shift using nonlinear finite element algorithms. *Med Image Comput Comput Assist Interv* 2009; 12: 300–307
- [442] Carter TJ, Sermesant M, Cash DM et al. Application of soft tissue modelling to image-guided surgery. *Med Eng Phys* 2005; 27: 893–909
- [443] Scholz M, Noack V, Pechlivanis I et al. Vibrography during tumour neurosurgery. *J Ultrasound Med* 2005; 24: 985–992
- [444] Fleming IN, Kut C, Macura KJ et al. Ultrasound elastography as a tool for imaging guidance during prostatectomy: initial experience. *Med Sci Monit* 2012; 18: CR635–CR642
- [445] Uramoto H, Nakajima Y, Ohtaki K et al. Intraoperative ultrasound elastography has little diagnostic benefit for deeper tumours of the lung. *Eur J Cardiothorac Surg* 2016; 49: 1538–1539
- [446] Parekattil S, Yeung LL, Su LM. Intraoperative tissue characterization and imaging. *Urol Clin North Am* 2009; 36: 213–221, ix

Noninvasive Tools and Risk of Clinically Significant Portal Hypertension and Varices in Compensated Cirrhosis: The “Anticipate” Study

Juan G. Abraldes,¹ Christophe Bureau,² Horia Stefanescu,³ Salvador Augustin,⁴ Michael Ney,¹ Hélène Blasco,² Bogdan Procopet,^{3,5} Jaime Bosch,^{5,6} Joan Genesca,⁴ and Annalisa Berzigotti,^{5,6} for the Anticipate Investigators

In patients with compensated advanced chronic liver disease (cACLD), the presence of clinically significant portal hypertension (CSPH) and varices needing treatment (VNT) bears prognostic and therapeutic implications. Our aim was to develop noninvasive tests-based risk prediction models to provide a point-of-care risk assessment of cACLD patients. We analyzed 518 patients with cACLD from five centers in Europe/Canada with paired noninvasive tests (liver stiffness measurement [LSM] by transient elastography, platelet count, and spleen diameter with calculation of liver stiffness to spleen/platelet score [LSPS] score and platelet-spleen ratio [PSR]) and endoscopy/hepatic venous pressure gradient measurement. Risk of CSPH, varices, and VNT was modeled with logistic regression. All noninvasive tests reliably identified patients with high risk of CSPH, and LSPS had the highest discrimination. LSPS values above 2.65 were associated with risks of CSPH above 80%. None of the tests identified patients with very low risk of all-size varices, but both LSPS and a model combining TE and platelet count identified patients with very low risk (<5%) risk of VNT, suggesting that they could be used to triage patients requiring screening endoscopy. LSPS values of <1.33 were associated with a <5% risk of VNT, and 26% of patients had values below this threshold. LSM combined with platelet count predicted a risk <5% of VNT in 30% of the patients. Nomograms were developed to facilitate point-of-care risk assessment. *Conclusion:* A significant proportion of patients with a very high risk of CSPH, and a population with a very low risk of VNT can be identified with simple, noninvasive tests, suggesting that these can be used to individualize medical care. (HEPATOLOGY 2016;64:2173-2184).

Liver cirrhosis is characterized by a long compensated phase, with a median survival from diagnosis of around 12 years. When decompensation occurs (variceal bleeding, jaundice, hepatic encephalopathy [HE], or ascites), the expected median survival is around 2 years.^(1,2) Although there are a number of well-validated scores for prognosis prediction and risk stratification in patients with decompensated cirrhosis, these are very limited in the case of compensated cirrhosis.⁽¹⁾ The two most widely validated

prognostic factors in compensated cirrhosis are the presence of clinically significant portal hypertension (CSPH),⁽³⁾ defined as a hepatic venous pressure gradient (HVPG) ≥ 10 mm Hg, and the presence of esophageal varices.⁽¹⁾ The presence of varices has the additional relevance of triggering a therapeutic intervention with either beta-adrenergic blockers or variceal ligation in the case these varices are at high risk of bleeding.⁽⁴⁾

The gold-standard tests to assess CSPH and varices are the measurement of HVPG through hepatic vein

Abbreviations: AUC, area under the curve; cACLD, compensated advanced chronic liver disease; CSPH, clinically significant portal hypertension; HCV, hepatitis C virus; HE, hepatic encephalopathy; HVPG, hepatic venous pressure gradient; IQR, interquartile range; kPa, kilopascals; LS, liver stiffness; LSM, liver stiffness measurement; LSPS, liver stiffness to spleen/platelet score; NITs, noninvasive tools; PSR, platelet/spleen ratio; ROC, receiver operating characteristics; TE, transient elastography measured by FibroScan; VNT, varices needing treatment.

Received June 29, 2016; accepted August 18, 2016.

Additional Supporting Information may be found at onlinelibrary.wiley.com/doi/10.1002/hep.28824/supinfo.

Copyright © 2016 by the American Association for the Study of Liver Diseases.

View this article online at wileyonlinelibrary.com.

DOI 10.1002/hep.28824

Potential conflict of interest: Dr. Bosch consults for and received grants from Conatus and Exallenz. He consults for Gilead.

catheterization and endoscopy, respectively.⁽⁵⁾ However, these tests, especially HVPG measurement, are relatively invasive and impractical for the frequent follow-up of these patients. This has fostered the interest in the use of noninvasive tools (NITs) for the assessment of patients with compensated cirrhosis, but these have not permeated clinical practice until very recently.⁽⁴⁾ Because of the observation that liver biopsy is an imperfect gold standard to mirror fibrosis and vascular remodeling in chronic liver disease, it has been proposed that the term “advanced chronic liver disease” should be used in alternative to “cirrhosis.” In recent years, liver stiffness (LS) measurement (LSM) by transient elastography (TE) emerged as a robust, objective, and numerical NIT for the diagnosis or exclusion of severe fibrosis/cirrhosis and of CSPH⁽⁶⁻⁸⁾ in compensated patients. Accordingly, the recent Baveno VI consensus conference on portal hypertension suggested that LSM can be used to identify patients having compensated advanced chronic liver disease (cACLD) and CSPH.

In addition, recent data suggested that LSM combined to platelet count and spleen size can accurately identify the patients carrying varices needing therapy.⁽⁹⁻¹¹⁾ In this regard, the recent Baveno VI consensus conference on portal hypertension suggested that the combination of LSM and platelet count can be used to reduce the number of unnecessary endoscopies. However, these criteria have not been validated yet and are a matter of debate.

A significant barrier for the translation of NITs into practice is the use of diagnostic performance measurements without direct clinical translation, such as sensitivity, specificity (which are reverse probabilities, indicating the chances of a positive or negative test

based on the presence or absence of disease),⁽¹²⁾ and receiver operating characteristics (ROC) curves (which inform the discriminative capacity of the test across the spectrum of values, but not the chances of having the target condition).⁽¹³⁾ Risk prediction modeling based on these NITs could be a more straightforward answer to the relevant clinical question, that is, what would be the risk of CSPH, varices (V), and VNT (medium-large varices or small with red signs) given a certain value of these noninvasive tests. This could increase the applicability of these tests to define decision thresholds to triage patients in which endoscopy could be avoided and define the probability of presenting CSPH to target the population at risk of decompensation with new therapies.

Therefore, the aim of this study was to develop continuous risk prediction models based on noninvasive tests to predict the risk of CSPH, varices, and VNT in a large, multinational cohort of compensated patients with cirrhosis who had paired noninvasive tests and endoscopy or HVPG measurements.

Patients and Methods

PATIENTS

In this cross-sectional study, we retrospectively analyzed data from 542 patients from four centers in Europe (one in Romania, one in France, and two in Spain) and one in Canada. Patients from the European centers were reported, in part, in previous publications.^(10,11,14,15) The cohort of patients from the

ARTICLE INFORMATION:

From the ¹Cirrhosis Care Clinic, Division of Gastroenterology (Liver Unit), University of Alberta, CEGIIR, Edmonton, Alberta, Canada; ²Service d'hépatogastroentérologie Hôpital Purpan CHU Toulouse, Toulouse France et Université Paul Sabatier, Toulouse, France; ³Hepatology Unit, Regional Institute of Gastroenterology and Hepatology “Octavian Fodor”; University of Medicine and Pharmacy “Iuliu Hatieganu”, Cluj-Napoca, Romania; ⁴Liver Unit, Department of Internal Medicine, Hospital Universitari Vall d'Hebron, Institut de Recerca Vall d'Hebron (VHIR), Universitat Autònoma de Barcelona, CIBEREHD, Barcelona, Spain; ⁵Hepatic Hemodynamic Lab, Liver Unit, Hospital Clinic, University of Barcelona, CIBEREHD, Barcelona, Spain; ⁶Hepatology, Swiss Liver Center, Universitätsklinik für Viszerale Chirurgie und Medizin (UVC/M), Inselspital, University of Bern, Switzerland.

ADDRESS CORRESPONDENCE AND REPRINT REQUESTS TO:

Juan G. Abraldes, M.D.
Division of Gastroenterology (Liver Unit)
University of Alberta
7-142F Katz Group Centre for Pharmacy &
Health Research (114 Street & 87 Avenue)
Edmonton, Alberta, Canada T6G 2E1
E-mail: juan.g.abraldes@ualberta.ca

Annalisa Berzigotti, M.D., Ph.D.
Inselspital, University of Bern
Department of Hepatology
University Clinic of Visceral Surgery and Medicine
MEM F807, Murtenstrasse 35, 3008
Bern, Switzerland
Tel.: +41316328727
E-mail: annalisa.berzigotti@insel.ch

Hospital Vall d'Hebron-Barcelona⁽¹¹⁾ was updated up to June 2014. Patients from the University of Alberta (Edmonton, Alberta, Canada) were reviewed specifically for this study and were identified with an automated search in the local medical record system, restricted to years 2010–2013.

The inclusion criteria for entering patients into the study cohort were: (1) cACLD of any etiology defined by LSM ≥ 10 kilopascals (kPa) according to the Baveno VI recommendations; (2) paired noninvasive tests (blood tests, TE, and/or ultrasound) and gastroscopy/HVPG within 3 months; and (3) absence of previous decompensation defined as ascites, variceal bleeding, HE, or jaundice. Exclusion criteria were: LS lower than 10 kPa; Child-Pugh greater than 6 points. We used these restrictive criteria with the aim of: (1) targeting the population in which these test would be used in clinical practice, given that all decompensated patients have CSPH and a very high prevalence of varices, which makes mandatory an upper endoscopy, and (2) narrowing the theoretical pretest probabilities of varices, which has been reported to be 30%–40% in compensated cirrhosis,^(16,17) and CSPH ($\sim 60\%$ –70% in most recent series; [Supporting Table S1](#)). No patients were treated with beta-blockers at the time of assessment.

PREDICTED OUTCOMES

The three outcomes under study were: (1) CSPH defined by an HVPG greater than 10 mm Hg⁽¹⁸⁾; (2) all-size varices (V); and (3) VNT, defined as large varices or small varices with red signs.⁽⁴⁾ HVPG was performed by experienced teams according to standard guidelines.⁽¹⁸⁾ Varices were classified as small or large according to the criteria used in each participating center. No consensus definition was agreed on beforehand.

PREDICTIVE MODELS

Table 1 shows the predictive models assessed in the present study, with the variables included in each model. We choose these models on the basis of data availability and extensive previous literature.^(9,10,19–23) TE was measured with a FibroScan device provided with M probe (Echosens, Paris, France)⁽⁶⁾ by experienced personnel with specific training and accreditation. The quality criteria used in each center for LSMs by TE were: 10 measurements obtained with a success rate $\geq 60\%$ and the interquartile range (IQR) should be $\leq 30\%$ of the median (IQR/M $\leq 30\%$).⁽⁸⁾ LSPS was calculated as described by Kim et al.⁽⁹⁾ Platelet to spleen ratio (PSR)

TABLE 1. Noninvasive Tests, and Variables Included in Each Model, Used for Risk Prediction in the Present Study

	LSM by TE	LSM by TE and Platelet Count	LSPS	PSR
LSM by TE	x	x	x	
Platelet count		x	x	x
Spleen diameter			x	x
No. of patients with paired endoscopy	518	498	286	286
No. of patients with paired HVPG	229	226	179	179

was calculated as described by Giannini et al.⁽²⁴⁾ Taking into account that spleen diameter (required to calculate LSPS and PSR) is provided inconsistently in ultrasound reports in some countries and thus would limit the use of these tests, we decided to also model the combination of LSM with platelet count.

DECISION THRESHOLDS

Though the aim of the study was to provide models to predict the probability of the outcomes across all the spectrum of values of the noninvasive tests, we provide examples of potential decision thresholds to triage patients for endoscopy (10% for all varices, 5% for VNT). The 5% risk of VNT was consensuated in the recent Baveno VI consensus conference⁽²⁵⁾ for the triage of patients with cirrhosis in need for screening endoscopy.

ETHICS

The ethics board of each participating center approved the study.

STATISTICAL ANALYSIS

We constructed risk prediction models with logistic regression in which the outcome variables were “CSPH,” “all varices,” and “varices needing-treatment.” For each outcome, we constructed four prediction models based on the sets of variables shown in Table 1. The models were internally validated and corrected for optimism with bootstrapping. This has been shown more efficient than a split-sample strategy.⁽²⁶⁾ For this purpose, 200 test data sets of the same size as the analysis data set were generated by random selection with replacement from the analysis data set. All reported performance parameters are based on the bootstrapped analysis. All model equations are provided in the [Supporting Table S2](#).

To assess the performance of the risk prediction models, we assessed discrimination and the calibration of the model. Discrimination refers to the ability to rank patients

TABLE 2. Baseline Demographic and Clinical Characteristics of Patients

	Patients With LSM by TE and Endoscopy (N = 518)	Patients With LSPS/PSR and Endoscopy (n = 286)	Patients With LSM by TE and HVPG (n = 229)	Patients With LSPS/PSR and HVPG (n = 179)
Age, mean years (SD)	58 (11)	59 (10)	60 (11)	60 (10)
Etiology of cirrhosis, %				
Alcohol	14	10	20	14
Alcohol + viral	3	3	3	3
Viral	70	79	66	73
NAFLD	6	3	5	4
Others	7	5	6	6
Prevalence of liver cancer, %	15 (96% BCLC 0 or A)	22 (100% BCLC 0 or A)	24 (100% BCLC 0 or A)	30 (100% BCLC 0 or A)
Prevalence of varices, %	43	47	40	42
Prevalence of varices needing treatment, %	13	16	14	17
Prevalence of CSPH, %			66	68
Percentage of patients with Child-Pugh 5 points, %	86	87	82	86

Abbreviations: NAFLD, nonalcoholic fatty liver disease; BCLC, Barcelona Clinic Liver Cancer.

according to their risk of the outcome variable. The discriminative ability was assessed by ROC curves analysis, with the area under the curve (AUC) as the main readout. Calibration refers to the ability to predict absolute risks (how closely the predicted probabilities agree with the actual risk of the outcome variable).⁽²⁷⁾ Calibration was tested by plotting the agreement of predicted and observed probabilities with a smooth nonparametric fit.^(28,29) Nomograms were based on the corrected logistic regression models. To assess whether the etiology of cirrhosis could modify the relationship between the predictive models and tested outcomes, we assessed the significance of an interaction term composed by etiology (alcohol, alcohol + hepatitis C virus [HCV], HCV, and others) and the non-invasive predictor. For all models, platelet count was capped at 150, given that the relationship between platelets and the risk of CSPH and varices, linear below 150, was flat above 150. Variable log transformation was used when this increased the performance of the models (Supporting Table S2). A preliminary analysis showed that adding more modeling flexibility with cubic splines (which would markedly increase the complexity of the predictive models) did not result in better performance.

Data were processed in SPSS and analyzed in the R platform with the packages ROCR⁽³⁰⁾ and rms.⁽²⁹⁾

Results

Table 2 shows the baseline characteristics of the patients included in the study. Viral hepatitis was the most common etiology of liver cirrhosis.

PREDICTION OF CSPH

Prevalence of CSPH was 66%. This is in keeping with previous reports (Supporting Table S1). Figure 1 shows model representation, ROC curves, and calibration plots of the different risk prediction models. Supporting Fig. S1 shows the nomograms for the prediction of CSPH, and Supporting Table S2 shows the model equations. The LSPS-based model showed the highest AUC (0.88) for CSPH. LSPS values of 0.75, 1.70, and 2.65 were associated with risks of CSPH of 20%, 50%, and 80%, respectively. Only 8% of patients had a predicted risk of CSPH <20% and none of <10%. Calibration of the model was excellent. TE also had an excellent discriminative value (AUC, 0.82), which was ameliorated by the addition of platelet count (AUC, 0.85). Calibration of the models was excellent, but, again, these models could not identify a subpopulation with low risk of CSPH. Performance of PSR was worse (AUC, 0.77), and the PSR-based model was significantly miscalibrated below predicted probabilities <50% (Fig. 1).

These results suggest that in a population of patients with Child-Pugh A compensated cirrhosis, NITs were useful to identify a population with a very high probability of CSPH.

PREDICTION OF VARICES

Prevalence of all-size varices was 42%. Figure 2 shows the representation of the models, with their respective ROC curves and calibration plots.

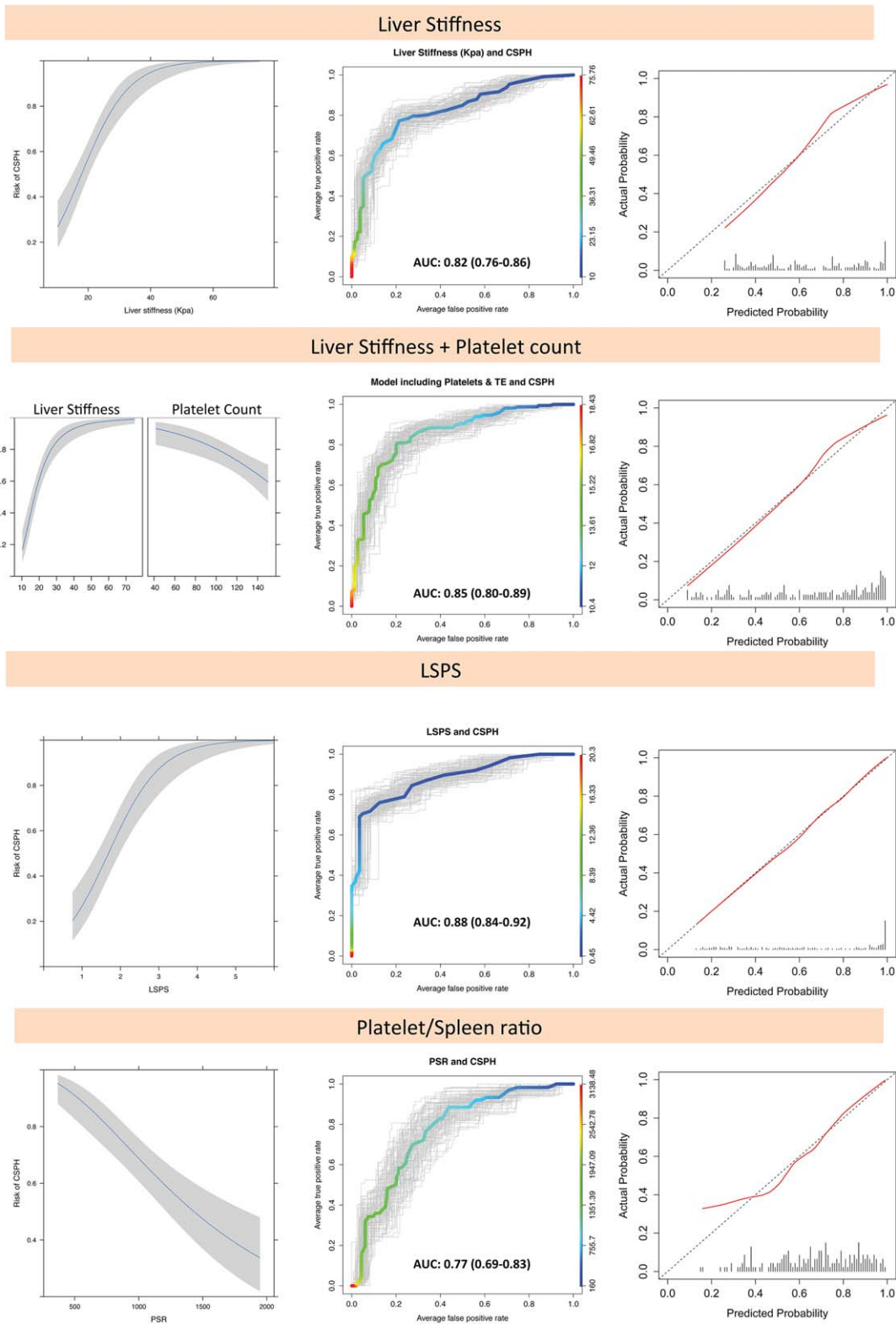


FIG. 1. Model representation, ROC curve, and calibration plot of the four models in predicting CSPH. In the ROC curves, the gray lines represent the 200 bootstrapped curves, and the colored line represents the median curve of the bootstrapped samples. In the calibration plot, the red line represents the smooth nonparametric fit of predicted versus observed probabilities. The lines over the x-axis represent a histogram with the distribution of the patients according to the predicted risk.

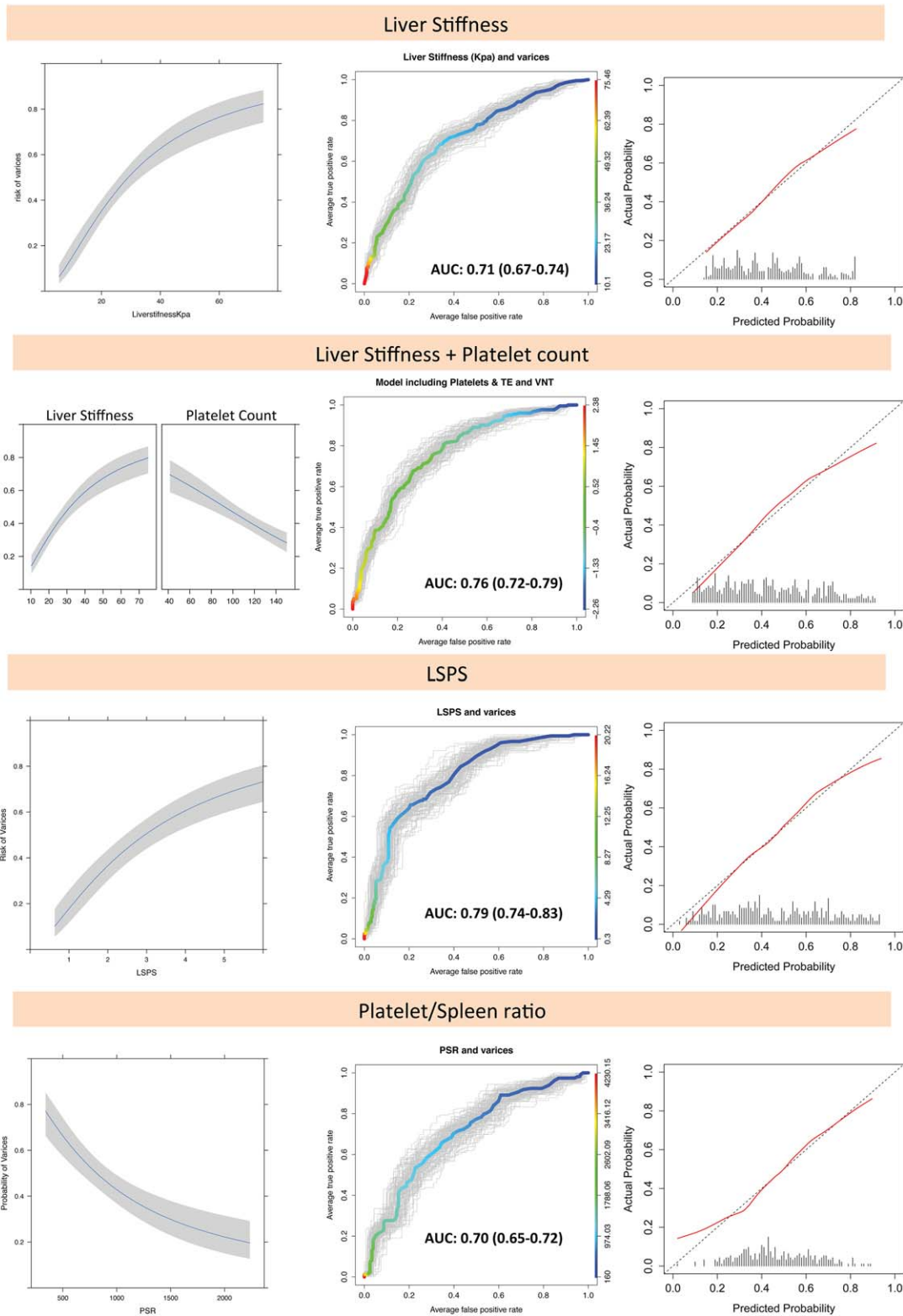


FIG. 2. Model representation (right column), ROC curves (middle column), and calibration plots (left column) of the four models in predicting all-size varices. In the ROC curves, the gray lines represent the 200 bootstrapped curves, and the colored line represents the median curve of the bootstrapped samples. In the calibration plot, the red line represents the smooth nonparametric fit of predicted versus observed probabilities. The lines over the x-axis represent a histogram with the distribution of the patients according to the predicted risk.

Supporting Fig. S2 shows the nomograms for the prediction of varices. The LSPS-based model had the best discriminative ability in predicting varices (AUC, 0.79). An LSPS of 0.63 was associated with a risk of varices of 10%. However, only 3% of the patients had an LSPS <0.63. LSM by TE, LSM by TE + platelet count, and PSR models still had acceptable discriminative value, but they could not identify a subgroup of patients with <10% risk of varices.

These results suggest that in a target population of patients with compensated cirrhosis Child-Pugh A with a pretest probability of varices of ~40%, none of the noninvasive models could identify a significant number of patients with a low probability of varices (<10%).

PREDICTION OF VNT

Prevalence of varices needing treatment was 13%. Figure 3 shows the representation of the different models, with their respective ROC curves and calibration plots. Figure 4 shows the predictive nomograms. LSPS showed the highest discriminative value for predicting VNT (AUC, 0.79). LSPS values of 1.33 were associated with a 5% risk of VNT, and 26% of the sample had values below this threshold. LSM by TE-platelet model was the second best model in terms of discriminative capacity. As shown in the nomogram (Fig. 4), a patient with platelet count $\geq 150,000$ and an LSM value of 20 kPa would have a predictive probability for VNT of 5%, and 30% of the patients showed a predictive probability of VNT below 5%. PSR also had good accuracy (AUC, 0.74), with values of 1,644 predicting a risk of VNT of 5%. The model including LSM by TE alone had the lowest discriminative capacity (AUC, 0.67). Values of 14 were associated with a 5% risk of VNT. The model with best calibration (the one with better agreement between predicted and observed probabilities) was that combining LSM by TE plus platelet count (Fig. 3). LSPS was significantly miscalibrated above predicted probabilities of 40%, and PSR was significantly miscalibrated above probabilities of 30%.

Altogether, these results suggest that LSPS, a combination of LSM by TE-platelet count, or PSR could be used to identify a relevant subset of patients with compensated cirrhosis and Child-Pugh A with a very low probability of VNT (<5%) in which endoscopy could be avoided.

INFLUENCE OF ETIOLOGY

Though the low number of patients with etiologies other than viral hepatitis limited the analysis, there were no significant interactions between the noninvasive models and the etiology of cirrhosis in any of the models, suggesting that etiology did not modify the relationship between the noninvasive models and the outcomes.

Discussion

In the present study, we provide a new way of approaching the use of NITs to predict key features of the natural history of patients with compensated cirrhosis; namely, we show that the numerical information derived from NITs can provide continuous, yet simple, risk measurement tools in the form of nomograms. Our study also allows to show that simple parameters, namely, LSM by TE, platelet count, and spleen diameter in different combinations, allow the clinician to reliably predict which patients have a very high risk of CSPH, thus allowing an early, noninvasive identification of patients at higher risk of developing clinical decompensation of cirrhosis. In addition, these tests could identify patients at very low risk of varices that need prophylactic treatment and thus that might not need an endoscopy. On the other hand, the same simple NITs cannot reliably identify the population of patients having a low risk of all-size varices. This can be, at least partly, explained by the fact that endoscopy is far from being a perfect gold standard for the diagnosis of gastroesophageal varices.⁽³¹⁾

A key point when approaching the use of diagnostic tests from the perspective of risk prediction is the major impact of the pretest probability of the condition in the posttest predictions obtained after applying the test. For this reason, it was extremely important to select for risk modeling a population with prevalences of the conditions under study comparable to those of the target population in which these tests are applied. There is a general agreement that prevalence of varices in patients with decompensated cirrhosis is high enough to warrant screening endoscopy; in addition, CSPH is always present in decompensated patients. Therefore, the niche for the noninvasive prediction of CSPH and varices would be patients with compensated cirrhosis, given that this population shows a much lower prevalence of CSPH (60%), varices (30%-40%),⁽¹⁶⁾ and even lower prevalence of VNT (10%-20%).^(10,32) This is the population included in this

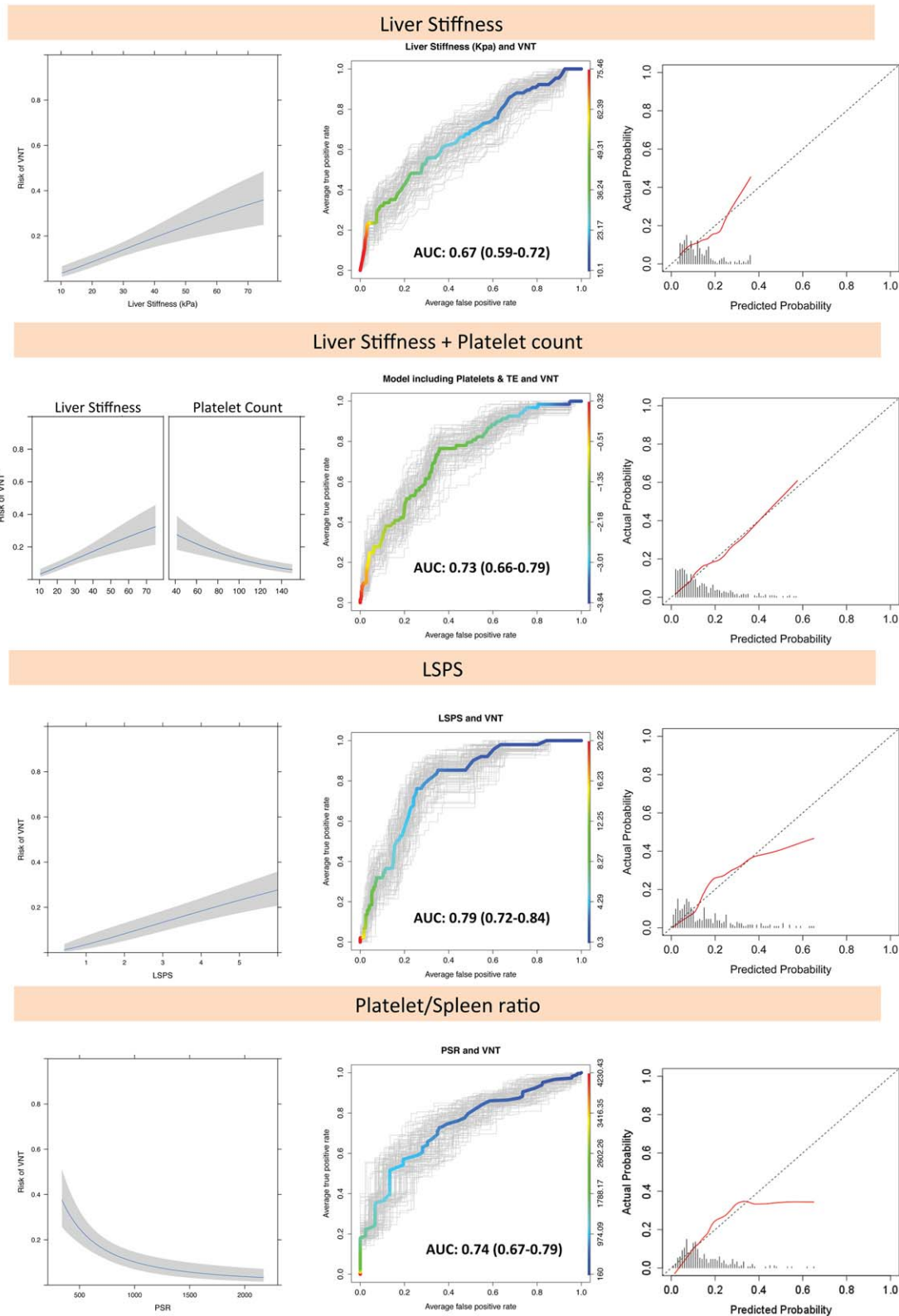


FIG. 3. Model representation, ROC curve, and calibration plot of the four models in predicting VNT, (defined as large varices or small varices with high-risk stigmata). In the ROC curves, the gray lines represent the 200 bootstrapped curves, and the colored line represents the median curve of the bootstrapped samples. In the calibration plot, the red line represents the smooth nonparametric fit of predicted versus observed probabilities. The lines over the x-axis represent a histogram with the distribution of the patients according to the predicted risk.

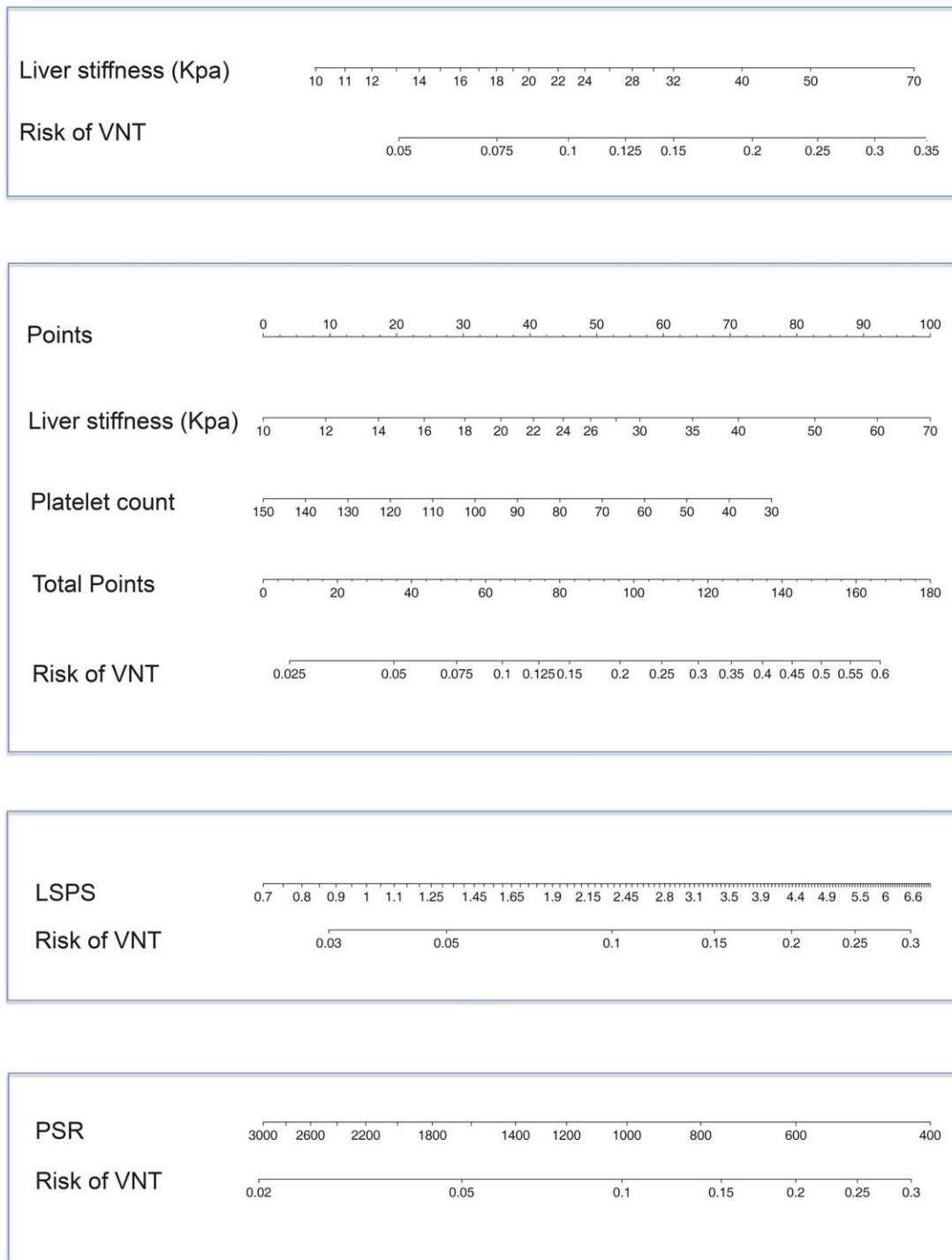


FIG. 4. Nomograms to predict the presence of VNT. In nomograms with one variable, to calculate the probability of VNT trace, a vertical line from the predictor to the risk axis. For the nomogram with two variables (LS and platelet count), trace a vertical line from each of the predictors' axis to the first line ("points"). Add the total points, and trace a vertical line from the "total points" axis to the risk axis to calculate the risk of VNT.

study, and the observed prevalence of varices is in keeping with these figures. It is important to note that the selection of a target population was the first step in our risk prediction approach (by applying the concept of compensated vs. decompensated cirrhosis and by applying the Child-Pugh score). The increasing introduction of NITs for the diagnosis of cirrhosis, and the introduction of the broader concept of cACLD,⁽⁴⁾ might result in the identification of patients at even earlier stages of disease with lower prevalence of varices. Whether these models would require recalibration if used in such populations will require further study.

The outcomes under assessment are of clinical relevance. On the one hand, the presence of CSPH in itself is associated with a 6-fold higher risk of decompensation,⁽³³⁾ and the presence of CSPH might serve to prioritize patients for new treatments, patient selection or stratification in clinical trials aimed at preventing decompensation, and patient selection for surgical treatment of hepatocellular carcinoma.⁽³⁴⁾ On the other hand, whereas the presence of any-size varices does not translate in a therapeutic decision, the presence of VNT has obvious therapeutic consequences, given that both endoscopic variceal ligation and nonselective beta-adrenergic blockers have been shown to decrease the risk of bleeding.⁽⁴⁾

Another relevant question addressed by this study is the use of decision thresholds in order to personalize the clinical decision-making process. This strategy is different from dichotomizing the predictive tool *ab initio*, which is associated with significant loss of information and, if done using the "optimal" data-driven cut off, introduces marked bias.⁽³⁵⁾ Though the selection of a decision threshold is required for taking a binary decision, the decision maker still knows the absolute risk of the outcome. For example, if the decision threshold to prompt screening endoscopy is 5%, and the patient has a greater than 5% risk, the physician making the decision still knows whether this risk is 6% or 30% and might act accordingly taking into account other clinical features of an individual patient (such as age or comorbidities). It is important to note that the choice of a decision threshold, even if is informed by a utility analysis, necessarily bears some degree of arbitrariness. A 5% decision threshold means that we are weighting the importance of a false negative (a patient who has VNT, but is not scoped as a result of the application of NITs) as 19 times more important than a false-positive result (a patient scoped, but with no VNT). This was considered reasonable at the latest Baveno consensus conference, in which a triage and

test associated with a less than 5% risk of missed VNT (a platelet count >150 G/L + an LSM by TE <20 kPa) was recommended.⁽⁴⁾ The ultimate validation of this strategy would require a randomized, controlled trial, comparing the incidence of the relevant outcome (variceal bleeding) if using this strategy to identify patients requiring treatment, with that of a universal endoscopy policy, including a cost and quality-of-life analysis.

Our study has several strengths. First, our predictive models were constructed in a large, multinational sample of patients, which increases the potential external validity of these models. Second, our approach did not involve intensive modeling with extensive variable selection, but was restricted either to one (LSM by TE) or two (LSM by TE and platelet count) variables, or to a preset combination of variables validated in previous studies (LSPS and PSR). This, together with internal validation with bootstrapping, reduces the chances of overfitting in model development or over-optimisms in the estimations of model performance. Third, we provide highly usable predictive tools, by including nomograms that allow for the prediction of the individual absolute risk of a given outcome in a given patient, and that could easily be converted to a web or electronic device-based application for point-of-care use. This differentiates this approach from traditional measurements of diagnostic performance, that require dichotomization of the noninvasive test and are therefore only applicable to groups, but not to individual patients.⁽¹²⁾ In addition, we show the limited value of ROC curves for real practice, given that they reflect the capacity for ranking patients according to their probability of the outcome, but do not inform about the usefulness of the model in individual risk prediction. For example, in the case of CSPH, NITs had a very high area under the ROC, but the tools could not identify patients at low risk of CSPH, and therefore could not be used to rule out this condition. In the case of VNT, with much lower areas under the ROC, models were useful to rule out the presence of VNT, obviating the need for endoscopy, although admittedly in a small subset of patients. Finally, avoiding traditional measurements of diagnostic performance eliminates the problem of how technical failures should be factored in these estimates.

The ANTICIPATE study has limitations. First, it does not incorporate spleen stiffness measurements, which have been suggested to have a high accuracy to predict varices⁽³⁶⁻³⁹⁾; in addition, data on LSM were obtained only with TE and not with newer

elastography techniques.⁽⁴⁰⁾ These data were not available for the present study, but it opens the opportunity to extend the modeling strategy proposed in this study to new multicenter collaborative studies using additional tools. Second, these data were a blend of prospectively and retrospectively collected data, which might limit the capacity for control of the quality of the TE and spleen diameter measurements. However, all participating centers had extensive experience with the techniques before the inclusion of patients in the study and used similar quality criteria. Third, the majority of the patients in this study had viral-related cirrhosis, and there were only a limited number of patients with other etiologies. We statistically explored whether there was heterogeneity in the predictive value of these techniques according to the etiology, or whether they would require different calibrations according to the underlying etiology, and our analysis did not detect significant interactions between etiology and predictions. Admittedly, the relatively low numbers somewhat limit the robustness of this analysis. In addition, this series predates the generalization of HCV treatment for patients with cirrhosis with direct antivirals. Therefore, the effect of viral clearance on the relation between noninvasive tests and the presence of varices or CSPH was not explored. Finally, though we used robust modeling techniques with internal validation, performance of these models in external samples should be assessed.

In summary, the ANTICIPATE study provides NITs for the prediction of relevant outcomes in patients with compensated cirrhosis. In particular, we show that simple and readily available NITs can predict the individual risk of portal hypertension and VNT in this population. Further studies should clarify whether these tests can be used as clinical decision tools to improve clinical outcomes in these patients.

Appendix

Additional ANTICIPATE investigators: University of Alberta, Edmonton, Alberta, Canada: Puneeta Tandon, Mang Ma, Sylvia Kalainy; Service d'hépatogastroentérologie Hôpital Purpan CHU Toulouse, Toulouse France et Université Paul Sabatier, Toulouse, France: Marie Angèle Robic, Jean Marie Péron; Hepatology Unit, Regional Institute of Gastroenterology and Hepatology "Octavian Fodor"; University of Medicine and Pharmacy "Iuliu Hatieganu", Cluj-Napoca, Romania: Monica Platon-

Lupsor, Radu I Badea; Liver Unit, Department of Internal Medicine, Hospital Universitari Vall d'Hebron, Institut de Recerca Vall d'Hebron (VHIR), Universitat Autònoma de Barcelona, CIBEREHD, Barcelona, Spain: Mónica Pons and Laura Millán. Liver Unit, Hospital Clinic, University of Barcelona, Barcelona, Spain: Juan Carlos Garcia-Pagan, Fanny Turon, Virginia Hernandez-Gea.

REFERENCES

- 1) D'Amico G, Garcia-Tsao G, Pagliaro L. Natural history and prognostic indicators of survival in cirrhosis: a systematic review of 118 studies. *J Hepatol* 2006;44:217-231.
- 2) D'Amico G, Pasta L, Morabito A, D'Amico M, Caltagirone M, Malizia G, et al. Competing risks and prognostic stages of cirrhosis: a 25-year inception cohort study of 494 patients. *Aliment Pharmacol Ther* 2014;39:1180-1193.
- 3) Ripoll C, Groszmann R, Garcia-Tsao G, Grace N, Burroughs A, Planas R, et al. Hepatic venous pressure gradient predicts clinical decompensation in patients with compensated cirrhosis. *Gastroenterology* 2007;133:481-488.
- 4) de Franchis R; Baveno VI. Expanding consensus in portal hypertension: report of the Baveno VI Consensus Workshop: stratifying risk and individualizing care for portal hypertension. *J Hepatol* 2015;63:743-752.
- 5) Abraldes JG, Araujo IK, Turon F, Berzigotti A. Diagnosing and monitoring cirrhosis: Liver biopsy, hepatic venous pressure gradient and elastography. *Gastroenterol Hepatol* 2012;35:488-495.
- 6) Castera L, Pinzani M, Bosch J. Non invasive evaluation of portal hypertension using transient elastography. *J Hepatol* 2012;56:696-703.
- 7) Vizzutti F, Arena U, Romanelli RG, Rega L, Foschi M, Colagrande S, et al. Liver stiffness measurement predicts severe portal hypertension in patients with HCV-related cirrhosis. *HEPATOLOGY* 2007;45:1290-1297.
- 8) Castera L, Forns X, Alberti A. Non-invasive evaluation of liver fibrosis using transient elastography. *J Hepatol* 2008;48:835-847.
- 9) Kim BK, Han KH, Park JY, Ahn SH, Kim JK, Paik YH, et al. A liver stiffness measurement-based, noninvasive prediction model for high-risk esophageal varices in B-viral liver cirrhosis. *Am J Gastroenterol* 2010;105:1382-1390.
- 10) Berzigotti A, Seijo S, Arena U, Abraldes JG, Vizzutti F, Garcia-Pagan JC, et al. Elastography, spleen size, and platelet count identify portal hypertension in patients with compensated cirrhosis. *Gastroenterology* 2013;144:102-111.e1.
- 11) Augustin S, Millan L, Gonzalez A, Martell M, Gelabert A, Segarra A, et al. Detection of early portal hypertension with routine data and liver stiffness in patients with asymptomatic liver disease: a prospective study. *J Hepatol* 2014;60:561-569.
- 12) Moons KG, Harrell FE. Sensitivity and specificity should be de-emphasized in diagnostic accuracy studies. *Acad Radiol* 2003;10:670-672.
- 13) Mallett S, Halligan S, Thompson M, Collins GS, Altman DG. Interpreting diagnostic accuracy studies for patient care. *BMJ* 2012;345:e3999.
- 14) Robic MA, Procopet B, Metivier S, Peron JM, Selves J, Vinel JP, Bureau C. Liver stiffness accurately predicts portal hypertension related complications in patients with chronic liver disease: a prospective study. *J Hepatol* 2011;55:1017-1024.

- 15) Procopet B, Cristea VM, Robic MA, Grigorescu M, Agachi PS, Metivier S, et al. Serum tests, liver stiffness and artificial neural networks for diagnosing cirrhosis and portal hypertension. *Dig Liver Dis* 2015;47:411-416.
- 16) D'Amico G, Pagliaro L, Bosch J. The treatment of portal hypertension: a meta-analytic review. *HEPATOLOGY* 1995;22:332-354.
- 17) Garcia-Tsao G, Sanyal AJ, Grace ND, Carey W. Prevention and management of gastroesophageal varices and variceal hemorrhage in cirrhosis. *HEPATOLOGY* 2007;46:922-938.
- 18) Bosch J, Abraldes JG, Berzigotti A, Garcia-Pagan JC. The clinical use of HVPG measurements in chronic liver disease. *Nat Rev Gastroenterol Hepatol* 2009;6:573-582.
- 19) Giannini E, Botta F, Borro P, Risso D, Romagnoli P, Fasoli A, et al. Platelet count/spleen diameter ratio: proposal and validation of a non-invasive parameter to predict the presence of oesophageal varices in patients with liver cirrhosis. *Gut* 2003;52:1200-1205.
- 20) Kim BK, Kim do Y, Han KH, Park JY, Kim JK, Paik YH, et al. Risk assessment of esophageal variceal bleeding in B-viral liver cirrhosis by a liver stiffness measurement-based model. *Am J Gastroenterol* 2011;106:1654-1662, 1730.
- 21) Castéra L, Le Bail B, Roudot-Thoraval F, Bernard PH, Foucher J, Merrouche W, Couzigou P, et al. Early detection in routine clinical practice of cirrhosis and oesophageal varices in chronic hepatitis C: comparison of transient elastography (FibroScan) with standard laboratory tests and non-invasive scores. *J Hepatol* 2009;50:59-68.
- 22) Castera L, Garcia-Tsao G. When the spleen gets tough, the varices get going. *Gastroenterology* 2013;144:19-22.
- 23) Giannini EG, Botta F, Borro P, Dulbecco P, Testa E, Mansi C, et al. Application of the platelet count/spleen diameter ratio to rule out the presence of oesophageal varices in patients with cirrhosis: a validation study based on follow-up. *Dig Liver Dis* 2005;37:779-785.
- 24) Giannini EG, Zaman A, Kreil A, Floreani A, Dulbecco P, Testa E, et al. Platelet count/spleen diameter ratio for the noninvasive diagnosis of esophageal varices: results of a multicenter, prospective, validation study. *Am J Gastroenterol* 2006;101:2511-2519.
- 25) Augustin S, Pons M, Santos B, Ventura M, Genesca J. Identifying compensated advanced chronic liver disease: when (not) to start screening for varices and clinically significant portal hypertension. In: de Franchis R, ed. *Portal Hypertension VI: Proceedings of the Sixth Baveno Consensus Workshop: stratifying risk and individualizing care*. Cham, Switzerland: Springer International AG; 2016:30-49.
- 26) Steyerberg EW, Harrell FE, Jr., Borsboom GJ, Eijkemans MJ, Vergouwe Y, Habbema JD. Internal validation of predictive models: efficiency of some procedures for logistic regression analysis. *J Clin Epidemiol* 2001;54:774-781.
- 27) Altman DG, Vergouwe Y, Royston P, Moons KG. Prognosis and prognostic research: validating a prognostic model. *BMJ* 2009;338:b605.
- 28) Harrell FE, Jr., Lee KL, Mark DB. Multivariable prognostic models: issues in developing models, evaluating assumptions and adequacy, and measuring and reducing errors. *Stat Med* 1996;15:361-387.
- 29) Harrell FE. *Regression Modeling Strategies with Applications to Linear Models, Logistic and Ordinal Regression and Survival Analysis*. New York: Springer; 2015.
- 30) Sing T, Sander O, Beerenwinkel N, Lengauer T. ROCr: visualizing classifier performance in R. *Bioinformatics* 2005;21:3940-3941.
- 31) Bendtsen F, Skovgaard LT, Sorensen TIA, Matzen P. Agreement among multiple observers on endoscopic diagnosis of esophageal varices before bleeding. *HEPATOLOGY* 1990;11:341-347.
- 32) Ding NS, Nguyen T, Iser DM, Hong T, Flanagan E, Wong A, et al. Liver stiffness plus platelet count can be used to exclude high-risk oesophageal varices. *Liver Int* 2016;36:240-245.
- 33) Ripoll C, Groszmann R, Garcia-Tsao G, Grace N, Burroughs A, Planas R, et al. Hepatic venous pressure gradient predicts clinical decompensation in patients with compensated cirrhosis. *Gastroenterology* 2007;133:481-488.
- 34) **Berzigotti A, Reig M, Abraldes JG, Bosch J, Bruix J.** Portal hypertension and the outcome of surgery for hepatocellular carcinoma in compensated cirrhosis: a systematic review and meta-analysis. *HEPATOLOGY* 2015;61:526-536.
- 35) Royston P, Altman DG, Sauerbrei W. Dichotomizing continuous predictors in multiple regression: a bad idea. *Stat Med* 2006;25:127-141.
- 36) Colecchia A, Montrone L, Scaiola E, Bacchi-Reggiani ML, Colli A, Casazza G, et al. Measurement of spleen stiffness to evaluate portal hypertension and the presence of esophageal varices in patients with HCV-related cirrhosis. *Gastroenterology* 2012;143:646-654.
- 37) Abraldes JG, Reverter E, Berzigotti A. Spleen stiffness: toward a noninvasive portal sphygmomanometer? *HEPATOLOGY* 2013;57:1278-1280.
- 38) Calvaruso V, Bronte F, Conte E, Simone F, Craxi A, Di Marco V. Modified spleen stiffness measurement by transient elastography is associated with presence of large oesophageal varices in patients with compensated hepatitis C virus cirrhosis. *J Viral Hepat* 2013;20:867-874.
- 39) Gao J, Ran HT, Ye XP, Zheng YY, Zhang DZ, Wang ZG. The stiffness of the liver and spleen on ARFI Imaging pre and post TIPS placement: a preliminary observation. *Clin Imaging* 2012;36:135-141.
- 40) **Procopet B, Berzigotti A, Abraldes JG, Turon F, Hernandez-Gea V, Garcia-Pagan JC, Bosch J.** Real-time shear-wave elastography: applicability, reliability and accuracy for clinically significant portal hypertension. *J Hepatol* 2015;62:1068-1075.

Author names in bold designate shared co-first authorship.

Supporting Information

Additional Supporting Information may be found at onlinelibrary.wiley.com/doi/10.1002/hep.28824/supinfo.